

Université Pierre et Marie Curie

École doctorale du Muséum d'Histoire Naturelle

« Sciences de la Nature et de l'Homme »

Laboratory Evolution Génome Comportement Ecologie (EGCE) UMR 247

Team Diversity, ecology and evolution of tropical insects

Thermal landscapes and pest dynamic in Andean tropical agrosystems

By Emile Faye

Doctoral thesis in Ecology

Supervision: Olivier Dangles

Defended on November 20th 2015

In front of a jury composed by:

M. Grémillet, David, DR, CNRS – CEFE

Reviewer

M. Goebel, François-Régis, DR, CIRAD – AIDA

Reviewer

M. Vinatier, Fabrice, CR, INRA – LISAH

Examiner

M. Pincebourde, Sylvain, CR, CNRS – IRBI

Examiner

Mme Maïbeche-Coisné, Martine, Professor, UPMC-iEES

Examiner

M. Dangles, Olivier, DR, IRD – EGCE

Supervisor

Université Pierre et Marie Curie

École doctorale du Muséum d'Histoire Naturelle

« Sciences de la Nature et de l'Homme »

Laboratoire Evolution Génomes Comportement Ecologie (EGCE) UMR 247

Équipe Diversité, écologie et évolution des insectes tropicaux

Paysages thermiques et dynamique de ravageurs des cultures dans les Andes tropicales

Par Emile Faye

Thèse de doctorat en Écologie

Dirigée par Olivier Dangles

Présentée et soutenue publiquement le vendredi 20 novembre 2015

Devant un jury composé de :

M. Grémillet, David, DR, CNRS – CEFE

Rapporteur

M. Goebel, François-Régis, DR, CIRAD – AIDA

Rapporteur

M. Vinatier, Fabrice, CR, INRA – LISAH

Examineur

M. Pincebourde, Sylvain, CR, CNRS – IRBI

Examineur

Mme Maïbeche -Coisné, Martine, Professeur, UPMC – iEES

Examineur

M. Dangles, Olivier, DR, IRD – EGCE

Directeur

ACKNOWLEDGEMENTS

To my advisor, Olivier Dangles, for teaching me Science and Research. For sharing with me your love for Ecology, your knowledge, methodologies and experiences. Thank you Olivier for always pulling me up, and for your enthusiasm for my research, for your guidance. I owe you a lot and hope we will keep working together for long. I'll do my best not to disappoint you. Special thank for your friendship as well.

To my wife, Sophie Cauvy, for your unconditional moral and scientific supports throughout these many years, for your ideas and advices (that I should have listen more carefully since the beginning) and for your commitment in many situations. Half of this would not have been possible without you. With love too.

To Sylvain Pincebourde, for presiding over my thesis scientific committee, for teaching me the concepts of thermal ecology, for continuously being attentive to my uncertainties and for being a pertinent adviser. Thank you for sharing with me your field knowledge and tips, and for your management of the paper on thermal cameras. Thank you as well for your warm welcoming during my stays in Tours, and for your friendship.

To François Rebaudo, for your advices and administrative assistance, for introducing me to R and for your unconditional help during statistical analysis. I am also grateful for your collaboration in many of my papers and for your friendship.

I would like to acknowledge the DEEIT team in Gif-sur-Yvette, especially Jean-Francois Silvain, for their hospitality during my stay in the lab (EGCE) and for their support to this work.

To Mario Herrera and Charlie Carpio for their agronomist expertise and help in the field. This study would have been logistically impossible to carry out without you two.

ACKNOWLEDGEMENTS

To the IRBI team (*Institut de Recherche sur la Biologie de l’Insecte*), for their hosting during my stays in Tours, especially to Jérôme Casas and Christelle Suppo for their welcome.

To David Gremillet, François-Régis Goebel, Fabrice Vinatier and Martine Maïbeche-Coisné for accepting of being part of the jury of this thesis and for examining this work.

To the *Pontificia Universidad Católica del Ecuador, Facultad de Ciencias Exactas y Naturales* and the *Laboratoy of Entomology* for always providing an enjoyable place to work, and for lending part of the material used in the experiments and laboratory analyses. Special acknowledgements to Alvaro Barragan and Veronica Crespo-Perez.

To the French *Institut de Recherche pour le Développement* in Quito (Ecuador) and in La Paz (Bolivia), with special thanks to Aída Melgarejo, Ivan Cangas, Alex Terrazas, and Marie Garino for their efficiency in administrative support and their friendships.

Finally, I would like to express my most sincere gratitude to my family and various friends from all over the world for their constant and unconditional moral and practical support since the beginning of my career in Biology. All my love and gratitude for my parents, my brothers and sisters, parents in laws, family in law and to Andrea Tamayo, Antonin Pépin, Benjamin Lehman, Clio Randimbivololona, Cristina Arias, Daniela Lopez, Bettina Heider, David Laurent, Delphine Lethimonier, Diane Sanchez, Estefanía Quenta, Fabien Anthelme, Flavia Tamayo, Felix Leger, Henry Huarez, Igor Stzepourginski, Isabel Moreno, Julien Viau, Justin Eyquem, Lucile Lejemble, Pauline Bonneviot, Pierre Semana, Pierre-Marie Assimon, Rafael Cardenas, Robin Cailon, Valeria Tamayo, Stef de Haan, and all I forgot ☺

ABSTRACT

In the context of global warming and increasing climatic variability, a major uncertainty that hampers effective pest management is related to the thermal characteristics of agricultural landscapes, which are known to have profound effects on insect pest dynamics. Moreover the spatial mismatch between the size of organisms and the scale at which climate data are collected and modelled is also a major barrier to better understand and predict pest distribution and dynamics.

In this thesis, we addressed the issue of considering microclimates experienced by crop pests in their environments with the main objective to infer their spatiotemporal distribution. Therefore, we focused on the following questions: 1) How to bridge the gap between the predictions of coarse-scale climatic models and the fine-scale climatic reality experienced by organisms (i.e. microclimates), 2) How to develop innovative technological approaches such as thermal infrared cameras and unmanned aerial vehicle as a tool for the study of crop pest thermal ecology, 3) to what extent the fine spatiotemporal variability in thermal heterogeneity of natural and agricultural landscapes is useful to understand pest dynamics, and 4) how to integrate microclimatic data in models predicting the interrelation between pest organisms and the microclimate of their environments.

This work revealed that microclimate substantially affects pest dynamics in agrosystems and may offer them opportunities to enhance their performances, as well as to buffer global warming effects within only few centimetres. Consequently, this thesis stresses the need of a better incorporation of microclimatic data into models of species distribution (and vulnerability to climate change) and evidences that microclimates might provide new insights towards agro-ecological pest management.

Keywords: microclimates, pest performances, Andean tropical agrosystems, thermal camera, unmanned aerial vehicle, thermal landscapes metrics.

RÉSUMÉ

Dans un contexte de changement climatique et d'augmentation de la variabilité du climat, une raison majeure qui freine le développement et l'adoption d'une gestion efficace des ravageurs des cultures est celle des caractéristiques thermiques des paysages agricoles, qui sont reconnues pour leur effet sur la dynamique ces ravageurs. De plus, la différence entre la taille des organismes considérés et les échelles auxquelles les données climatiques sont collectées et modélisées est une problématique clé pour comprendre et prédire la distribution des ravageurs des cultures.

Dans ce travail de thèse, nous explorons la prise en compte des microclimats ressentis par les ravageurs des cultures dans leur environnement afin de mieux déduire leur distribution spatiotemporelle. Par conséquent, cette thèse s'est intéressée à: 1) réduire les différences d'échelles entre les prédictions des modèles climatiques globaux et la fine échelle spatiotemporelle des microclimats vécus par les organismes, 2) développer des approches techniques innovantes, comme la combinaison de caméras thermiques avec des drones aéroportés, pour faciliter l'étude de l'écologie thermique des ravageurs des cultures dans leur milieu, 3) déterminer dans quelle mesure la caractérisation de l'hétérogénéité thermique spatiotemporelle des paysages agricoles est utile pour comprendre les dynamiques des ravageurs des cultures et 4) comment intégrer les microclimats dans les modèles de prédiction des ravageurs des cultures.

Ce travail montre que les microclimats conditionnent partiellement la dynamique des ravageurs des cultures dans les agrosystèmes et peuvent leur fournir des opportunités pour améliorer leur performances (et atténuer les effets du changement climatique) dans quelques centimètres carrés seulement. Par conséquent, cette thèse a montré l'importance d'une meilleure prise en compte des microclimats dans les modèles de distribution d'espèces (et de vulnérabilité face au changement climatique). Finalement, ce travail a révélé que l'étude des

microclimats pourrait ouvrir de nouvelles voies de lutte intégrée agro-écologiques contre les ravageurs des cultures.

Mots clés: microclimats, agrosystems Andins, ravageurs des cultures, caméra thermique, drone, indices spatiaux de paysages thermiques.

FOREWORDS

This work has resulted in 5 scientific manuscripts (3 published, 1 accepted after major revisions, and 1 to submit – 4 as a first author), 2 posters, and 6 oral presentations in international conferences and workshops.

LIST OF PAPERS:

1. **Faye, E.**, Herrera, M., Bellomo, L., Silvain, J. F., & Dangles, O. (2014). Strong discrepancies between local temperature mapping and interpolated climatic grids in tropical mountainous agricultural landscapes. **PLoS ONE** 9(8): e105541.
2. Parsa, S., Morse, S., Bonifacio, A., Chancellor, T. C., Condori, B., Crespo-Pérez, V., Hobbs Shaun L. A., Kroschel, J., Bai, M. N., Rebaudo, F., Sherwood, S. G., Vanek, S. J., **Faye, E.**, Herrera, M. A., & Dangles, O. (2014). Obstacles to integrated pest management adoption in developing countries. **Proceedings of the National Academy of Sciences**, 111(10), 3889-3894.
3. **Faye, E.**, Dangles, O., & Pincebourde, S. Distance makes the difference in thermography for ecological studies. **Journal of Thermal Biology**. Doi: 10.1016/j.jtherbio.2015.11.011.
4. **Faye, E.**, Rebaudo, F., Yáñez, D., Cauvy-Fraunié, S. & Dangles O. (2015). A toolbox for studying thermal heterogeneity across spatial scales: from unmanned aerial vehicle imagery to landscape metrics. **Methods in Ecology and Evolution**. Doi: 10.1111/2041-210X.12488.
5. **Faye, E.**, Herrera, M. A., Carpio, C., Rebaudo, F., & Dangles, O. Does heterogeneity in crop canopy microclimate matter for pests? Evidence from aerial high-resolution thermography. To submit to **Journal of Applied Ecology**.

CONFERENCES:

- **2012:** International workshop and summer course on Advances in non-homogeneous environmental turbulences. **Talk:** *Thermal landscape dynamics in agricultural systems of the High Andes*. 12-16th of June 2012. Villanova, Spain.
- **2013:** 11th INTECOL international congress. **Talk** in the Agricultural ecology symposia: *Thermal landscape dynamics and related insect pest performance in mountain agrosystems*. 18-23rd of August 2013. London, United Kingdom.
- **2014:** Heteroclim international workshop entitled ‘The responses of organisms to climate change in heterogeneous environments’. **Poster:** Distance makes the difference in thermography for ecological studies. 10-14th of June 2014. Loches, France.
- **2014:** International conference of the IRSTEA/IGN entitled ‘Drones et moyens légers aréoportés d’observation: recherche, développement et applications’. **Talk:** *Un hélicoptère pour la caractérisation de l’hétérogénéité thermique des agrosystèmes et la compréhension de la dynamique des ravageurs dans les hautes Andes d’Équateur (3500 m)*. 24-26th of June 2014. Montpellier, France.
- **2014:** Workshop at the UMMISCO (Unité de Modélisation Mathématique et Informatique des Systemes COMplexes) laboratory, entitled ‘Réseaux de capteurs/surveillance environnementale’. **Talk:** *High resolution U.A.V. thermal imagery for the study of pest dynamics in the tropical Andes*. 3-4th of June 2014, Bondy, France.
- **2015:** 3rd Global Science conference on Climate Smart Agriculture. **Poster:** *Microclimate drives pests in complex agricultural landscapes: how to monitor and analyse fine-scale climate data?* **Granting of a scholarship.** 18th of March 2015. Montpellier, France.

INVITED CONFERENCE:

- **2014:** at the International Centre of Potato (CIP – CGIAR), **2 talks** entitled *Uses of thermography and U.A.V. for research: techniques and opportunities*. 2-3rd of April 2014. Lima, Peru.

FUNDING:

This work was conducted within the project MAN-PEST “Adaptive management in insect pest control in thermally heterogeneous agricultural landscapes” (ANR-12-JSV7-0013-01) and the project MICROCLIMITE “From global to micro-climate change” (ANR-10-BLAN-1706-02) both funded by the Agence Nationale pour la Recherche (ANR, www.agence-nationale-recherche.fr). A financial support of the McKnight Foundation (www.mcknight.org) and the International Centre of Potato (CIP) to EF during the fieldwork of this study is greatly acknowledged. I am also grateful to the IRD PPR Pest Obs project entitled “Hétérogénéité des températures et ravageurs des cultures dans les paysages agricoles andins (Equateur – Pérou – Bolivie)” for providing funds for travelling across south America. I finally truthfully acknowledge the Sorbonne Universités, Université Pierre-Marie Curie Paris VI for my 3 years PHD grant.

ADDITIONAL INFORMATION:

This thesis was mainly conducted in South America at the *Pontificia Universidad Católica del Ecuador* and at the *French Institute for Development* in Quito (Ecuador), and at the *Universidad Mayor San Andrés* and the *French Institute for Development* in La Paz (Bolivia) but also at the IRD/CNRS EGCE *Laboratoire Évolution, Génomes Comportement*, Ecologie, *Université Paris-Sud II* in Gif sur Yvette (France). Fieldwork was performed nearby Salcedo in Ecuador, Piura in Peru and in Tours in France.

During this thesis, I collaborated with the organisation of the *HeteroClim workshop* in Loches, France in 2014 and at the Thermal Ecology Summer School in the *Pontificia Universidad Católica del Ecuador* in 2015.



Images and videos media that relate to this thesis can be found at www.emilefaye.com in the Media tab. Particularly, short-films on the use of thermal cameras and UAV for studying the microclimates in agricultural landscapes are presented.

TABLE OF CONTENTS

ACKNOWLEDGEMENTS	5
ABSTRACT	7
RÉSUMÉ	8
FOREWORDS	10
TABLE OF CONTENTS	14
INTRODUCTION	19
I. Thermal ecology from individual to landscapes	21
1. Thermal ecology of organisms: basics concepts	21
a. Thermal performances in fluctuating environments	22
b. Thermoregulation strategies	24
2. Microclimates	32
a. Definition and use in the scientific community	32
b. Organism – environment interactions: the microclimate components	35
c. Operative temperatures	38
d. Scales in microclimates.	40
<i>i. Temperature variations in time</i>	40
<i>ii. Thermal heterogeneity at different spatial scales</i>	41
e - Scale mismatch and methods to study ecologically-relevant microclimates	46
3. Microclimates in agrosystems: from agro-climatology to thermal agrosapes	52
a. History of microclimate research in agriculture	52
b. Contributions of precision agriculture	54
c. Pest performances in thermal agrosapes	56
II. Thesis justification	59
1. Microclimates and climate change	59
2. Methods for characterizing thermal heterogeneity at relevant spatial scales and resolutions in agricultural landscapes	60
3. Microclimates for understanding pest occurrence and distribution in agricultural landscapes	61
III. Study site	63
1. Tropical Andes	63
a. Geography and geology	63
b. Climate settings	64
c. Implications for agriculture	66
2. Agricultural landscapes of the study site	68
3. Pests	74
a. Overview of pest in the study site	74
b. Overview of the potato tuber moth complex	76
IV. Objectives and thesis plan	80
Chapter I: Microclimates and pests <i>in silico</i>	80
Chapter II: Methods for assessing thermal heterogeneity in agricultural landscapes	80
Chapter III: Microclimates and pests in situ	81
PLATES	83

CHAPTER I - Microclimates and pests <i>in silico</i>	87
Strong discrepancies between local temperature mapping and interpolated climatic grids in tropical mountainous agricultural landscapes	90
Abstract	90
Introduction	90
Materials and Methods	91
1. Study area	91
2. Temperature data collection	91
3. Global solar radiations	92
4. Data analyses	92
4.1. Times series analyses using Fourier transforms	92
4.2. Thermal landscape analyses	95
4.3. Pest performance in thermal landscape	95
Results	97
1. Local vs. global air temperature discrepancies in thermal landscapes	97
2. Temperature discrepancies due to microclimate in agricultural landscapes	97
3. Thermal performance curve using local vs. interpolated temperatures	97
Discussion	98
1. LAI-based and elevation-based climate heterogeneity	98
2. Fine scale variations in temperature vs. climatic units	99
3. Microclimates and species distribution models	99
References	100
Supporting Information	101
 CHAPTER II - Methods for assessing thermal heterogeneity in agricultural landscapes	111
PART I	113
Distance makes the difference in thermography for ecological studies	116
Abstract	117
1. Introduction	118
2. Materials and Methods	122
2.1. The thermal infrared cameras	122
2.2. Experimental design	122
2.2.1. Thermal test card in different environments	122
2.2.2. TIR shots at increasing distances	123
2.2.3. Differences among surfaces of different structural complexity	125
2.2.4. Surface temperature excess	125
2.3. Data analysis	126
3. Results	128
3.1. Thermal test card in different environments	128
3.2. Effect of surface structural complexity	129
3.3. Surface temperature excess distributions vs. distance	131
4. Discussion	133
4.1. Lower atmosphere composition effect	133
4.2. Pixel size effect	134
4.3. Effect of surface structural complexity	135
4.4. Guidelines for the use of thermography with regards to shooting distance	136
4.5. Conclusion	137
References	138
Supporting Information	143

PART II	155
A toolbox for studying thermal heterogeneity across spatial scales: from unmanned aerial vehicle imagery to landscape metrics	158
Summary	158
Introduction	158
Materials and Methods	159
1. Step 1: Data acquisition with UAV flights	159
a- The UAV system and sensors	159
b- Ground control points	160
c- Meteorological conditions during flights	160
d- Flight description	160
e- TIR surface emissivity	160
2- Step 2: Mapping	161
a- Image geotagging	161
b - RGB / TIR orthophotos generation	161
3 - Step 3: GIS workflow (Fig.1 – GIS workflow and Fig. 3)	161
4 - Step 4: Spatial analyses in R (Fig. 1 – Spatial analysis in R)	162
Study case	162
Results	164
Discussion	164
References	166
Supporting Information	168
CHAPTER III- Microclimates and pests <i>in situ</i>	177
Does heterogeneity in crop canopy microclimate matter for pests? Evidence from aerial high-resolution thermography	180
Abstract	181
Introduction	182
Materials and methods	184
Data acquisition in the field	184
Study area	184
Solar radiation recordings	185
Acquisition of aerial TIR and visible images	185
Pest assessment	187
Image treatment and data sets	187
Image processing	187
Pests' optimal temperatures data	188
Data analyses	189
Results	192
Spatiotemporal heterogeneity in crop surface temperatures	192
Thermal microenvironments and crop pests	194
Discussion	199
Thermal heterogeneity at relevant spatial scale for pests	199
Spatiotemporal heterogeneity of microclimates	200
Linking microclimates to pest distribution	201
References	203
Supporting Information	209

DISCUSSION	217
I. Microclimates: Is exactness in the details?	219
1. Scale effects in microclimates	219
2. Is microclimate enough?	224
3. Does microclimate reduce tropical mountain passes?	226
II. Thermal ecology for agronomists	230
1. Pest control based on thermal ecology?	230
2. Moving to experimental approaches	232
3. Pest modelling for agro-ecological purposes	235
III. Putting thermal ecology into practices in developing countries	237
1. The importance of data in the tropics	237
2. UAV: Limits and promises for developing countries	240
3. The broader picture: facing obstacles to IPM	243
REFERENCES	245
GENERAL APPENDICES	263
Appendix S1: Press communications	265
Appendix S2: Posters	273
Appendix S3: Obstacles to integrated pest management adoption in developing countries	275

INTRODUCTION

I. Thermal ecology from individual to landscapes

1. Thermal ecology of organisms: basics concepts

The phenotype of living organisms is highly influenced by their environment ([Gillooly *et al.* 2001](#), [Angilletta 2009](#), [Kingsolver 2009](#)): environmental features substantially drive organism's traits. The physiology, behaviour, abundance and distribution of organisms are shaped by dozens of environmental variables that can be classified into three main components ([Andrewartha & Birch 1960](#)): weather (temperature, solar radiation...), resource (predation, food availability...), and species interactions (intra- and interspecific, such as competition, parasitism...), which all define a place where to live (i.e. the habitat). Even though organisms might be influenced by a high number of variables, usually only a few account for most of the variability observed in life-history patterns and population dynamics ([Andrewartha & Birch 1960](#), [Wilson 1992](#)). In the case of ectothermic organisms, which constitute the vast majority of terrestrial biodiversity ([Wilson 1992](#), [Brown *et al.* 2004](#)), temperature is a key environmental factor ([Gillooly *et al.* 2001](#), [Bale *et al.* 2002](#), [Angilletta 2009](#), [Bonebrake & Deutsch 2012](#)). Temperature drives most biological and ecological processes from organisms' energetics, growth dynamics, survival, and reproduction ([Cossins & Bowler 1987](#), [Kingsolver & Woods 1997](#), [Savage *et al.* 2004](#), [Frazier *et al.* 2006](#)) to spatial patterns of population density, richness and biogeographical distribution ([Brown *et al.* 2004](#), [Gilbert 2004](#), [Bonebrake & Deutsch 2012](#), [Estay *et al.* 2014](#)). The importance of temperature in affecting life at many levels lies on its influence on biochemical reaction rates, metabolic rates, and nearly all other rates of biological activity ([Gillooly *et al.* 2001](#), [Pörtner 2002](#), [Brown *et al.* 2004](#)). Since the beginning of the twentieth century, thousands of studies on the temperature effects on biological processes have been published and this thematic has resurfaced in the last decades due to the growing importance of research on global climate change effects.

a. Thermal performances in fluctuating environments

Organisms' responses to environmental variables are commonly depicted by performance curves (Huey & Stevenson 1979, Angilletta 2009) that describe performance along a continuous environmental gradient. Angilletta (2009) defines performance as "any measure of an organism's capacity to function, usually expressed as a rate or a probability." Non-exhaustively, these performances include locomotion (e.g., McConnell & Richards 1955, Hirano & Rome 1984, Weinstein 1998, Dillon *et al.* 2012), immune function (e.g., Mondal & Rai, 2001), sensory perception (e.g., Stevenson *et al.* 1985, Dillon *et al.* 2012), foraging ability (e.g., Ayers & Shine 1997), courtship (e.g., Navas & Bevier 2001), and rates of feeding, growth, survival, reproduction and development (e.g., Huey & Stevenson 1979, Kingsolver & Woods 1997, Frazier *et al.* 2006, Crespo-Pérez *et al.* 2013, Logan *et al.* 2014). All these variables respond rapidly (and usually reversibly) to changes in temperature (Angilletta 2009).

In the case of responses to temperature, these curves are commonly referred to as thermal performance curves (TPCs). TPCs are characterized by key properties, including an unimodal shape, a negative skewness at one of their tail, and a finite breadth (Angilletta 2009) and are commonly described with several metrics (Fig. 1): TPC rises with temperature (of the environment or body organism) from a minimum critical temperature (CT_{min}) to an optimum temperature ($Topt$) at which performance is maximal (P_{max}). Then it drops to a critical thermal maximum (CT_{max}). Critical temperatures, CT_{min} and CT_{max} , operationally define the performance limits or thermal tolerance of an organism (see Lutterschmidt & Hutchison 1997 for a review). The thermal breadth (Tbr) or performance breadth is the range of temperatures over which performance is greater than, or equal to, an arbitrary level of performance, usually expressed as a percentage of the maximal performance level (e.g. 50% in Fig. 1).

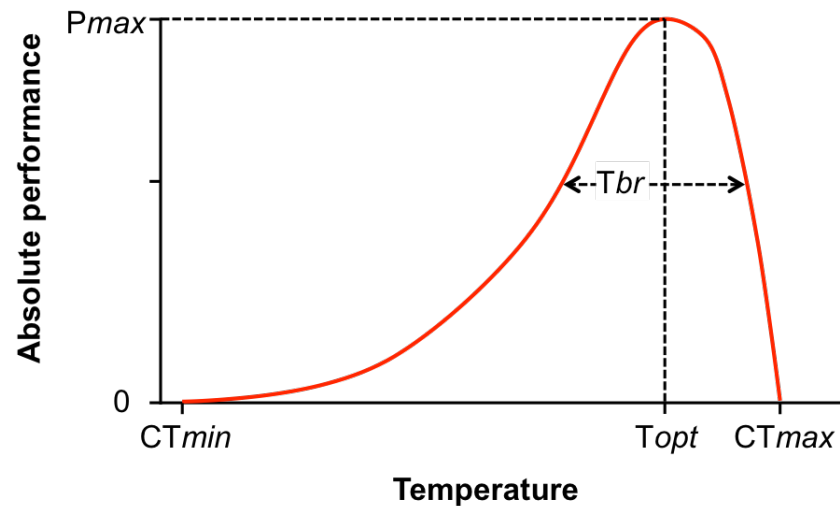


Figure 1: A typical thermal performance curve as a function of the temperature of the environment or organism's body. $Topt$ is optimum temperature at which performance is maximized, $CTmin$ and $CTmax$ are minimum and maximum temperatures at which performance is greater than zero, Tbr is thermal breadth and $Pmax$ is maximal performance at the optimum temperature. Adapted from [Huey & Stevenson \(1979\)](#).

TPCs describe the direct effect of temperature on organism fitness ([Huey & Stevenson 1979](#), [Angilletta 2002](#), [Frazier et al. 2006](#)) and can be fitted mathematically to obtain performance models that relate specific performances to temperature. For a given species, TPCs differ in their thermal optimum, breadth and limits depending on the type of performance assessed ([Huey & Stevenson 1979](#)). Thus, thermal performance models provide a physiological framework for ecologists to understand the responses of organisms to environmental temperatures.

A drawback of TPCs is that they are generally built under stable temperature conditions along a defined gradient ([Barbour & Racine 1967](#), [Huey & Stevenson 1979](#), [Angilletta 2006](#)), while most organisms experience fluctuating temperature conditions in their environment ([Geiger 1965](#)). Because of the variability of the climatic environment experienced by organisms (see paragraph I.2.), TPCs are difficult to build from field

measurements and are usually defined in the laboratory, along a gradient of constant temperatures in closed apparatus (Barbour & Racine 1967). Temperature heterogeneity in time and in space has been shown to strongly modulate the performances of ectothermic organisms (Wu *et al.* 2014, Vázquez *et al.* 2015). For instance, Gilchrist (1995) found that performance breadth was strongly modified by the stability of the thermal environment within generations. Estay *et al.* (2014) showed that population growth rate depends on the interaction between mean temperature and thermal variability (i.e., the standard variation). Finally, Vasseur *et al.* (2014) pointed that temperature-dependent growth rates of 38 ectothermic invertebrate species calculated with mean temperature changes alone differ substantially from those incorporating changes to both mean and variation. Existing predictions of performance models based on insect responses measured under constant temperatures may therefore yield different and less realistic results than predictions of models that include the effect of temperature fluctuation on organism's biology (Gilbert *et al.* 2004). Therefore, as pointed out by Bozinovic *et al.* (2011), to predict organism's responses to their environments, ecologists must understand the patterns of thermal variation and the mechanisms by which animals cope with such variation within their environment.

b. Thermoregulation strategies

Organisms have evolved many strategies to face the thermal heterogeneity of their environment (Angilletta 2009). These strategies can be placed in a general conceptual framework defined by two dimensions (Fig. 2). The first dimension describes the degree to which an organism's performance depends on its temperature (i.e., the thermal sensitivity), ranging from organisms whose performance depends strongly on temperature (thermal specialists) to organisms that perform well over a broad range of temperature (thermal generalists). The second dimension describes the degree to which an organism regulates its

temperature (i.e., thermoregulation), ranging from organisms that maintain a nearly constant body temperature (perfect thermoregulators) to organisms that conform to their environmental temperature (perfect thermoconformers).

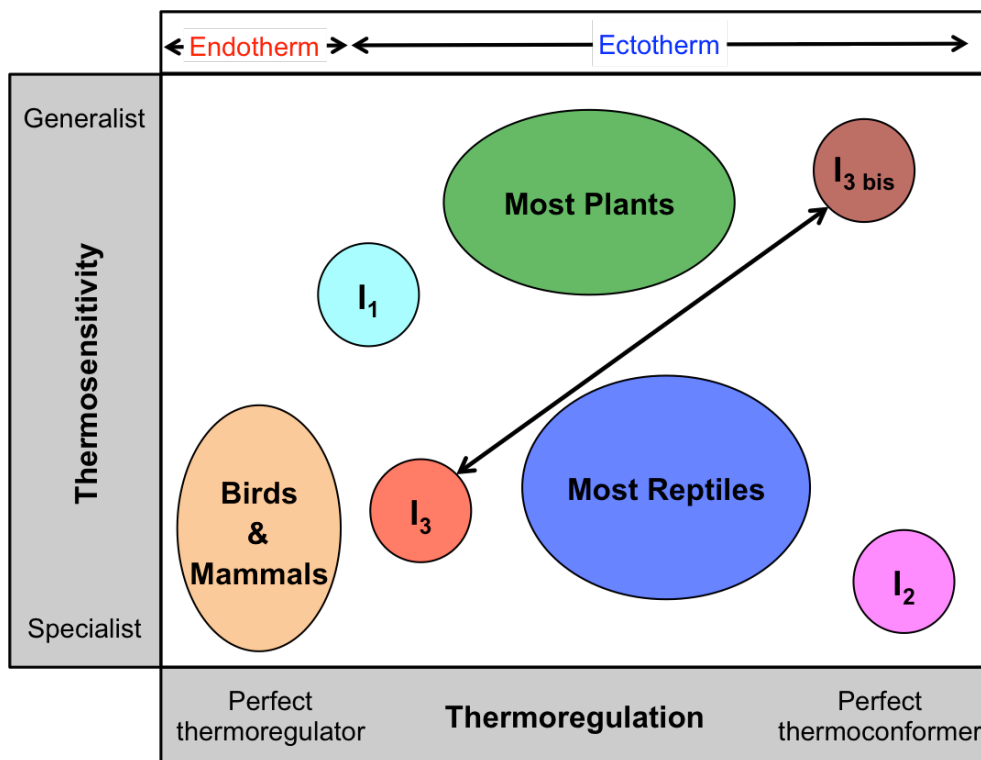


Figure 2: Main strategies for coping with thermal heterogeneity include different combinations of thermosensitivity and thermoregulation. I_1 , I_2 , I_3 indicate different insect species. Coloured areas define the extent of intra-specific variation. A strategic set can change across phenology as exemplified by the arrow connecting two sets for the same species. Modified from [Angilletta 2009](#).

In this framework, endotherms (from the Greek “*endon*” = “within” and “*thermē*” = “heat”) are thermal specialists (which depend strongly on temperature) that thermoregulate precisely. Endotherms rely predominantly on the heat from internal metabolic processes

(Cossins & Bowler 1987, Prinzinger *et al.* 1991): they maintain their body at a metabolically favourable temperature, largely by the use of the heat released by their internal body functions. For instance, human beings are perfect thermoregulators and specialist with a body temperature stabilized at 37.5°C.

On the other hand, ectotherms (from the Greek “*ektós*” = “outside” and “*thermē*” = “heat”) rely on environmental heat sources, which permit them to operate at very economical metabolic rates, i.e., with low energetic costs (Sears & Angilletta 2015). Their internal physiological sources of heat are relatively small or quite negligible in controlling body temperature (e.g., plants, small insects; Huey & Stevenson 1979, Cossins & Bowler 1987, Brown 2004). Therefore, ectotherms regulate their body temperature making use of their abiotic environments. Within ectothermy, tremendous variations occur in terms of thermosensitivity and thermoregulation. For instance, most reptiles are specialists as their performance strongly depends on temperature, but their thermoregulation depends on behavioural capacities (see below, Dawson 1975, Gilchrist 1995). Insects can be found everywhere within this conceptual diagram from thermoregulators such as honeybees (Harrison *et al.* 1996) to strict thermoconformers such as *Drosophila melanogaster* (Dillon *et al.* 2009). Remarkably, the same species can even shift from one position to another within thermoregulation. Indeed, an individual may be a perfect thermoregulator during its diapause and a thermoconformer for the rest of its life cycle (Danks 2004). Likewise, nocturnal moths are thermoconformers, but shift to thermoregulators during the pre-flight and flight activity periods, because they warm up by contracting their wing muscles before flying (Heath & Adams 1967, Heinrich 1993).

Additionally, an individual may use behavioural and physiological mechanisms, or both, to regulate its temperature within a narrower (or larger) range than the range of environmental temperatures (Bartholomew 1966, Smith 1979, Huey 1974, Kearney *et al.* 2009). Physiological thermoregulation includes heat production by metabolism or muscles activity (Benzinger *et al.* 1961, Harrison *et al.* 1996), evaporative cooling (i.e., by heat cutaneous loss, panting, salivation or sweating, Heinrich 1993, Prange 1996), control of blood flow into body appendage (Steen & Steen 1965, Smith 1979), and control of heart-beating rate (Heinrich 1993, Fleisher *et al.* 1996). Behavioural thermoregulation is used by a wide range of organisms, from tiny insects to mega-herbivores, for selecting environmental temperatures that maximize physiological performances or that buffer extreme events (Kearney *et al.* 2009). Those behaviours encompass seasonal adaptation for specific performances (Danks 2004), habitat choice through locomotion and dispersion (Kinahan *et al.* 2007, Dillon *et al.* 2012, Briscoe *et al.* 2014, Sears & Angilletta 2015 and see Fig. 3), postural adjustments of the body or parts of the body (Huey 1974, Kingsolver 1985, Heinrich 1990, 1993, Kemp & Krockenberger 2002 and see Fig. 4), social behaviour (Gilbert *et al.* 2008, Kadochová & Frouz 2013), environmental engineering (Korb 2003), and body part abscission (Pincebourde *et al.* 2013).

For example, [Briscoe *et al.* \(2014\)](#) showed how the arboreal koala *Phascolarctos cinereus* copes with extreme heat events in south-eastern Australia via a behavioural thermoregulation mechanism: during warm events koalas enhance conductive heat losses (see below paragraph I.2.b.) by hugging tree trunks that are substantially cooler than ambient air temperature (Fig. 3).

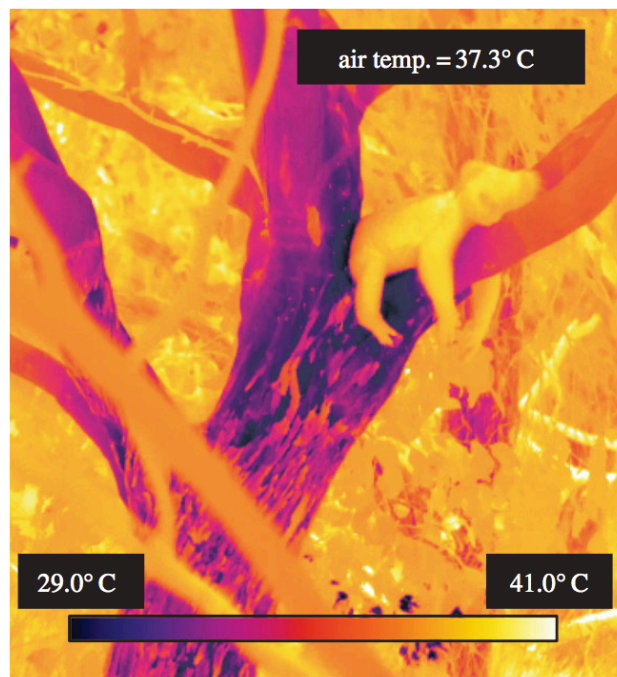


Figure 3: Thermal image of a koala hugging the cool lower limb of a tree, illustrating a posture typically observed during hot weather in Australia. From [Briscoe *et al.* \(2014\)](#).

As another example, [Kingsolver \(1985\)](#) illustrated the reflectance basking phenomena used by Pierid butterflies (Lepidoptera: Pieridae) as a behaviour that involves the use of the wings as solar reflectors, which direct solar radiation into the body to increase their thoracic temperature (Fig. 4). Pierid butterflies orient the inclination of their wings toward the sun (i.e., a thermoregulatory posture) to increase thoracic temperatures through radiative heat (see below paragraph I.2.b.), in order to reach their optimal temperature for taking off and flying (between 29 and 40°C), even when the temperature of their environment is lower.

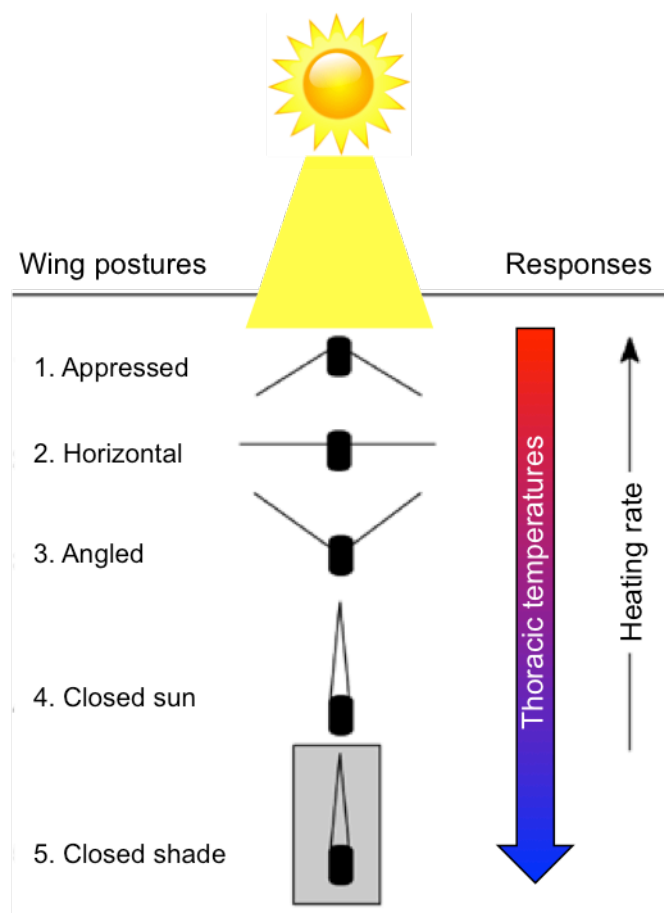


Figure 4: Butterfly wing posture classifications as a behavioural thermoregulation mechanism for the regulation of thoracic temperatures. Adapted from [Kingsolver \(1985\)](#) and [Kemp & Krockenberger \(2002\)](#).

The ability of many ectotherms to avoid potentially lethal body temperatures and to increase the time spent at optimal temperatures has obvious and profound effects on its physiology and fitness ([Kingsolver 2009](#), [Dillon *et al.* 2012](#)). While endotherms thermoregulate their body temperatures using their own metabolic processes regardless of their environmental temperatures (Fig. 5), many ectotherms thermoregulate throughout a combination of physiological and behavioural mechanisms that allow them to deal with the spatial and temporal heterogeneity of their environment (e.g., to avoid the risk of thermal death or to maximize diverse performance traits). In this thesis, we will focus on ectothermic insect pests that are perfect thermoconformers and possess a body temperature closely related to the temperature of their environment (see Fig. 5).

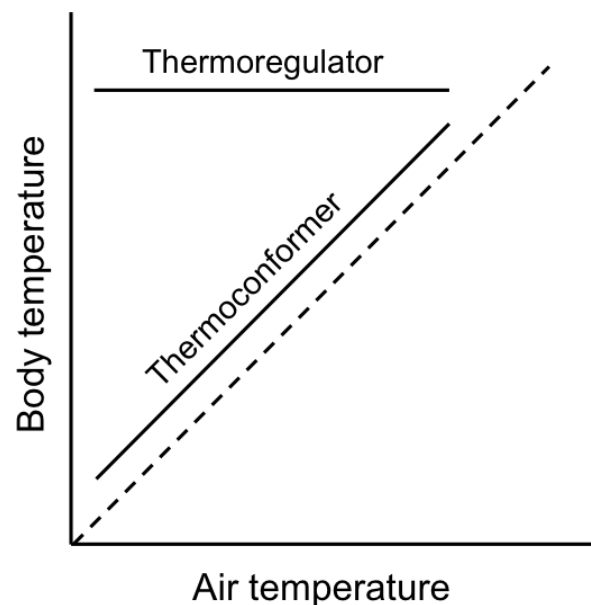


Figure 5: Relationship between air temperature and body temperature define thermoregulation strategies. Adapted from [Angilletta \(2009\)](#).

Temperature is a critical parameter that influences a variety of biological and environmental processes. Environmental temperatures shape the thermally-dependent performances of organisms and consequently condition their occurrences and distributions. Therefore, organisms have evolved many physiological and behavioural strategies to cope with the thermal heterogeneity of their environment. Ectothermic organisms face the environmental conditions by taking advantage of its spatiotemporal variability. Thus, understanding the functioning of the spatiotemporal heterogeneity of the thermal environment available for a study organism (i.e., its microclimates) and the mechanisms by which organisms cope with such variation relative to their physiological sensitivities is primordial for an accurate comprehension of organism occurrence, fitness and distributions. Indeed, forecasting the impacts of climate on organisms requires that we understand the details of how microhabitats filter environmental fluctuations, and whether heterogeneity at small scales is sufficient to allow organisms to find and exploit optimal and favourable conditions.

2. Microclimates

a. Definition and use in the scientific community

The study of the relationships between organisms and climate is a classic question in ecology and has a long history (e.g., Cloudsley-Thompson 1962, Geiger 1965, Woodward 1987, Jones 1992, Pielke *et al.* 1998). Microclimate is usually defined as the climate experienced by an organism in its habitat. While Geiger (1965) initially defines microclimate as “the climate near the ground”, it is now more broadly defined as the result of a combination of biophysical processes shaped by the surrounding environment, which causes climatic conditions to differ from macroclimates (Kearney *et al.* 2014, Storlie *et al.* 2014). Ecologists and agronomists were first interested in what temperatures should be considered among the variety of temperatures that occur at fine spatial scales (Fig. 6), and then in what features of the environment shaped the microclimates.

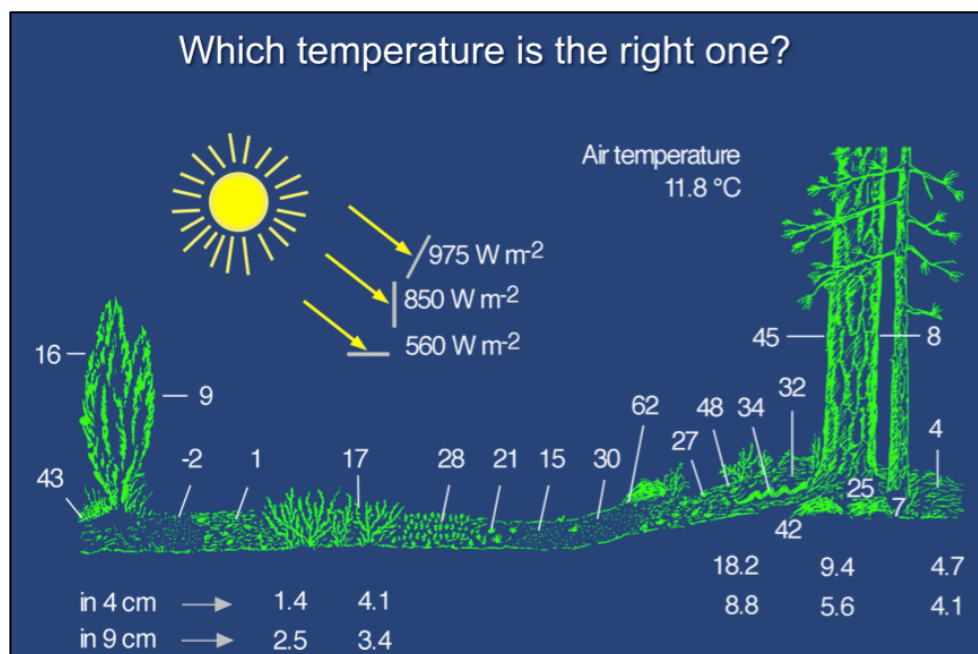


Figure 6: Schematic representation of the spatial heterogeneity of temperatures occurring in a typical ecological landscape. Adapted from Körner (2013).

Microclimates reflect the filtering of global climatic conditions by abiotic and biotic structures present in the environment (e.g., rocks of different sizes, soils of different compositions, topography of the ground surface, moisture, canopy density, etc.). This filtering happens through biophysical processes that involve environmental factors including air and surface temperatures, precipitation, radiation, and wind speed (Geiger 1965, Gates 1980, Jones 1992, Hannah *et al.* 2014).

To illustrate the evolution of microclimates in scientific research, we searched and collected in the ISI Web of Science database, the number of published papers (i.e., papers, letters, editorials and reviews only) per year since 1940, that included the keyword topics “TS= (Microclimate* OR Microclimatic)”. Then, we refined the query using studies written in English and sorted the results by research areas available in ISI Web of Science database (Environment & Ecology, Plant sciences, Agriculture, Entomology, Meteorological sciences and others).

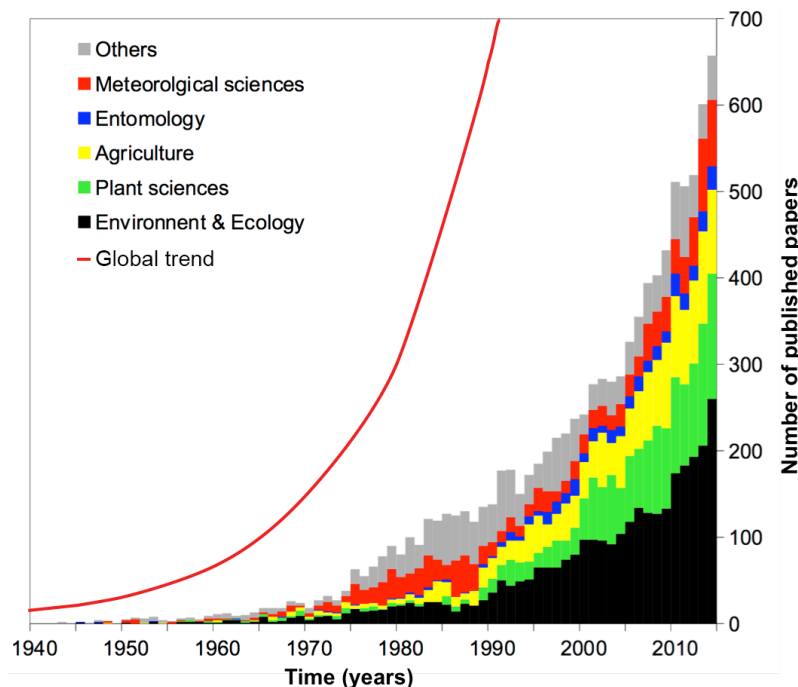


Figure 7: Number of ISI Web of Science publications between 1940 and 2014 referring to microclimates (see text above for definition). Publications (i.e. papers, letters, editorials and reviews only) were sorted by research areas (Environment & Ecology, Plant sciences, Agriculture, Entomology, Meteorological sciences and others). The global rate of published paper per year (+11%, Van Noorden 2014) is displayed as a red curve.

The number of published works involving microclimatic issues has increased exponentially since 1940 (Fig. 7). Results showed that the strong increase in microclimate-focused studies (from <10 in 1950 and >650 in 2014) is mainly due to an intensification of works in the ecology, plant sciences and agriculture areas. These three last research areas represent 40, 22, and 15% of published works in 2014, respectively. Contrastingly, studies focusing in microclimates in entomology have shown a low rate of increase (low increased of blue bars in Fig. 7). However, these increasing trends are to be nuanced for two reasons (see [Van Noorden 2014](#) for details): academic databases such as the ISI Web of Science increased their coverage by 3% a year (i.e., no database captures everything) and the global scientific output increased by 8-9% every year.

b. Organism – environment interactions: the microclimate components

The flow of heat between organisms and their environment occurs through a variety of physical processes, which depend on the environment considered ([Gates 1980](#)). In the case of an ectothermic terrestrial organism, four physical processes contribute significantly to the microclimate experienced by an organism: radiation, conduction, convection, and evaporation (Fig. 8). Each component that composes the habitat of the organism (e.g. plants, ground, rocks, water elements, living organisms, air) relies on these processes and will experience heat exchange among each other.

Radiation. The insect depicted in Fig. 8 gains heat mainly from the radiation absorbed by its body surface. Incoming radiations include the short-wave radiations from the sunbeam that reach the body surface directly (i.e. direct radiations; [Porter & Gates 1969](#)). Part of the sunbeam (mainly UV and blue radiations between 270 and 450 nm) is scattered in terms of quantity, spectral properties and angular distribution by particles in the atmosphere. Reflected radiations are all radiations coming from the sunbeam that are mirrored by terrestrial objects such as rocks, soils, vegetation and clouds. The other part is composed by long-wave radiations emitted by all other surroundings (i.e., thermal radiations from 7.5 to 14 μm , [Jones 1992](#)). Infrared thermal radiations are also emitted by the body surface of the terrestrial ectotherm and are thus responsible for the radiative losses (heat loss by radiation; [Church 1960](#), [Bakken et al. 1989](#)) itself dependent on the physical properties of organism's body (e.g. its emissivity; [Rubio et al. 1997](#)).

Conduction. It is the heat transfer within a body or between the organism and the surrounding objects that occurs only through physical contact. The transfer of heat by conduction occurs through microscopic diffusion and collisions of particles within the body ([Gates 1980](#), [Bakken 1992](#)). Therefore, heat transfers through conduction increase with increasing contact between the body and other solid elements, principally the ground. In the case of thermal conduction, heat spontaneously flows from a warmer to a colder body or part of the body. Therefore, thermal conduction within the body reduces differences in temperature between the body surface (that receives the radiations) and the inner and cooler body parts ([Church 1960](#)).

Convection. Convective heat transfer (or convection) is the transfer of heat from one place to another by the movement of fluids (mainly air in this case). Convection is caused by the variation in density of the air when temperatures are dissimilar. When the air is in contact with a warmer surface (e.g., the body), its molecules separate and scatter, causing the air to be less dense. As a consequence, this warm air is displaced while the cooler air (denser) sinks. The warmer part of the air transfers heat towards the cooler one, thereby decreasing organism's body temperature ([Gates 1980](#)). Convection heat transfers is reversible (depending on the thermal difference between air and body) and dependent on the body surface in contact with the air ([Vogel 1970](#), [Jones 1992](#)). Small ectotherms loose less heat by convection than bigger organisms.

Evaporation. Evaporative cooling (e.g., sweating) happens when water from body surfaces evaporates, changing from liquid to gas. The energy needed to evaporate the water is taken from the body in the form of heat. In the case of an insect in a warm environment, if the heat needed for evaporation can be drawn from the body, body temperature can be prevented from increasing or even lowered below that of the environment ([Porter & Gates 1969](#), [Prange 1996](#)). However, an insect in a hot environment would be gaining heat from its surroundings at the same time it is attempting to cool down. Despite their relatively impermeable exoskeletons some minimal level of evaporation from an insect occurs at warm temperatures. The rate of evaporation increases with increasing body surface area and by the movement of the air over the surface. As the amount of steam (water at the gas phase) that air can hold increases non-linearly with temperature, water loss is likely to be greater at higher temperatures ([Gates 1980](#)). Additionally a high difference between the two temperatures induces strong evaporative cooling, which is the unique way for organisms to decrease their body temperature when the temperature of the environment is higher than the body temperature ([Jones 1992](#)).

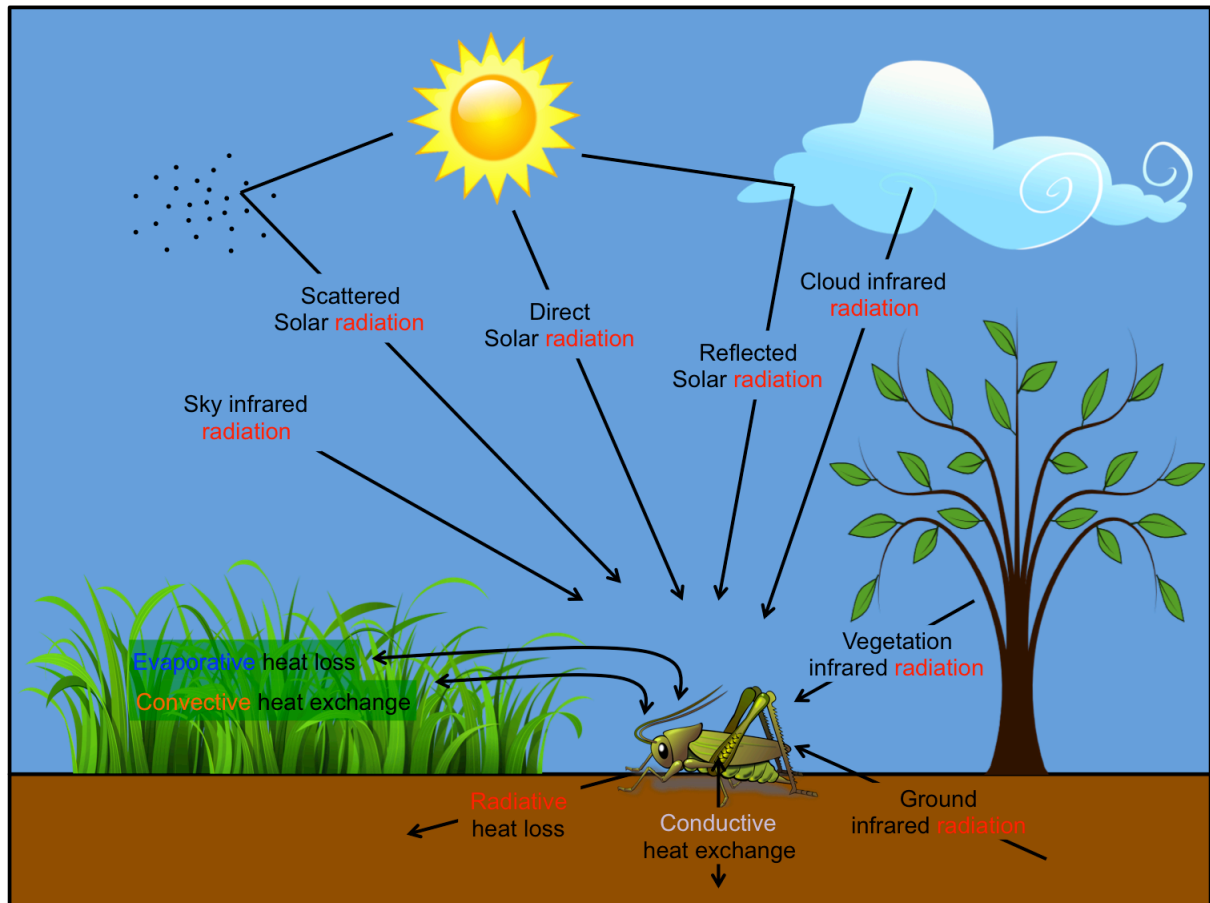


Figure 8: Schematic representation of the biophysical processes that occurs in the elaboration of the microclimatic environment of a terrestrial ectotherm. Routes of heat exchange between the organism and its environment include radiation, conduction, convection, and evaporation. Adapted from Angilletta (2009) and Kearney *et al.* (2014).

Temperature of an organism determines the capacity for heat to flow between the organism and its environment ([Angilletta 2009](#)). Under environmental conditions, the heat flows between the body and the environment occur simultaneously in gains and losses. This relationship relies on the biophysical interaction of the thermal properties of the body (e.g., size, shape, solar reflectance) and the environmental factors including air and surface temperature, humidity, precipitation, radiation, and wind speed as defined by its habitat (e.g., slope, aspect, shading; [Bakken 1992](#), [Kearney *et al.* 2014](#)). The organism will heat or cool until it reaches a steady-state temperature. At this steady state, the organism continues to exchange heat with its environment, but gains and losses cancel each other.

c. Operative temperatures: linking microclimatic heterogeneity and biotic responses

Given the complexity of processes controlling climatic conditions experienced by an organism in its environment, the concept of operative temperature is used to understand how environmental conditions influence the body temperature of an organism. The operative temperature is the steady-state temperature of an organism in a particular microclimate in the absence of metabolic heating and evaporative cooling ([Bakken 1992](#), [Angilletta 2009](#)). This temperature characterizes the thermal environment as perceived by the organism, independently of any physiological thermoregulation. Thus, operative temperatures deliver a thermal index that allows a single-number representation of the complex thermal environment. They can be measured directly using various biophysical figurines of the study organism ([Bakken 1992](#)): temperature sensors installed in figurines that mimic the key biophysical characteristics of the organism's body (e.g., with the same external properties of the animal such as size, colour and matter, [Helmuth & Hofmann 2001](#), [Seebacher & Shine 2004](#), [Langer & Fietz 2014](#)) or in freshly dead bodies ([Kingsolver 1985](#), [Kemp &](#)

[Krockenberger 2002](#)). For example, biophysical models of frogs made of gelatine (i.e., agar-agar) and tinted with the same colour of the studied organism that include a precise thermometer are used to mimic frog body and record operative temperatures in a specific environment (Fig. 9). Biophysical figurines permit to explore the thermal environment at the same spatial scale experienced by organism, and can be replicated relatively easily to measure conditions at multiple sites. However, these empirical measurements should to be made at relevant spatiotemporal scales.

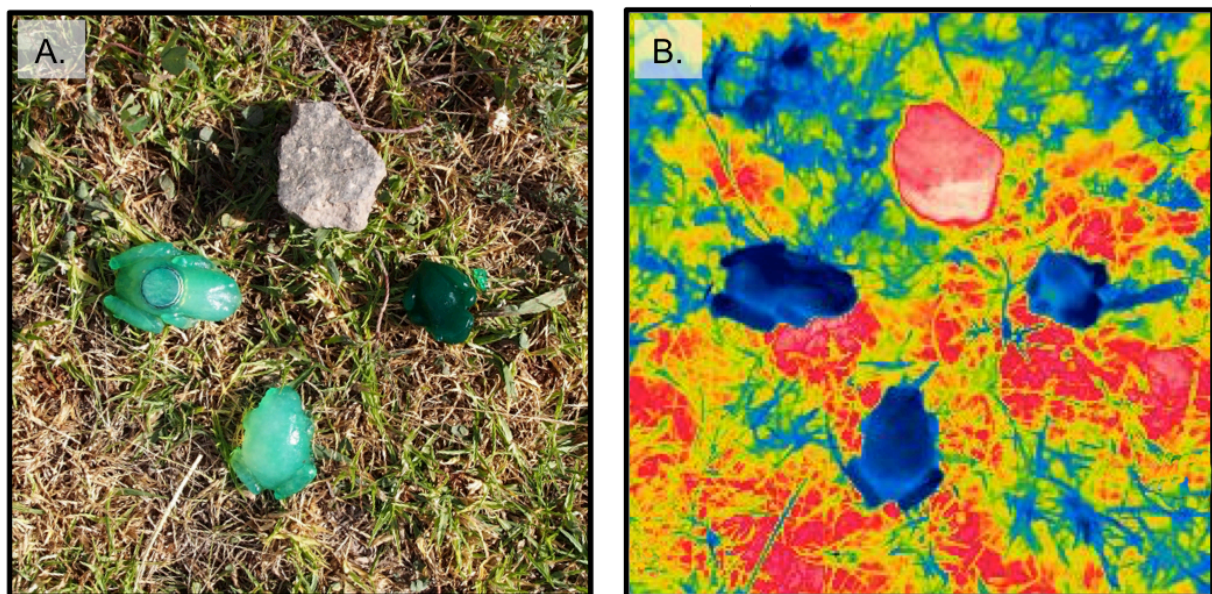


Figure 9: Visual (A.) and thermal infrared (B.) images of frog's biophysical figurines that record operative temperatures in their microenvironment. Surface temperatures ranged from 17 to 30°C. The enclosed-body thermometer appears on the left frog in the visual image. Figurines from Andrés Merino of the *Pontificia Universidad Católica del Ecuador*. Photos credits: Emile Faye and Sylvain Pincebourde.

d. Scales in microclimates.

The temperature experienced by organisms in their environments can be totally different from the conditions measured by a conventional weather station placed 2 m above ground level (defined by the World Meteorological Organisation). Worldwide a large body of literature has acknowledged that weather stations can misrepresent the thermal environment of living organisms (Cloudsley-Thompson 1962, Holmes & Dingle 1965, Geiger 1965, Weiss *et al.* 1988, Jones 1992, Bennie *et al.* 2008, Angilletta 2009, Scherrer & Koerner 2010, Sears *et al.* 2011, Sears & Angilletta 2015, Suggitt *et al.* 2011, Dobrowski 2011, Graae *et al.* 2012, Buckley *et al.* 2013, Hannah *et al.* 2014, Kearney *et al.* 2014, Scheffers *et al.* 2014a,b, Woods *et al.* 2016). Therefore, it is important to consider the climatic heterogeneity experienced by organisms at different temporal and spatial scales.

i. Temperature variations in time

Time has a significant effect on temperature variations at both macro- and micro-scales. The motion of the earth combined with the radiation from the sun drives a continuous redistribution of heat throughout the planet within time. Thus, living organisms must deal with thermal changes on a variety of temporal scales (Wang & Dillon 2014). First, environmental temperatures cycle daily because of the periodic exposure to solar radiation due to the rotation of the earth around its axis (Rojas *et al.* 2014). Second, environmental temperatures change seasonally because of the tilt of the earth as it orbits the sun. Third, environmental temperatures change quickly and unpredictably with atmospheric conditions (wind speed, cloud cover, etc.). Consequently, mean temperatures alone do not provide a complete understanding of these periodic patterns (Camacho *et al.* 2015). By concentrating on climate means, the actual impact of climate on biological systems and organisms is probably being seriously mis-estimated (Paaajmans *et al.* 2013, Thornton *et al.* 2014). Climate

variability and extreme events are not only of critical importance for understanding the biological responses of living organisms (Easterling *et al.* 2000, Rhines & Huybers 2013) but also are expected to be exacerbated by climate change (Karl *et al.* 1995, IPCC 2014), with strong implications for predicting species performances in a changing environment (e.g., Sheldon & Tewksbury 2014, Vasseur *et al.* 2014).

ii. Thermal heterogeneity at different spatial scales

In addition to the temporal variability, the spatial heterogeneity is also one of the main issues of microclimate research. Spatial scale at which climatic data are studied and modelled ranged from the global scale, the regional scale, the local scale, to the organism's scale.

At the global scale: The thermal data collected by weather stations all over the world allow mapping environmental temperatures on a global scale (New *et al.* 2002, Hijmans *et al.* 2005). To construct such maps, one must convert the extremely patchy distribution of thermal records into a regularly spaced grid (Fig. 10). Temperatures between weather stations are interpolated by fitting regression models to the available data using latitude, longitude, and elevation as independent variables (see Hijmans *et al.* 2005 for details). Results are “high-resolution” coarse-scale models of temperature indices (e.g., monthly mean, minimum, and maximum temperature). The spatial resolution obtained by these global models of interpolation reaches at best 0.86 km². Indeed, the overall low density of available climate stations prevents surface temperature models to capture of all the variation that may occur at a resolution of 1 km, particularly in tropical mountainous areas (Hijmans *et al.* 2005).

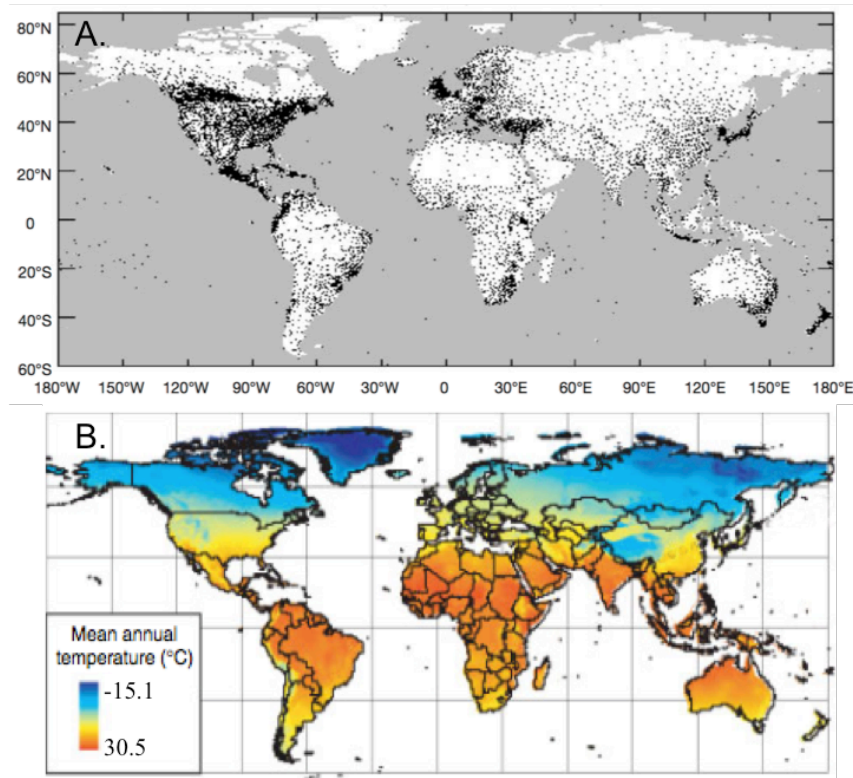


Figure 10: A. Distribution map of the air temperature weather stations available worldwide. For mean temperature, in total 24542 weather stations were used for creating the WordClim database. B. Map of the modelled mean temperatures at a 30 arc second (almost 1 km close to the Ecuador line) resolution. Adapted from Hijmans *et al.* (2005).

At the regional scale: capturing fine-grain environmental patterns at regional scales cannot be accomplished easily using conventional sampling techniques (i.e., standard weather stations) because of the structural complexity of the landscape ([Lookingbill & Urban 2003](#)) and the resulting thermal heterogeneity. Therefore, studies at the regional scale usually combine empirical fine-grain monitoring of climate (with a large number of miniaturized thermometers evenly distributed in space) with correlative models based on landscape features ([Chuanyan et al. 2005](#), [Ashcroft et al. 2012](#)). Elevation, topography and slope are some of the main landscape features that influence the drivers of climate heterogeneity at the regional scale ([Dobrowski 2011](#)). These topoclimatic effects (i.e., spatial estimates of climate as it varies with topographic position in the landscape) result mainly from differences in slope orientation and angle towards solar radiation and wind ([Bennie et al. 2008](#)). Therefore, solar radiation is commonly used as a predictor variable in modelling temperature in complex terrain at the regional scale (Fig. 11).

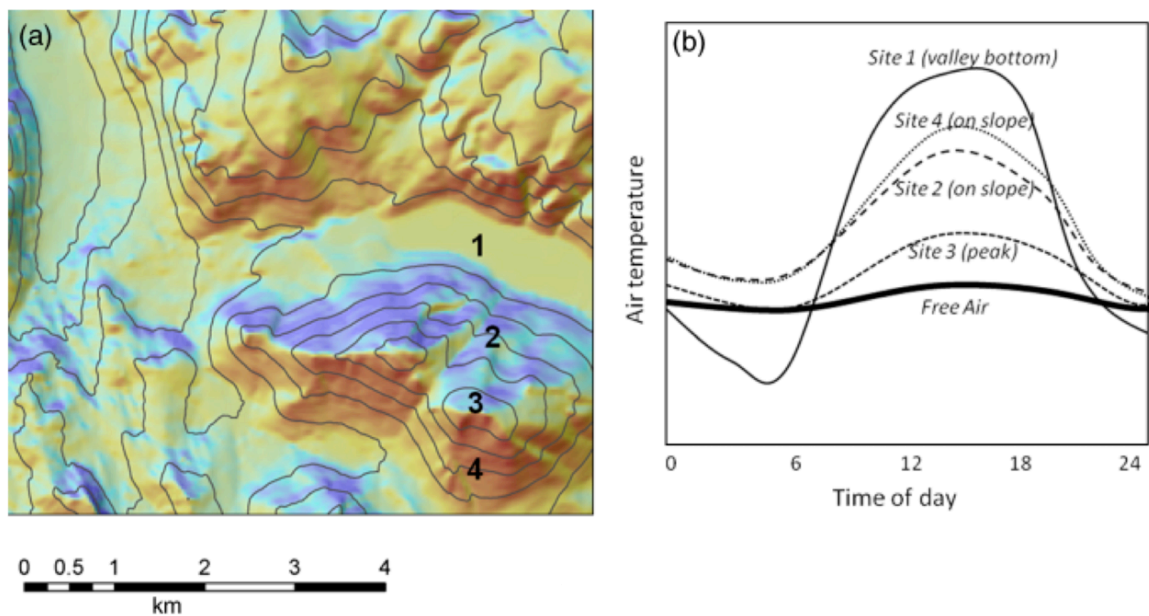


Figure 11: Representation of the influence of landscape position on air diurnal temperature variation. (a) Shaded relief map shows areas of high (warm colours) and low (cool colours) solar insolation with the locations of four temperature-monitored sites. (b) Pattern of diurnal temperature patterns for sites 1 to 4. From [Dobrowski \(2011\)](#).

At the local scale: The local scale is an intermediate between the regional scale (that might extent from one to hundreds of square kilometres) and the organism scale (basically the environment of an organism, i.e., from few millimetres to meters). Thermal heterogeneity at the local scale could be defined as the environment experienced by a study organism along its life cycle. Therefore the local scale mainly depends on the body size of the focal organism and its capacities to move within the environment: a spatial scale of 1 m² may be long for a 1-mg ant but short for a 1-kg lizard (Sears *et al.* 2011, Sears & Angilletta 2015). However, assessing microclimates at the local scale is not straightforward because of the variety of abiotic and biotic elements making up this scale: topography and macroclimate interactions but also micro-topography of the ground surface, vegetation and plant canopy structure, nearby organism interactions, areas of water, rocks or other local objects (Woods *et al.* 2016). All elements interact with each other and with macroscale conditions thereby leading to a fine-scale mosaic of climate (Fig. 12).

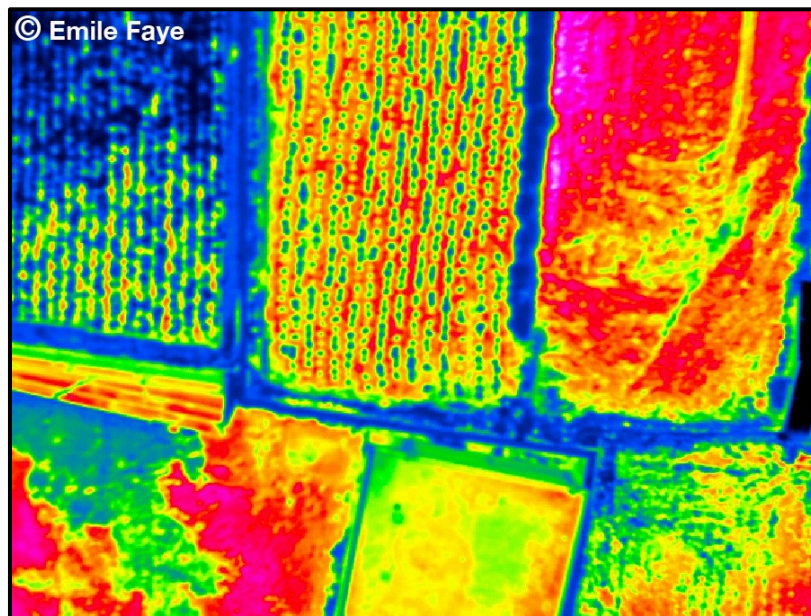


Figure 12: Thermal infrared image of an agricultural landscape pinpointing the thermal heterogeneity available for an ectothermic pest at the local scale. The extent of the image is 32 x 24 metres and temperatures range from 12 to 43°C. Blue colours show cold temperatures and red colours show warm temperatures. Photo credits: Emile Faye.

Among all the spatial scales of microclimates, the local scale has been the least studied (e.g., [Sears *et al.* 2011](#), [Sears & Angilletta 2015](#), [Woods *et al.* 2016](#)) mainly because of methodological limitations in climate heterogeneity quantification.

At the organism scale: Organism scale corresponds to the spatially restricted extent in which an organism occurs at a defined time. This scale is one of the most studied by biophysical researchers who seek understanding organism-environment interactions throughout thermal budgets ([Vogel 1970](#), [Gates 1980](#), [Kingsolver 1985](#), [Jones 1992](#), [Kingsolver 2009](#), [Saudreau *et al.* 2009](#)). For instance, [Pincebourde & Casas \(2006a,b\)](#) studied the modifications of the thermal environment inside a mine of an apple tree leaf by the leaf-mining insect *Phyllonorycter blancardella* (Lepidoptera: Gracillariidae).

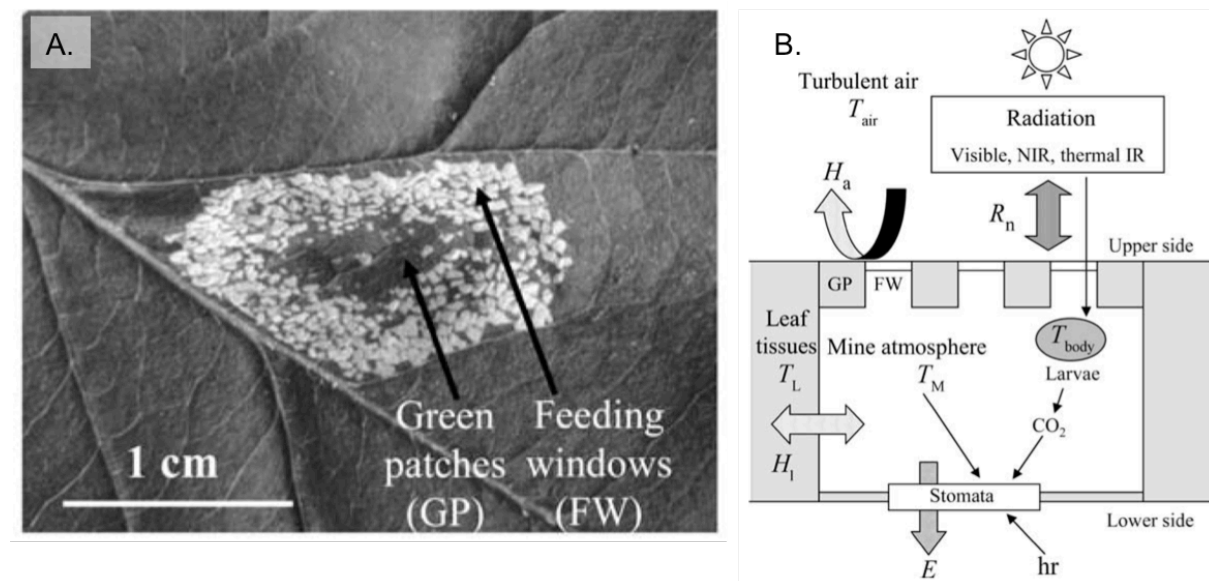


Figure 13: Microhabitat of the leaf-mining moth *Phyllonorycter blancardella*. A. The larva develops inside the apple leaf tissues, within a mine (representing a surface of 1 cm²). The feeding activity of a larva results in the formation of feeding windows (FW). Green patches (GP) correspond to intact chlorophyll-containing leaf tissues remaining in the mine. B. Schematic cross section of a mine and determinants of heat transfer. Adapted from [Pincebourde & Casas \(2006a\)](#).

Plant tissue modifications by the miner alter leaf solar radiations absorbance and gas exchange (Fig. 13), which results in an increase of 5°C in temperature inside the mined leaf compared to intact leaves (Pincebourde & Casas 2006a). These organism-modified microclimates influence in turn the performances of leaf-dwelling insects (Pincebourde & Casas 2006b). Studying the microclimates at such fine scales is relatively accessible due to the variety of technologies available (e.g., thermometer, thermocouple, distributed temperature optic fibre, automatized greenhouse or climate chamber) and because most of the experiments can be performed under controlled conditions.

e. Scale mismatch and methods to study ecologically-relevant microclimates

Scale gap in thermal ecology: Potter *et al.* (2013) recently highlighted the spatial mismatch between the size of organisms and the resolution at which climate data are collected and modelled (Fig. 14). The majority of living organisms on earth are smaller than a few centimetres (May 1988) whereas the spatial resolution of climate data used in species distribution models is often of one to many kilometres. In their meta-analysis, Potter *et al.* (2013) showed that the resolutions of the climate grids used in species distribution models are, on average, 10,000-fold larger than studied animals, and 1,000-fold larger than studied plants. Interestingly, the mismatch between insect body length and the climatic grid length is one of the largest of all. Strikingly, their study also revealed that two climatic database were predominantly used in species distribution models (the two peaks in the grid-size density plots in Fig. 14): the grid scales of 1 and 10 km² which correspond to the resolution of one of the most widely used and readily available climate database, the WorldClim (Hijmans *et al.* 2005).

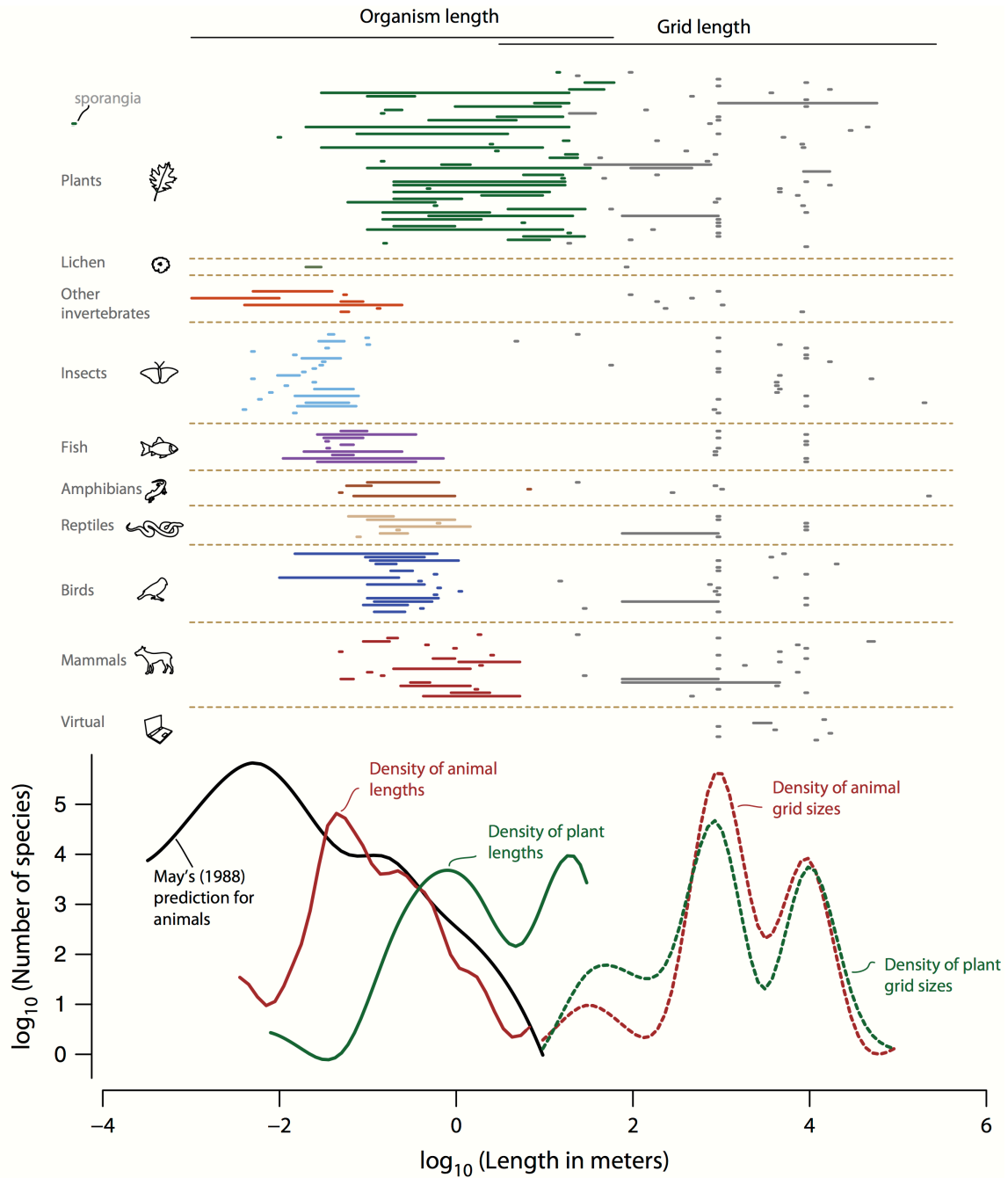


Figure 14: Lengths of grid cells from published species distribution models (SDMs) compared to the lengths of the animals and plants they studied. Coloured dots indicate the body size of a species from one study; coloured horizontal lines indicate a range of body sizes if the study used multiple species. The corresponding grey dots and lines indicate the grid size (or range of sizes) of climate variables used in that study. The black density plot is a spline fitted to data from May's 1988 paper [(May, 1988), Figure 6], which represents his estimate of the body size distribution of all terrestrial animals. Density plots of the rest of the terrestrial data are shown at the bottom for comparison. Adapted from Potter *et al.* (2013).

[Woods *et al.* \(2016\)](#) have proposed a conceptual framework to link macro- and microscale (Fig. 15). Macroclimates interact with living and non-living objects in the environment to produce a complex mosaic of microclimates. Organisms, such as small mobile ectothermic pests, that experience such fine-scale mosaics, may actively thermoregulate by sampling the local microclimatic heterogeneity of their environment. Finally, the physiology of ectotherms transduces thermal experiences into performances (as described above), which in turn influences demographic parameters (i.e., rates of growth and survival).

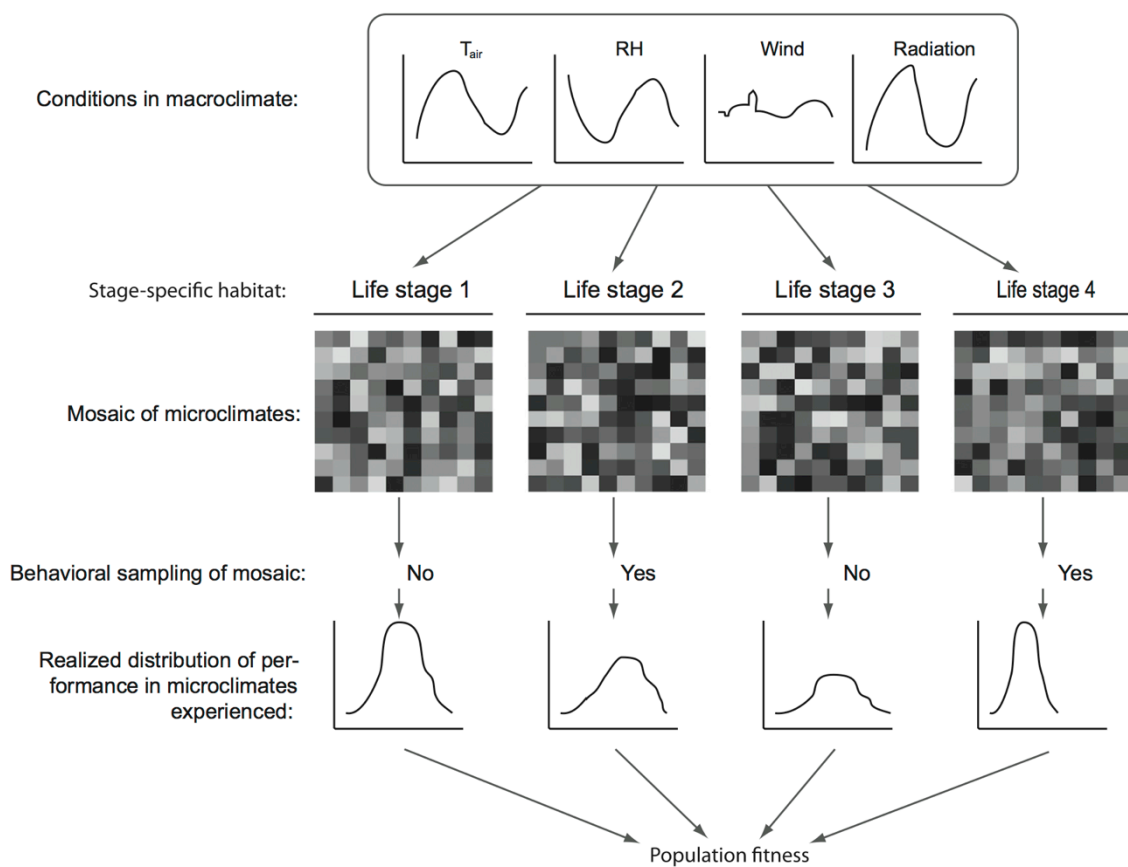


Figure 15: Diagram of the connections between macroclimate, microclimates and the performances of a population of ectotherms. Adapted from [Woods *et al.* \(2016\)](#).

Current methods for bridging the scale gap: modelling and empirical monitoring. Assessing the spatiotemporal thermal heterogeneities that occur at relevant scale for the study organism is a major issue for everyone who want to accurately estimate organism

occurrences and distribution. Consequently, several methodologies have been developed to study microclimates and their effects on organisms and species. Stochastic weather generators (e.g., the Worldclim) produce synthetic time series of weather data for a location, based on the statistical characteristics of observed weather at that location ([Furrer & Katz 2007](#)). Therefore, combined with operative temperatures recorded in the field, stochastic weather generators allow modelling microclimates. This method has proven a powerful interpolative tool for defining and projecting climatic envelopes ([Guisan & Thuiller 2005](#), [Elith & Leathwick 2009](#)). However, such correlative microclimatic models are not well suited for obtaining a detailed understanding of the climatic constraints limiting species distributions, since processes are only captured implicitly ([Dormann *et al.* 2012](#)). Moreover, statistical correlative models may not be extrapolated over other extents because they can only be applied to the conditions under which they were fitted.

Another way to accurately model the microclimatic conditions experienced by an organism is using mechanistic models ([Kearney & Porter 2009](#), [Buckley *et al.* 2010](#)). Complex mathematical functions based on the fine analyses of the biophysical processes between the structural properties of the environment and the body allow assessing and estimating both microclimates and body temperatures ([Gates 1980](#)). These mechanistic models, known as thermal budgets or energy budgets, use fundamental knowledge of the interactions between process variables to define the model structure. Therefore, they do not require much data for model development and validation. This kind of models can be interpolated over large landscapes (when inputs data are available) to assess spatial and temporal variations of microclimatic conditions at wider scales. Recently, [Kearney *et al.* \(2014\)](#) developed the *microclim* model that quantifies key microclimatic parameters at macro-scales (i.e., continental) for all terrestrial landmasses, with a relatively fine spatial (15 km²) and temporal resolution (hours). However, the model requires a large amount of specific

values as inputs such as air temperature, wind speed, relative humidity and cloud cover, soil properties (such as conductivity, specific heat, density, solar reflectivity, emissivity, surface wetness of the soils), as well as the elevation, slope and aspect of the surface. Mechanistic predictions of local microclimates, hourly, across continental scales, create new opportunities for understanding how organisms respond to their environments ([Hannah *et al.* 2014](#)).

Global mechanistic models of microclimates such as the one developed by [Kearney *et al.* \(2014\)](#) allows providing key parameters of microclimates, but the spatial resolution is still far from the empirical interpolation-based models (e.g., 15 square kilometres for [Kearney *et al.* \(2014\)](#), compared to 1 square kilometre for [Hijmans *et al.* 2005](#)), and even further from the resolution at which organisms experience their environment. Despite their sophistication these models still fail to accurately portray environments in terms of the magnitude of climatic variables and their heterogeneity through space and time, which are important for the performance of individuals.

Microclimates are driven by interactions between complex biophysical processes, the structural composition of the environment and the macroclimate features. Consequently, the heterogeneity of microclimates creates complex thermal mosaics that change across time and space. Temperatures gathered from weather stations are unlikely to represent biologically-relevant operative temperatures. Quantifying these spatiotemporal heterogeneities of temperature can be made through statistical and mechanistic models or empirically at various spatial scales from large (global and regional) to fine (local and organism) scales with diverse resolutions. Since spatial heterogeneity in the thermal environment as perceived by a given organism is likely to have important consequences on its occurrence and performances, one might conclude that quantifying the thermal heterogeneity of microclimates constitutes a major challenge for researchers interested in predicting responses of organism to their environment at a relevant scale. The same concern arises when considering agricultural landscape and crop pests. Indeed, by the variety of plant phenologies and structures, agricultural landscapes provide ectothermic inhabitants, including crop pests, with a massive but still poorly studied, heterogeneity of microclimates.

3. Microclimates in agrosystems: from agro-climatology to thermal agroscales

a. History of microclimate research in agriculture

Climates and microclimates have long been studied within an agricultural perspective (see yellow bars in Fig. 7) and the existence of specific journals on these thematic highlights the strong interests of agronomists for this issue (e.g., *Journal of Agricultural Meteorology* first published in 1943, *Journal of Applied Meteorology and Climatology* in 1962, and *Agricultural and Forest Meteorology* in 1964). Agroclimatology aims at studying the interaction between local climate features (e.g., temperature, humidity, wind, radiations) and agricultural variables (e.g., growth rate, yield, leaf development). The main objective is to use climatological information to improve farming practices and increase agricultural productivity in both quantity and in quality. Previous studies that related the physical components of climate with crop production (Leopold 1964, Monteith & Elston 1971, Chang 1974, Jones 1992) showed that crop growth and yield were sensitive to temperature in various ways (e.g., Watson & Baptiste (1938) on plant weight, Cooper (1964) and Peacock (1975) on leaf development, Langridge & McWilliam (1967) on photosynthetic rate). However, most crop microclimate studies before 1970, such as Broadbent (1950) for potatoes, Waterhouse (1955) for grasslands, Stoskopf & Klinck (1966) for oats, Rosenberg (1966) for sugar beets and Colville (1968) for corns, were performed on plants under controlled environments rather than in the field.

Later, various studies focused on the interactions between microclimates and crops *in situ* (i.e., within the field in real conditions, Baldocchi *et al.* 1983). Colville (1968), Stigter & Baldy (1995) and Sharaiha & Battikhi (2002) showed that the spatial arrangements of the plants within a field (i.e., plant spacing, intercropping rows of various species) strongly affected the microclimates experienced by plants and may lead to increases in crop yields, compared to single crop farming (i.e., monoculture). Indeed, relevant spatial arrangements in

crop fields increased light interception (enhancing the photosynthesis process) and decreased the evapotranspiration rate. [Batugal *et al.* \(1990\)](#) showed that intercropping potatoes with corns provided partial shade to the potato plants during strong radiation events, thereby reducing air and ground temperatures (temperature reducing systems), and improving tuber production. [Sharaiha & Kluson \(1994\)](#) reported that both air and soil temperatures required for fava bean nitrogen fixation were significantly more optimal when fava bean was planted in association with peas or lettuce as compared with fava bean monocultures. [Smart \(1985\)](#) showed that plant canopy structure enhanced grapevine yield and quality by modifying radiation interception rate and moisture. Moreover, microclimate beneath tree canopy in agroforestry systems protected crop plants (such as coffee) against extreme climatic events by providing shades and lower air temperatures than the above tree canopy air temperatures ([Hardwick *et al.* 2014](#)). [Tompkins *et al.* \(1993\)](#) and [Suh *et al.* \(2002\)](#) showed how agronomic practices and canopy closure influenced the infestation of crop diseases and pests by modifying the components of the in-field microclimates (*Septoria sp* in wheat field and *Trichogramma exiguum* in cotton field, respectively). Also, [Willmer *et al.* \(2008\)](#) reported how intra-field microclimates constrained the distribution patterns of raspberry beetle (*Byturus tomentosus*). Until recently, most studies focused on multiple point measurements of microclimates rather than continuous assessments of microclimates that occur at larger scales. Therefore, and unfortunately, these descriptors carried limited information about the spatial heterogeneity of temperatures in agricultural landscapes.

b. Contributions of precision agriculture

The recent and topical development of precision agriculture and remote sensing domains has brought new insights for the assessment of the thermal heterogeneity across agricultural landscapes. In particular, the development of thermal infrared cameras has opened new opportunities to quantify the spatial heterogeneity of microclimates in agrosystems (Inagaki *et al.* 2008, Meron *et al.* 2010, Agam *et al.* 2014, Bellvert *et al.* 2014, Petach *et al.* 2014). Infrared thermography is an imaging method that records infrared waves emitted by an object in the electromagnetic spectrum within the range of light – from 7.5 to 14 μm (Fig. 16). Radiation readings are converted into surface temperature by the thermal infrared camera taking into account the ambient conditions and emissivity (Rubio *et al.* 1997).

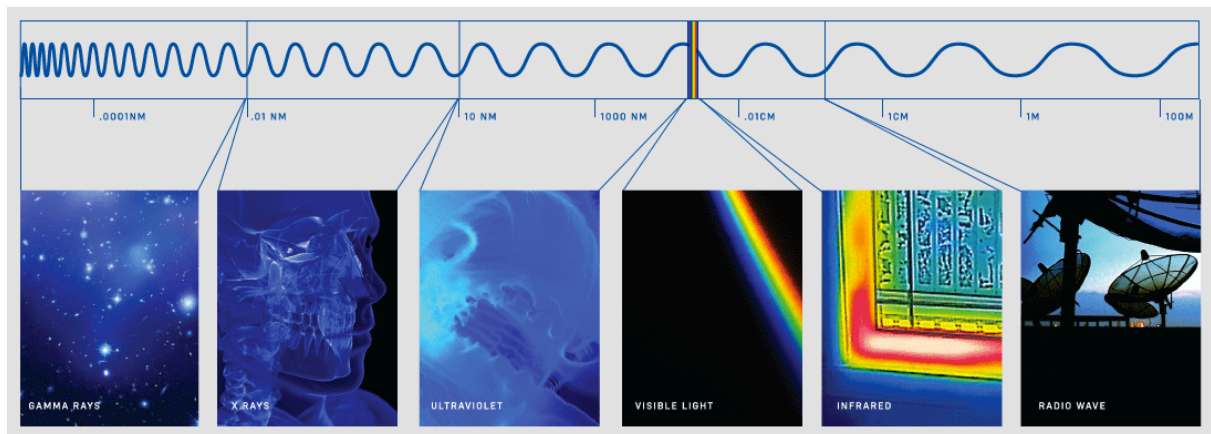


Figure 16: Schematic representation of the electromagnetic spectrum. The electromagnetic spectrum extends from below the low frequencies used for modern radio communication to gamma radiation at the short-wavelength (high-frequency) end, thereby covering wavelengths from thousands of meters down to a fraction of the size of an atom. Thermal infrared correspond to from 750 to 1400 nm.

Thermal infrared images allow the study of surface temperature patterns over a large spatial extent and are widely applied to precision agriculture issues. Thermal remote sensing is the capture of thermal infrared images from aircraft-based or satellite-based sensors. These images provide spatially distributed estimations of land surface temperatures over large-scale

areas ([Anderson *et al.* 2007](#), [Kuenzer & Dech 2013](#)). Surface temperatures are measured by satellite sensors such as Landsat, AVHRR, MODIS and ASTER ([Kalma *et al.* 2008](#)). Once the atmospheric component corrections performed (e.g., particles and water vapour, [Quattrochi & Luval 1999](#), [Glenn *et al.* 2007](#)), thermal remote sensing provides accurate values of surface temperatures (i.e., an accuracy of less than $\pm 1^{\circ}\text{C}$, see [Hook & Prata \(2001\)](#), [Jacob *et al.* \(2004\)](#) and [Coll *et al.* \(2005\)](#) for details). Thermal remote sensing in precision agriculture yields continuous measurements of surface thermal heterogeneity of agricultural landscapes ([Kuenzer & Dech 2013](#)) and allows quantifying crop indices based on temperatures ([Moran *et al.* 1997](#), [Glenn *et al.* 2007](#), [Kalma *et al.* 2008](#)). For instance, evapotranspiration and soil moisture or Crop Water Stress Index (CWSI) can be spatially estimated through remotely sensed crop surface temperatures ([Soer 1980](#), [Moran *et al.* 1994](#), [Berni *et al.* 2009](#), [Meron *et al.* 2010](#)).

Even more recently, thermal remote sensors placed on unmanned aerial vehicles (UAVs) provide low-cost approaches to meet the critical requirements of fine spatial and temporal resolutions over agricultural landscapes (Plate 1). Autonomously operated, flying low and slow, UAVs offer scientists new opportunities for scale-appropriate measurements of the thermal landscapes. Few recent studies illustrated the use of this novel technology for resolving agronomical issues: crop water stress index is the first coming output from high-resolution thermal infrared images as it allows to map the spatial variability in water status across agricultural landscapes at very fine spatial resolutions (Fig. 17, [Zarco-Tejada *et al.* 2012](#), [Gonzalez-Dugo *et al.* 2013](#), [Bellvert *et al.* 2014](#)). UAV's thermal imaging has also been used as an indicator of field's infestation by diseases ([Calderón *et al.* 2014](#)). The spatial resolution of the thermal infrared maps obtained in those studies were at best of 20, 30, 40 and 49 cm per pixel on a spatial extent of 0.2, 11, 1.2, 42 ha for [Calderón *et al.* \(2014\)](#),

Bellvert *et al.* (2014), Zarco-Tejada *et al.* (2012) and Gonzalez-Dugo *et al.* (2013), respectively.

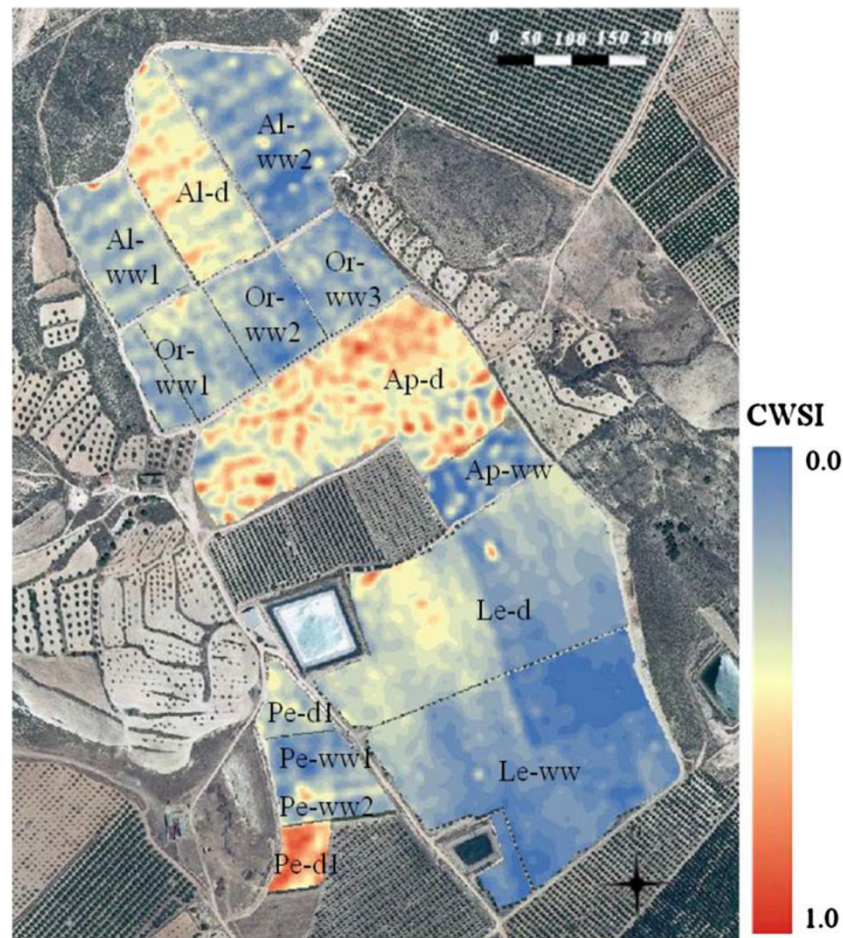


Figure 17: Map of the Crop Water Stress Index (CWSI) of an orchard landscape in southeastern Spain. CWSI was built from thermal infrared images yielded from a UAV platform. From [Gonzalez-Dugo *et al.* \(2013\)](#).

c. Pest performances in thermal agrosapes

Being ectotherms, pests respond to the rules of physiological and behavioural thermoregulation and temperature dependency of their performances (development, fecundity and survival) as presented in paragraph I-1. Maximal pest growth occurs under optimal temperature ranges, but when a pest is exposed to extreme low or high temperatures, development rates are reduced, reproduction fails, and if exposed sufficiently long enough, death occurs (see paragraph I-1 and Fig. 18). That is why precise information on pests'

thermal responses is crucial for understanding their occurrence and dynamics (Travis *et al.* 2011). However, pests' responses to temperature may differ if exposed to constant or fluctuating temperature regimes (Gilbert *et al.* 2004, Davis *et al.* 2006, Wu *et al.* 2014, Vázquez *et al.* 2015). Thus, pest population dynamics in highly variable environmental conditions may differ from those in more constant ones. This may be especially the case in environments, like complex agricultural landscapes of the Tropical Andes, where temperatures tend to vary within a 30°C range within a day (Dangles *et al.* 2008) and where the spatial composition of the landscape favours the spatial heterogeneity of temperatures. Under fluctuating (in time) temperature regimes, Davis *et al.* (2006) found that aphid *Myzus persicae* (Sulzer) had higher optimal and upper developmental thresholds (Fig. 18).

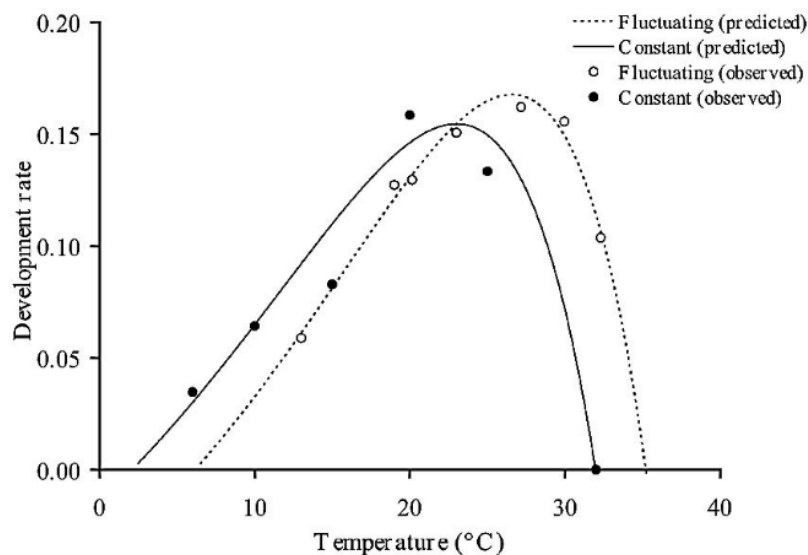


Figure 18: Constant and fluctuating temperature dependent development rate observed for the peach tree pest *Myzus persicae* (Sulzer). Adapted from Davis *et al.* (2006).

The relationship between experienced temperatures and the developmental rate of pests is crucial for understanding a variety of biological processes that occur in agricultural landscapes (e.g., pest infestation in the field). To accurately estimate this relationship, the thermal component of pests' ecological niches is of major interest to understand both patterns and processes of their occurrence and distribution dynamics in agricultural landscapes.

Microclimate has long been studied throughout an agricultural perspective. Many works have depicted the relationship between one-location microclimate and various crop factors (e.g., yield, growth). Then, the apparition of thermal remote sensing has permitted to study the spatiotemporal thermal heterogeneity within agricultural landscapes. Very recently, thermal sensor on-board unmanned aerial vehicles brought new insights for the study of microclimates at spatiotemporal scales relevant for the study of crop related phenomena. These new technical innovations would permit agronomists to bridge the gap between the body lengths of the studied organism (e.g., plants or insects) and the spatiotemporal resolution of the climatic data of their studies. Therefore, quantifying the heterogeneity of the thermal environment experienced by ectothermic pests becomes accessible and repeatable at the extent of agricultural landscapes (i.e., the local scale) and offer news approaches for studying pest issues in thermal agroscares. Because crop pests are ectothermic organisms that respond to the rules of temperature dependency for their performances, the thermal environment in which they evolved plays a key role in shaping population dynamics.

II. Thesis justification

Based on the literature review presented above, we identified three key remaining challenges to be overcome for improving our general understanding of microclimate patterns. These challenges are particularly relevant in agrosystems but could also be of interest to other types of ecosystems.

1. Microclimates and climate change

Climate change affects ecological and evolutionary responses of living organisms represents across multiple biomes and organizational scales. Indeed, climate warming will modify ecosystem structure and functioning, lead to the extinction of the populations of some species (Parmesan 2006) while increasing levels and distribution ranges of others, such as crop pests and disease vectors (Chakraborty & Newton 2011, Luck *et al.* 2011). As it has been widely projected that global warming would yield an increase in climate variability (IPCC 2014) leading to novel global climatic landscapes, efforts have started to focus on predicting how species, and their distributions, will respond to future climates (Bale *et al.* 2002, Parmesan 2006, Buckley *et al.* 2013, Paaajmans *et al.* 2013, Hannah *et al.* 2014, Kingsolver & Buckley 2015). To assess species' response to climate change, mapped environmental data coarsely resolved in time and space are commonly used. However, coarsely resolved temperature data are typically inaccurate for predicting temperatures in microhabitats used by an organism (see above paragraph I.2.d.ii). Consequently, climatic niches and species distribution models based on the coarse-scale climatic data for forecasting the species' response to climate change are likely to misestimate of species biogeographical shifts (Storlie *et al.* 2014). Moreover, microclimates have recently been studied for their capacities to buffer organism's exposure to climate change (Scherrer & Körner 2011, De Frenne *et al.* 2013, Hannah *et al.* 2014, Scheffers *et al.* 2014a, Woods *et al.* 2014, Maclean *et al.* 2015) and even to hamper evolutionary responses (i.e., adaption and acclimation) in the face of climate change (Buckley

et al. 2015, Kingsolver & Buckley 2015). For instance, Lenoir *et al.* (2013) suggested that fine-grained thermal variability over tens of metres (i.e., spatial microclimate) exceeds much of the climate warming expected for the coming decades. Such spatial variability in temperature provides local buffering to mitigate future climate-change impacts within one square kilometre only. Consequently, accurately predicting how organisms will respond to climate change requires deepening our knowledge about the thermal heterogeneities in space and time that occur in the environment experienced by an organism, thereby radically reducing the mismatch between the spatial scales of climatic data and the body size of the organism studied.

2. Methods for characterizing thermal heterogeneity at relevant spatial scales and resolutions in agricultural landscapes

One of the main challenges in microclimatic studies concerns climatic data collection (Potter *et al.* 2013). Sampling microclimates perceived by a given species at relevant scales and resolutions is of critical importance for future research on microclimate issues. However, predicting temperature heterogeneity at fine resolutions over large areas is not straightforward using existing methods such as thermal remote sensing. Indeed, a fundamental requirement for providing useful remote sensing products is the capacity to combine both high spatial resolution (the closest possible to the organism body size) and temporal resolution adapted for the target organism or crop (Moran *et al.* 1997, Kuenzer & Dech 2013). Current thermal imaging satellite-based products have limited application in crop management due to the low spatial resolutions provided: microbolometer sensors used in remote sensing commonly offer c.a. 100 m pixel size thermal images (ASTER and Landsat images, Kalma *et al.* 2008, Berni *et al.* 2009, Kuenzer & Dech 2013), a spatial resolution that is impractical for site-specific agricultural applications, thereby limiting the usefulness of remote sensing products for fine-scale thermal agricultural landscape studies. Alternatives based on airborne sensors can

deliver higher spatial resolutions and are more flexible in terms of repeatability. Airborne remote sensing has demonstrated capabilities for vegetation climatic condition monitoring due to high spatial thermal resolutions used, ranging between 1 and 2 metres per pixel, enabling for instance the detection of water-stressed trees in orchards for site-specific field management (Berni *et al.* 2009). However, the high operating costs and long turnaround times due to high volume of data acquired have so far intensively limited the use of airborne and satellite data for research activities. Additionally, the spatial resolution provided by these technological means is still far from the fine-scale spatial resolution needed over large spatial areas such as agricultural landscapes.

3. Microclimates for understanding pest occurrence and distribution in agricultural landscapes

Despite centuries of effort, we are still far from a complete integrate pest management of insect pests (Chakraborty & Newton 2011, Bebber *et al.* 2014, Sakschewski *et al.* 2014). Global population is increasing, and projections suggest that a system that currently keeps a billion people hungry will have to feed an extra three billion within the next 50 years (Birch *et al.* 2011). If future world demand is to be met, food production must virtually double by the year 2050 (Tilman *et al.* 2011). One potential approach of meeting this demand is the control of pests, which globally consume (pre- and post-harvest) the amount of food sufficient to feed more than 1 billion people (Birch *et al.* 2011, Oerke 2006). In the context of global warming and increasing climatic variability, a major uncertainty that hampers effective pest management is that related to the thermal characteristics of agricultural landscapes, which are known to have profound effects on insect pest dynamics (e.g., Dangles *et al.* 2008). Therefore, comprehending the impacts of microclimates available in agricultural landscapes on pest performances and small-scale distribution is of prime importance to further integrate those relationships in performance and species distribution models.

The thesis was developed in the context of thermal agricultural landscapes and pest temperature-dependent performances that we presented above. The microclimatic challenges exposed here acted as drivers of this work, and can be retrieved throughout the entire thesis. For improving our general understanding of microclimate patterns and their consequences on ectothermic organisms, the agrosystems of the tropical Andes provide a perfect and relevant study site in regards to these microclimatic challenges, for various reasons that are explained in the following part. In the sections that follow, we firstly present the study region and study site where our experiments were set up, and then expose the main objectives of this thesis.

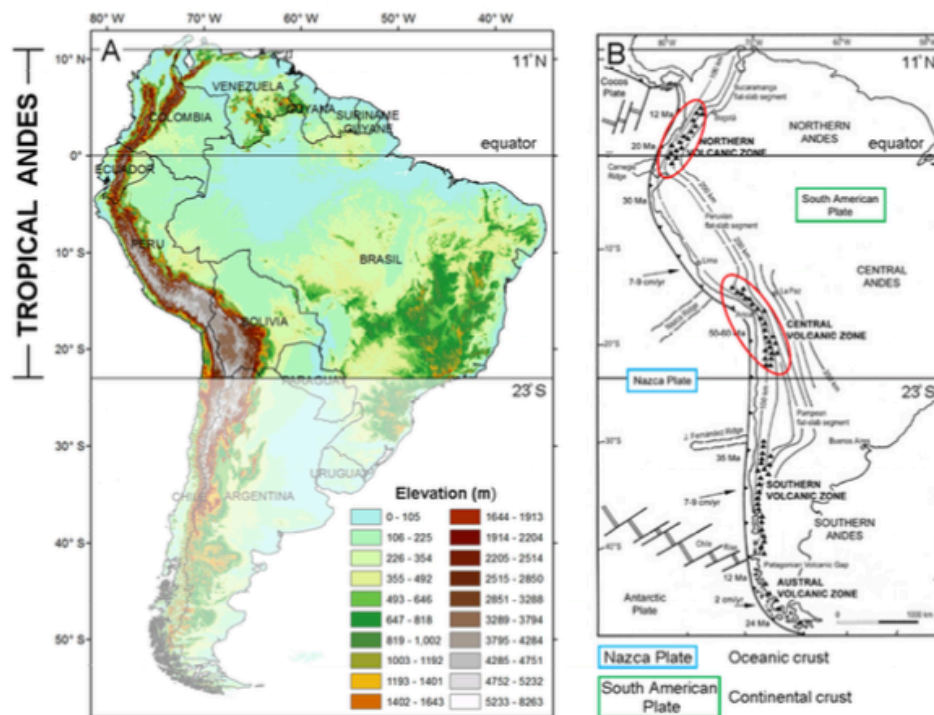


Figure 19: A. Elevation map of South America. The tropical Andes extend between 11°N to 23°S from western Venezuela to north Chile, and Argentina, encompassing Colombia, Ecuador, Peru and Bolivia. A 30 arc-second digital elevation model was used to build this map within ArcGis (10.2). B. Geological map of South America. Tropical Andes include two volcanic zones: the northern and central one (red circles). From [Cauvy-Fraunié \(2014\)](#).

III. Study site

1. Tropical Andes

a. Geography and geology

The tropical Andes are located in South America and extend over 1.5 million km² (area over 1000 m a.s.l.) from 11°N to 23°S, i.e. from west Venezuela to north Chile and Argentina, encompassing Colombia, Ecuador, Peru and Bolivia (Fig. 19; [Tovar *et al.* 2013](#)). It is the longest and widest mountainous region in the tropics worldwide, occupying an elevation range from 1000 m up to 6768 m a.s.l. (Mt. Huascarán in Peru). The Tropical Andes are primarily composed by parallel high mountain chains (two in Venezuela, Ecuador, South Peru and Bolivia, and three in Colombia) with a large number of snow-capped peaks (96 summits), and a vast mountain plain, the Peruvian-Bolivian Altiplano ([Josse *et al.* 2011](#)).

The Andes are the result of the Cenozoic (i.e., ~ 65.5 million years ago) tectonic shortening of the South American plate margin caused by the subduction of oceanic crust, the Nazca plate (Fig. 19; [Sobolev & Babeyko 2005](#), [Capitanio *et al.* 2011](#)). While the compression of the western rim of the South American plate is the primary cause of the Andes rise, volcanic activity (as a result of subduction of the Nazca plate), is also a significant phenomenon in the building of the Andes ([Stern 2004](#)). Indeed, the Andes are the world's second highest orogenic belt and include at least 200 active quaternary volcanoes, occurring in four separate segments referred to as the Northern, Central, Southern, and Austral Volcanic Zones (Fig. 19).

b. Climate settings

Unlike temperate zones, seasonal variations in temperature are small in the tropics (Fig. 20-A.) and seasonal markers such as day length variation are absent. Seasonality, as defined by [Bonebrake & Deutsch \(2012\)](#), is the intra-annual standard deviation of mean monthly temperature. These authors consider areas with low (or absent) seasonality as any area with a measure of seasonality below 4°K, which roughly corresponds to tropical and subtropical global isotherms ([Legates & Willmott 1990](#)). Seasonality in temperature is strongly dependent upon latitude with the most seasonal areas occurring at high northern latitudes (Fig. 20-A.). In the study area, seasonality measured across a 4 year sampling of air temperature was evaluated at 1°K (see appendix 6 of Chapter I). Even though the tropical Andes lack a clear seasonality in temperature, this region does present temporal variability in precipitation: precipitation patterns mainly result from a combination of events such as *El Niño Southern Oscillation* event which causes annual or sometimes decadal oscillations leading to increases of rain or draught depending on the location ([Poveda et al. 2011](#)) and the easterly flow of moisture from the Amazon Basin ([Vizy & Cook 2007](#), [Poveda et al. 2011](#)). Roughly, precipitation patterns in the tropical Andes are quite complex and difficult to predict and contribute to the high heterogeneity of the landscapes.

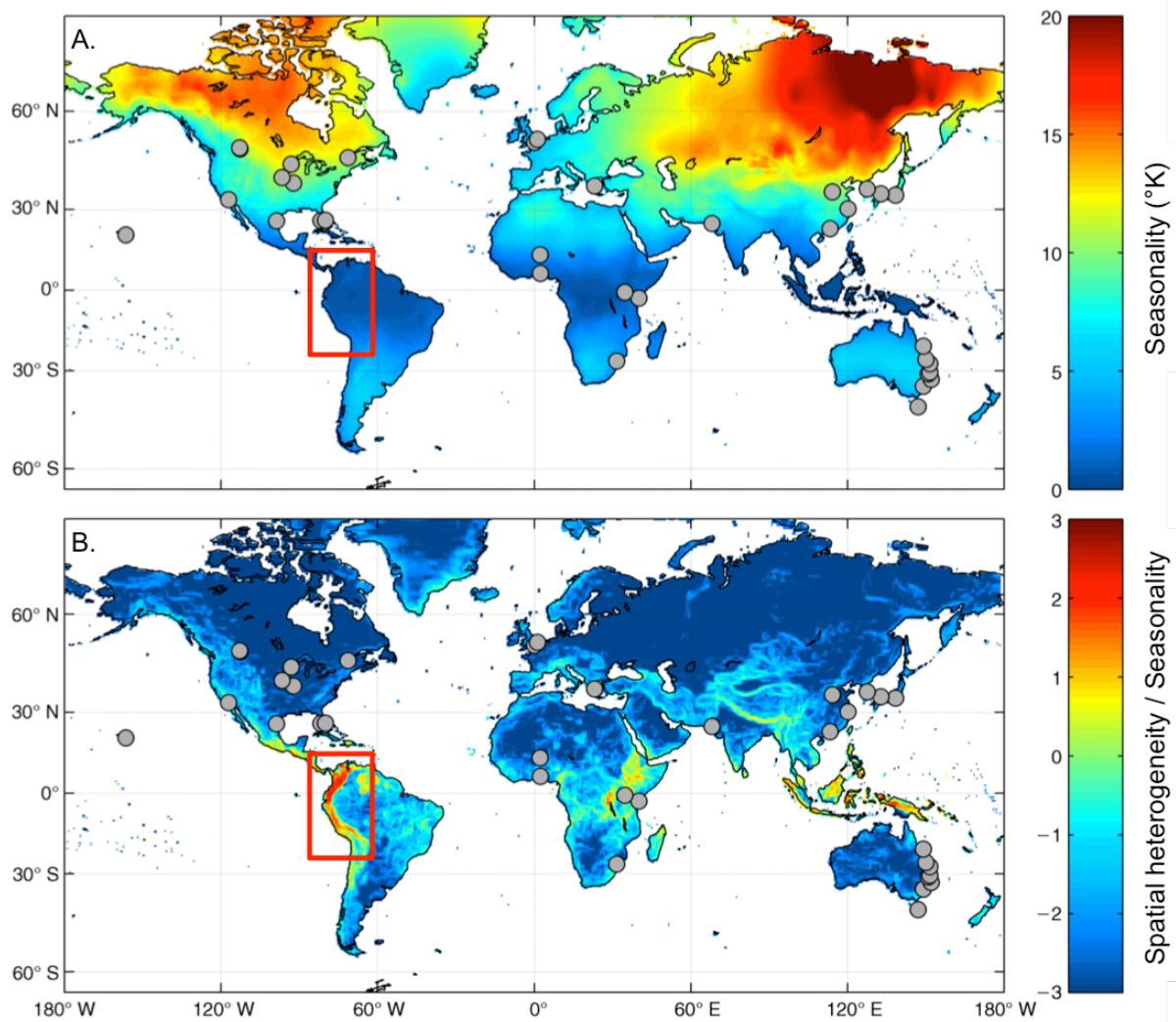


Figure 20: A. Seasonality (standard deviation, in °K at 0.58° resolution) within a year, represented globally. B. The log of the non-dimensional ratio of spatial heterogeneity in the thermal environment (standard deviation, in °K at 0.58° resolution), to seasonality plotted globally. Blue regions represent locations where seasonality exceeds spatial heterogeneity and red locations represent regions where spatial heterogeneity exceeds seasonality. Red squares delimit the tropical Andes. Adapted from [Bonebrake & Deutsch \(2012\)](#).

Although displaying a lack of seasonality, the tropical Andes are characterized by strong spatial gradients in climatic variables mainly associated with changes in elevation ([Young 2009](#), [Josse et al. 2011](#)). Spatial heterogeneity at the regional scale in tropical Andean landscapes is indeed remarkable (mountaintops can exceed 6000 m.a.s.l. with adjacent valley bottoms reaching 3000-4000 m below) and is probably the most important feature that shapes

climates and natural ecosystems (McCain 2007, Young 2009). Consequently, by dividing the regional scale spatial heterogeneity of temperature with the measure of seasonality, Bonebrake & Deutsch (2012) showed that the spatial heterogeneity in temperature strongly exceeds seasonality in the tropical Andes, illustrating the relevance of this region for studying spatial-temperature-related patterns (Fig. 20-B.). Moreover, due to the high elevation of this region and its tropical location, diurnal temperatures vary more within days (up to 30°K variation) than within months and years (less than 1°K): the pattern of hot days and cold nights overshadows temperature variations through the year (Dangles *et al.* 2008).

c. Implications for agriculture

The specific spatiotemporal climatic patterns occurring in the tropical Andes have led to particular land uses (Otero & Onaindia 2008). Indeed, unlike high altitude landscapes in temperate regions, which are commonly regarded as relatively pristine places, tropical mountains have a long history of human occupation and impact (Young 2009). Agriculture is one of the first consequences of this anthropogenic implantation. Agricultural systems are organised in agroecological belts along the gradients of elevation and climate (Becker *et al.* 2007), ranging from low elevations up to 4500 m a.s.l. Numerous crops are cultivated in these belts of the tropical Andes (Millones 1982, Knapp 1991): in the lowlands (from 1000 to 2000 m a.s.l.) the major crops are banana (*Musa acuminata* L.), coffee (*Coffea arabica* L.), cacao (*Theobroma cacao* L.), rice (*Oryza sativa* L.), sugar cane (*Saccharum angustifolium* L.), african palm, tomato (*Solanum lycopersicum* L.) and tropical fruits such as mango (*Mangifera indica* L.), avocado (*Persea americana* L.), naranjilla (*Solanum quitoense* L.), pineapple (*Ananas comosus* L.), coconut (*Cocos nucifera* L.), etc. The major crops in the highlands (from 2000 to 4500 m a.s.l.) are potato (*Solanum tuberosum* L.), corn (*Zea mays* L.), broad bean (*Vicia faba* L.), barley (*Hordeum vulgare* L.), wheat (*Triticum aestivum* L.), pea (*Pisum*

sativum L.), soybean (*Glycine max* L.), quinoa (*Chenopodium quinoa* L.), lupin (*Lupinus mutabilis* L.), alfalfa (*Medicago sativa* L.) and cultivated grasses for farm animal breeding.

Due to the lack of seasonality in the region, crops can be planted, grown and harvested all year round (as illustrated by the steady CO₂ assimilation by plants throughout the year in Ecuador, Fig. 21), thereby creating agricultural landscapes made up of a wide variety of crops at different phenological stages (stages of maturation). This is a critical advantage for studying microclimates in agricultural landscapes because at the same time and over small area, all vegetation-based microclimates are encountered (see below).

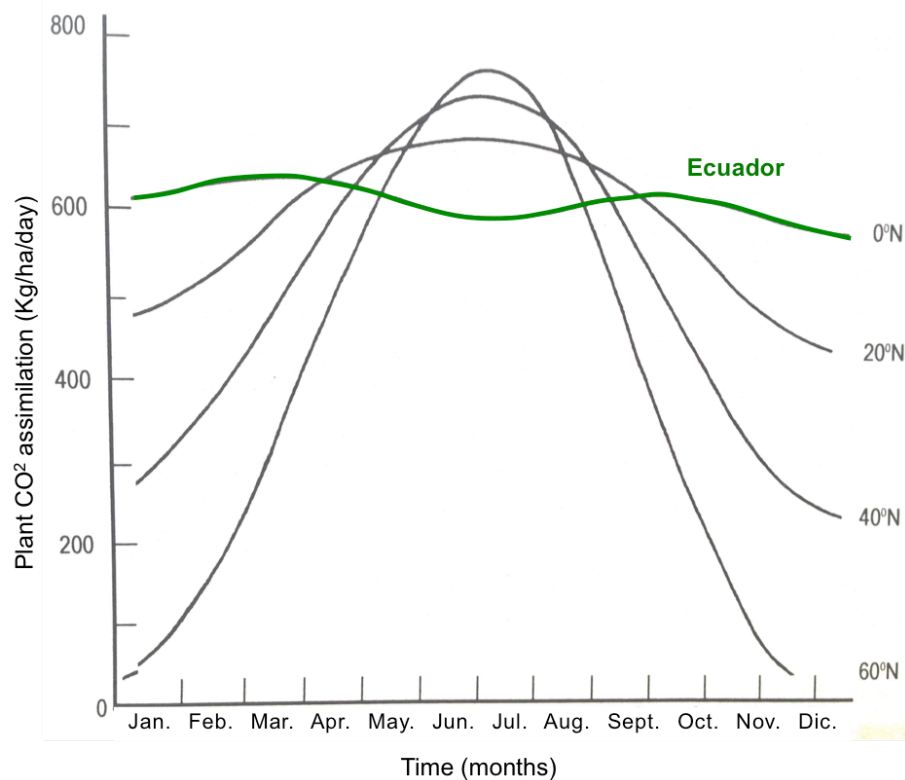


Figure 21: CO₂ plant assimilation (in Kg/ha/day) throughout time of the year for different latitudes of the northern hemisphere. Simulations are performed under clear sky day for a mature green plant. The green line represents Ecuador. Adapted from [Penning & Laar \(1982\)](#).

2. Agricultural landscapes of the study site

The main study site of this work was located 115 km south from the equatorial line ($01^{\circ}01'36''\text{S}$, $78^{\circ}32'16''\text{W}$) in the Cotopaxi province of Ecuador (Fig. 22). It spreads out on a 20-km^2 elevation transect ranging from 2,600 to 3,800 m a.s.l., which broadly corresponds to the elevation belt of potatoes in Ecuador (Pumisacho & Sherwood 2002). The gradient had a southwest exposure and an average slope of 9.5° (± 5.2). The study area is marked by an altitudinal gradient in temperature with mean monthly air temperature roughly decreasing by 0.6°K every 100 m of elevation (McCain 2007), featured by a mean monthly air temperature of $13.26 \pm 0.4^{\circ}\text{C}$ at 2800m, $10.86 \pm 0.6^{\circ}\text{C}$ at 3200m, and $9.36 \pm 0.4^{\circ}\text{C}$ at 3600 m a.s.l.

In this study area, agriculture is the main component of the economy with many people depending directly or indirectly on agricultural activities (MAGAP, *Ministerio de Agricultura, Ganadería, Acuacultura y Pesca de Ecuador*, 2014). Agriculture activity is mainly based on small farm units with most fields < 1 Ha (Fig. 23). Agricultural productivity faces many challenges associated with climate change and extreme events, limited access to technology and infrastructure (related to both elevated costs and remoteness of many sites), low margins of gains faced by the volatile market prices, lack of people's education, and institutional changes that weaken the internal social organization and cause cultural erosion in the Andean society (Perez *et al.* 2010, FAO *Food and Agriculture Organisation* 2014).

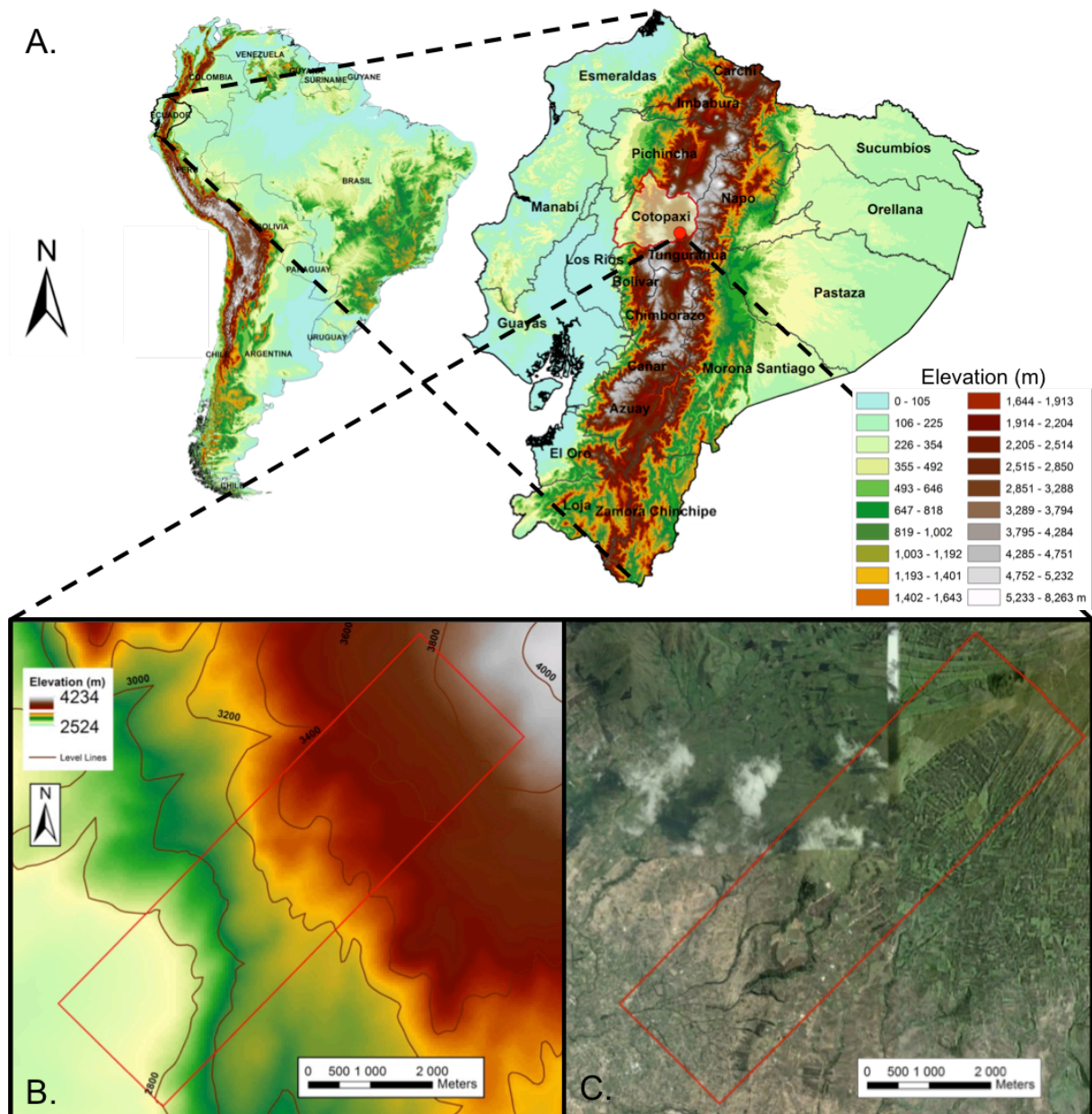


Figure 22: Maps of our main study site. A. Location of the study site in South America and Ecuador. B. Elevation gradient ranging from 2800 to 3600 m a.s.l. within the study area (red square of 20 km²). C. Visual orthophoto of the complex agricultural landscapes of the study site (www.igm.gob.ec). All map were made using ArcGIS (10.2). Elevation gradients in A. and B. are based on a 200 and 30 m digital elevation models, respectively.



Fig. 23: Agricultural landscapes on the study area are complex humanized spaces relying mainly on family farming systems. Photo credits: IRD – Emile Faye.

Like other tropical mountain regions, Ecuadorian Andean landscapes have been intensely fragmented by long-term human influences, mainly related to agricultural practices (Young 2009) that have transformed the region into a complex mosaic of cultivated fields, housing, and roads (Fig. 23 and 24). These intensively humanized landscapes, dominating the altitudinal belt between 2600 and 3800 m, are typically composed by field crops of potato (*Solanum tuberosum*), broad bean (*Vicia faba*), corn (*Zea mays*), alfalfa (*Medicago sativa*), and pastures, natural grasslands (called paramos) and a few forest patches (Fig. 24).

This cultivated mosaic, emerging from the steady climatic conditions of the region and the organization of cropping systems by farmers, is characterized by the spatial arrangement of the fields. A variety of practices such as soil tillage, sowing, weeding, fertilization, harvest

and the farmer objectives of crop production will contribute in shaping the agricultural landscapes (Vasseur *et al.* 2013). Within the study area, landscape heterogeneity in composition and structure evolve following the studied gradient: lower elevations are dominated by small fields (0.36 ± 0.1 Ha) of potato, corn, broad bean, and pasture while the higher elevations had larger fields (0.76 ± 0.3 Ha) of mainly potato and pasture for breeding (Fig. 24). This cultivated mosaic is not just heterogeneous in space but also strongly dynamic (i.e., temporal heterogeneity) due to crop phenology, and the cropping system (i.e., crop rotations). Several factors drive the temporal organisation of the cropping system by farmers. Among them, environmental factors (i.e., soil, slope, exposure, elevation), production resources (work capacity, available equipment) and the accessibility to the fields (i.e., the spatial configuration of field patterns, distance and scattering of fields in relation to the farm building) are crucial in choosing crop practices and rotations.

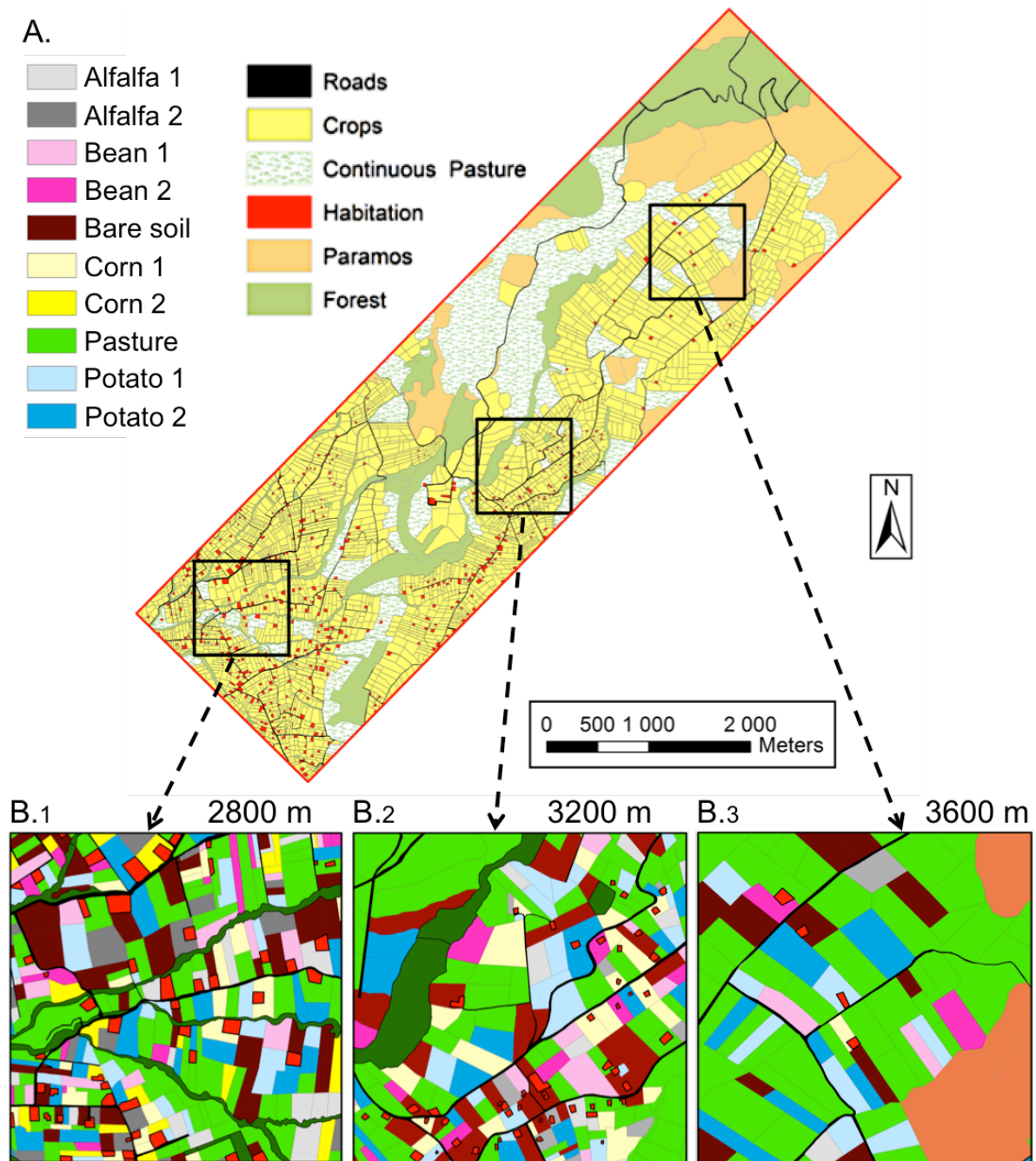


Figure 24: Land uses and cropping systems shape the complex agricultural landscapes in the study area. A. Patchy land uses between crops, pastures, habitation, forest and paramos (natural grasslands in the tropical Andes). B. Focuses on the cropping system at a given time on three 1-km² plots. Crops are numbered based on their stages of maturation (phenological stage 1 and 2). All maps were made in ArcGIS 10.2.

The steadiness of the macroclimatic conditions combined with an altitudinal gradient and a high complexity of the landscape structure (crop types and phenologies) make this study region highly relevant for the study of microclimates at the local scale (see below paragraph III-2). This spatiotemporal heterogeneity provides the opportunity to study the crop-based microclimates during vegetation growth and over small area under identical macroclimates.

In summary, the spatiotemporal organization of agricultural practices, determined by various driving factors, specifically environmental characteristics of fields, on-farm resources and logistic constraints, lead to complex spatiotemporal agricultural landscapes in the Ecuadorian Andes. This spatiotemporal heterogeneity provides the opportunity to study the crop-based microclimates during vegetation growth and over small area under identical macroclimates. Moreover, the spatiotemporal heterogeneity of composition and structure in agricultural landscapes will be decisive for insect population distribution and persistence ([Benton *et al.* 2003](#), [Bianchi *et al.* 2006](#), [Fahrig *et al.* 2011](#), [Vasseur *et al.* 2013](#)).

3. Pests

a. Overview of pests in the study site

The emergence and propagation of agricultural pests constitute important threats to agriculture in the region and worldwide (Bebber *et al.* 2014). Losses caused by pests are estimated to approach 60-70% in available crop production and storage in developing countries (Thomas 1999, Oerke 2006, Nwilene *et al.* 2008). In Ecuador, agricultural landscapes offer a wide variety of crops at different stages of maturation, implying that a great diversity of crop pests can be found all year round (*Instituto Nacional de Investigaciones Agropecuarias del Ecuador* INIAP, Brader 1982, Young 2009). In this thesis, we focused on the potato crop pests because of the economic importance of this crop in the study region and worldwide (Pumisacho & Sherwood 2002). Indeed, after cereals, potato is the most important cultivated crop in the world. Potatoes are produced in almost every country and each year more than 320 million metric tons are produced (Hijmans 2001, Harris 2012). In Ecuador, potatoes constitute a central element of household and national economies, contributing with more than 7 % of the country's Gross Domestic Product (GDP; Devaux *et al.* 2010). Although the tropical Andes are the centre of origin of potatoes, they contribute with only 1.38 % of world production. Recently, production has increased in this region, but yields are still considerably lower than the world average: 7 t/ha in Ecuador while the average yields in developed countries reach 42 to 88t/ha (Hijmans 2001, Pumisacho & Sherwood 2002). Andean farmers face constant problems with potato production, some of them related to climate (such as frost, hail or draught) or market prices, but mainly to pests and diseases which have been estimated to cause losses in production of 32% in the country (Pumisacho & Sherwood 2002, Keller 2003).

In the study region, the major potato pests and diseases (Plate 2) are fungus such as *Phytophthora infestans* L. (potato late blight; Nowicki *et al.* 2012, Sparks *et al.* 2014), viruses

such as the Potato yellow mosaic *begomovirus* L. (Robert *et al.* 1986, Morales *et al.* 2001), epitrix such as the tuber flea beetle *Epitrix tuberis* L. (Vernon & Thomson 1993), the Andean potato weevil *Premnotrypes spp.* L. (Alcázar & Cisneros 1997, Kühne 2007), the leafminer *Liriomyza huidobrensis* L. (Parrella 1987, Huang 2007), the aphid *Myzus persicae* L. (Campbell *et al.* 1974, Davis *et al.* 2006), thunderflies such as thrips *Frankliniella tuberosis* L. (Gaum *et al.* 1994, Chaisuekul & Riley 2005), the potato beetle *Leptinotarsa decemlineata* L. (Hare 1990, Alyokhin *et al.* 2008) and the potato tuber moth complex (*Tecia solanivora* Povolny, *Symmetrischema tangolias* Gyeen, *Phthorimaea operculella* Zeller; Lepidoptera: Gelechiidae; Pollet *et al.* 2004, Crespo-Perez *et al.* 2011, Rebaudo & Dangles 2011). All of these pests and diseases are climate-dependent in various or at least one stage of their life development (see their respective references).

Despite the large number of potato pests, this thesis mainly focused on the potato tuber moth (PTM) complex, because it represents an ideal focal group for various reasons. First, PTM are one of the most important threats to potato production worldwide and in the study area, in particular *P. operculella* (Rondon 2010, Pollet *et al.* 2004). Indeed, losses in yield caused by these three species in the potato fields of the Ecuadorian Andes are considerable, especially in the poorest regions (Pumisacho & Sherwood 2002, Dangles *et al.* 2008). Second, PTM are strict thermoconformers that evolved in all potential habitats in agricultural landscapes (i.e., air, vegetation and ground layers and storage structures; Hanafi 1999, Keller 2003, Keasar *et al.* 2005, Sporleder *et al.* 2004, Dangles *et al.* 2008). Additionally, PTM are Lepidoptera that have dispersal capacities that permit them to move within the agricultural landscape up to 250 m (maximum dispersal distance per individual; Rondon 2010, Crespo-Pérez *et al.* 2011). Last but not least, the PTM complex in the Andes has long been studied by our team which gathered relevant information on temperature related performances (Dangles *et al.* 2008, Herrera & Dangles 2012, Dangles *et al.* 2013, Crespo-Perez *et al.* 2013),

anthropogenic-based pest dynamics in complex agricultural landscapes (Rebaudo *et al.* 2011, Crespo-Perez *et al.* 2011), participative and adaptative integrated pest management throughout social organisation (Dangles *et al.* 2010, Rebaudo & Dangles 2011, Rebaudo & Dangles 2013, Rebaudo & Dangles 2015), species interactions (Dangles *et al.* 2009, Crespo-Pérez *et al.* 2014) and others (e.g., genetics Puillandre *et al.* 2008).

b. Overview of the potato tuber moth complex

PTM adult females lay their eggs on rough surfaces such as soil, potato tuber eyes, or leaf under-surfaces. After hatch, larvae of the three species dig into the soil until finding a potato tuber where they burrow deep tunnels in order to feed (Fig. 25). *S. tangolias* and *P. operculella* larvae can also feed on stems and leaves of potato plants. When fully grown, larvae leave their host and pupate in the soil near the bases of plants, in leaf remains, leftover potatoes, near stored potatoes, or in other suitably sheltered sites (see Fig. 25 for a graphic description of PTM life-cycle). Infestation is often highest in traditional potato storage (tubers heaped under a basic shelter), which offers optimal conditions for PTM development and expansion, such as protection from coldest temperatures and against rainfall (Keasar *et al.* 2005). Under the climatic settings of the study region and the resulting desynchronized complex agricultural landscapes, PTM can survive and be active all year round since they have constant favourable conditions in terms of climate and food resource. Thus, they thrive and propagate all year round more easily than in temperate countries (Crespo-Perez *et al.* 2013). These conditions explain why neither diapause nor seasonal rhythms have been reported for these species at any elevation in Ecuador. This implies that their thermal limits and population dynamics are defined spatially rather than seasonally (Dangles *et al.* 2008).

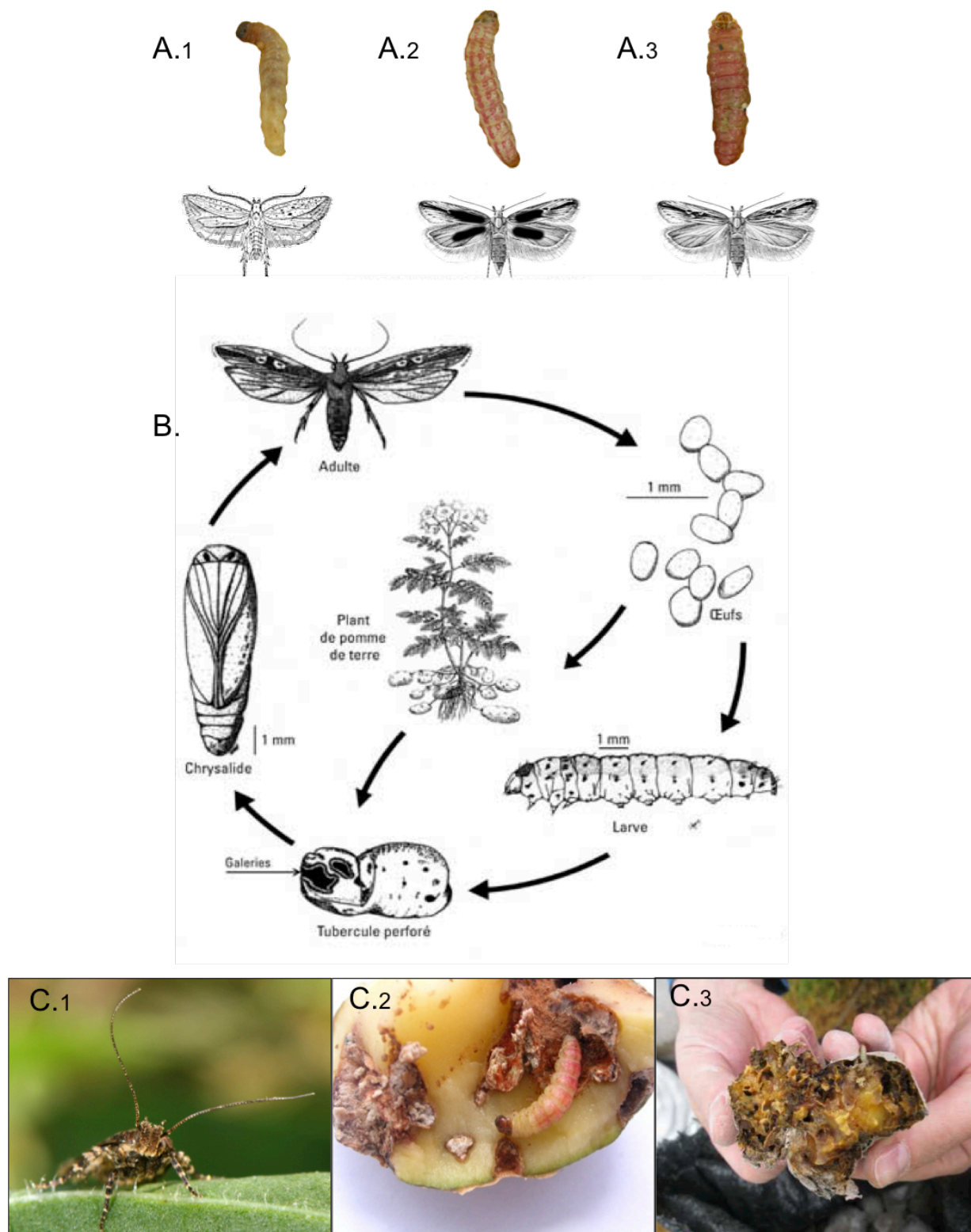


Figure 25: Overview of the potato tuber moth complex. A. Larvae and adults of 1) *Phthorimaea operculella* 2) *Symmetrischema tangolias* 3) *Tecia solanivora*. B. PTM life cycle. C. *Tecia solanivora* 1) adult in the field, 2) larva living inside a potato tuber, and 3) damaged potato with galleries made by PTM larvae. Photo credits: C.1 – IRD Olivier Dangles and C.2 and C.3 IRD – François Rebaudo.

An important characteristic of the complex of pest species is that they differ in their physiological responses to temperature, which affects their spatial distribution across climatically heterogeneous landscapes (Dangles *et al.* 2008). The performance curves representing the temperature dependent survival rate, developmental rate, and fecundity (in number of eggs per female) for these three species are presented in Figure 26. Temperature dependent survival and developmental rates were based on the non-linear thermodynamic model developed by (Sharpe & DeMichele 1977) and modified by (Schoolfield *et al.* 1981). Fecundity was based on the Weibull function, as described and fitted in previous studies on these crop pests (Crespo-Pérez *et al.* 2011, Rebaudo *et al.* 2011, Rebaudo & Dangles 2011). Generally, survival along temperature gradients presents an inverted U shape, with low survival at high and low temperatures. Insect development occurs within a definite temperature range, with a lower threshold temperature – near which development asymptotically approaches zero (because insects often survive for long periods at cold temperatures with little or no development, e.g., during diapause) – and an optimum one of fastest development above which it declines abruptly to a lethal maximum temperature. Then, temperature related fecundity has been shown to present a bell shaped curve extending in a minimum and maximum temperature range. These temperature-dependent functions are the basis for modelling the spatiotemporal dynamics of potato tuber moth invasion under thermally heterogeneous environment.

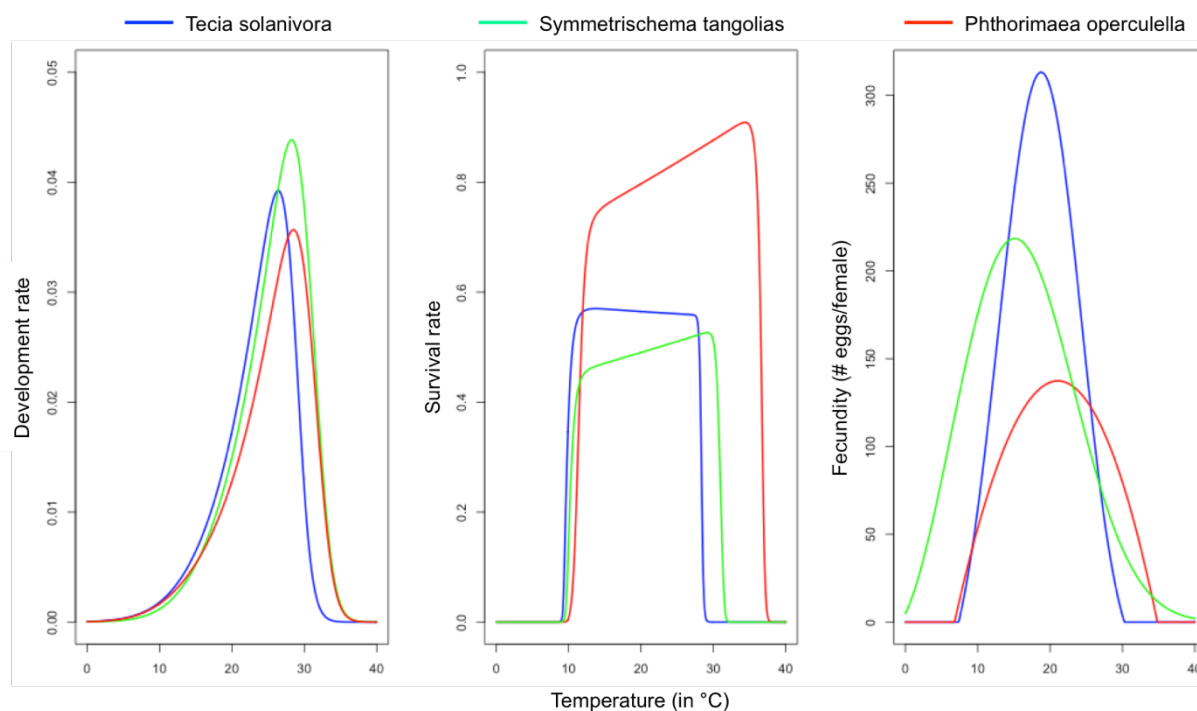


Figure 26: Thermal performance curves for adults of the three species of the potato tuber moth complex. Blue, green and red lines represent *Tectia solanivora*, *Symmetrischema tangolias*, and *Phthorimaea operculella* performances, respectively. Based on data from [Crespo-Perez *et al.* \(2011\)](#) for development and survival rate and [Rebaudo & Dangles \(2011\)](#) for fecundity.

In this general scientific context and face to the presented challenges, this thesis focused on improving our general understanding of the microclimate patterns experienced by ectothermic pests in their habitat following three main objectives.

IV. Objectives and thesis plan

The overall objective of this thesis was *to quantify thermal microclimates in spatially heterogeneous agricultural landscapes and point out their relevance for the understanding of crop pest dynamics*. This overall objective is divided into three specific objectives, each of them corresponding to a chapter of this manuscript.

- **Chapter I: Microclimates and *in silico* pests**

In the first chapter of this thesis, we aim at empirically recording microclimate data at fine spatiotemporal scales in complex agricultural landscapes to compare them to global climatic models with coarse-scale resolutions. Our goal was to provide quantitative information on the limitation of coarse-scale climate data to capture the reality of the climatic environment experienced by living organisms. Then, the objective was to highlight *in silico* the consequences of these discrepancies for the modelling and forecast of pest occurrences.

- **Chapter II: Methods for assessing thermal heterogeneity in agricultural landscapes**

While in the Chapter I of this thesis we used standard methods of thermal ecology for pointing out the importance of considering microclimates when evaluating pest performances in agricultural landscapes, the second Chapter focused on the development of new methodologies to better assess the spatiotemporal heterogeneities of microclimatic temperatures in the field at relevant spatial scales and resolutions for studying pests. This part aims at overcoming the challenge of bridging the gap between the coarse-scale resolutions of the climatic dataset used in a majority of species distribution models and the body length of the study organism (Potter *et al.* 2013). This Chapter is divided in two parts: the first one focuses on a potential pitfall of the use of thermal camera related to the distance between the

study organism and the thermal camera and the second part consists in the development of a toolbox for the monitoring and spatial characterization of microclimates considering the results revealed in the Chapter I and Chapter II part 1.

- **Chapter III: Microclimates and pests *in situ***

Finally, the third Chapter of this manuscript endeavours to combine *in situ* fine scale thermal measurement of crop fields based on the methodologies developed in Chapter II with an in-field sampling of crop pest infestations. Indeed, limited by the technical possibilities for studying the spatiotemporal heterogeneity of microclimates in an agricultural context, agronomists still rarely focused on the effects of the spatiotemporal structure and composition of crop microclimates on pest occurrences. The aim of this chapter was precisely to understand the relationship between crop microclimates and pest occurrences in potato fields.

PLATES

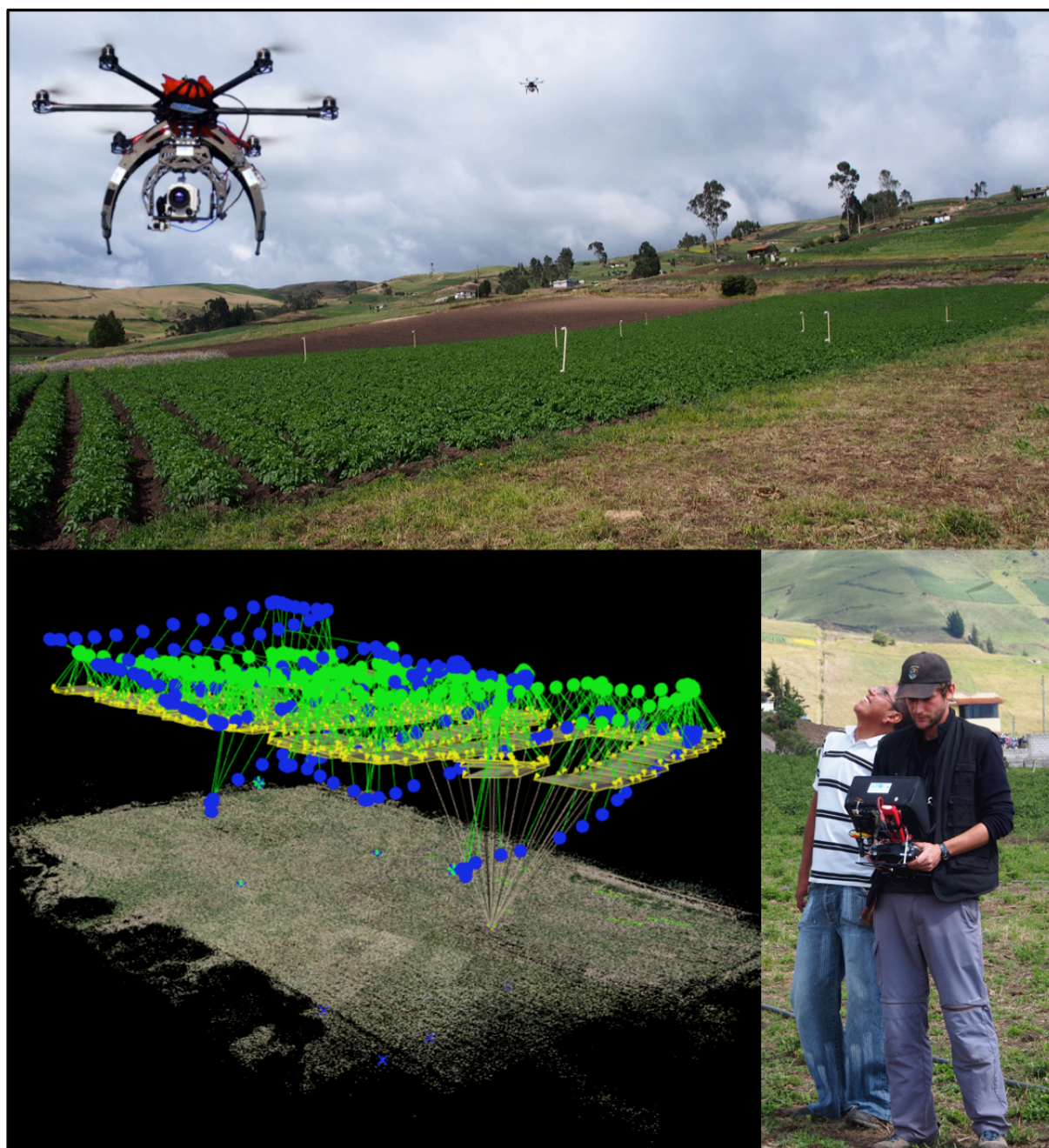


Plate 1: Flying UAV with visual and thermal sensors for high-resolution agricultural remote sensing. Top: Flying over an agricultural landscape of the Ecuadorian Andes (2850 m.a.s.l.). Bottom left: densified three-dimensional point cloud reconstruction of the visual scene. Bottom right: piloting UAV with remote control and control partner.

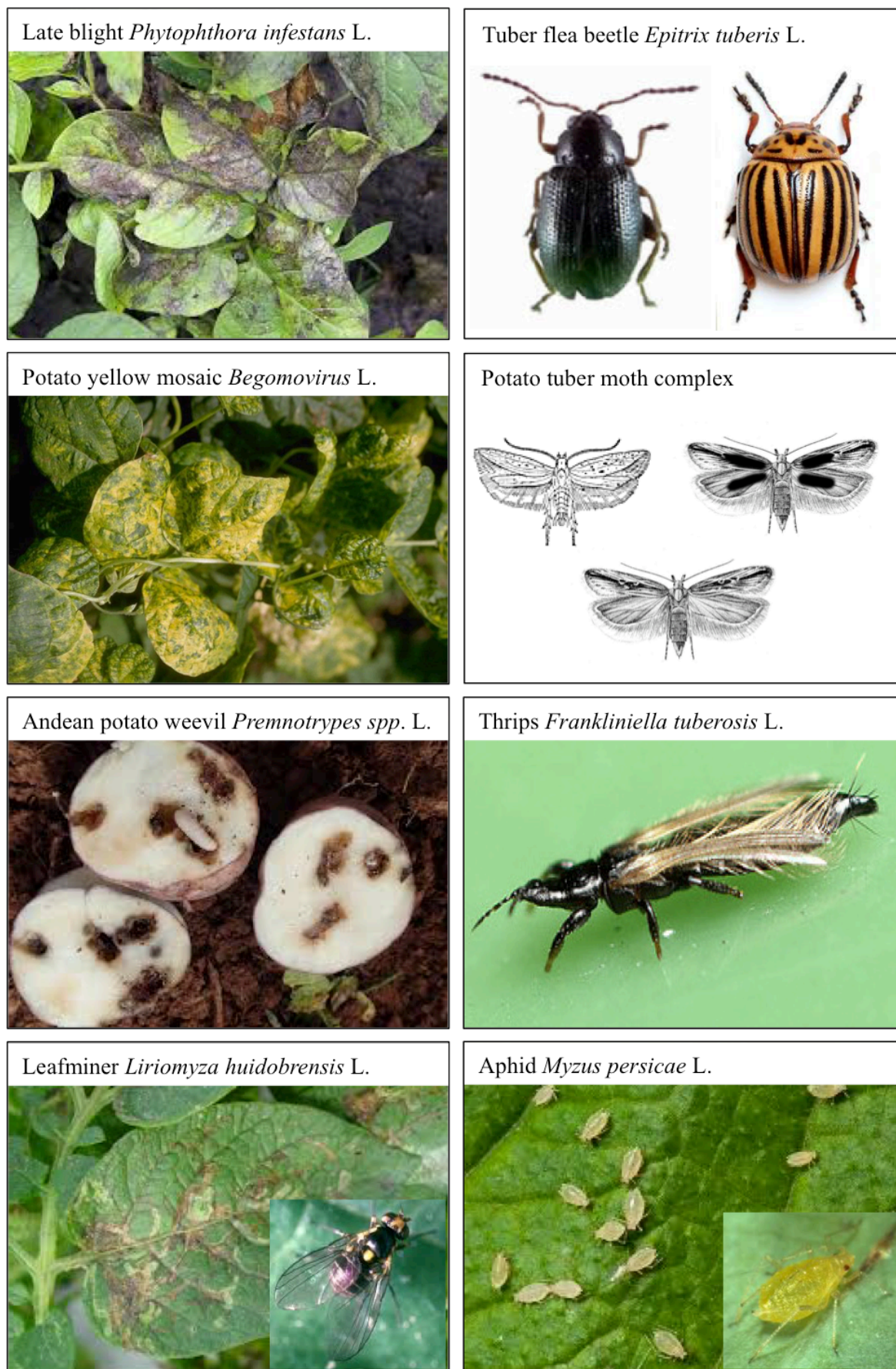


Plate 2: Major potato pests and diseases present in the study area.

CHAPTER I

Microclimates and pests *in silico*

This first chapter of this thesis addressed the need of quantifying the scale gap between the temperature data modelled at coarse spatial scales and the climatic reality experienced by organisms in their microhabitats and to highlight the consequences of this scale gap onto species performances estimations. We therefore used common techniques of data recording used in ecology (large number of temperature loggers) for measuring fine spatiotemporal scales data of temperatures experienced by crop pest over their life cycles (i.e., air, air-inside canopy and soil temperatures). Then, these empirically recorded temperatures were featured and compared to coarse-scale interpolated temperatures of the WorldClim; thereby providing quantitative information on the limitation of coarse-scale climate data to capture the reality of the climatic environment experienced by living organisms.

This study was applied to the tropical agricultural landscape of the study area where we recorded microclimates at 108 localities. In each locality, we documented the crop type, the phenology of the crop with the leaf area index and the elevation. We finally explored the limitations of using the WorldClim to infer the potential performance of a potato crop pest compared to the empirically recorded temperatures.

This work was performed in collaboration with the Entomological laboratory of the Pontificia Universidad Católica del Ecuador and the Mediterranean Institute of Oceanography (MIO), Toulon University, France. This chapter is one publication published in 2014 in ***Plos one***:

- **Faye, E.**, Herrera, M., Bellomo, L., Silvain, J. F., & Dangles, O. (2014). Strong discrepancies between local temperature mapping and interpolated climatic grids in tropical mountainous agricultural landscapes. *PloS One*, **9**(8), e105541.

doi:[10.1371/journal.pone.0105541](https://doi.org/10.1371/journal.pone.0105541).



Strong Discrepancies between Local Temperature Mapping and Interpolated Climatic Grids in Tropical Mountainous Agricultural Landscapes

Emile Faye^{1,2,3*}, Mario Herrera³, Lucio Bellomo⁴, Jean-François Silvain¹, Olivier Dangles^{1,3,5*}

1 Institut de Recherche pour le Développement (IRD), UR 072, Laboratoire Evolution, Génomes et Spéciation, UPR 9034, Centre National de la Recherche Scientifique (CNRS), Gif sur Yvette, France et Université Paris-Sud 11, Orsay, France, **2** UPMC Univ Paris06, Sorbonne Universités, Paris, France, **3** Facultad de Ciencias Exactas y Naturales, Pontificia Universidad Católica del Ecuador, Quito, Ecuador, **4** Mediterranean Institute of Oceanography (MIO) CNRS/INSU, IRD, UM 110, Université de Toulon, La Garde, France, **5** Instituto de Ecología, Universidad Mayor San Andrés, Cotacota, La Paz, Bolivia

Abstract

Bridging the gap between the predictions of coarse-scale climate models and the fine-scale climatic reality of species is a key issue of climate change biology research. While it is now well known that most organisms do not experience the climatic conditions recorded at weather stations, there is little information on the discrepancies between microclimates and global interpolated temperatures used in species distribution models, and their consequences for organisms' performance. To address this issue, we examined the fine-scale spatiotemporal heterogeneity in air, crop canopy and soil temperatures of agricultural landscapes in the Ecuadorian Andes and compared them to predictions of global interpolated climatic grids. Temperature time-series were measured in air, canopy and soil for 108 localities at three altitudes and analysed using Fourier transform. Discrepancies between local temperatures vs. global interpolated grids and their implications for pest performance were then mapped and analysed using GIS statistical toolbox. Our results showed that global interpolated predictions over-estimate by 77.56–10% and under-estimate by 82.16–12% local minimum and maximum air temperatures recorded in the studied grid. Additional modifications of local air temperatures were due to the thermal buffering of plant canopies (from 2–2.7°C during daytime to 1.3°C during night-time) and soils (from 2–4.9°C during daytime to 6.7°C during night-time) with a significant effect of crop phenology on the buffer effect. This discrepancies between interpolated and local temperatures strongly affected predictions of the performance of an ectothermic crop pest as interpolated temperatures predicted pest growth rates 2.3–4.3 times lower than those predicted by local temperatures. This study provides quantitative information on the limitation of coarse-scale climate data to capture the reality of the climatic environment experienced by living organisms. In highly heterogeneous region such as tropical mountains, caution should therefore be taken when using global models to infer local-scale biological processes.

Citation: Faye E, Herrera M, Bellomo L, Silvain J-F, Dangles O (2014) Strong Discrepancies between Local Temperature Mapping and Interpolated Climatic Grids in Tropical Mountainous Agricultural Landscapes. PLoS ONE 9(8): e105541. doi:10.1371/journal.pone.0105541

Editor: Michael Sears, Clemson University, United States of America

Received: March 12, 2014; **Accepted:** July 24, 2014; **Published:** August 20, 2014

Copyright: © 2014 Faye et al. This is an open-access article distributed under the terms of the Creative Commons Attribution License, which permits unrestricted use, distribution, and reproduction in any medium, provided the original author and source are credited.

Data Availability: The authors confirm that all data underlying the findings are fully available without restriction. All temperature time-series used in this work are within the Supporting Information files of the paper.

Funding: This work was partly conducted within the project "Adaptive management in insect pest control in thermally heterogeneous agricultural landscapes" (ANR-12-JSV7-0013-01) funded by the Agence Nationale pour la Recherche (ANR, <http://www.agence-nationale-recherche.fr/>). A financial support of the McKnight Foundation (<http://www.mcknight.org/>) to EF during the fieldwork of this study is greatly acknowledged. The funders had no role in study design, data collection and analysis, decision to publish, or preparation of the manuscript.

Competing Interests: The authors have declared that no competing interests exist.

* Email: ehfaye@gmail.com (EF); olivier.dangles@ird.fr (OD)

Introduction

Bridging the gap between the predictions of coarse-scale climate models and the fine-scale climatic reality of species is increasingly recognized as a key issue of climate change biology research [1,2,3,4]. Despite decades of study on microclimates [5,6,7,8] and evidence for habitat-related and topographical variations in local temperatures and their relevance for species ecology [2,9,10,11,12,13], most attempts to understand and model species distributions still do not integrate spatially-explicit fine-scale climatic data (e.g. [14,15,16]). Many work use global model of temperature interpolation to examine species vulnerability to climate change and, doing so, ignore the critical issue of habitat complexity in climate buffering [4,5,17]. Indeed, climate surfaces

used in species distribution models (SDMs) are rarely generated or interpolated to a resolution finer than 1 km² (e.g. WorldClim database), a resolution that is still very coarse relative to the home ranges or body size of most species [13,18]. For instance, [8] showed that climate grid lengths used in SDMs are, on average, 10,000-fold larger than studied animals, and 1,000-fold larger than studied plants. Their meta-analysis showed that the WorldClim was the most widely used climatic dataset in global SDMs. As this commonly used coarse scale climatic data in SDMs overlook the spatiotemporal thermal heterogeneity experienced by organisms, there is an urgent need for a more sophisticated use of these datasets for making inferences about biological processes that are driven by hour to hour operative temperatures of organisms.

An important yet poorly studied issue in climate change biology is to quantify to what extent climatic conditions differ between widely used 1 km² interpolated grid cells of global climatic database and real-world landscapes of similar areas. While it is now well-known that most organisms, especially tiny ectotherms such as insects and other arthropods, do not experience the climatic conditions recorded at weather stations [9,12,18], there is little quantitative information on the spatial and temporal heterogeneity at the landscape scale of local climatic conditions (i.e. conditions at biologically relevant scales, e.g., from cm to km for insects) and their consequences for organisms' performance. A better quantification of the climatic conditions of ecologically-relevant habitats over relatively large landscape scales (e.g., 1 km²) is therefore a necessary first step to better incorporate dynamical microclimate into global distribution models.

Here, we investigate the sources of variance between global interpolated and local temperatures by examining 1) how well WorldClim predicts local air temperatures in our study region (the tropical Andes), 2) to what extent temperatures in crop canopies and soils differ from local air temperatures, and 3) how relevant is to use WorldClim to infer the potential performance of an insect crop pest. Addressing these questions is not an easy task as the mosaic of climatic habitats relevant for small ectothermic species at a 1-km² scale in real-world landscapes may be outstandingly complex. In this study, we focused on highland agricultural landscapes of the tropical Andes as most prior similar data came from low elevation and temperate agroecosystems. In such systems, most crop pests experience, over their entire life cycle, climatic conditions in three well-defined environmental layers (air, air inside-canopy and soil) and these conditions are remarkably stable over the year [19]. In this context, we firstly decided to map over replicated 1-km² climatic grid cells the ecologically relevant local temperatures for ectothermic crop pests in agricultural landscapes, and to compare these maps to interpolated temperature grid cells of the widely used WorldClim database. We used Fourier analysis applied to local temperature time-series as a tool to fit daily variations of temperature and to feature microclimate discrepancies in space and in time (both in terms of amplitude and phase). We then explored the implication of our thermal landscape mapping for pest performance by comparing temperature frequencies in our grid cells with the temperature-dependent growth curve of the potato tuber moth (*Plutella maculipennis*), a major crop pest species in the region and worldwide.

Materials and Methods

1. Study area

The Ecuadorian Andes are characterized by a low seasonality, with mean temperatures varying more within days (up to 1.8 K variation) than within months and years (less than 0.6 and 0.2 K variations, respectively, see [19]). This region exhibits a marked altitudinal gradient in temperatures (between 2000 and 4000 m) with mean monthly air temperature roughly decreasing by 0.6 K every 100 m of elevation [20]. Agricultural landscapes dominate the altitudinal belt between 2600 and 3800 m, and are typically composed by small field crops (mainly potato (*Solanum tuberosum* L., broad bean *Vicia faba* L., corn *Zea mays* L., alfalfa *Medicago sativa* L., and pasture), natural grasslands (*paramos*) and a few forest patches [21]. Under the climatic conditions of the region, crops can be planted and harvested all year round, thereby creating a landscape mosaic of a wide variety of crops at different phenological stages.

Our study area was located 115 km south from the equatorial line (01°01'36"S, 78°29'60"W) in the Cotopaxi province of

Ecuador. It spread out on a 20-km² elevation transect (2,356–3,800 m), ranging from 2,600 to 3,800 m a.s.l. The gradient had a Southwest exposure and an average slope of 9.5° (based on a 30 m resolution digital elevation model). To investigate the elevation effect on local vs. global interpolated temperature variations, we divided our study area into three 400 m altitudinal belts which correspond to natural floors in the hillside (2,600–3,000 m, 3,000–3,400 m, and 3,400–3,800 m) with a mean monthly temperature of 13.2 ± 0.4 °C, 10.8 ± 0.6 °C, and 9.36 ± 0.4 °C, respectively. Beyond temperature, these belts also differed in terms of landscape composition (Appendix S1 in Supporting Information), with lower elevations dominated by small fields (0.3 ± 0.1 Ha) of potato, corn, broad bean, and pasture while the higher band had larger fields (0.67 ± 0.3 Ha) of mainly potato and pasture. Working in these agricultural landscapes no requires specific permissions expect the kind agreement of the field owner. The presented study did not involve endangered or protected species.

2. Temperature data collection

In each of the three-altitudinal belts, we measured temperature regimes in six habitats (five crops and natural grasslands) where insect pests can be found. In each habitat, we defined three layers: air, air inside-canopy (referred as "air canopy" in the text) and soil. These layers are all used by most insect pests over their life cycle: air layer by adults, air canopy layer by adults and leaf-eating larvae and pupae, soil layer by tuber feeding larvae and pupae. In each layer of each habitat, temperature was recorded with a 1 min time step using data loggers (Hobo U23-001-Pro-V2 internal temperature loggers, Onset Computer Corporation, Bourne, USA) with an accuracy of 0.21 °C over the 0–50 °C range and a resolution of 0.02 °C at 25 °C. According to [4], 1) air loggers were fixed on a wooden stake at 1 m high to overstep most crop canopies and sheltered by a 20 cm² white plastic roof to minimize solar radiation heating; the roof was itself placed 5 cm above the logger to avoid warming by greenhouse effect, 2) air canopy loggers were placed 0.3 m high inside vegetation 5 cm below large leaves to minimize the effect of direct solar radiation and 3) soil loggers were buried 0.1 m into the ground where roots and tubers grow (see Appendix S2 for photographs). In each field, only one logger per layer measured the temperatures. Those triplets of loggers were located at the centre of the field to avoid edge effect (see Appendix S3 for an analysis of the spatial variability of temperatures within a field and [22]). As vegetation land cover influences microclimate beneath and around plants, see [5,6], we repeated these 54 measurements (3 elevations × 6 habitats × 3 layers) for three classes of leaf area index (LAI) [23] defined as follows: 0 (bare soil), 0.01–0.5 for and 0.5 of LAI. Minimum LAI was fixed to 0.01 to avoid confusion with bare soil and allowed enough leaf area to place the loggers underneath. At each measurement site, LAI values were visually estimated (twice) measuring the ratio of leaf area within a 1-m² quadrant sub-divided into 0.1 m² cells delimited by strings. This indirect method did not account for leaves that lie on each other however it relates to shaded areas that influence inside-canopy and soil microclimates [23].

Each of the 162 measurement combinations (3 altitudinal belts × 6 habitats × 3 layers × 3 LAI classes) was replicated 1–3 times depending on availability of habitats at a given elevation and phenology stage. In total 324 independent temperature time series were acquired over 15 days between September and December 2011 (data available in Appendices S9, S10 and S11). Importantly, under the climatic conditions of the study area, 15-days time series characteristics did not differ from those obtained over one year (see Appendix S4 for details). At each measurement site, we

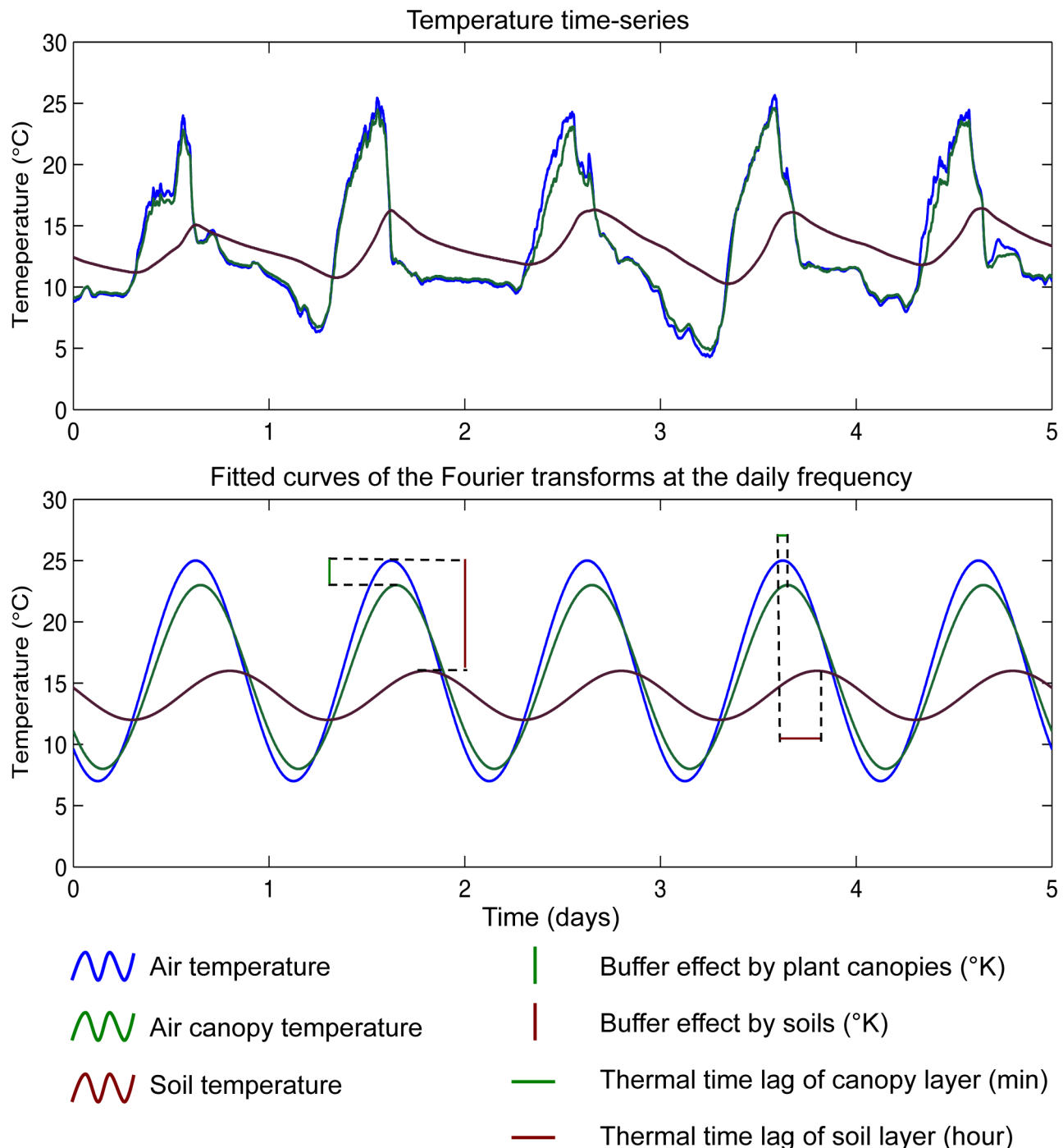


Figure 1. Fit of temperature time series with discrete Fourier transforms at the daily frequency
doi:10.1371/journal.pone.0105541.g001

K_{cr} Air temperatures are in blue, crop

recorded the UTM-WGS84 geographic coordinates with a handheld GPS Garmin Oregon 550 (Garmin, Olathe, USA).

3. Global solar radiations

Infrared and visible radiations (expressed in Watt/m^2) were monitored in each altitudinal belts using a LI-1400 LI-COR datalogger equipped with a LI-200 pyranometer sensor (LI-COR, Lincoln, USA) placed perpendicular to gravity. Between 9:00 AM and 4:00 PM, mean global solar radiations ranged from 500 to

1000 watts/m^2 , with temporal variability mainly induced by short-term changes in cloud cover.

4. Data analyses

4.1. Times series analyses using Fourier transforms. Air and air canopy temperature time series showed extreme events during a few minutes that were certainly due to strong radiations experienced at the study sites these affected loggers recording despite their plastic roofs. Therefore, we found

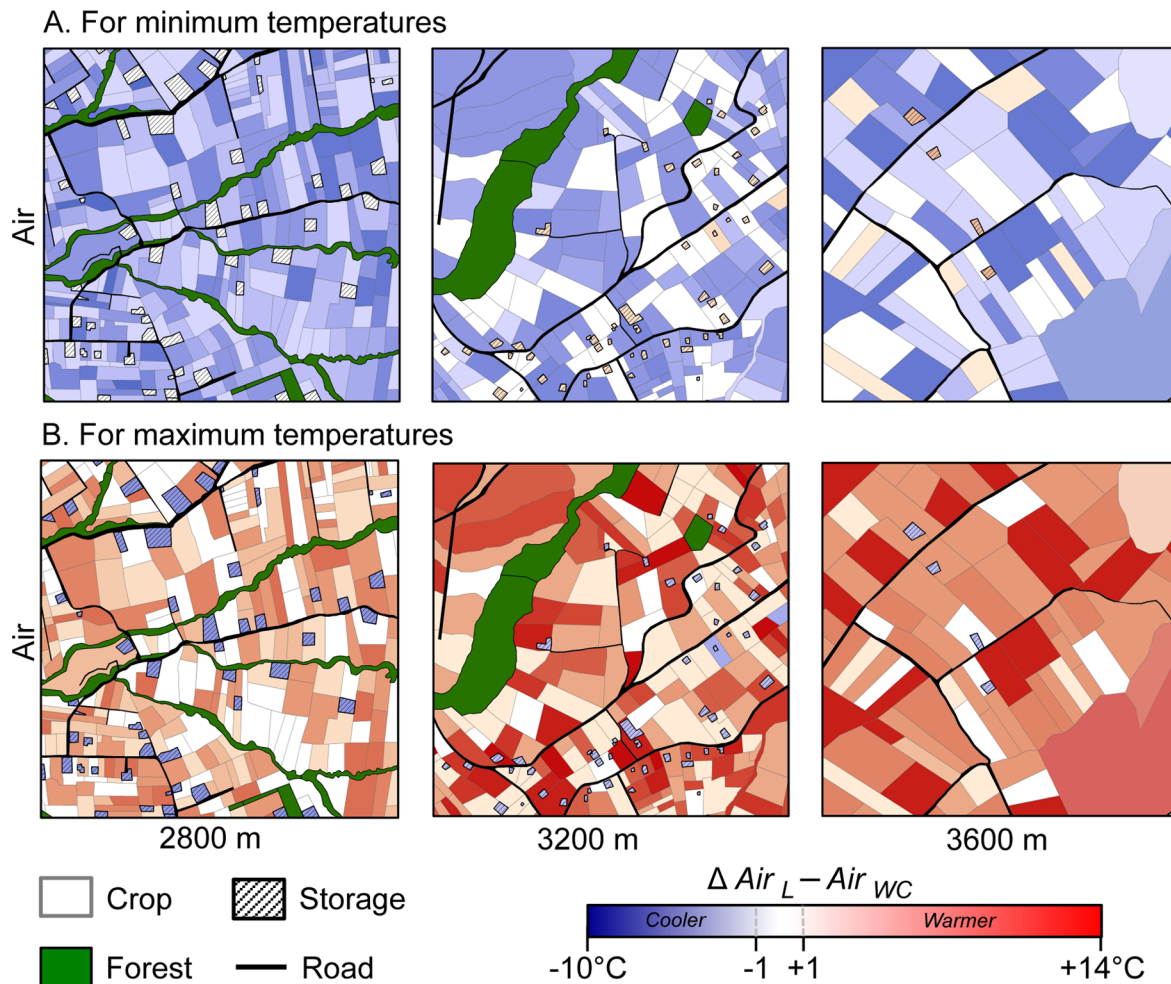


Figure 2. Maps showing the differences between local air temperatures and the WorldClim interpolated minimum (A) and maximum (B) ($\Delta \text{Air}_L - \text{Air}_{WC}$). Blue colours indicate $\Delta \text{Air}_L - \text{Air}_{WC} < 0$, i.e. area where local air temperatures are cooler than those gave by WorldClim. Red colours indicate $\Delta \text{Air}_L - \text{Air}_{WC} > 0$, i.e. area where air local temperatures are warmer than the ones gave by the WorldClim. White colours $\Delta \text{Air}_L - \text{Air}_{WC} = 0$ indicate areas where air WorldClim temperatures equate air local temperatures ($\pm 1^\circ\text{C}$). The extent and position of each square is equal to the spatial resolution of the WorldClim database: 30-arc sec that is the equivalent of 0.86 km^2 for the study area. Temperatures in storages were obtained from [26]. doi:10.1371/journal.pone.0105541.g002

relevant to fit our time series data with a discrete Fourier transform (DFT) at the daily frequency k_d (Fig. 1) as this allowed averaging daily minimum and maximum temperatures while limiting the effect of short extremes (mainly for maximum). Moreover fitting temperature time series with the DFT allowed us to circumvent (or partially resolve) the issue of comparing time series with different temporal resolution: a sinusoid built from a daily time step time series will be accurate enough to compare with another sinusoid built from a one minute time step time series (our operative temperatures vs. global climatic models).

DFT analyses allowed us estimating two important descriptors of the time series at the daily frequency: the amplitude A_d and the phase w_d of the DFT (see Appendix S5 for details). The thermal amplitude allowed us to measure the thermal buffer effect in Kelvin between air and canopy layers and air and soil layers (Fig. 1 and Appendix S5). The phase allowed us to measure the thermal time lag expressed in minute in inside-canopy and soil layers with respect to the air layer (Fig. 1 and Appendix S5). Thermal time lag therefore quantifies the time delay in time series to reach their maximum between air vs. canopy and air vs. soil

layers. This is an important climatic parameter to test whether microclimate conditions below canopy (canopy and soil layers) would track air conditions with some time lag depending on habitat characteristics.

We also ran DFT analyses on a four-year monitoring (2008–2012) of air temperatures (recorded at one meter high with half an hour time step with the same shelter process described above) to measure the seasonality. Analyses were performed for the three-altitudinal belts of the study area (2800, 3200, 3600 m) by reading the amplitude at the seasonal frequencies (91, 182 and 364 days, see Appendix S6). On average the Fourier transform amplitudes at 91, 182 and 364 days were 0.14 ± 0.01 , 0.44 ± 0.04 , $0.97 \pm 0.03 \mu\text{K}$ indicating that the seasonality was negligible in the study area [24].

All Fourier analyses were performed in MATLAB R2011a (Mathworks, Natick, USA). The effects of habitat, elevation, LAI classes and the interaction “elevation \times LAI classes” on daytime and high-time DFT amplitudes and on DFT thermal time lag were assessed using a two-way ANOVA with Bonferroni corrections. When habitat was found significant, we ran post-hoc

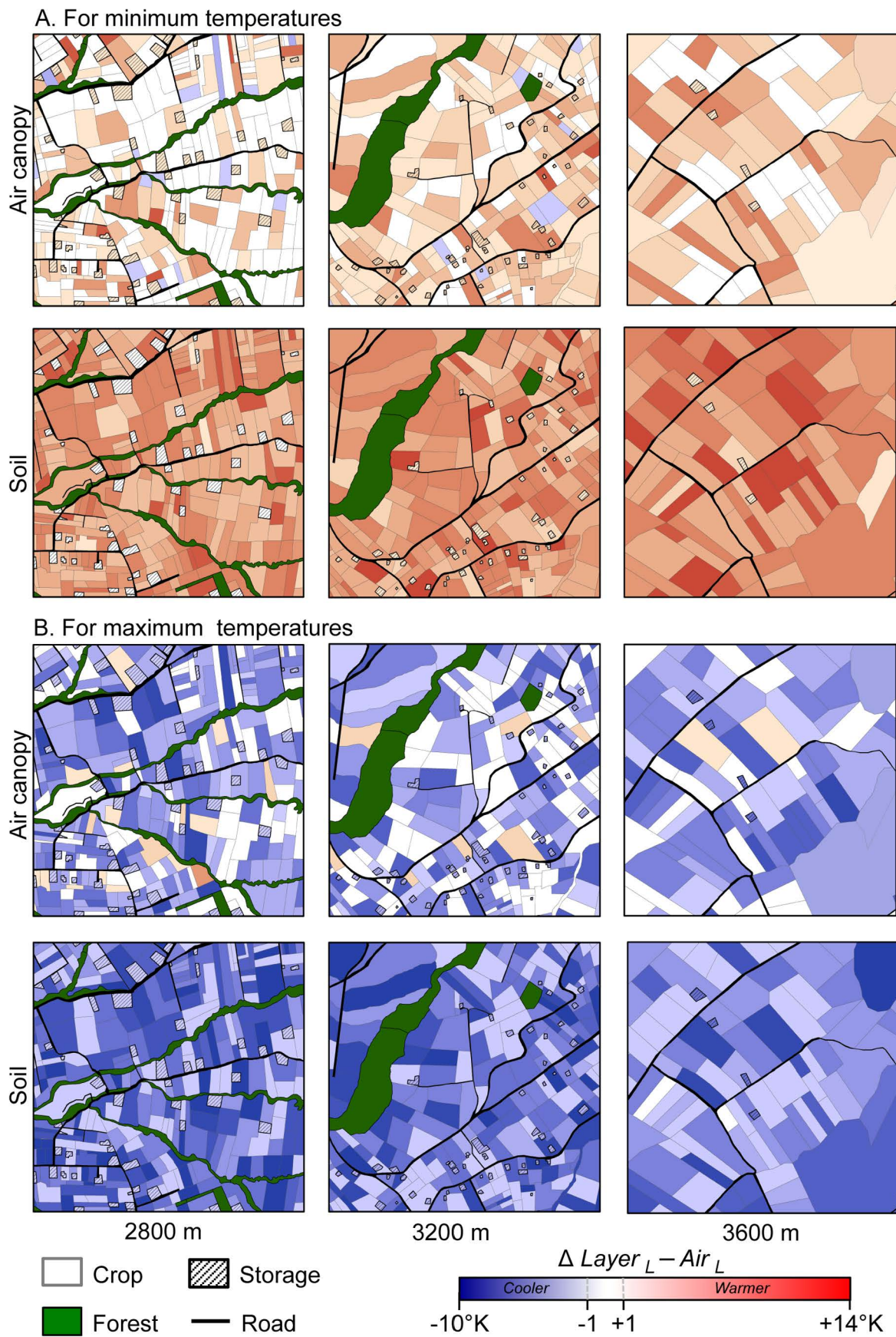


Figure 3. Maps showing the differences between local air canopy and soil temperatures with the air local for minimum (A) and maximum (B) ($\Delta Layer_L - Air_L$). Colour code is given in Figure 2.
doi:10.1371/journal.pone.0105541.g003

multiple comparisons using a Tukey HSD test to identify differences among habitats. All statistical analyses were performed in R version 3.0.0 (R Development Core Team 2012).

4.2. Thermal landscape analyses. To compare local temperatures with global interpolated climate data employed in species distribution models, we considered one of the most widely used and readily available climate database, WorldClim [25]. The WorldClim database is a set of global climate layers (interpolated averages of monthly minimum, maximum and mean 1.5 m high air temperatures from weather stations spread out worldwide) with a spatial resolution of 30 arc seconds. Close to equator, this resolution is equivalent to squares of 0.86 km. In each altitudinal belt, we selected one WorldClim grid cell with homogenous slope (between 5.4 and 7.9), micro-topography and exposition (south-west). Based on a digitized municipal cadastre (from the town council of Salcedo, Cotopaxi province) and a 5-m resolution digital orthophoto (Ecuadorian Military Geographical Institute, www.igm.gob.ec/site/index.php), we built the digital landscape of each grid cell in ArcGIS 10.01 (ESRI, Redlands, USA). In addition to the six studied habitats, crop storage infrastructures were also included into the digital maps as they significantly modify air temperature patterns, offering optimal conditions for crop pest development [26]. Outside air vs. inside air storage-temperature relationships for different elevations were derived from measurements made by [26] within the same area with

similar temperature data design (see Fig. 1 in Appendix A2 of their paper). Roads and woodlots were also indicated on the maps even if they were not included in the temperature comparison analysis, as they do not constitute relevant habitats for crop pests.

In order to simulate landscape thermal heterogeneity, crop habitats were attributed with one crop type (potato, broad bean, corn, alfalfa or pasture) and one LAI classes (0, 0.01–0.5, 0.5) based on a survey of 85 sites in the region, in which we quantified landscape composition (% of each crop and LAI classes) in 100-m radius sampling circles (see Appendix S7). For each habitat, we assigned the corresponding air, air canopy and soil temperature values at each elevation. Finally, since we were particularly interested in minimal and maximal values, as they are the most biologically relevant for ectothermic crop pests [4], we focused on minimum and maximum temperatures obtained from the DFT analyses and the WorldClim database.

Afterwards, we decomposed the variance of temperatures between global interpolated grids and local temperatures measured in agricultural landscapes by mapping the differences in minimum and maximum temperatures between the air local temperatures (Air_L) and the WorldClim interpolated temperatures (Air_{WC}) for the three studied grid cells. Then, to illustrate the part of the variance due to microclimate effects, we mapped the differences in minimum and maximum temperatures between measured local air canopies, soil temperatures ($Layer$) and the air local temperatures (Air_L) for the three studied grid cells.

4.3. Pest performance in thermal landscape. As a final step of our analysis, we explored the implication of our thermal landscape mapping for pest performance by comparing temperature frequencies in our grid cells with the temperature-dependent growth curve of a major crop pest species in the region: *Phthorimaea operculella* (Lepidoptera: Gelechiidae). This pest is considered one of the most important potato pests worldwide, but also attacks a wide variety of other crops such as tomato (*Solanum lycopersicum* L.), eggplant (*Solanum melongena* L.) or tobacco (*Nicotiana tabacum* L.) (see [27] for a review). *P. operculella* feeds on different part of the plant (leaves, stems, and tubers) and also tubers in storage structures [26,28]. In agricultural landscape, *P. operculella* is abundant in virtually all types of habitats (even far from its host plant) because 1) this pest is able to fly over large distances (100–250 m) to infest suitable host plants [29] and 2) a significant quantity of tubers are left in the field after harvest, and are rapidly colonized by the moth before the following crop is planted. It is therefore common to observe infested potato plants in corn or broad bean fields. These left-over potatoes are well known by farmers and agronomists as significant obstacle to the control of these pests [28].

The temperature-dependent growth rate curve of *P. operculella* larvae (in day⁻¹) over a 0–40°C range was obtained using published temperature-response data of laboratory experiments performed in the Andean region (see [30] for details). PTM development rate data were then modeled with the [31] equation as modified by [32]:

$$DFT = \frac{\frac{dT}{298.16} \exp \left[\frac{e}{R} \left(\frac{1}{298.16} - \frac{1}{T} \right) \right]}{1 + \exp \left[\frac{f}{R} \left(\frac{1}{g} - \frac{1}{T} \right) \right] + \exp \left[\frac{h}{R} \left(\frac{1}{i} - \frac{1}{T} \right) \right]}$$

where T is temperature in Kelvin ($^{\circ}C + 273.15$), $R = 1.987$, and d , e , f , g , h , and i estimated parameters. This model has been widely used to describe the kinetics of insect development based on several assumptions about the underlying developmental control

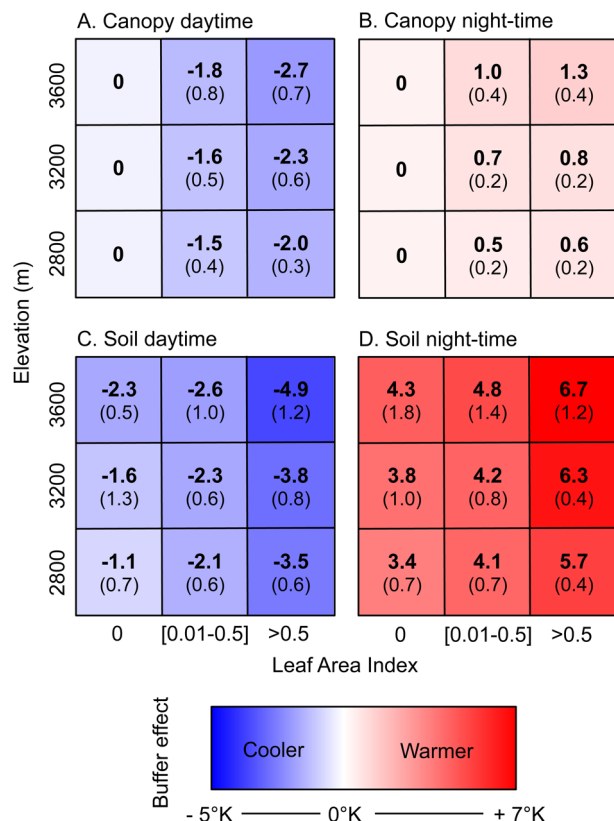


Figure 4. Mean thermal buffering from Fourier transforms at the daily frequency for canopy (A, B) and soil temperatures (C, D) as a function of elevation and leaf area index. (A, C) show the daytime temperature excursion with respect to air, whereas (B, D) are the equivalent results for night-time temperatures. The 95% interval of confidence is given between brackets. Blue colours show colder temperatures than air. Red colours show warmer temperatures than air. doi:10.1371/journal.pone.0105541.g004

Table 1. Results of the two-way ANOVA with a Bonferroni correction on the effects of habitat, elevation, LAI and elevation6 LAI terms on daytime and night-time DFT amplitudes and thermal time lag on inside-canopy and soil temperature time series.

Effect	Canopy				Soil			
	Df	Mean sq	F value	P value	Df	Mean sq	F value	P value
Daytime amplitude								
Habitat	5	6.282	3.370	0.007*	5	5.745	2.466	0.036
Elevation	2	12.491	6.701	0.002*	2	5.722	2.456	0.089
LAI	1	40.171	21.551	0.001*	1	136.78	58.705	0.001*
Elevation 6 LAI	2	2.513	1.348	0.263	2	0.292	0.125	0.882
Residuals	132	1.864			127	2.330		
Night-time amplitude								
Habitat	5	0.936	3.895	0.002*	5	1.390	0.839	0.525
Elevation	2	4.539	18.896	0.001*	2	2.143	1.293	0.278
LAI	1	1.083	4.509	0.035	1	157.52	95.041	0.001*
Elevation 6 LAI	2	1.754	7.302	0.010	2	0.097	0.059	0.943
Residuals	132	0.240			127	1.657		
Thermal Time Lag								
Habitat	5	0.001	1.297	0.269	5	0.009	3.881	0.003*
Elevation	2	0.001	5.777	0.004*	2	0.024	10.139	0.001*
LAI	1	0.001	29.322	0.001*	1	0.022	9.165	0.003*
Elevation 6 LAI	2	0.001	2.374	0.097	2	0.005	2.334	0.101
Residuals	132	0.001			127	0.002		

Bold* indicates significant results ($P < 0.05$).
doi:10.1371/journal.pone.0105541.t001

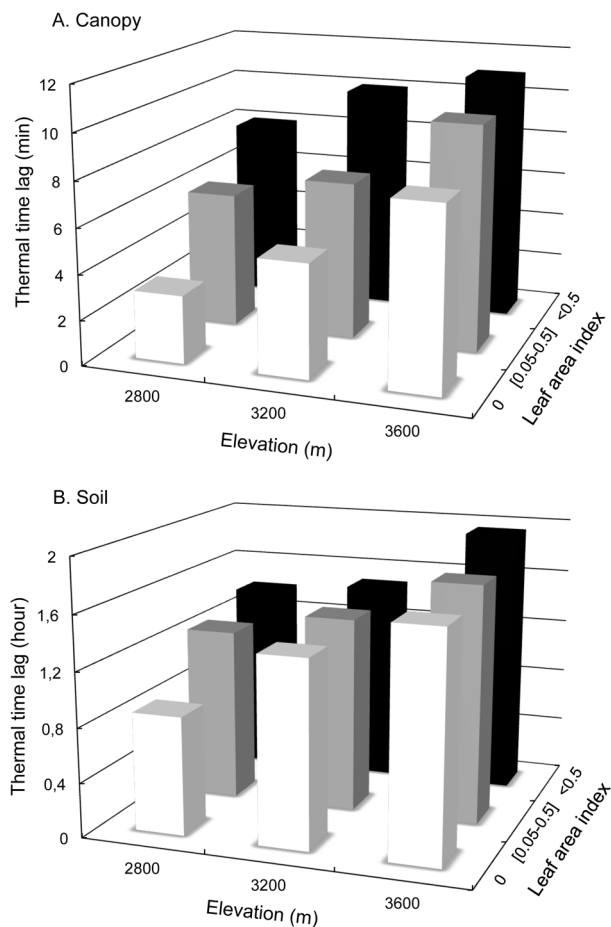


Figure 5. Thermal time lag from Fourier transforms at the daily frequency for canopy (A) and soil temperatures (B) as a function of elevation and leaf area index. The z-axis (log+1 transformed) is expressed in minutes (A) and in hours (B). doi:10.1371/journal.pone.0105541.g005

enzymes. For instance, it has been used to describe poikilotherms' temperature-dependent development [33].

We then compared the growth rate performance curve of *P. operculella* for local temperature distribution (canopy and soil layer temperatures) and for global interpolated ones (e.g., Fig. 3 in [3]). Distributions of canopy and soil minimum, maximum and mean temperatures were extracted from the three digitized landscapes using the geostatistical analyst extension of ArcGIS. Canopy and soil temperature frequencies were expressed as the percent of total grid cell area. The growth performance model of *P. operculella* given by Eqn. 1 was implemented with WorldClim minimum and maximum temperatures and the local minimum, maximum and mean temperature distribution. This allowed estimating insect growth rate within the range of WorldClim and measured field data.

Results

1. Local vs. global air temperature discrepancies in thermal landscapes

Differences in average minimum and maximum temperatures between local air temperatures and the global coarse grain interpolated air temperatures from the WorldClim ($Air_L - Air_{WC}$) were mapped for the three studied grid cells (Fig. 2). While

minimum local air temperatures were cooler than those predicted by WorldClim in 77.56 10% of the studied areas (blue areas, average $\min D Air_L - Air_{WC} = 2.29^{\circ}K$) maximum local air temperatures were warmer than extrapolated temperatures in 82.16 12% of the studied areas (red areas, average $\max D Air_L - Air_{WC} = +5.6^{\circ}K$). This pattern was not influenced by elevation. Notably, for all elevations, local mean air temperatures were quite well predicted by the WorldClim ($\pm 2.1^{\circ}K$) as in average 55.36 3.4% of the studied areas felt in the range of $Air_L - Air_{WC} \# 1^{\circ}K$ (Appendix S8).

2. Temperature discrepancies due to microclimate in agricultural landscapes

Differences in average minimum and maximum temperatures between local canopy and soil temperatures and local air temperatures ($D Air_L$) were mapped for the three studied grid cells (Fig. 3). Overall, canopy and soil areas were always cooler than maximum air temperature and were always warmer than air minimum temperatures resulting in a general buffer effect of minimum and maximum air temperatures by canopy and soil layers. The buffer effect on air temperatures was significantly stronger for soil than for canopy layer (see Fig. 4, Student's t-test, $t = 2.27.10$ and $t = 4.52$, $P = 0.001$ for night-time and daytime, respectively). Interestingly, the buffer effect on air temperatures by soil was higher during night-time than daytime (Fig. 4D) while the opposite pattern was found in crop canopy (Fig. 4A).

Elevation had a significant effect on air temperature buffering in the canopy layer but not in the soil layer (Table 1). Contrastingly, LAI had a highly significant thermal buffering effect in both soils (night and daytime) and canopies (daytime, see Table 1). Buffer effect on air temperatures by bare soil (e.g. without plant cover, $LAI = 0$) ranged from $2.1.1^{\circ}K$ to $2.2.3^{\circ}K$ for daytime and from $3.4^{\circ}K$ to $4.3^{\circ}K$ for night-time. Crop type had no significant effect on buffering patterns except for potato in which higher buffer effects were recorded (Post-Hoc HSD test, $P = 0.05$).

Overall, thermal time lag was much shorter in canopies (7.56 2.6 min) than in soils (1.5 0.3 hours, Fig. 5). LAI classes had a significant positive effect on thermal time lag for both canopy and soil layers (Table 1). On average, thermal time lag increased by 2 min. in canopies and 30 min. in soils between two LAI classes. Similarly, elevation had a significant positive effect on thermal time lag for both canopy and soil layers (Table 1) with an average increase of 2 0.3 min. in canopies and of 60 31 min. in soil between two altitudinal belts (Fig. 5).

3. Thermal performance curve using local vs. interpolated temperatures

To assess the implication of local vs. global interpolated temperature discrepancies for crop pest performances, we plotted the frequency distribution of the minimum (blue bars), maximum (red bars) and mean local (stripped bars) temperatures and those given by WorldClim (from minimum to maximum temperature, shaded region in the background) with the temperature-dependent growth rate curve of the potato moth *P. operculella* (Fig. 6). As a general pattern, global interpolated temperature ranges predicted lower growth rates of *P. operculella* than those predicted by local temperatures at all elevations, in both inside-canopy and soil layers (where the pest lives most of their time). While mean temperature distribution generally fell within the WorldClim min-max range, extreme temperatures (and especially maximum ones) largely exceeded this range.

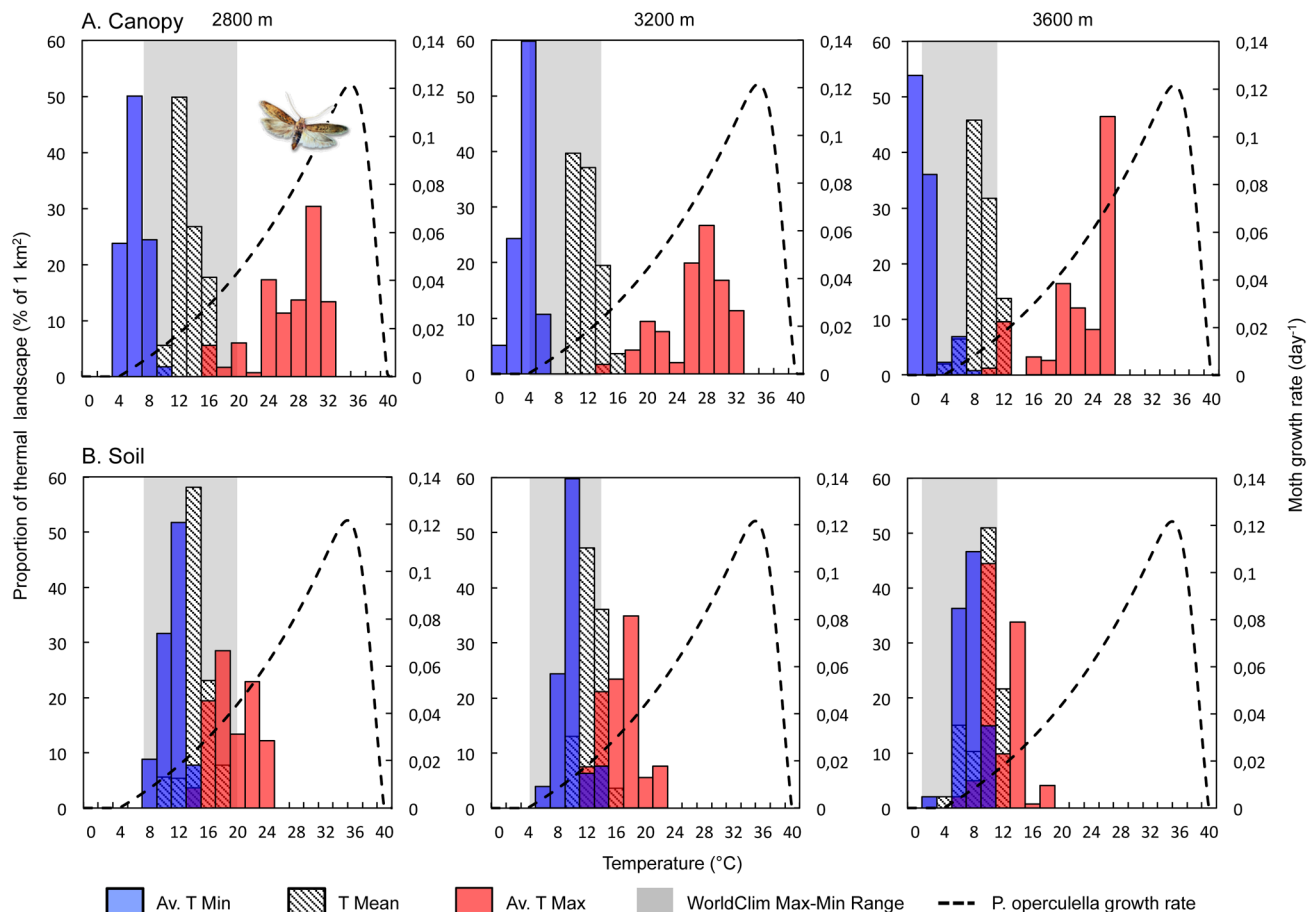


Figure 6. Superimposed plot of the temperature-dependent growth rate curve of the potato moth *Phthorimaea operculella* (dashed line) and the frequency distribution (% of area) of average minimum (blue), maximum (red) and mean (striped) temperatures for canopy and soil layers at the three studied elevations. Grey (shaded) bands in the background represent the WorldClim minimum and maximum temperature range. doi:10.1371/journal.pone.0105541.g006

The WorldClim estimations predicted *P. operculella* growth rates ranging between 0.007 and 0.045 day^{-1} at 2800 m, and between 0 and 0.018 day^{-1} at 3600 m, the maximum rates being slightly lower than those predicted by soil temperatures (0.068 day^{-1} at 2800 m and 0.037 day^{-1} at 3600 m). These differences were exacerbated in canopy layers where estimated maximum growth rates were 2.6–4.3 times higher than those predicted by WorldClim (0.118 day^{-1} at 2800 m and 0.079 day^{-1} at 3600 m). Discrepancies between WorldClim and local temperature-based growth rate estimations were not significantly affected by elevation (One-way ANOVA, $F = 7.79$, $P = 0.219$ and $F = 1.67$, $P = 0.419$ for canopies and soils, respectively).

Discussion

Accurate predictions of the responses of organisms to climate change using SDMs require knowledge of microclimates at spatial and temporal scales relevant for studied organisms [13,34,35]. To our knowledge, our study is the first to quantify the thermal heterogeneity among a set of agricultural habitats at fine spatial and temporal scales and to compare those thermal microhabitats to the most widely used global climatic dataset in SDMs. By documenting the mosaic of thermal habitats found in tropical agricultural landscapes, our study confirms previous evidence that microclimates strongly differ from nearby macroclimates due to

the variability of air motion and solar radiation patterns created by complex topographies with heterogeneous elevation, slope angle, exposure or roughness [1,7,18,36]. Our study therefore supports the view that results from the long tradition of agrometeorological studies on microclimates (e.g. [6,17,22]) have to be revived in the new context of microhabitat modelling for predicting the response of organisms to climate change.

1. LAI-based and elevation-based climate heterogeneity

In contrast to many previous studies (see [7] for a review), our objective was not to examine the well-documented effect of topography on local temperatures but rather to examine the less-known effects of habitat types and vegetation land cover on thermal landscape features. We found significant thermal time lag and buffer effects on air temperatures by plant and soil layers below crop canopies during night-time and daytime. The top of canopies reflects and absorbs part of the solar radiation during the day, allowing less energy to reach the layers (plants and soils) below canopies. During the night, infrared heat released from both the ground and plants is partly held back by the canopy above [5]. As a consequence plants and soils limit night-time cooling and daytime warming [6], leading to a significant buffer effect of minimum and maximum temperatures [1,4,17]. That is also why we found a buffer effect on air temperatures by soil higher during

night-time than daytime and the opposite pattern for crop canopies.

Our results indicate a strong effect of elevation on thermal buffering and thermal time lag by canopy and soil layers. This could result from the combination of a negative relationship between elevation and air temperature and a positive relationship between elevation and solar radiation exposure, part of which is absorbed by plants and soils [6]. As a result, the difference between air temperature and canopy and soil temperature increased with elevation. Interestingly, the modifications of local temperatures by habitats and LAI were of the same magnitude (from 2.70 to 4.82°C in average) than that generated by topography-related factors [7,36], supporting the need to better consider habitat effects on microclimates.

2. Fine scale variations in temperature vs. climatic units

Our findings show that the complex agricultural mosaic resulting from habitat types and LAI classes at the landscape scale was a major modifier of the thermal patterns in the studied tropical highlands. More importantly, our findings revealed that, at best, 55% of landscape habitats had real mean air temperatures that were well estimated by WorldClim predictions while in average less than 20% of these areas had minimum and maximum air temperatures well estimated. Additional thermal discrepancies between large and fine-scale temperatures resulted from heterogeneity in crop types and phenologies. This strongly supports the view that the common use of the WorldClim database arrayed into 1-km² grids may not adequately capture the reality of the climatic environment experienced by living organisms, in particular tiny ectothermic species [2,3,13,18]. It is important to note that to obtain the highest level of thermal heterogeneity we chose a complex mountainous agricultural study area that provided boundary conditions for climate modelling. Indeed, these mountainous areas provide strong climatic gradients and extreme habitat fragmentation which combined with un-seasonal agrosystem make up a mosaic of thermal patches that expanded the difficulties to faithfully assess climatic parameters for modelling [25]. In view of the urgent need of fine scale climate data with large extent [2,8,35] more research is necessary to develop accurate up- or down-scaling methods, in mountainous locations where thermal heterogeneity is large, and may be needed to properly describe the ecologically significant microclimates [7,37].

3. Microclimates and species distribution models

From tiny insects to mega-herbivores, it is well recognized that species ecology is strongly influenced by micro-climatic features of the landscape [2,10,11,12,13] yet quantitative information on how thermal landscape heterogeneity may affect species performance is scarce. Short-scale differences in temperatures may provide opportunities for individual organisms, even with limited dispersal capabilities, to escape unfavourable microclimates or to maximize physiological performances by selecting preferred microclimates [38,39]. Our analysis showed that predictions of *Peroporella* growth rates strongly differed between Wordclim-based and locally-measured temperatures, suggesting that global species distribution models using global coarse-scale climatic datasets without further microclimate modelling could be strongly limited to accurately predict species occurrence and performance, in particular that of ectotherms living in habitats such as mountain slopes. Such a spatial heterogeneity in thermal patches, where climatic conditions are strongly modified, provides a mosaic of favourable, sub-optimal or lethal thermal habitats that directly influences the performance of natural populations of ectotherms.

Coarse-extent modeling of microclimate is currently one of the major obstacles to predicting how organism will react to their experienced environments and forecast their distribution under climate change [8]. To date, two main types of models have been shown to provide relatively accurate, continent-wide calculations of microclimate: statistical model and mechanistic model [13]. The first one is statistical as the variables are not deterministically but stochastically related. These models perform statistical correlation of species occurrences with climatic data and have proven to be powerful interpolative tools for defining and projecting climatic envelopes [40,41]. A disadvantage of these statistical models is that they can only be applied to the conditions under which they are fitted. On the other hand, mechanistic models of the climatic responses of organisms [13,34] use fundamental knowledge of the interactions between process variables to define the model structure. Therefore they do not require much data for model development and validation. One of them is the Microclim model recently developed by [35,42] for all terrestrial landmasses except Antarctica which quantify key microclimatic parameters at macro-scales, with a relatively fine spatial (15 km²) and temporal resolution (hours). The microclimatic parameters such as wind velocity, humidity, and solar radiation allow building energy and mass budgets of organisms, and therefore serve as key inputs for biophysical models of species distributions.

It is important to highlight that a better spatiotemporal resolution in temperature patterns should go in pair with the development of more accurate temperature-based population dynamics models to integrate it [2,13,34,43]. Existing predictions of models based on insect response measured in constant temperatures may yield different and less realistic results than those from predictions of models that include the effect of real temperature fluctuation on insect biology [33]. For example, to date, we still do not know the impact of a few hours of warm temperature for the performance of ectotherm species at longer time scales [33]. In this context, fine-scale spatiotemporal temperature mapping has revealed a key step for any studies aiming at understanding, predicting and managing the responses of species distributions to climate change.

Supporting Information

Appendix S1 Habitat and field size distribution in the three studied altitudinal belts. (PDF)

Appendix S2 Photos of the temperature recording experiment. (PDF)

Appendix S3 Spatial variability of temperatures within a field. (PDF)

Appendix S4 Comparison of time series analysis outputs using 15 days vs. 1-year temperature data. (PDF)

Appendix S5 Fourier analysis description. (PDF)

Appendix S6 Seasonality measured on four year air temperature time series with Discrete Fourier Transform. (PDF)

Appendix S7 Crop habitat composition survey used in the study area. (PDF)

Appendix S8 Local and global air mean temperature discrepancies mapping.
(PDF)

Appendix S9 Microclimate temperature time-series used in this work # 1.
(ZIP)

Appendix S10 Microclimate temperature time-series used in this work # 2.
(ZIP)

Appendix S11 Microclimate temperature time-series used in this work # 3.
(ZIP)

References

- Scherrer D, Korner C (2011) Topographically controlled thermal-habitat differentiation buffers alpine plant diversity against climate warming. *J Biogeogr* 38: 406–416.
- Bennie J, Hodgson JA, Lawson CR, Holloway CTR, Roy DB, et al. (2013) Range expansion through fragmented landscapes under a variable climate. *Ecol Lett* 117: 285–229.
- Logan ML, Huynh RK, Precious RA, Calsbeek RG (2013) The impact of climate change measured at relevant spatial scales: new hope for tropical lizards. *Global Change Biol* 19: 3093–3102.
- Scheffers BR, Edwards DP, Diesmos A, Williams SE, Evans TA (2013) Microhabitats reduce animal's exposure to climate extremes. *Global Change Biol* 20: 495–503.
- Geiger R (1965) *The climate near the ground*. Cambridge, USA.
- Jones HG (1992) *Plants and microclimate: a quantitative approach to environmental plant physiology*. Cambridge University Press, Cambridge.
- Dobrowski SZ (2011) A climatic basis for microrefugia: the influence of terrain on climate. *Global Change Biol* 17: 1022–1035.
- Potter KA, Woods HA, Pincebourde S (2013) Microclimatic challenges in global change biology. *Global Change Biol* 19: 2932–2939.
- Cloudsley-Thompson JL (1962) Microclimates and the distribution of terrestrial arthropods. *Annu Rev Entomol* 7: 199–222.
- Tracy CR (1977) Minimum size of mammalian homeotherms: role of the thermal environment. *Science* 198: 1034–1035.
- Willmer PG (1982) Microclimate and the environmental physiology of insects. *Adv Insect Physiol* 16: 1–57.
- Unwin DM, Corbet SA (1991) *Insects, plants and microclimate*. Richmond Publishing Company Ltd.
- Kearney M, Porter W (2009) Mechanistic niche modelling: combining physiological and spatial data to predict species' ranges. *Ecol Lett* 12: 334–350.
- Beaumont LJ, Pitman AJ, Poulsen M, Hughes L (2007) Where will species go? Incorporating new advances in climate modelling into projections of species distributions. *Global Change Biol* 13: 1368–1385.
- Deutsch CA, Tewksbury JJ, Huey RB, Sheldon KS, Ghalambor CK, et al. (2008) Impacts of climate warming on terrestrial ectotherms across latitude. *P Natl Acad Sci USA* 105: 6668–6672.
- Warren RJ, Chick L (2013) Upward ant distribution shift corresponds with minimum, not maximum, temperature tolerance. *Global Change Biol* 19: 2082–2088.
- Suggitt AJ, Gillingham PK, Hill JK, Huntley B, Kunin WE, et al. (2011) Habitat microclimates drive fine-scale variation in extreme temperatures. *Oikos* 120: 1–8.
- Sears MW, Raskin E, Angilletta MJ (2011) The world is not flat: defining relevant thermal landscapes in the context of climate change. *Integr Comp Biol* 51: 666–675.
- Dangles O, Carpio C, Barragan AR, Zeddam JL, Silvain JF (2008) Temperature as a key driver of ecological sorting among invasive pest species in the tropical Andes. *Ecol Appl* 18: 1795–1809.
- McCain CM (2007) Could temperature and water availability drive elevational species richness patterns? A global case study for bats. *Global Ecol Biogeogr* 16: 1–13.
- Dangles O, Carpio FC, Villares M, Yumisaca F, Liger B, et al. (2010) Community-based participatory research helps farmers and scientists to manage invasive pests in the Ecuadorian andes. *Ambio* 39: 325–335.
- Baldocchi DD, Verma SB, Rosenberg NJ (1983) Microclimate in the soybean canopy. *Agr Meteorol* 28: 321–337.
- Wilhelm WW, Ruwe K, Schlemmer MR (2000) Comparisons of three-leaf area index meters in a corn canopy. *Crop Sci* 40: 1179–1183.
- Fitzpatrick EA (1964) Seasonal distribution of rainfall in Australia analysed by Fourier methods. *Archiv Meteorologie, Geophysik und Bioklimatologie* 13: 270–286.
- Hijmans RJ, Cameron SE, Parra JL, Jones PG, Jarvis A (2005) Very high resolution interpolated climate surfaces for global land areas. *Int J Climatol* 25: 1965–1978.
- Crespo-Perez V, Rebaudo F, Silvain JF, Dangles O (2011) Modeling invasive species spread in complex landscapes: the case of potato moth in Ecuador. *Landscape Ecol* 26: 1447–1461.
- Rondon S (2010) The potato tuberworm: a literature review of its biology, ecology, and control. *Am J Potato Res* 87: 149–166.
- Hanafi A (1999) Integrated pest management of potato tuber moth in field and storage. *Potato Res* 42: 373–380.
- Cameron PJ, Walker GP, Penny GM, Wigley PJ (2002) Movement of potato tuberworm within and between crops, and some comparisons with diamondback moth. *Environ Entomol* 31: 65–75.
- Crespo-Pérez V, Dangles O, Re'gnière J, Chuine I (2013) Modeling temperature-dependent survival with small datasets: insights from tropical mountain agricultural pests. *Bul Entomol Res* 103(03): 336–343.
- Sharpe PJH, DeMichele DW (1977) Reaction-kinetics of poikilotherm development. *J Theor Biol* 64: 649–670.
- Schoolfield RM, Sharpe PJH, Magnuson CE (1981) Non-linear regression of biological temperature-dependent rate models based on absolute reaction-rate theory. *J Theor Biol* 88: 719–731.
- Gilbert E, Powell JA, Logan JA, Bentz BJ (2004) Comparison of three models predicting developmental milestones given environmental and individual variation. *B Math Biol* 66(6): 1821–1850.
- Buckley LB, Urban MC, Angilletta MJ, Crozier LG, Rissler LJ, et al. (2010) Can mechanism inform species' distribution models? *Ecol Lett* 13: 1041–1054.
- Kearney M, Shamakhya A, Tingley R, Karoly DJ, Hoffmann AA, et al. (2013) Microclimate modelling at macro scales: a test of a general microclimate model integrated with gridded continental-scale soil and weather data. *Global Change Biol* Doi : 10.1111/2041–210X.12148.
- Scherrer D, Korner C (2010) Infra-red thermometry of alpine landscapes challenges climatic warming projections. *Global Change Biol* 16: 2602–2613.
- Fridley JD (2009) Downscaling climate over complex terrain: high finescale (1000 m) spatial variation of near-ground temperatures in a montane forested landscape. *J Appl Meteorol Clim* 48: 1033–1049.
- Kinahan AA, Pimm SL, van Aarde RJ (2007) Ambient temperature as a determinant of landscape use in the savanna elephant, *Loxodonta africana*. *J Therm Biol* 32: 47–58.
- Dillon ME, Liu R, Wang G, Huey RB (2012) Disentangling thermal preference and the thermal dependence of movement in ectotherms. *J Therm Biol* 37: 631–639.
- Guisan A, Thuiller W (2005) Predicting species distribution: offering more than simple habitat models. *Ecol Lett* 8: 993–1009.
- Elith J, Leathwick JR (2009) Species distribution models: ecological explanation and prediction across space and time. *Annu Rev Ecol Evol* 40: 677–697.
- Kearney MR, Isaac AP, Porter WP (2014) microclim: Global estimates of hourly microclimate based on long-term monthly climate averages. *Scientific Data* 1.
- Bakken GS, Angilletta MJ (2014) How to avoid errors when quantifying thermal environments. *Func Ecol* 8: 96–107.
- Bloomfield P (2004) *Fourier analysis of time series: an introduction*. Wiley-Interscience, New York, USA.

Acknowledgments

We are grateful to the city council of Salcedo (Cotopaxi, Ecuador) for providing the digital shape files of the study area cadastre. We also thank all farmers who collaborated with us during fieldwork. And finally, we gratefully acknowledge Dr. Pincebourde S. and Dr. Duyck F. for their constructive scientific comments and suggestions.

Author Contributions

Conceived and designed the experiments: EF OD. Performed the experiments: EF MH. Analyzed the data: EF LB OD. Contributed reagents/materials/analysis tools: EF LB OD. Contributed to the writing of the manuscript: EF LB JFS OD.

Supporting Information of “Faye, E., Herrera, M., Bellomo, L., Silvain, J. F., & Dangles, O. (2014). Strong discrepancies between local temperature mapping and interpolated climatic grids in tropical mountainous agricultural landscapes. *PLoS ONE* 9(8): e105541”.

Appendix S1 : Habitat and field size distribution in the three studied altitudinal belts.

Appendix S2 : Photos of the temperature recording experiment.

Appendix S3: Spatial variability of temperatures within a field.

Appendix S4 : Comparison of time series analysis out- puts using 15 days vs. 1-year temperature data.

Appendix S5: Fourier analysis description.

Appendix S6: Seasonality measured on four year air temperature time series with Discrete Fourier Transform.

Appendix S7: Crop habitat composition survey in the study area.

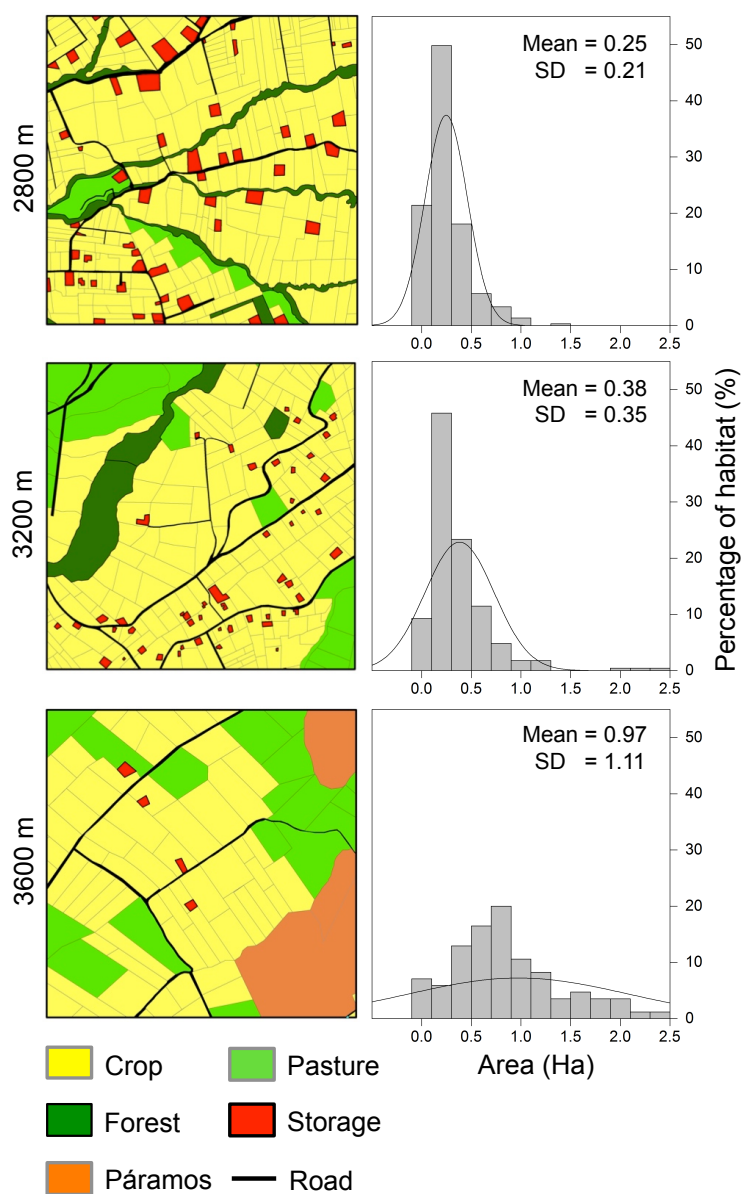
Appendix S1: Habitat and field size distribution in the three studied altitudinal belts.

Figure S1: Habitat mapping of the three studied 1-km² grid cells at their respective elevations (2800, 3200 and 3600 m) and the corresponding frequency distribution histograms of field areas.

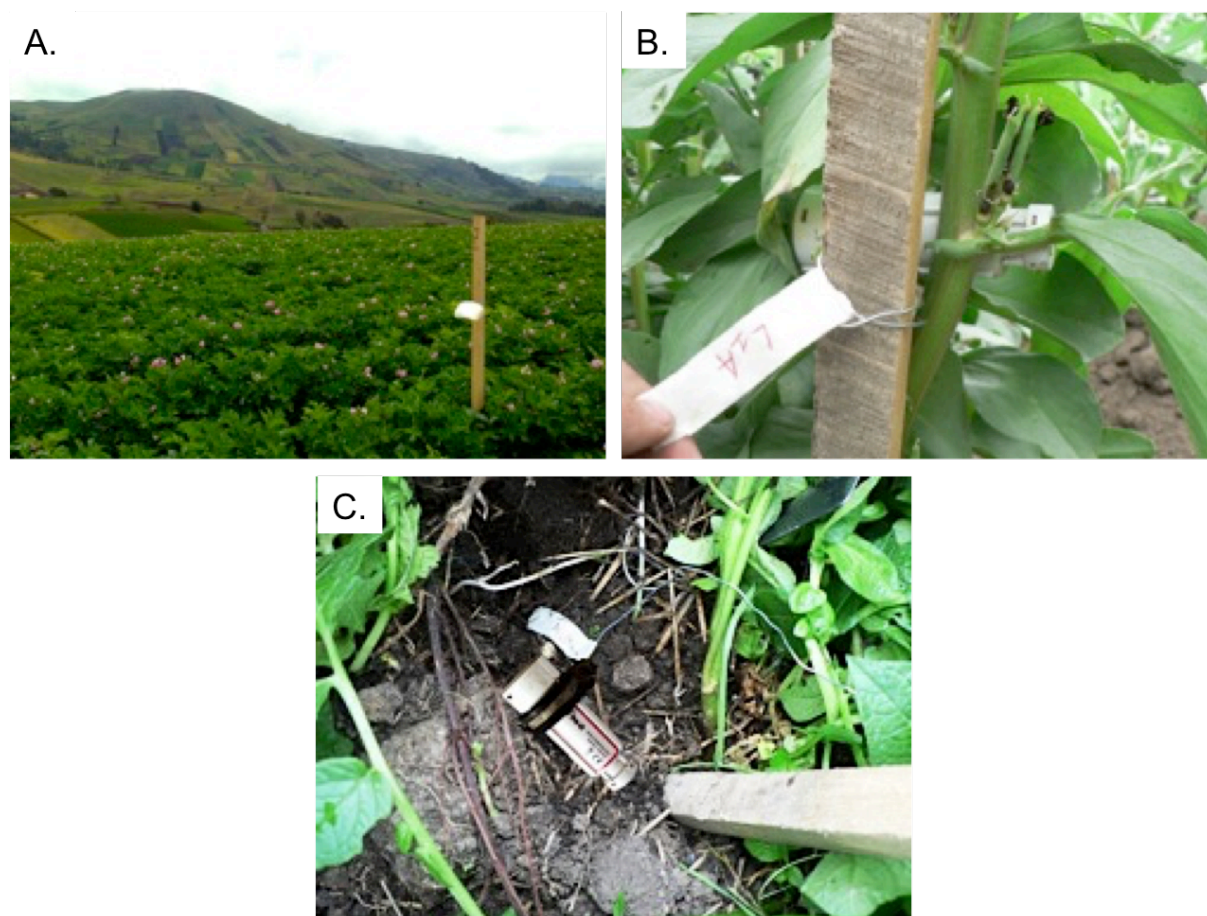
Appendix S2: Photos of the temperature recording experiment.

Figure S2: Photos of the temperature recording experiment. Photograph A. 20 cm² white plastic shelter placed 5 cm above the air logger fixed on a wooden stake at 1 m high in a fully-grown potato field. Photograph B. Air canopy logger (Hobo U23-001 Pro V2 internal temperature loggers, Onset Computer Corporation, Bourne, USA) placed 0.3 m high inside vegetation 5 cm below large leaves in a fully-grown broad bean field. Photograph C. Soil logger (Hobo U23-001 Pro V2 internal temperature loggers, Onset Computer Corporation, Bourne, USA) placed 10 cm inside ground before burial.

Appendix S3: Spatial variability of temperatures within a field.

Edge effect, micro-topography and LAI variations within a field can strongly change the microclimate of plant and soil layers creating heterogeneous thermal conditions at the field scale [6, 17, 22]. To address this issue, in a parallel experiment we measured air, air canopy and soil temperatures at six different locations within the same field. Measurements were replicated in 4 fields with area ranging from 596 to 672 m² of in order to capture to variability of field size in the study area. Fields were located between 2900 and 3000 m and were composed of fully-grown potatoes. Temperatures were recorded over one month using loggers (Hobo U23-001 Pro V2 internal temperature loggers, Onset Computer Corporation, Bourne, USA, 1 min time step) arranged as described in the main document (see part 2.2). Figure S3 shows that the discrete Fourier transformed amplitudes at the daily frequency of the one-month temperature time series did not vary among field location for both canopy and soil layers in the 4 replicate fields.

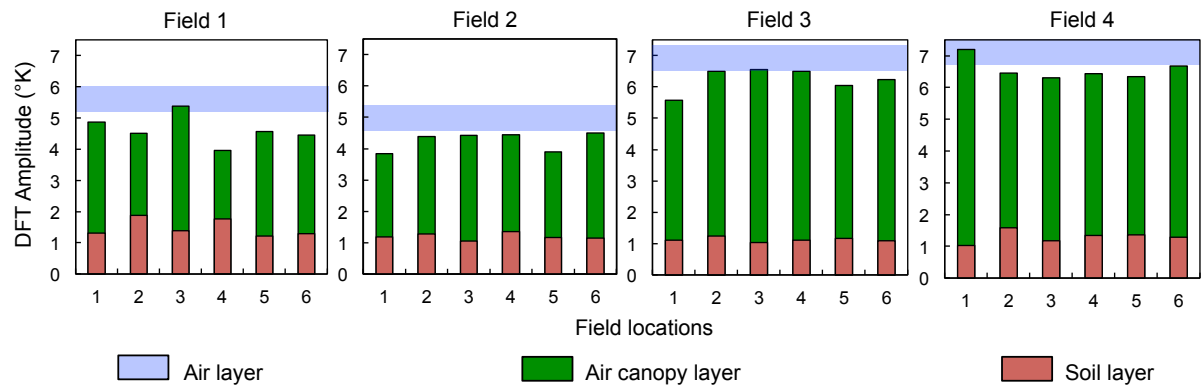


Figure S3: Histogram of the DFT amplitudes of air (light blue), canopy (green) and soil (brown) layers in the 4 fields studied.

Appendix S4: Comparison of time series DFT analyses outputs using 15 days vs. 1-year temperature data.

We assessed the relevance of using 15-days temperature time series as a good proxy of climatic conditions occurring over longer time scales (one year) using data from a four-year monitoring (2008-2012) of air temperatures, at three elevations in the study area. Air temperatures were measured using loggers (Hobo U23-001 Pro V2 internal temperature loggers, Onset Computer Corporation, Bourne, USA), covered by a plastic roof and fixed on a wooden stake 1 m high (see main document part 2.2 for details). Using the same Fourier transform analysis described in the main document, we then compared daily discrete Fourier transform amplitude A_d of 15-days air temperature time series vs. 1-year air temperature time series chosen randomly over the 4-year database. We ran between 10 and 50 pairs of time series (15 days vs. a year) for each elevation, the starting for each time series being chosen randomly among the three first years of the four-year air temperature data. We found a highly significant positive relationship between the amplitude of the 15-days and the 1-year Fourier transform at the daily period (see Fig S4). The slope of the 15-days vs. 1-year curve did not significantly differ from the 1:1 slope (ANCOVA, $df = 114$, $F = 2.08$, $p > 0.05$). The small variations observed between both slopes are likely the result of sporadic meteorological phenomena such as storms or hails.

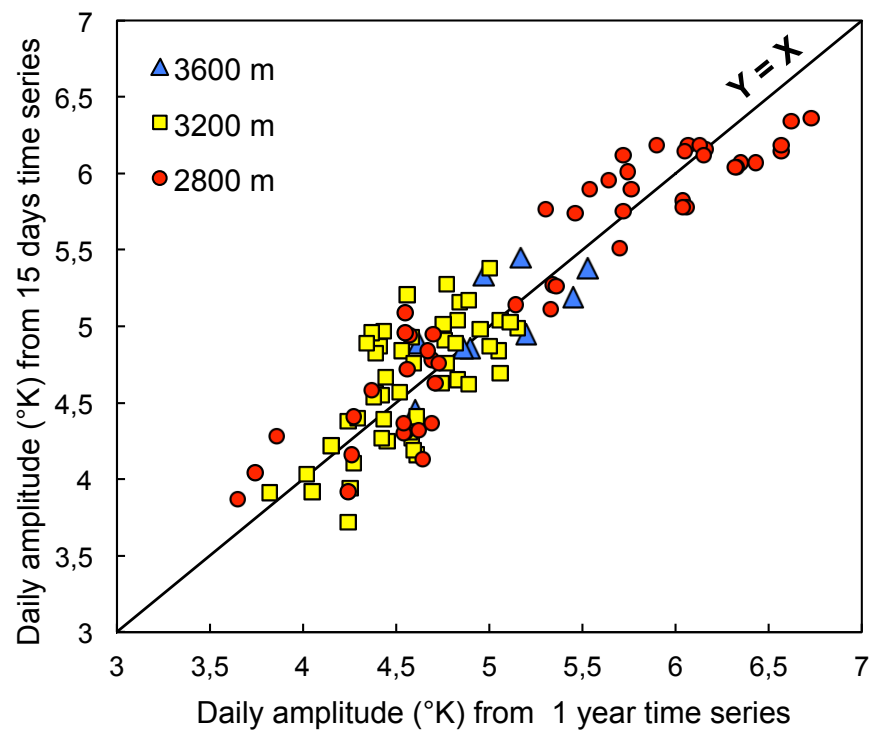


Figure S4: Scatter plot of Fourier transform amplitude for the daily frequency of a 15 days air temperature time series vs. a 1-year air temperature time series at three elevations.

Appendix S5: Fourier analysis description.

The Discrete Fourier Transform (DFT) used in this study was defined as follow:

$$X_k = \frac{1}{N} \sum_{n=0}^{N-1} x_n e^{-i2\pi k \frac{n}{N}}, \quad k = 0, \dots, N-1 \quad (\text{eqn 1})$$

where X_k , the Fourier transform complex coefficient, is the frequency domain representation of the signal time series x_n at the k_{th} frequency, N is the total number of samples of the time series, and i is the imaginary unit (see [36] for details). The amplitude A_d and the phase ϕ_d of the DFT are defined by definition (\triangleq) as follows:

$$A_d \triangleq |X_{k_d}| \quad (\text{eqn 2})$$

$$\phi_d \triangleq \arg(X_{k_d}) \quad (\text{eqn 3})$$

The thermal amplitude allowed us to measure the thermal buffer effect in Kelvin (see Fig. 1) between air and canopy layers (β^p) and air and soil layers (β^s), by calculating the difference of the DFT amplitudes as follows:

$$\begin{cases} \beta^p \triangleq A_d^a - A_d^p \\ \beta^s \triangleq A_d^a - A_d^s \end{cases} \quad (\text{eqn 4})$$

where A_d^a , A_d^p and A_d^s are the DFT amplitudes at the daily frequency for air, air canopy and soil time series, respectively (see equation 2).

As we were interested in amplitude differences between air vs. air canopy and air vs. soil for maximum and minimum daily temperatures, we then defined the daytime (M) and night-time (m) temperature excursions between air vs. plant canopy ($\epsilon_{M,m}^p$) and air vs. soil ($\epsilon_{M,m}^s$) as follows:

$$\begin{cases} \epsilon_M^p \triangleq A_0^a - A_0^p + \beta^p \\ \epsilon_M^s \triangleq A_0^a - A_0^s + \beta^s \end{cases} \quad (\text{eqn 6})$$

$$\begin{cases} \epsilon_m^p \triangleq A_0^a - A_0^p - \beta^p \\ \epsilon_m^s \triangleq A_0^a - A_0^s - \beta^s \end{cases} \quad (\text{eqn 7})$$

with A_0 is the mean DFT value of the time series.

The phase allowed us to measure the thermal time lag τ_d expressed in minute in

canopy (τ_d^p) and soil layers (τ_d^s) with respect to the air layer (see Fig. 1) by calculating the difference of the DFT phases as follows:

$$\begin{cases} \tau_d^p \triangleq \frac{24}{2\pi} (\phi_d^p - \phi_d^a) \\ \tau_d^s \triangleq \frac{24}{2\pi} (\phi_d^s - \phi_d^a) \end{cases} \quad (\text{eqn 8})$$

where ϕ_d^a , ϕ_d^p and ϕ_d^s are the DFT phases at the daily frequency for air, air canopy and soil time series, respectively (see equation 3).

All Fourier analyses were performed in MATLAB R2011a (The Mathworks Inc., Natick, USA).

Appendix S6: Seasonality measured on four-year air temperature time series with Discrete Fourier Transform.

Period (days)	Mean amplitude of the discrete Fourier transform (°K)		
	2800 m	3200 m	3600 m
91	0.14 (+/- 0.3)	0.15 (+/- 0.1)	0.12 (+/- 0.2)
182	0.41 (+/- 0.18)	0.49 (+/- 0.15)	0.43 (+/- 0.13)
364	0.94 (+/- 0.15)	1.01 (+/- 0.17)	0.96 (+/- 0.11)

Table S6: Mean amplitudes in Kelvin of the discrete Fourier transform at the seasonally frequencies (91, 182 and 364 days) of four year monitoring of air temperatures (recorded at 1 meter high with half an hour time step with the same shelter process describe above between 2008-2012) for the three altitudinal belts of the study area (2 replicates for each elevation).

Appendix S7: Crop habitat composition survey in the study area.

Crop habitat composition in the study area was measured in 85 independent locations at different altitudes between 2008 and 2012. The relative area of each crop type (in %) was visually estimated by two observers in a 100-m radius circle around each location. The mean of the two observations was then calculated. The phenological stage of each crop was also recorded.

Elevation	Potato	Broad bean	Corn	Alfalfa	Pasture
2800 m	20.9	13.4	18.4	16.5	30.8
3200 m	24.1	13.3	15.9	12.5	34.2
3600 m	27.3	9.1	6.6	7.6	49.4

Table S7: Mean crop composition (%) at three altitudes used to parameterize thermal landscape mapping (see Fig. 2 & 3 in the main document). The number of independent location were N = 43, 25, 17 at 2800, 3200, and 3600 m, respectively.

Appendix S8: Local and global air mean temperature discrepancies mapping.

Differences in mean temperatures between local air temperatures (extracted from the Fourier transform) and the global coarse grain interpolated air temperatures from the WorldClim ($\Delta \text{Air}_L - \text{Air}_{WC}$) were mapped for the three studied grid cells (Fig. S8). Generally, local air temperatures were 1.4°K warmer than the global interpolated ones. Mean temperature discrepancies were of $0.3 \pm 1^\circ\text{K}$, $1.7 \pm 1.6^\circ\text{K}$ and $2.3 \pm 1.5^\circ\text{K}$ at 2800 m, 3200 m and 3600 m respectively. For the three studied grid cells minimum of average temperature discrepancies was -2°K and maximum reached $+8^\circ\text{K}$. As a consequence, $44.6 \pm 3.4\%$ of the studied areas were either under-estimated or over-estimated by the global climatic models ($\pm 1^\circ\text{K}$).

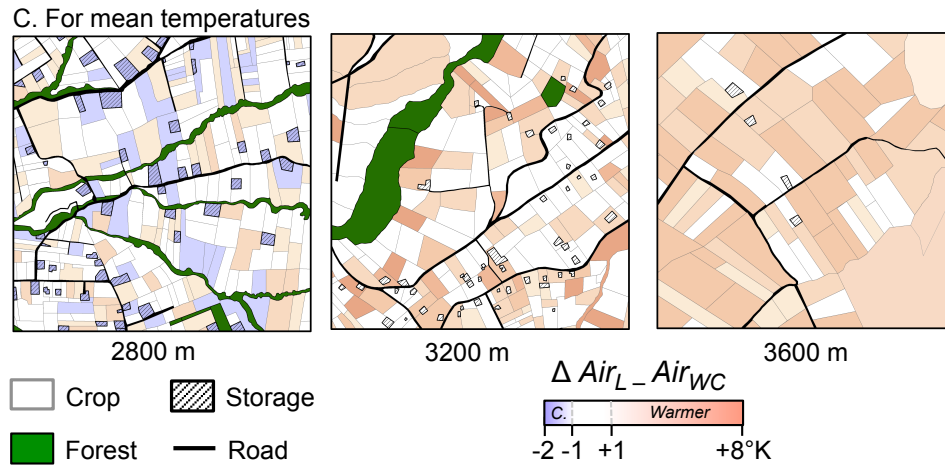


Figure S8: Maps showing the differences between the measured local air temperatures and the WorldClim interpolated temperatures for mean values ($\Delta \text{Air}_{Local} - \text{Air}_{WorldClim} = \Delta \text{Air}_L - \text{Air}_{WC}$). Blue colours indicate $\Delta \text{Air}_L - \text{Air}_{WC} < 0$, i.e. area where local air temperatures are cooler than the ones gave by WorldClim, red colours indicate $\Delta \text{Air}_L - \text{Air}_{WC} > 0$, i.e. area where air local temperatures are warmer than the ones gave by the WorldClim, and white colours $\Delta \text{Air}_L - \text{Air}_{WC} = 0$ indicate areas where air WorldClim temperatures equate air local temperatures ($\pm 1^\circ\text{C}$). The extent and position of each square is equal to the spatial resolution of the WorldClim database: 30-arc sec that is the equivalent of 0.86 km^2 for the study area. Each side of square has a 925 m length. The temperature dataset for storages was obtained from [26].

CHAPTER II

Methods for assessing thermal heterogeneity in agricultural landscapes

PART I

While in the Chapter I of this thesis, we used standard methods of thermal ecology for pointing out the importance of considering microclimates when evaluating pest performances in agricultural landscapes, this second Chapter focused on the development of new methodologies to better assess the spatiotemporal heterogeneities of microclimatic temperatures at relevant spatial scales.

The first part of this chapter focused on one critical and poorly studied pitfall of the uses of thermal infrared cameras in ecological and biological studies to measure the thermal heterogeneity of species' habitats: we studied how short variation in the shooting distance (i.e., distance between the thermal camera and the study object) could lead to misestimates of the spatial heterogeneity of object surface temperatures. This work was performed in Tours, France in collaboration with the 'Institut de Recherche sur la Biologie de l'Insecte' (IRBI) of the François Rabelais University and the French National Center for Scientific Research (CNRS). This first part of the Chapter II is made of one publication currently accepted after major revisions in *Journal of Thermal Biology*:

- **Faye, E., Dangles, O., & Pincebourde, S. (2015).** Distance makes the difference in thermography for ecological studies. *Journal of Thermal Biology*. Doi: 10.1016/j.jtherbio.2015.11.011.

Moreover, this study has been presented at the *Heteroclim international workshop* the 10-14th of June 2014 with the poster in Appendix S2. Finally, we illustrated the uses of thermal cameras on agricultural landscapes by 2 short movies available at:

- [TIR/VIS Time lapses of Ecuadorian agricultural landscapes. 2014.](#)
- [TIR and VIS comparaison on the study site. 2014.](#)



Title: Distance makes the difference in thermography for ecological studies

Authors: E. FAYE^{a,b,c}, O. DANGLES^a, S. PINCEBOURDE^d

Affiliations:

^a UMR EGCE, IRD-247 CNRS-UP Sud-9191, 91198 Gif-sur-Yvette cedex, France.

^b Sorbonne Universités, UPMC Univ Paris 06, IFD, 4 Place Jussieu, 75252 Paris cedex 05, France.

^c Pontifica Universidad Católica del Ecuador, Facultad de Ciencias Exactas y Naturales, Quito, Ecuador.

^d Institut de Recherche sur la Biologie de l’Insecte (IRBI, CNRS UMR 7261), Faculté des Sciences et Techniques, Université François Rabelais, Tours 37200, France.

Corresponding authors: Emile Faye - ehfaye@gmail.com; Sylvain Pincebourde - sylvain.pincebourde@univ-tours.fr

Abstract

Surface temperature drives many ecological processes and infrared thermography is widely used by ecologists to measure the thermal heterogeneity of species' habitats. However, the potential bias in the temperature readings caused by the shooting distance (between the surface to be measured and the camera) is still poorly acknowledged. We examined the effect of shooting distance from 0.3 to 80 m on a variety of thermal metrics (mean temperature, standard deviation, patch richness and aggregation) to depict the relationship between those metrics and the shooting distance under various weather conditions and for different structural complexity of the studied surface (various surfaces with vegetation). We found that the shooting distance is a key modifier of the absolute temperature measured by thermal infrared camera. A non-linear relationship between shooting distance and mean temperature, standard deviation and patch richness led to a strong under-estimation of the thermal metrics within the first 20 m and then a slight decrease between 20 to 80 m from the object. Also, solar radiation enhanced the bias with increasing distance. Therefore, surface temperatures were underestimated as shooting distance increased and thermal mosaics were homogenised at long distance with a much stronger bias in the warmer than the colder parts of the distributions. The under-estimation of thermal metrics due to shooting distance was explained by the lower atmosphere composition and the pixel size effect. The structural complexity of the surface had little effect on the surface temperature bias. Finally, we provide general guidelines for ecologists to minimize inaccuracies caused by the distance from the studied surface in thermography.

Keywords: thermography; thermal bias; shooting distance; microclimate; leaf temperature.

1. Introduction

Surface temperature drives many physical, chemical, biological and ecological processes and is among the most influent factors for life across all biomes including marine, terrestrial and freshwater ecosystems (Oke 1987, Kingsolver 2009). Several methodologies have been developed to measure surface temperatures. Among them, infrared thermography is the only non-invasive method, and major developments over the past decades significantly improved our understanding of temperature-related patterns in ecological sciences (Quattrochi & Luvall 1999, Cilulko *et al.* 2013, Lathlean & Seuront 2014). Originally, infrared thermography was developed mainly for industrial, medical and military applications (Vollmer & Möllmann 2010), and it was first used for ecological research in the late sixties (e.g., studies on seal thermoregulation, Ørtisland 1968, and on white-tailed deer detection, Croon *et al.* 1968). Over the last four decades, infrared thermography has been increasingly used in various fields of biology including thermal physiology (Hill *et al.* 1980, Pincebourde *et al.* 2012, Woods 2013, McCafferty *et al.* 2013), marine ecology (Lathlean & Seuront 2014), plant sciences (Jones 2002, 2013, Pincebourde & Woods 2012, Caillon *et al.* 2014), agronomy (Jackson *et al.* 1981, Jones 2002, Inagaki *et al.* 2008, Meron *et al.* 2010, Bellvert *et al.* 2013, Faye *et al.* 2015), and landscape ecology (Scherrer & Körner 2010, Tonolla *et al.* 2010).

Infrared thermography is an imaging method that records infrared waves emitted by an object in the electromagnetic spectrum after the visible range of light – from 7.5 to 14 μm – as a result of the molecular motion (Vollmer & Möllmann 2010). The radiation readings are then converted into surface temperature by the Thermal Infra-Red (TIR) camera taking into account the ambient conditions and emissivity. TIR images allow the study of surface temperature patterns over a broad range of spatial scales from sea and land surface satellite mapping (Kerr & Ostrovsky 2003) to landscape (Scherrer & Korner 2010) and organism scales (Tattersall & Cadena 2010, Pincebourde *et al.* 2013). Recent advances in thermal

imaging technology – increasingly lightweight and hand-held – and a reduction in the cost of thermal cameras have facilitated its uses and opened new area of investigation in ecological sciences ([Lathlean & Seuront 2014](#)).

However, despite its increasing use, relatively few studies have addressed or reviewed the potential pitfalls and limits of thermal imaging (Clark 1976, Quattrochi & Luvall 1999, Minkina & Dudzik 2009, [Cilulko *et al.* 2013](#), [Lathlean & Seuront 2014](#)). Weather conditions (e.g. solar radiation and rainfall) are known to affect TIR outputs leading to misinterpretation of organism body temperatures. Also, the emissivity of an object – i.e. the ability of an object to emit thermal radiation – and the viewing angle between the camera and the object can affect the surface temperature measurements ([Clark 1976](#)). Last, the distance between the object and the TIR camera is among the main factors supposed to impact temperature values in TIR images ([Cilulko *et al.* 2013](#)). Like any image, TIR images are composed of pixels, and the portion of object surface area included in a single pixel directly depends on the shooting distance – with larger area included in each pixel as shooting distance increases. Then, when the surface is thermally heterogeneous, neighbouring surface patches of different temperature merge together with increasing distance. To our knowledge, however, the net effect of increasing shooting distance on temperature readings by TIR camera has never been quantified. At best, TIR images are acquired at equal distances from the study organism allowing accurate estimates of relative temperature differences between patches ([Inagaki *et al.* 2008](#), [Tonolla *et al.* 2012](#), [Caillon *et al.* 2014](#)).

Here, we examined the effect of shooting distance (in the range of 0.3 to 80 m) on TIR thermal metrics that are commonly used to quantify the spatial heterogeneity of object temperatures (e.g., mean temperature, standard deviation, patch richness and aggregation). The aims of this study were 1) to characterize the relationship between those thermal metrics and the shooting distance, 2) to assess the effect of weather conditions (solar radiation) on this

relationship, and 3) to test whether the structural complexity of the studied surface affected this relationship. We first shot the same object surface (a thermal test card corresponding to a regular mosaic of black and white patches) under various global solar radiation levels with two similar TIR cameras placed at different distances. We then shot three object surfaces with different structure under identical global solar radiation with the two TIR cameras placed at various distances. The object surfaces consisted in a thermal test card under constant environmental conditions in the laboratory, a green wall covered by a deciduous woody vine scene, and an oak-beech forest edge offering a more complex scene. Additionally, we performed a TIR close-up shooting (0.3 m) of the plant leaves to assess how actual leaf temperatures shaped the surface temperature distribution from each shooting distance and compare the micro-scale thermal heterogeneity of the leaves to the one of the entire surface. Generally, we expected that the distance between the thermal camera and the studied object would lead to errors in the absolute surface temperature because of the pixel size effect. We also expected this bias to be more pronounced when the surface is heated by solar radiation. Finally, under similar abiotic conditions, structurally complex surfaces are supposed to deliver more thermal heterogeneity than simpler ones and we hypothesized that the temperature measurements of these complex surfaces would be more affected by the shooting distance. Based on the TIR images obtained with two thermal cameras, we calculated thermal metrics and compared them among distances for various solar radiation levels and structural surfaces.

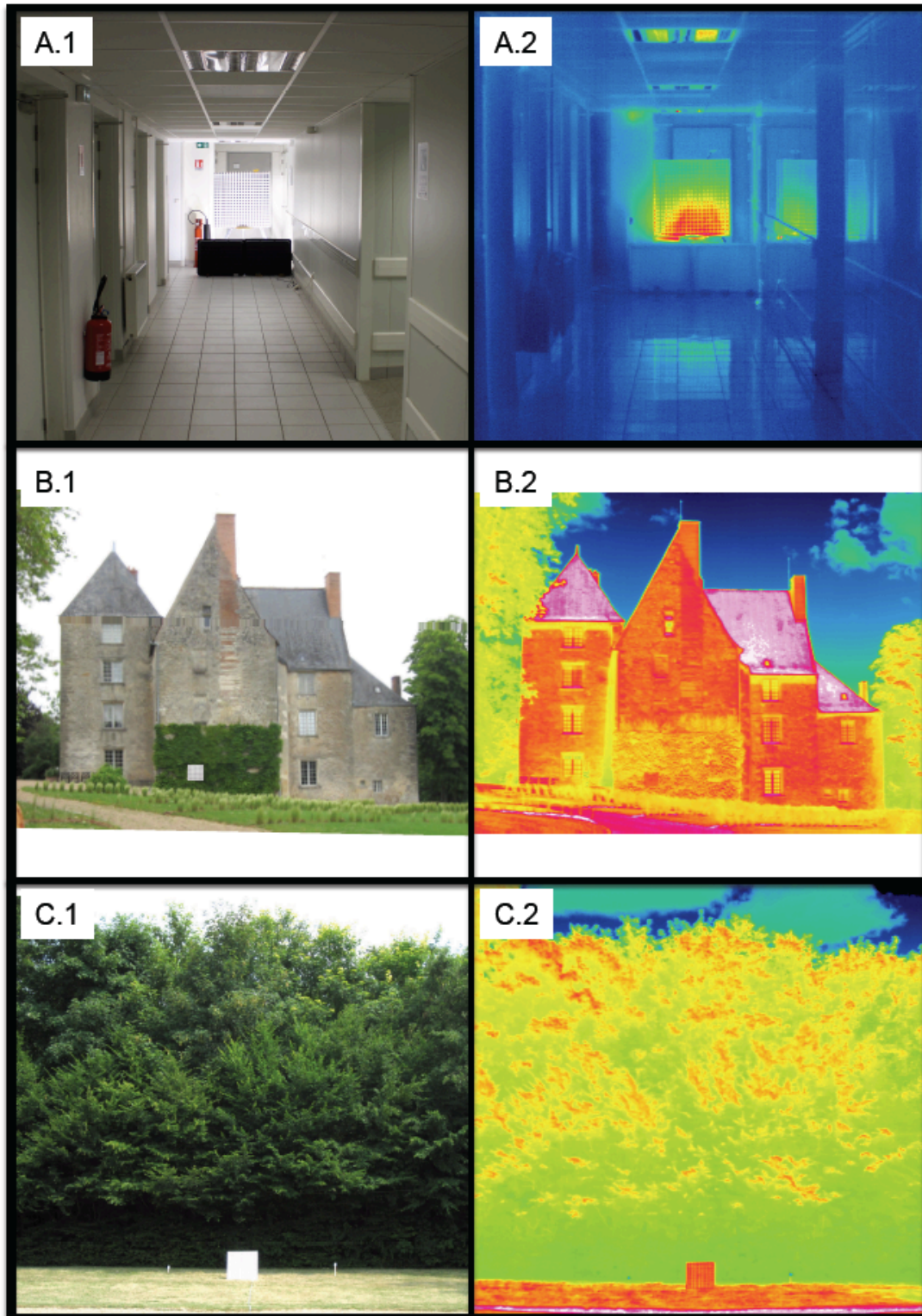


Figure 1: RGB images (A.1, B.1, C.1) and TIR images (A.2, B.2, C.2) of the 1-m² thermal test card placed in the three environments (laboratory A., green wall B. and wood edge C.) – Photos credits: Emile Faye (IRD) and Sylvain Pincebourde (CNRS).

2. Materials and Methods

2.1. The thermal infrared cameras

TIR images were acquired using two similar TIR cameras recording the long-wave infrared radiation emitted by objects in the spectral range from 7.5 to 14 μm . They were equipped with uncooled micro-bolometer sensors and converted the infrared radiation readings into temperatures within the -20 to 120°C calibration range. TIR images were processed assuming an emissivity of 1 for every surface because our interest was to quantify the discrepancies in spatial thermal heterogeneity between TIR images of the same surface taken at different distances – i.e. comparing relative values instead of measuring actual temperature values (Clark 1976, Rubio *et al.* 1997). Therefore, surface temperature refers to the brightness surface temperature in this work (Norman 1995). The first TIR camera (called fixed TIR camera, see below) was equipped with a 320×240 pixels micro-bolometer focal plane array (B335, FLIR Systems, Wilsonville, OR, USA). The second TIR camera (called mobile TIR camera, see below) was equipped with a 640×480 pixels micro-bolometer focal plane array (HR research 680, VarioCAMs, InfaTec GmbH, Dresden, Germany). These two TIR cameras were similar enough in terms of thermal sensitivity, accuracy, and spatial resolution to compare TIR data among them (Appendix 1).

2.2. Experimental design

2.2.1. Thermal test card in different environments

We studied a 1-m² thermal test card, made of 400 black and 400 white tiles of 2.5 cm² each, which delivered a well-characterized geometry and dimensions resulting in a predictable thermal pattern, with the black tiles reaching higher surface temperatures than the white ones when hit by radiation (Fig. 1). We placed the thermal test card vertically in three different environments that differed in term of abiotic parameters (exposure, temperature and global

solar radiation). The first environment – *the laboratory environment* – was a 50 m long corridor without window in our laboratory (Institut de Recherche sur la Biologie de l’Insecte, Tours, France) wherein air temperature and humidity were maintained constant by an air-cooling system, thereby resulting in a homogeneous environment along the hall (21.7°C and 63% of humidity; see Appendix 2). Global radiation was generated using two heat lamps (250 watts each) positioned on the ground one meter in front of, and oriented toward, the thermal test card (A.1 and A.2 in Fig. 1).

The second and third environments were outdoor, at the castle named *Château de Saché* in the Loire Valley, France (49°14’45’’N, 0°32’41’’E, at a mean elevation of 77 m a.s.l.). In July 2013, when the study took place, mean daily temperature reached 20°C (27.7 and 13.9 °C for mean maximum and minimum respectively) and photoperiod lasted almost 10 hours (Météo France, 2013). Thus, the plants reached their fully-grown phenology with the highest vegetation density in canopies at that time (Körner & Basler 2010). At this site, we first placed the thermal test card in front of a South-exposed green wall of the castle – *the green wall environment* – facing a flat area free of any obstacles (B.1 and B.2 in Fig. 1). Then, we positioned the thermal test card in front of a West-exposed wood edge in the court of the castle – *the wood edge environment* – facing a flat area free of any obstacles (C.1 and C.2 in Fig. 1).

2.2.2. TIR shots at increasing distances

To test whether the distance between the TIR camera and the object had an effect on the thermal metrics of surfaces, we used synchronised shots between the two TIR cameras placed at different distances in each of the three environments (laboratory, green wall and wood edge). Synchronising shots allowed us to compare TIR images taken under exactly the same environmental conditions – i.e. solar radiation and air temperature (Appendix 1) – thus giving

the effect of shooting distance directly. The fixed TIR camera was placed at a minimum distance from the surface so that it could capture a large extent: 2 m from the thermal test card in the laboratory, 3 m from the green wall and 10 m from the wood edge. The fixed TIR camera was considered to provide the most accurate absolute values of surface temperatures, and the highest level of thermal heterogeneity, as it was placed at the shortest distance. The mobile TIR camera shot from distances to the fixed camera of 1, 2, and 7 m – i.e. distance at which Δ pixel size ≥ 0 (Appendix 1, Figure 2) – and up to 48, 57 and 70 m in the laboratory, green wall and wood edge environments, respectively. One TIR shot was taken simultaneously with the two IRCs (less than 2 sec. differences between the two cameras, and each shot was repeated twice) at fourteen Δ distances (defined as the distance between the mobile and the fixed TIR cameras, see Appendix 3) along a straight and perpendicular transect to the surface to avoid view angle effects on temperature readings (Clark 1976). In total, we performed eight TIR shooting transects (two for the laboratory environment, three for the green wall environment and three for the wood edge environment) collecting up to 448 TIR images under various abiotic conditions (8 TIR shooting transects \times 14 Δ distances \times 2 repetitions \times 2 IRCs). At the end of each transect for the outdoor environments, we also took TIR images of leaf surfaces with the fixed TIR camera positioned at a 0.3 m distance from the vegetation surface (Appendix 4). Leaf surface temperature was measured for 15 shaded leaves and 15 leaves exposed to direct solar radiation. Initially, the leaves were selected randomly and thereafter the same leaves were measured during each session.

TIR cameras were switched on at least ten minutes before the beginning of each shooting to allow sensor stabilization. They were fixed on two professional tripods (MN 190X ProB, Manfrotto, Bassano Del Grappa, Italy) at 1.5 m above the ground to obtain a 90° view angle to the surface (Clark 1976). Simultaneously to each TIR image, we recorded global

solar radiation (in W/m^2) using a datalogger equipped with a pyranometer sensor facing the sky vault (datalogger LI-200 and pyranometer LI-400, LI-COR, Lincoln, OR, USA).

2.2.3. Differences among surfaces of different structural complexity

To examine whether surface complexity modulated the effect of shooting distance on TIR outputs, we used surfaces differing in their structural complexity: 1) the thermal test card surface was the less structurally complex because of its well-defined two-patches composition in one plan; 2) the fully-grown grape ivy green wall (*Parthenocissus tricuspidata*) covering the south-exposed wall of the castle – background of the green wall environment – was a more structurally complex surface because of the various inclination angles of the leaves that composed its almost two dimensional layout – the depth of the ivy cover did not exceed 20 cm; 3) the third level of complexity consisted in a fully-grown wood edge composed of oak-trees (*Quercus robur* L.), beech-trees (*Fagus sylvatica* L.), and hornbeam-trees (*Carpinus betulus* L.) – background of the wood edge environment –, which provided a highly complex surface composed of various patches in a three-dimensional configuration with tens of meters in depth that increased the compositional heterogeneity. For each set of outdoor TIR images, we worked on two 1-m^2 areas: the 1-m^2 thermal test card (see above) and a 1-m^2 area of vegetation placed just beside the thermal test card in the green wall and wood edge environments (see TIR images in Appendix 5).

2.2.4. Surface temperature excess

In order to determine the surface temperature excess – i.e. positive or negative deviation between pixel temperature values of the TIR images and ambient air temperature –, we measured ambient air temperatures using a set of temperature loggers (Hobo U23-001-Pro-V2, Onset Computer Corporation, Bourne, USA) placed within 5 cm behind the leaves and

the thermal test card. The loggers were always shadowed and homogeneously distributed (20 loggers inside the green wall and the wood edge, and 10 behind the thermal test card, see photographs in Appendix 6). Temperatures were recorded every 10 seconds with an accuracy of $\pm 0.21\text{K}$ and a resolution of 0.02K at 25°C . We standardized the TIR images using these air temperatures, which allowed us direct comparisons of the leaf and the surface temperature excesses in the two outdoor environments, regardless of their absolute temperature dissimilarities.

2.3. Data analysis

For each TIR image from the two TIR cameras, we marked the same 1-m^2 area of the thermal test card and the same 1-m^2 area of the vegetation surface (Appendix 5). Pixel temperature values on these 1-m^2 surfaces were extracted from raw images with ThermaCam Researcher software (FLIR Systems) and IRBIS 3 software (Infatec GmbH), for the fixed and the mobile TIR camera, respectively. We then calculated several thermal landscape indices from these pixel temperature matrices using FRAGSTATS (University of Massachusetts, Landscape Ecology Lab, Amherst, MA, USA): 1) mean temperature and standard deviation, providing a descriptive summary of the patch metrics for the entire landscape, 2) patch richness, calculated as the number of patch types present in a landscape and describing its compositional make-up (McGarigal & Marks 1994), 3) the aggregation index, often referred as landscape texture, which quantifies to what extent temperature pixels of the same value were spatially aggregated (He *et al.* 2000).

To analyse the effect of shooting distance on thermal metrics, we plotted the deviation in mean temperature (ΔT_{mean} in Kelvin), standard deviation (ΔSD in Kelvin), patch richness ($\Delta \text{patch richness}$) and aggregation ($\Delta \text{aggregation}$ in percentage) against the $\Delta \text{Distance}$ (m) between the two TIR cameras (mobile camera minus fixed camera) for each surface. Those

plots were represented for the various solar radiation levels in the three different environments (from 65 to 915 W/m²) and also for the three different surfaces – test card, green wall, wood edge – under similar and stable clear sky conditions (solar radiation of 890 ±133 W/m²).

We then searched for a general pattern in the change of thermal metrics with shooting distance by standardizing surface temperatures according to air temperatures (Appendix 6). We plotted density curves of surface temperature excess of the thermal test card in the laboratory and in the green wall environment as function of shooting distance, and also of the entire green wall surface and of the entire wood edge surface under clear sky conditions. For the outdoor environments, leaf surface temperature distributions were added to the plots to assess how actual leaf temperatures (i.e., leaf surface temperature distribution at high spatial resolution) shaped the surface temperature distribution from each shooting distance. For this analysis, we used the surface temperature excess matrices – the surface temperature distributions minus the mean ambient air temperature recorded by the temperature loggers behind the leaves at the same time than the TIR images (Appendix 6). Densities were used to leave aside the effect of decreasing pixel number with increasing distance on the distribution curves, since the number of temperature pixels in the focused areas decreased with distance. As temperature density distributions were normal, they were fitted using Gaussian function in Table curve 2D (V5.01, Systat Software Inc., Chicago, Illinois, USA) as follows:

$$D = a + b e^{\left[-0.5\left(\frac{T_{ex}-c}{d}\right)^2\right]} \quad (\text{eqn 1})$$

where a , b , c , d are parameters, D the density predicted and T_{ex} the temperature excess in K. The accuracy of the fits (R^2 and standard deviation) of each density curve fitted is given in Appendix 7. We performed an analysis of variance (ANOVA) with the R package ‘stats’ version 3.1.1 (R Development Core Team 2014) to analyse the effects of the shooting

distance, the radiation level and their interactive influences on the surface temperature excess distributions.

3. Results

3.1. Thermal test card in different environments

Overall, the distance between the mobile and the fixed TIR cameras had a significant effect on all thermal metrics for the thermal test card (ΔT_{mean} , ΔSD , $\Delta \text{Patch richness}$ and $\Delta \text{Aggregation}$; Fig. 2). Within the first 20 m separating the two TIR cameras, ΔT_{mean} , ΔSD , and $\Delta \text{Patch richness}$ strongly decreased, from 0 to -3.4 K, -2.5 K and -1200 patches, respectively. At distances from 20 m to 70 m, this decrease was much less pronounced as it did not exceed -1K, -0.8K, -400 patches for ΔT_{mean} , ΔSD , and $\Delta \text{Patch richness}$ respectively. T_{mean} , SD , and Patch richness were therefore increasingly under-estimated as the distance between the two TIR cameras increased. By contrast, indoor TIR measurements on the 1-m² thermal test card showed a linear relationship with shooting distance, but thermal metrics were also under-estimated at increasing distances (red squares in Fig. 2). Moreover, global radiation levels influenced the magnitude of this error: for instance at 40 m, mean temperatures were under-estimated by about 3.3K and 1.5 K at radiation levels of $915 \pm 20 \text{ W/m}^2$ and $65 \pm 5 \text{ W/m}^2$, respectively (Fig. 2 A). In other words, the surface temperature of solar-heated objects was more under-estimated than relatively cooler surfaces at the same distance. A similar pattern was found with ΔSD (Fig. 2 B). By contrast, $\Delta \text{aggregation}$ increased with distance (Fig. 2 D).

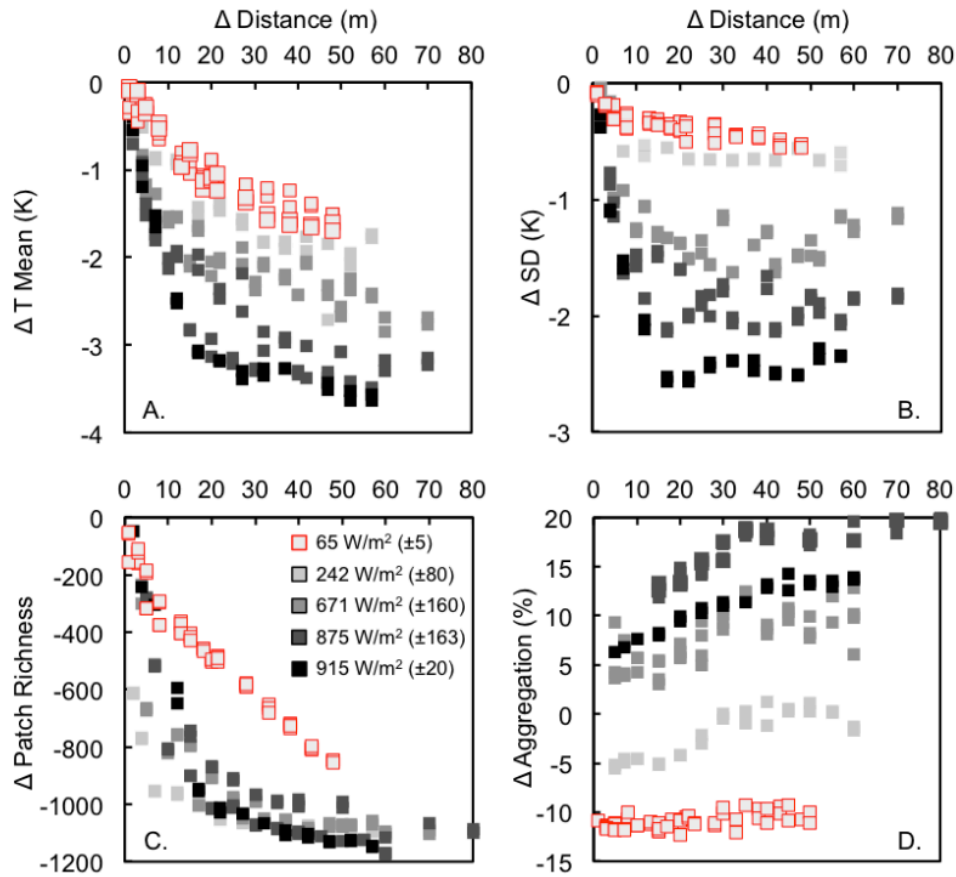


Figure 2: Scatter plots of the thermal indices' deviation between the mobile and the fixed TIR cameras' images of the 1-m² thermal test card under various levels of solar radiation against the Δ Distance (m) – the distance between the two TIR cameras (mobile minus fixed). Negative values indicate that the metric is under-estimated by the mobile camera. (A) ΔT mean (K), (B) ΔSD (K), (C) Δ Patch richness and (D) Δ Aggregation (%). Red squares are the indoor TIR shootings at radiation level 65 W/m². Solar radiation varied from 242 W/m² to 915 W/m² in the outdoor green wall environment.

3.2. Effect of surface structural complexity

Overall, we found no effect of the surface structural complexity on the relationship between thermal metrics and shooting distance. The same decreasing pattern with increasing distance was found for the three structurally different surfaces (thermal test card surface, green wall vegetation surface and wood edge surface) and for ΔT_{mean} , ΔSD , Δ Patch richness (and a

similar increasing pattern for Δ Aggregation). However, under similar solar radiation, surfaces had different TIR responses. The thermal heterogeneity of the wood edge surface, the more structurally complex, was less under-estimated with increasing distance than the green wall and the thermal test card surfaces (Fig. 3 A and B).

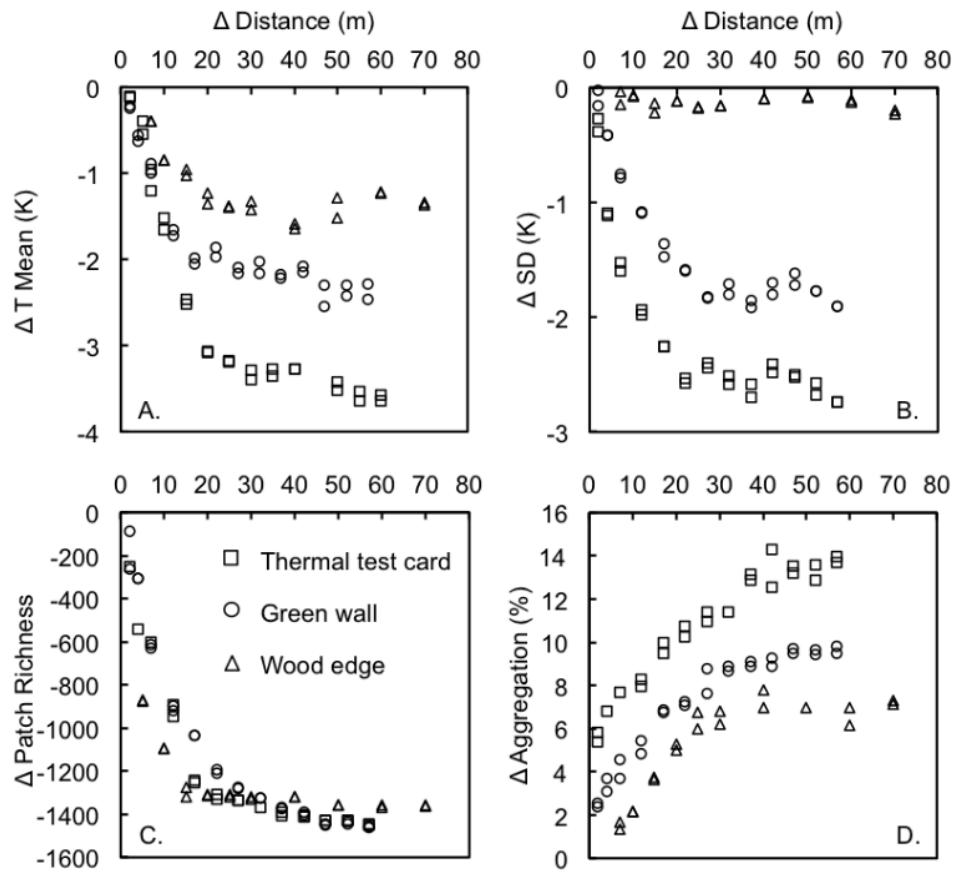


Figure 3: Scatter plots of thermal indices' deviation between the mobile and the fixed TIR cameras' images of the 1-m² thermal test card in the green wall environment, and of the 1-m² vegetation surface in the green wall and wood edge environments, against the Δ Distance (m) – distance between the two IRCs (mobile minus fixed). (A) ΔT mean (K), (B) ΔSD (K), (C) Δ Patch richness, and (D) Δ Aggregation. Solar radiation was 890 ± 133 W/m² for all points.

3.3. Surface temperature excess distributions vs. distance

Overall, temperature excess distributions shifted down to lower values with increasing distance (Fig. 4). Under similar radiation levels, this shift was larger for the thermal test card (up to -3 K; Fig. 4 B) than for the green wall and the wood edge surfaces (Fig. 4 C, D, respectively). The range of excess temperature of the distribution curves – i.e. the spatial variation of temperature – decreased with increasing distances, from 7K at 5 m to 2K at 60 m for the 1-m² thermal test card in the green wall environment (Fig. 4 B). This diminution was larger for the 1-m² thermal test card than for the green wall and the wood edge surfaces under similar solar radiation (Fig. 4 B,C,D). As a consequence, the maximum density increased with increasing distance between the surface and the TIR camera. The maximum density at 5 m for the thermal test card outdoor reached 0.18 while it increased up to 0.90 at 60 m (Fig. 4 B).

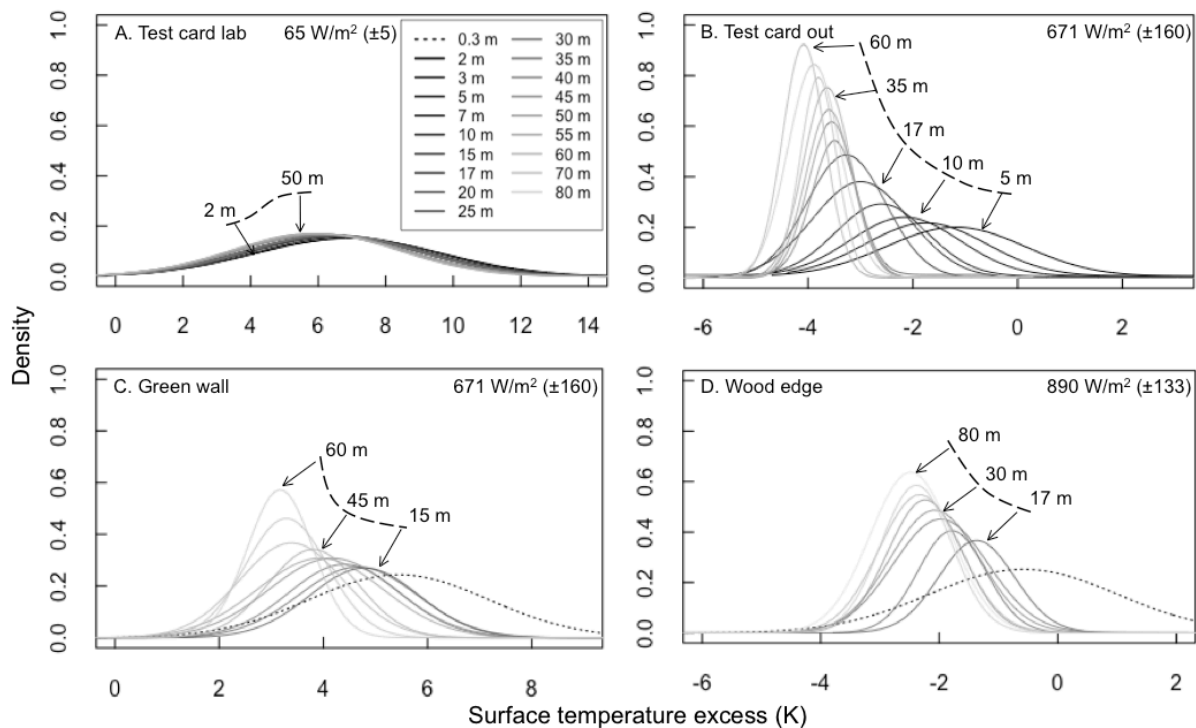


Figure 4: Density distribution of the surface temperature excess (K) obtained from TIR images of the mobile TIR camera at various distances for the 1-m² thermal test card in the laboratory and in the green wall environments (A. and B. respectively), of the whole surface of the green wall (C.) and of the whole surface of the wood edge (D.) under clear sky conditions. Dashed curves in C. and D. represent the leaf surface temperature distributions from TIR images taken at 0.3 m from individual leaves of the green-wall and the wood-edge respectively (see Appendix 4).

Therefore, increasing distances caused both an under-estimation of the extreme temperature and a spatial homogenization of the temperatures. We also found that the shooting distance significantly modify the surface temperature distribution in the outdoor environments (ANOVAs in Table 1). Leaf temperature distributions, taken at a distance of 0.3 m from the surface in the outdoors environments (dashed curves in Fig. 4 C, D) showed larger temperature range and lower density maximum than the entire vegetation background in the green wall and wood edge environments. Note that the shooting distance has no significant effect on the temperature distributions for the 1-m² thermal test card in the indoor laboratory environment (ANOVA in Table 1, $F_A = 0.761$, $P_A = 0.383$). Nevertheless, they shifted downward up to -1K with increasing distance, which is less than for the outdoor surfaces (Fig. 4 A).

Parameter	F value		P value	
Distance	^A 0.761	^B 49.510	^A 0.383	^B <0.001
	^C 31.742	^D 16.843	^C <0.005	^D <0.01
Radiation	^A 0.079	^B 34.372	^A 0.778	^B 0.047
	^C 0.317	^D 0.116	^C 0.574	^D 0.683
Dist x Rad	^A 0.039	^B 1.119	^A 0.844	^B 0.29
	^C 2.108	^D 1.331	^C 0.147	^D 0.21

Table 1: Results of ANOVA for the effects of shooting distance, radiation level and their interaction on the density distribution of the surface temperature excess used in Fig. 4. Temperature distributions were obtained from TIR images taken with the mobile TIR camera at various distances for the 1-m² thermal test card in the laboratory and in the green wall environments (A. and B. respectively), of the whole surface of the green wall (C.) and of the whole surface of the wood edge (D.). Values in bold indicates significance ($P < 0.05$).

4. Discussion

TIR imagery is widely used to record object/organism surface temperatures and quantify their spatial heterogeneities in ecological studies. However, some key parameters in thermography may strongly impact the TIR outputs. In the present study, we show that the distance between the TIR camera and the object affected the thermal metrics used for featuring thermal heterogeneity of surfaces. Overall, we found that the shooting distance strongly modified the absolute temperature measured by the TIR camera. The relationship found between distance and the mean temperature, standard deviation and patch richness for the outdoors environments was non-linear, indicating a strong effect within the first 20 m and only a slight decrease between 20 to 80 m. As a result, average surface temperatures were underestimated when increasing the shooting distance. Interestingly, increasing the shooting distance homogenised thermal mosaics with a much stronger bias in the warmer than the colder part of the distributions. To our knowledge, this effect of shooting distance has never been quantified before. This quantification is critical for future studies that aim at assessing the thermal heterogeneity available for animals and plants (see below). Below, we explain this shooting distance effects by the lower atmosphere composition, the size of pixels, and the influence of global solar radiation on structurally complex surfaces.

4.1. Lower atmosphere composition effect

The underestimation of the mean temperature, standard deviation and patch richness might occur because of the composition of the ambient atmosphere. Recently, [Minkina & Dudzik \(2009\)](#) evidenced absorption of the infrared radiation (emitted by objects) by gases and particles present in the lower atmosphere between the object and the TIR camera. For instance, air humidity, fog, snow, and dust can significantly distort the TIR readings ([Minkina & Dudzik 2009](#)). This effect of atmospheric composition is suggested by the linear negative

relationship between the thermal metrics and the distance in the indoor environment, wherein abiotic parameters such as air temperature and humidity were more homogeneous in space and in time (see red squares at 65 W/m^2 in Fig. 2). Indeed, the temperature surface distributions of the TIR images for thermal test card in the laboratory environment shifted downward by no more than 1K from 1 to 50 m, and both the maximum density and the temperature range did not change with distance in this stable environment (Fig. 4 A). By contrast, the lower atmosphere composition in the outdoor environments was probably heterogeneous along our transects. For example, the camera may have received more infrared radiation coming from nearby surfaces at close than at moderate and long distances (boundary layer properties, see [Oke 1987](#)). This effect can explain the non linear decrease of thermal metrics in outdoor transects (Fig. 4 B). Moreover, concurrently with other studies ([Clark 1976](#), [Minkina & Dudzik 2009](#), [Vollmer & Möllmann 2010](#), [Jones 2013](#)), we found that global radiation level altered TIR outputs and therefore modified the relationship between shooting distance and the thermal metrics. Indeed, global radiation heat up the small portions of the surface that are perpendicular to the sun position, while the portions at a lower angle to the sun remain close to ambient air temperature, increasing thereby the spatial heterogeneity of surface temperatures. This effect probably amplifies the pixel size effect (see below), leading to an even larger under-estimation of thermal metrics.

4.2. Pixel size effect

TIR cameras are equipped with a sized sensor that provides a fixed number of pixels for any shooting distance. Therefore, the pixel size relies upon the shooting distance (Appendix 1): the further you shoot, the bigger is the pixel size. This change in pixel size with distance inevitably induces modifications of the thermal information recorded by the TIR camera. Indeed, the physical borders between an object, or a thermal patch, and its surrounding may

be included in the same single pixel depending on the shooting distance, and in this case the pixel simply integrates the TIR information coming from both elements – i.e. a combination of sub-pixel temperatures (Murphy *et al.* 2014). The integration of sub-pixel temperatures likely reduces the level of heterogeneity in the TIR images. This effect is well illustrated by the response of the aggregation index to shooting distance: thermal patches became more aggregated as shooting distance increased (Fig. 4). The aggregation index relies on the number of pixels composing the landscape (McGarigal & Marks 1994, He *et al.* 2000). Indeed, the number of pixels composing a 1-m² surface area decreases with distance, causing thereby an 'apparent' increase in aggregation.

4.3. Effect of surface structural complexity

The relationship between shooting distance and thermal metrics was only weakly influenced by the structural complexity of the surfaces (thermal test card, green wall, and wood edge). This is a quite unexpected result as the interaction between a high level of radiation and the roughness of the surface is known to generate a highly diverse mosaic of temperature patches according to simple geometrical rules (Oke 1987). We therefore expected a high spatial heterogeneity in surface temperature for the wood edge because of its three dimensional structure. The background of the wood edge, however, corresponded to a deep, shaded part of the wood, which may contribute to homogenize the TIR image. Indeed, under identical weather conditions (including solar radiation) the three structurally different surfaces showed different thermal metric responses (Appendix 8), i.e. a lower thermal heterogeneity for the wood edge surfaces than for the green wall surfaces. We also acknowledge that by starting at a Δ distance of 7 m in the wood edge environment, we may have missed much of the thermal effect. On the contrary, the thermal test card surface, although less structurally complex, showed a higher heterogeneity in temperatures than for the two other surfaces under identical

abiotic conditions. The thermal test card is emitting TIR directly as function of incoming energy, while in the case of the green wall and the wood edge environments, the eco-physiology of plant leaves managed radiation loads and modulate their (highest) surface temperatures by transpiring (Jones 2013). Therefore, the structural composition alone is not sufficient to infer the heterogeneity of surface temperature at local scale.

4.4. Guidelines for the use of thermography with regards to shooting distance

We present some major guidelines to minimize inaccuracies due to the distance between studied object and TIR cameras. Firstly, to yield accurate and absolute TIR measurements, emissivity of the object should be fixed in the settings of the camera according to emissivity tables (Clark 1976), and global solar radiation must be recorded while shooting to proceed within similar irradiance conditions. When applicable, IR shots should be taken at low solar irradiance or during night to avoid underestimations of the results. Additionally, to minimize the sub-pixel temperature combination onto the physical borders of the studied surface, we would recommend removing the surface boundary edge – i.e. the boundary pixels – in the TIR image. However, this precaution will not exclude the inaccuracies due to sub-pixel temperature combination onto the thermal patches that composed the surfaces.

Secondly, the relationship between the shooting distance and the accuracy of the TIR images must be considered for data analysis. TIR studies should anticipate the influences of lower atmosphere composition (especially when outdoor) and of the shooting distance-related pixel size. Thus, we recommend reducing the shooting distance at the lowest possible distance (when feasible) to yield more accurate absolute surface temperatures. If not, atmospheric radiative transfer models could be used to correct the surface temperatures depending on atmospheric composition. For instance, MODTRAN®6 (MODerate resolution atmospheric TRANsmission) solves the radiative transfer equation including the effects of molecular and

particulate absorption/emission of the atmosphere present between the thermal sensor and the studied object ([Berk *et al.* 2014](#)).

The size of the body organism is also a key parameter that constrains the use of thermography and the determination of the shooting distance. Indeed, surface temperatures significantly affect the performance of small living organisms mainly (e.g. insects and rocky shore crustaceans, when the heat budget is driven by conduction mainly), while the thermal budget of bigger animals is more influenced by the ambient air properties (convective heat loss). In particular, solar radiation warm up the surface of animal's body, increasing thereby the deviation between internal and skin temperatures. However, these effects are expected to remain minor for small, dry-skin ectotherms with low thermal inertia such as most arthropods, and plant surfaces. Nevertheless, TIR shooting distance should be selected depending on the size of the organism to maximize the number of pixels covering the object. For example, at a distance of 20 m, the pixel size was about 2 cm² with our best TIR camera (Appendix 1). The opportunities for behavioural thermoregulation can therefore only be assessed at 20 m and below for organisms with body size > 2 cm, assuming that the organism itself integrates surface temperatures throughout its whole body ([Woods *et al.* 2015](#)).

4.5. Conclusion

In conclusion, our study reveals that the distance between the object and the TIR camera is a major modifier of the measured thermal heterogeneity. Shooting distance causes errors and underestimations of the absolute surface temperatures. Researchers should therefore select the shooting distance as the result of a conscious trade-off between body size, the features of their TIR camera (field of view especially), the hypothetical surface temperature (if the object surface temperature is heated), and the level of accuracy of the TIR results they need in their

studies. These recommendations apply for any field of research where thermography can be used.

Acknowledgements

We are grateful to Christelle Breion (www.musee-balzac.fr) for allowing us to work in the *Château de Saché*, and Sophie Cauvy-Fraunié for her help in the fieldwork. Thanks to Damien Legaie for clarifying comments on the manuscript. This work was partly conducted within the project Microclimite “From global to micro-climate change” (ANR-10-BLAN-1706-02) and the project “Adaptive management in insect pest control in thermally heterogeneous agricultural landscapes” (ANR-12-JSV7-0013-01) funded by the Agence Nationale pour la Recherche (ANR, <http://www.agence-nationale-recherche.fr/>).

References

- Bellvert, J., Zarco-Tejada, P. J., Girona, J., Fereres, E. 2013. Mapping crop water stress index in a ‘Pinot-noir’ vineyard: comparing ground measurements with thermal remote sensing imagery from an unmanned aerial vehicle. *Precis. Agric.* 1-16.
- Berk, A., Conforti, P., Kennett, R., Perkins, T., Hawes, F., van den Bosch, J. 2014. MODTRAN6: a major upgrade of the MODTRAN radiative transfer code. In *SPIE Defense+ Security* (pp. 90880H-90880H). International Society for Optics and Photonics.
- Caillon R., Suppo C., Casas J., Woods H., Pincebourde S. 2014. Warming decreases thermal heterogeneity of leaf surfaces: implications for behavioural thermoregulation by arthropods. *Func. Ecol.* DOI: 10.1111/1365-2435.12288.
- Cilulko, J., Janiszewski, P., Bogdaszewski, M., Szczygielska, E. 2013. Infrared thermal imaging in studies of wild animals. *Eur. J. Wildlife Res.* **59**(1), 17-23.

- Clark, J.A. 1976. Effects of surface emissivity and viewing angle on errors in thermography. *Acta Therm.* **1**, 138–141.
- Croon, G.W., McCullough, D.R., Olson, C.E., Queal, L.M. 1968. Infrared scanning techniques for big game censusing. *J. Wildlife Manage.* **32**, 751–759.
- Faye, E., Rebaudo, F., Yáñez, D., Cauvy-Fraunié, S. & Dangles O. (2015). A toolbox for studying thermal heterogeneity across spatial scales: from unmanned aerial vehicle imagery to landscape metrics. *Meth. Ecol. Evol.*, In press.
- He, H. S., DeZonia, B. E., Mladenoff, D. J. 2000. An aggregation index (AI) to quantify spatial patterns of landscapes. *Land. Ecol.* **15**(7), 591-601.
- Hill, R.W., Christian, D.P., Veghte, J.H. 1980. Jackrabbit ears: surface temperatures and vascular responses. *Science*, **194**, 436–438.
- Inagaki, M. N., Nachit, M. M. 2008. Visual monitoring of water deficit stress using infra-red thermography in wheat. In *The 11th International Wheat Genetics Symposium proceedings Edited by Rudi Appels Russell Eastwood Evans Lagudah Peter Langridge Michael Mackay Lynne*. Sydney University Press.
- Jackson, R. D., Idso, S. B., Reginato, R. J., and Pinter, P. J. 1981. Canopy temperature as a crop water stress indicator. *Water Resour. Res.* **17**(4), 1133-1138.
- Jones, H. G. (2013). *Plants and microclimate: a quantitative approach to environmental plant physiology*. Cambridge University Press. Third edition.
- Jones, H. G., Stoll, M., Santos, T., De Sausa, C., Chaves, M. M., Grant, O. M. 2002. Use of infrared thermography for monitoring stomatal closure in the field: application to grapevine. *J. Exp. Bot.* **53**(378), 2249–2260.
- Kerr, J. T., Ostrovsky, M. 2003. From space to species: ecological applications for remote sensing. *Trends Ecol. Evol.* **18**(6), 299-305.
- Kingsolver, J. G. 2009. The Well-temperated biologist. *Am. Nat.* **174**(6), 755-768.

- Lathlean, J., Seuront, L., 2014. Infrared thermography in marine ecology: methods, previous applications and future challenges. *Mar. Ecol. Prog. Ser.* **514**, 263-277.
- Körner, C., Basler, D. 2010. Phenology under global warming. *Science* **327**(5972), 1461-1462.
- McCafferty, D. J., Gilbert, C., Thierry, A. M., Currie, J., Le Maho, Y., Ancel, A. 2013. Emperor penguin body surfaces cool below air temperature. *Biol. Lett.* **9**(3), 1112-1192.
- McGarigal, K., Marks, B.J. 1994. *Fragstats: Spatial Pattern Analysis Program for Quantifying Landscape Structure*. Oregon state university, Forest science department, Corvallis.
- Meron, M., Tsipris, J., Orlov, V., Alchanatis, V., Cohen, Y. 2010. Crop water stress mapping for site-specific irrigation by thermal imagery and artificial reference surfaces. *Precis. Agri.* **11**(2), 148-162.
- Minkina, W., Dudzik, S. 2009. *Uncertainties of Measurements in Infrared Thermography, in Infrared Thermography: Errors and Uncertainties*. John Wiley and Sons, Ltd, Chichester, UK. DOI: 10.1002/9780470682234.ch5
- Murphy, S. W., Oppenheimer, C., de Souza-Filho, C. R. 2014. Calculating radiant flux from thermally mixed pixels using a spectral library. *Remote Sens. Environ.* **142**, 83-94.
- Norman, J. M., Becker, F. 1995. Terminology in thermal infrared remote sensing of natural surfaces. *Remote Sens. Rev.* **12**(3-4), 159-173.
- Oke, T. R. 1987. *Boundary layer climates* (Vol. 5). Routledge, Taylor and Francis Group, New York.
- Ørtisland, N.A. 1968. Variations in the body surface temperature of the harp seal. *Acta Physiol. Scand.* **73**, 35–36.

- Pincebourde, S., Woods, H. A. 2012. Climate uncertainty on leaf surfaces: the biophysics of leaf microclimates and their consequences for leaf-dwelling organisms. *Func. Ecol.* **26**(4), 844-853.
- Pincebourde, S., Sanford, E., Casas, J., Helmuth, B. 2012. Temporal coincidence of environmental stress events modulates predation rates. *Ecol. Lett.* **15**(7), 680-688.
- Pincebourde, S., Sanford, E., Helmuth, B. 2013. Survival and arm abscission are linked to regional heterothermy in an intertidal sea star. *J. Exp. Biol.* **216**(12), 2183-2191.
- Quattrochi, D. A., Luvall, J. C. 1999. Thermal infrared remote sensing for analysis of landscape ecological processes: methods and applications. *Landscape ecol.* **14**(6), 577-598.
- R Development Core Team 2005. *R: A Language and Environment for Statistical Computing*. R Foundation for Statistical Computing, Vienna, Austria. URL <http://www.R-project.org>.
- Rubio, E., Caselles, V., Badenas, C., 1997. Emissivity measurements of several soils and vegetation types in the 8–14 mm wave band: analysis of two field methods. *Remote Sens. Environ.* **59**(3), 490–521.
- Scherrer, D., Koerner, C., 2010. Infra-red thermometry of alpine landscapes challenges climatic warming projections. *Glob. Change Biol.* **16**(9), 2602–2613.
- Tattersall, G. J., Cadena, V. 2010. Insights into animal temperature adaptations revealed through thermal imaging. *Imag. Sc. J.*, **58**(5), 261-268.
- Tonolla, D., Acuña, V., Uehlinger, U., Frank, T., Tockner, K. (2010) Thermal heterogeneity in river floodplains. *Ecosystems* **13**(5), 727–740.
- Vollmer, M., Möllmann, K. P. 2010. *Infrared thermal imaging: fundamentals, research and applications*. John Wiley and Sons.

- Woods, H. A., 2013. Ontogenetic changes in the body temperature of an insect herbivore. *Func. Ecol.* **27**(6), 1322-1331.
- Woods, H. A., Dillon, E. M., Pincebourde, S., 2015. The roles of microclimatic diversity and of behaviour in mediating the responses of ectotherms to climate change. *J. therm. biol.* DOI: 10.1016/j.jtherbio.2014.10.002.

Supporting Information of “Faye, E., Dangles, O., & Pincebourde, S. (2015). Distance makes the difference in thermography for ecological studies. *Journal of Thermal Biology*. Doi: 10.1016/j.jtherbio.2015.11.011.

Appendix 1: Features of the two TIR cameras used in the study

Appendix 2: Abiotic conditions for the three environments during the main experiment

Appendix 3: Δ distance points used for the fixed and mobile TIR cameras

Appendix 4: High resolution TIR shooting of leaf surfaces

Appendix 5: 1-m² studied areas on the TIR images in the green wall and the wood edge environments.

Appendix 6: Photographs showing the exact locations of the loggers recording the air ambient temperature in the three studied environments.

Appendix 7: Accuracy of the fitted density curves used in Fig. 4

Appendix 8: Thermal heterogeneity of the studied surfaces

Appendix 1: Features of the two TIR cameras used in the study

The thermal sensitivity (smallest temperature change or difference that can be detected) of the fixed TIR camera (B335, FLIR Systems, Wilsonville, OR, USA) was $< 0.05\text{K}$ at 30°C , and the measurement accuracy (accuracy of the absolute temperature) was $\pm 2\text{K}$. An 18 mm lens was used with the fixed camera that resulted in a spatial resolution or Instantaneous Field Of View (IFOV) of 1.35 mrad (i.e. $25 \times 19^\circ$ FOV). The thermal sensitivity of the mobile TIR camera (HR research 680, VarioCAMs, InfaTec GmbH, Dresden, Germany) was $< 0.03\text{K}$ at 30°C , and the measurement accuracy was $\pm 1.5\text{K}$. A 30 mm lens was used with the mobile camera that resulted in a spatial resolution or IFOV of 0.8 mrad (i.e., $30 \times 23^\circ$ FOV).

We tested whether the slight technical differences between the two cameras can cause bias in the surface temperature measurements. Both TIR cameras were mobiles in this additional experiment. The two cameras were moved together and TIR images were taken simultaneously at each shooting distance. The differences between the two TIR cameras are small enough to be ignored (Fig. S1_#1). Indeed, in the three environments, the mean temperature measured from the TIR images of the thermal test-card differed between the two cameras by only $0.42 \pm 0.27^\circ\text{C}$ on average, and this difference was not altered by shooting distance. Similarly, the standard deviation of temperature from the thermal test card varied by only $0.17 \pm 0.12^\circ\text{C}$ between the two cameras along the distance and for the three environments (Fig. S1_#1).

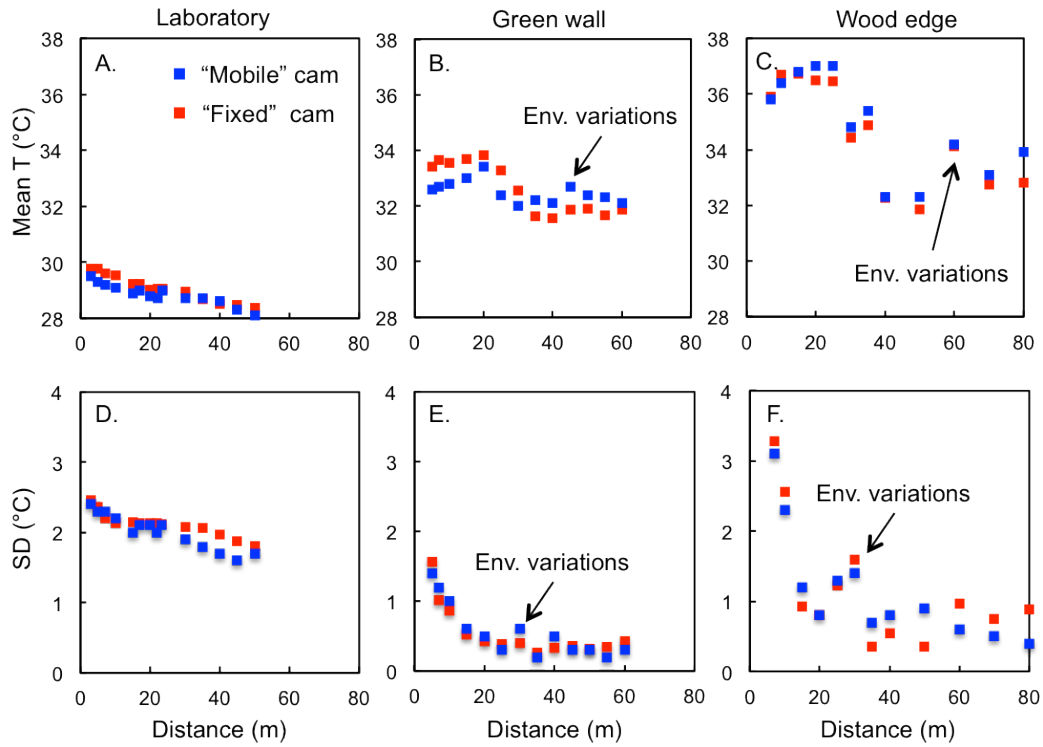


Figure S1_#1: Scatter plots of the mean temperatures and standard deviation (in °C) of the thermal test card TIR images taken from various distance with the two TIR cameras in the three studied environments. Environmental variations (radiation and/or ambient air temperature) caused sudden fluctuations in the thermal metrics but they did not influence the comparison of the performance between the two cameras.

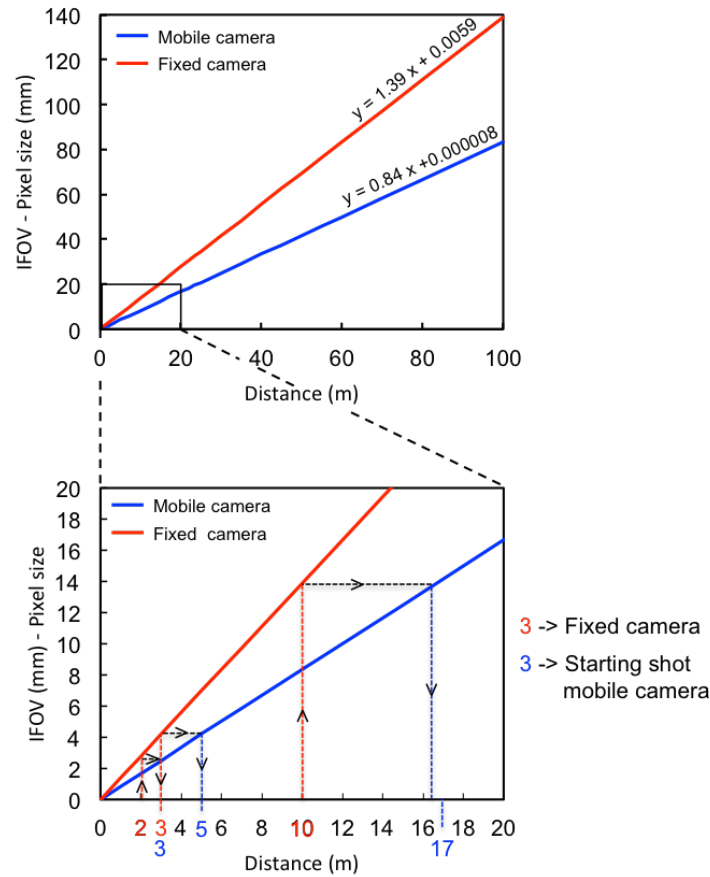


Figure S1_#2: Scatter plot of pixel size as function of distance for the mobile and the fixed TIR camera. The blue and red lines are the pixel size (or Instantaneous Field Of View) of the mobile and fixed TIR cameras, respectively. Red numbers on the x-axis are the distances at which the fixed TIR camera has been placed during the experiment (2, 3, and 10 m for the laboratory, the green wall and the wood edge environments, respectively). The blue numbers on the x-axis are the respective distances (from the surface) at which the mobile TIR camera has been placed for starting the shooting (3, 5, and 17 m for the laboratory, the green wall and the wood edge environments, respectively). Those distances insured a difference of pixel size between the two cameras positive or equal to zero ($\Delta \text{pixel size} \geq 0$ when the pixel size of the mobile TIR camera exceeded the pixel size of the fixed TIR camera). Therefore the mobile TIR camera started shooting 1 m from the fixed TIR camera in the laboratory, 2 m from the fixed TIR camera in front of the green wall and 7 m from the fixed TIR camera in front of the wood edge.

Appendix 2: Abiotic conditions for the three environments during the main experiment

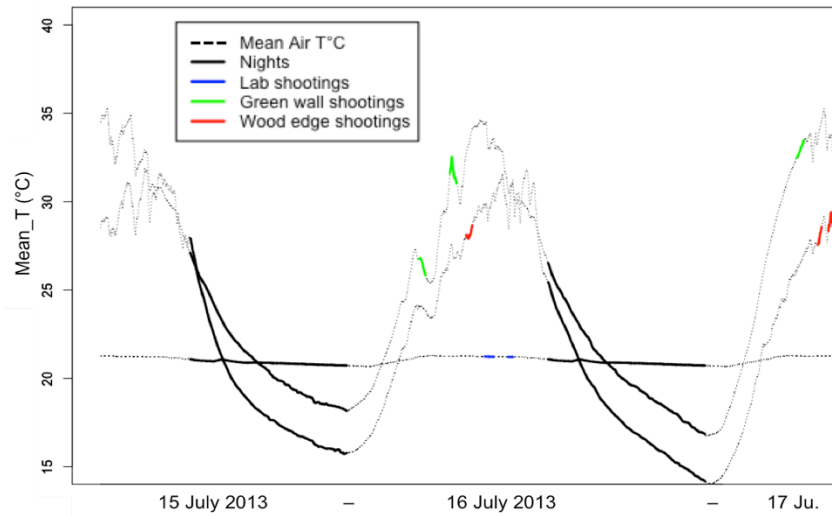


Figure S2: Scatter plot of mean air temperature in the three environments during the main experiment. Thin dotted lines show the mean ambient air temperature of the three environments, thick black lines the night-time air temperatures and thick coloured lines the air temperatures during the IR shooting sessions in their respective environment. For each TIR shooting set, we measured shadowed air temperature and relative humidity every 10 seconds using a thermo-hygrometer (Thermo-hygro clock AW-1, TC direct, Hillside, IL, USA) and global solar radiation (in W/m^2) using a datalogger equipped with a pyranometer sensor facing the sky vault (datalogger LI-200 and pyranometer LI-400, LI-COR, Lincoln, OR, USA) in each environment.

Environment	TIR shooting transects	Air T ($^{\circ}\text{C} \pm \text{SD}$)	Relative Humidity ($\% \pm \text{SD}$)	Radiation ($\text{W/m}^2 \pm \text{SD}$)
Laboratory	1	21.7 ± 0.5	63 ± 0	65 ± 5
	2	21.7 ± 0.5	63 ± 0	65 ± 5
Green wall	1	26.2 ± 0.4	59 ± 2.2	242 ± 80
	2	28.3 ± 0.5	48 ± 2	915 ± 21
	3	29.1 ± 1.2	49 ± 6	660 ± 140
Wood edge	1	29.8 ± 0.8	44 ± 12	680 ± 180
	2	28.3 ± 1	51 ± 4.2	866 ± 215
	3	29.7 ± 0.7	47 ± 2.4	884 ± 49

Table S2: Abiotic conditions during the TIR shootings

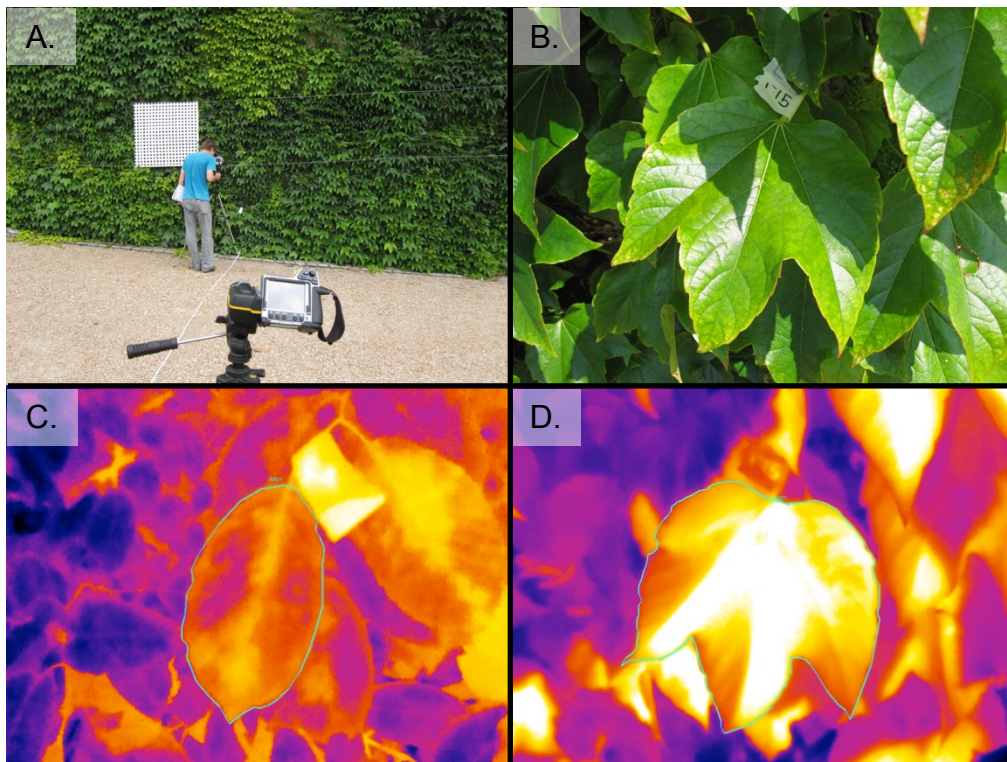
Appendix 3: Δ distance points used for the fixed and mobile TIR cameras

Laboratory			Green wall			Wood edge		
A	B	C	A	B	C	A	B	C
2	2	1	3	5	2	10	17	7
	5	3		7	4		20	10
	7	5		10	7		22	12
	10	8		15	12		25	15
	15	13		17	15		27	17
	17	15		23	20		30	20
	20	18		25	22		32	22
	22	20		30	27		35	25
	25	23		35	32		40	30
	30	28		40	37		45	35
	35	33		45	42		50	40
	40	38		50	47		60	50
	45	43		55	52		70	60
	50	48		60	57		80	70

A = Fixed TIR camera distance from the surface (m). B = Mobile TIR camera distance from the surface (m). C = Δ distance (m), distance between the mobile and the fixed TIR cameras.

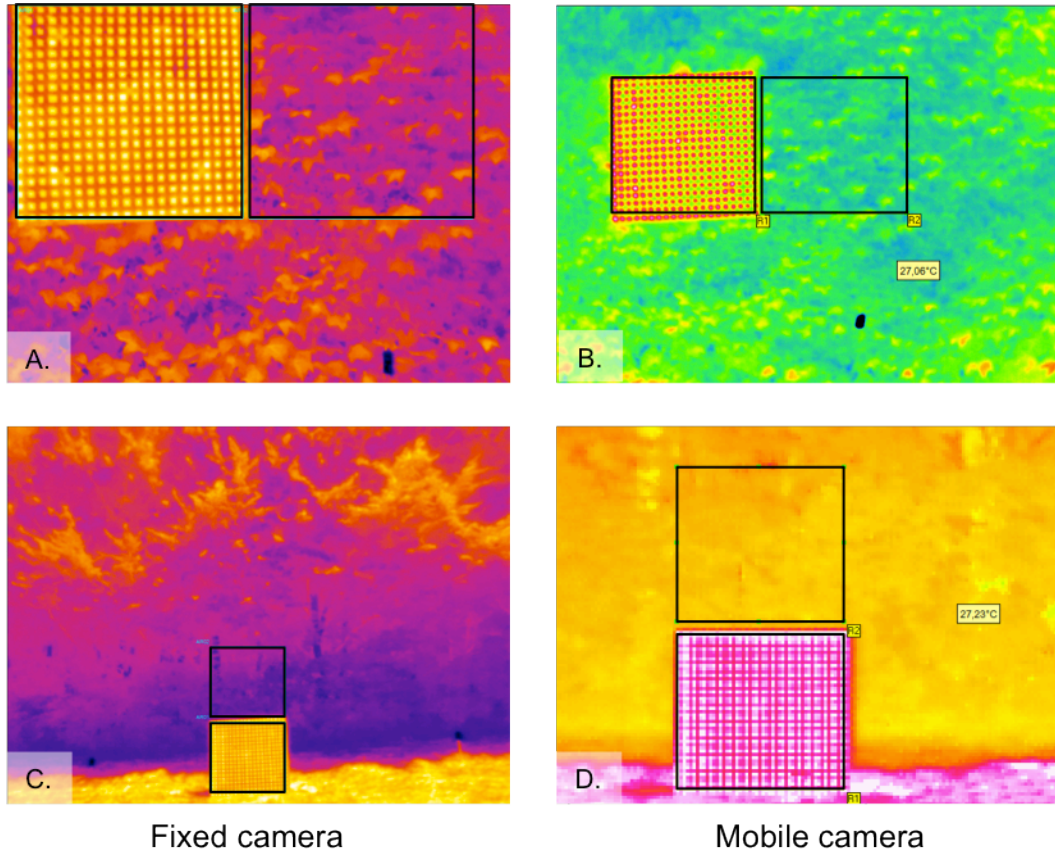
Appendix 4: High resolution TIR shooting of leaf surfaces

We determined the leaf surface temperature heterogeneity at high spatial resolution (close up). We shot 15 identified leaves in the two vegetation surfaces (green wall and wood edge) with the mobile TIR camera at 0.03 m distance right after each of the 6 shooting sessions performed in the outdoor environments. Half of these leaves were shadowed and half of them were sunny. As for the main experiment, air temperature, relative humidity and solar radiations have been recorded during each leaf shot.



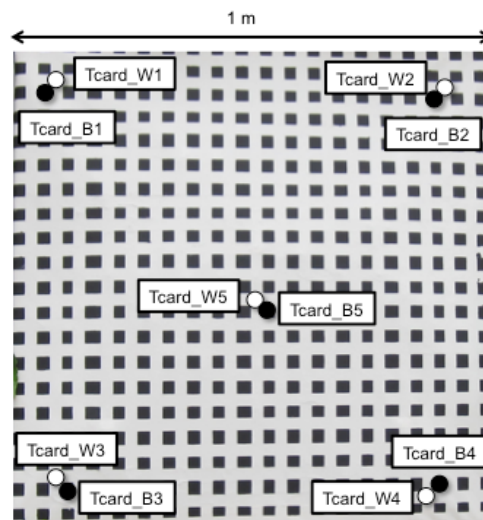
Photographs S4: A- TIR shooting of leaf surfaces at high spatial resolution in the green wall environment. B and D are visual and infrared images, respectively, of the leaf #15 in the green wall environment. This leaf was one of the sunny leaves. C- TIR image of one of the shadowed leaves in the forest edge environment. The contour of the leaves has been drawn in the TIR image analysis software.

Appendix 5: 1-m² studied areas on the TIR images in the green wall and the wood edge environments.

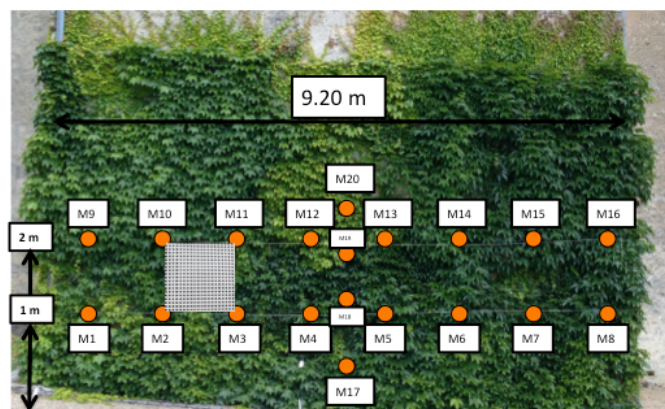


Photographs S5: False coloured TIR images of the thermal test card and the vegetation surface areas taken simultaneously with the fixed (A and C) and the mobile TIR cameras (B and D). A- is a TIR image taken with the fixed TIR camera at 3 m from the thermal test card and the green wall surfaces. B- is the simultaneous TIR image taken with the mobile TIR camera at 7 m from the fixed camera (i.e. at 10 m from the green wall surface). C- is a TIR image taken with the fixed TIR camera at 10 m from the thermal test card and the wood edge surfaces. D- is the simultaneous TIR image taken with the mobile TIR camera at 70 m from the fixed TIR camera (i.e. at 80 m from the wood edge surface) zoomed in at 600% for visual convenience. Black delimitations are the 1-m² areas used for analysis in the main study, for thermal test card and vegetation surfaces respectively.

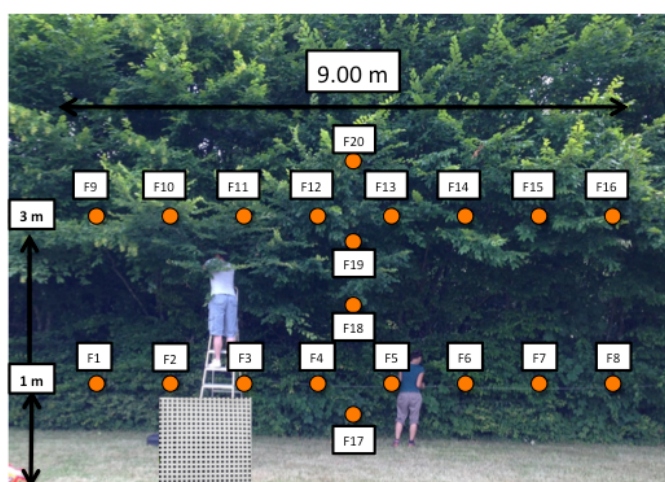
Appendix 6: Photographs showing the exact locations of the loggers recording the air ambient temperature in the three studied environments.



Thermal test card



Green wall



Wood edge

Appendix 7: Accuracy of the fitted density curves used in Fig. 4

	Distance (m)	R ²	SD	t-value	95%IC	95%IC
Figure 4 A.	2	0.8520	0.0025	-0.2672	-0.0056	0.0043
	5	0.8686	0.0023	-0.2559	-0.0053	0.0041
	7	0.8605	0.0025	-0.3997	-0.0060	0.0040
	10	0.8523	0.0026	-0.4185	-0.0063	0.0041
	15	0.8161	0.0029	-0.3530	-0.0069	0.0048
	17	0.8205	0.0029	-0.3619	-0.0069	0.0048
	20	0.8344	0.0028	-0.3321	-0.0065	0.0046
	22	0.8423	0.0027	-0.3711	-0.0064	0.0044
	25	-	-	-	-	-
	30	0.8797	0.0023	-0.3889	-0.0056	0.0038
	35	0.8806	0.0023	-0.4563	-0.0057	0.0036
	40	0.8806	0.0023	-0.4563	-0.0057	0.0036
	45	0.8886	0.0022	-0.4443	-0.0054	0.0035
	50	0.8755	0.0024	-0.4436	-0.0059	0.0038
Figure 4 B.	5	0.8653	0.0020	2.8252	0.0017	0.0099
	7	0.9244	0.0017	1.0406	-0.0017	0.0053
	10	0.9935	0.0009	-0.2942	-0.0020	0.0015
	15	0.9736	0.0015	0.2365	-0.0027	0.0034
	17	-	-	-	-	-
	20	0.4332	0.0100	0.4451	-0.0155	0.0244
	25	0.9999	0.0001	0.5583	-0.0002	0.0003
	30	0.3950	0.0116	0.4073	-0.0185	0.0279
	35	0.9998	0.0002	0.9914	-0.0002	0.0006
	40	0.9998	0.0002	0.9914	-0.0002	0.0006
	45	1.0000	0.0000	-1.1185	0.0000	0.0000
	50	0.8673	0.0052	0.7335	-0.0066	0.0143
	55	1.0000	0.0000	-1.1304	0.0000	0.0000
	60	0.9999	0.0001	0.9913	-0.0001	0.0004
Figure 4 C.	0.3	0.9655	0.0014	-0.6359	-0.0037	0.0019
	15	0.9902	0.0052	63.9144	0.3194	0.3401
	17	-	-	-	-	-
	23	0.9966	0.0005	-0.8143	-0.0014	0.0006
	25	0.9970	0.0005	-0.8000	-0.0013	0.0006
	30	0.9805	0.0012	-0.4913	-0.0030	0.0018
	35	0.9785	0.0012	-0.5276	-0.0031	0.0018
	40	0.9785	0.0012	-0.5276	-0.0031	0.0018
	45	0.9789	0.0014	-0.5652	-0.0037	0.0021
	50	0.9849	0.0011	-0.2813	-0.0025	0.0019
	55	0.9994	0.0002	-1.0438	-0.0007	0.0002
	60	0.9935	0.0009	-0.0440	-0.0018	0.0017

Figure 4 D.	Distance (m)	R ²	SD	t-value	95%IC	95%IC
	0.3	0.9206	0.0021	0.0159	-0.0041	0.0042
	17	0.9642	0.0012	1.0809	-0.0011	0.0036
	20	0.9470	0.0172	26.1394	0.4159	0.4848
	25	0.9777	0.0012	0.3484	-0.0019	0.0028
	30	0.9789	0.0013	0.9455	-0.0014	0.0038
	35	0.9997	0.0001	0.9899	-0.0001	0.0003
	40	0.9994	0.0002	1.0681	-0.0002	0.0005
	50	0.9972	0.0005	0.1728	-0.0010	0.0012
	60	0.9865	0.0008	1.1128	-0.0007	0.0024
	70	0.9721	0.0015	0.0101	-0.0030	0.0030
	80	0.9889	0.0011	0.0030	-0.0021	0.0021

Table S7: Statistics of the fits of the Gaussian function used to fit the temperature density distributions versus distance. The distance (m) is the shooting distance of the mobile TIR camera. For each shooting distance, we performed a Gaussian fit, giving the R², the standard deviation (SD), the t-value and the 95% confidence interval (95%IC below and above).

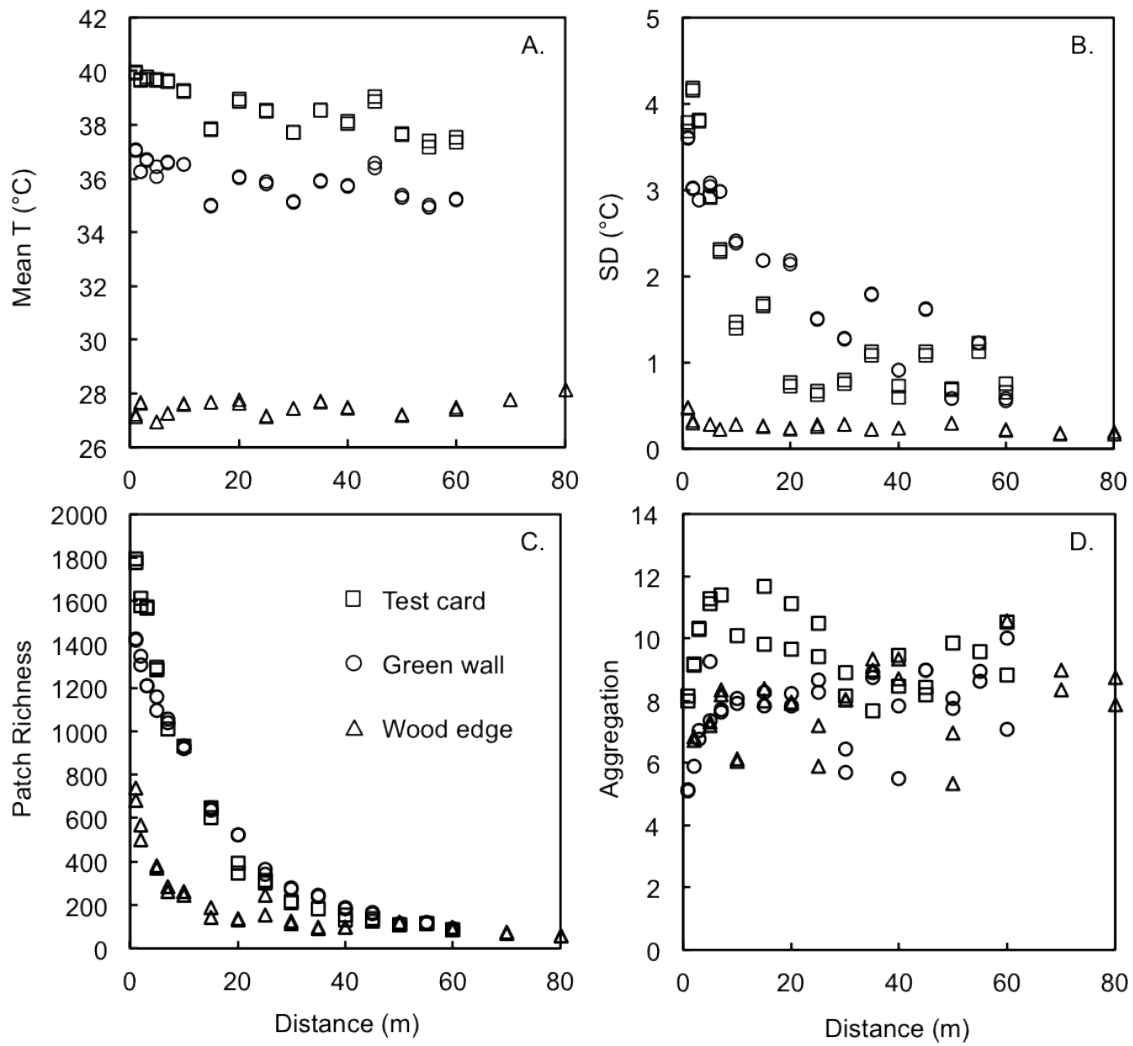
Appendix 8: Thermal heterogeneity of the studied surfaces

Figure S8: Under similar solar radiation level ($890 \pm 133 \text{ W/m}^2$), we shot with the mobile TIR camera the 1-m^2 thermal test card, the 1-m^2 green wall surface and 1-m^2 wood edge surfaces. We plotted the mean temperature in °C (A), the standard deviation in °C (B), the patch richness (C) and the aggregation index (D) of these surfaces against the absolute distance (m) between the mobile TIR camera and the surface. The thermal test card had a mean temperature exceeding the mean of the green wall by $2.74 (\pm 0.37 \text{ K})$ on average and exceeding the mean of the wood edge by $10.73 (\pm 1.36 \text{ K})$ on average. This pattern was found at all distance from 1 m to 80 m from the surface. Patch richness strongly decreased with distance from almost 1800, 1500 and 800 patches for the test card, green wall and wood edge surface respectively to no more than 120 at 60 - 80 m, due to the pixel size effect.

PART II

The second part of Chapter II consists in the development of an integrative and quantitative toolbox for the monitoring and spatial characterization of microclimates across spatial scales. This part aims at overcoming the challenge of bridging the gap between the coarse-scale resolutions of the climatic dataset used in a majority of species distribution models and the body length of the study organism (Potter *et al.* 2013). In this study, we proposed an integrative toolbox that brings together procedures of unmanned aerial vehicle, thermal imagery, orthomosaic, GIS classification and spatial metrics. We applied this toolbox to the case of the agricultural landscapes in Ecuador for assessing the effect of plant phenology on high-resolution spatial metrics of surface temperatures, with implications for ectothermic pest dynamics.

This work was performed in collaboration with the ‘Instituto Espacial Ecuatoriano’ (IEE) and the ‘Escuela Politécnica Nacional’ del Ecuador (EPN) - Escuela de Formación de Tecnólogos (ESFOT). The second part of this methodological Chapter is one publication accepted and currently in press in *Methods in Ecology and Evolution*:

- **Faye, E.,** Rebaudo, F., Yáñez, D., Cauvy-Fraunié, S. & Dangles O. (2005). A toolbox for studying thermal heterogeneity across spatial scales: from unmanned aerial vehicle imagery to landscape metrics. **Methods in Ecology and Evolution**. Doi: 10.1111/2041-210X.12488

Moreover, this study has been presented at the 3rd Global Science conference on Climate Smart Agriculture the 18-23rd of March 2015 with the poster in Appendix S2. Finally, we illustrated the uses of UAV for studying thermal landscapes by 2 short movies available at:

- [UAV showcase IRD. 2013.](#)
- [Un dron para estudiar los microclimas en los Andes Ecuatorianas. 2015.](#)



A toolbox for studying thermal heterogeneity across spatial scales: from unmanned aerial vehicle imagery to landscape metrics

Emile Faye^{1,2,3*}, François Rebaudo¹, Danilo Yáñez-Cajo^{4,5}, Sophie Cauvy-Fraunière^{1,2} and Olivier Dangles^{1,3}

¹UMR EGCE, IRD-247 CNRS-UP Sud-9191, 91198 Gif-sur-Yvette Cedex, France; ²Sorbonne Universités, UPMC Univ Paris 06, IFD, 4 Place Jussieu, 75252 Paris Cedex 05, France; ³Pontificia Universidad Católica del Ecuador, Facultad de Ciencias Exactas y Naturales, Quito, Ecuador; ⁴Ministerio de Defensa Nacional (MIDENA), Instituto Espacial Ecuatoriano (IEE), Guagacalle, Quito, Ecuador; and ⁵Escuela Politécnica Nacional (EPN) - Escuela de Formación de Tecnólogos (ESFOT), Ladron de Guevara E11-253, Quito, Ecuador

Summary

1. A major barrier for the scientific community of climate change biologists is the spatial mismatch between the size of organisms and the resolution at which global climate data are collected and modelled. Thus, the development of integrative and quantitative tools for the monitoring and spatial characterization of microclimates across spatial scales is a key issue for climate change ecologists.
2. We proposed an integrative toolbox for quantifying the spatial heterogeneity in surface temperatures by bringing together procedures of unmanned aerial vehicles, thermal imagery, orthomosaic, GIS classification and spatial metrics. This toolbox permits to yield high-resolution visual and infrared orthoimages that are processed into a GIS for selecting surfaces of interest in the landscape (e.g. soil, vegetation). Then, the thermal matrices of selected surfaces (i.e. temperature values of the pixels belonging to the selected surfaces only) are processed within R to generate a variety of thermal landscape metrics (e.g. thermal patch richness and density, thermal aggregation and cohesion index).
3. We applied this toolbox to the thermal characterization of mountainous agricultural landscapes in Ecuador with implications for ectothermic pest dynamics. UAV flights at a height of 60 m above-ground level allowed us to acquire high-resolution visual and thermal images (1 and 5 cm/pixel, respectively) for 12 potato fields with a mean surface of $1017 \pm 117 \text{ m}^2$. Landscape metrics on plant and soil surfaces showed that crop phenology drives the spatial patterns of surface temperatures and strongly modifies the overall thermal ecology of crop fields, with potential implications for ectothermic pest occurrence and dynamics.
4. Overall, our toolbox affords a timely and innovative methodological framework to better assess the thermal heterogeneity of natural landscapes across a wide range of spatial scales. In particular, this toolbox would be of topical interest for ecologists trying to bridge the gap between the resolution of their climatic data and the body size of their study organisms.

Key-words: ectotherm, high-resolution thermal imagery, microclimate, plant phenology, spatial metrics, temperature heterogeneity, UAV

Introduction

The study of microclimate has recently triggered renewed interest as it is a major issue to connect global and local climate change and forecast species' physiological responses and distributions in the future (Gillingham et al. 2012; Potter, Woods & Pincebourde 2013; Woods, Dillon & Pincebourde 2014; Sears & Angilletta 2015). Microclimatic conditions can deviate substantially from those represented by gridded climatic layers (Faye et al. 2014; Hannah et al. 2014; Scheffers et al. 2014b) and might offer opportunities to modify biotic responses to

global warming (Scheffers et al. 2014a; Storlie et al. 2014; Pincebourde & Casas 2015). There is therefore an urgent need to better quantify microclimates across spatial scales so that mechanistic models at the individual levels can be better incorporated into models of species distribution and vulnerability to climate change (Potter, Woods & Pincebourde 2013). However, monitoring microclimates at relevant scales for organism is not an easy task. The spatial and temporal patterns of microclimatic variation are highly heterogeneous, and climate change at global scale generates even more complex variability to predict climatic conditions at local scales (Woods, Dillon & Pincebourde 2014).

*Correspondence author. E-mail: ehfaye@gmail.com

The quantification of microclimates across spatial scales (from individuals to landscapes) can be potentially revolutionized by the recent development and increased access of unmanned aerial vehicles (UAVs). Autonomously operated, flying low and slow, UAVs offer scientists new opportunities for scale-appropriate measurements of ecological phenomena (Watts, Ambrosia & Hinkley 2012; Anderson & Gaston 2013; Marris 2013; Floreano & Wood 2015). When equipped with appropriate sensors, UAVs can deliver thermal data with spatial and temporal resolutions suited to thermal ecology investigations. This technological innovation has been applied to the study of microclimates in several recent ecological and agronomical studies (Berni et al. 2009; Tonolla et al. 2012; Haselwimmer, Prakash & Holdmann 2013; Dugdale, Bergeron & St-Hilaire 2015). While these studies provide ecologists with some information on UAV technology and use of thermal images, we currently lack an integrative methodological framework for combining up-to-date procedures for UAV systems, thermal imagery, orthophotograph generation, GIS classification and spatial metrics for the characterization of ecologically relevant thermal patterns.

Here, we propose a comprehensive methodological framework, from UAV thermal imagery to landscape metrics, for assessing the thermal heterogeneity of natural landscapes across a wide range of spatial scales. Our methodology employs an UAV equipped with visual and thermal infrared (TIR) cameras to yield high-resolution images processed into mapping software to obtain orthorectified visual and thermal images of high resolution. These orthophotographs are processed in a GIS for selecting surfaces of interest in the visual and thermal landscape (e.g. soil, vegetation). After the surfaces' emissivities (value of object's ability to emit thermal radiation) have been set at the appropriate value, the thermal matrices of selected surfaces (i.e. temperature values of the pixels belonging to the selected surfaces only) are processed within R to generate a variety of thermal landscape metrics (e.g. thermal patch richness and density, thermal aggregation and cohesion index). We applied this methodological framework to the case of agricultural landscapes in the tropical Andes by assessing the effect of plant phenology on high-resolution spatial metrics of surface temperatures.

Materials and methods

The methods described below follow the different steps summarized in Fig. 1.

STEP 1: DATA ACQUISITION WITH UAV FLIGHTS

The UAV system and sensors

High-resolution thermal imagery (e.g. <5 cm) can be acquired by the use of an unmanned aerial vehicle (UAV). We used a multi-copter (Drone-RC, PIXTIM, Messein, France) equipped with a DJI Wookong-M autopilot (DJI Inc., Shenzhen, China) with GPS receiver and barometer, a stabilized gimbal and a 900 MHz data-link that allowed a continuous radio link for inflight monitoring and control from computer. The image acquisition was performed

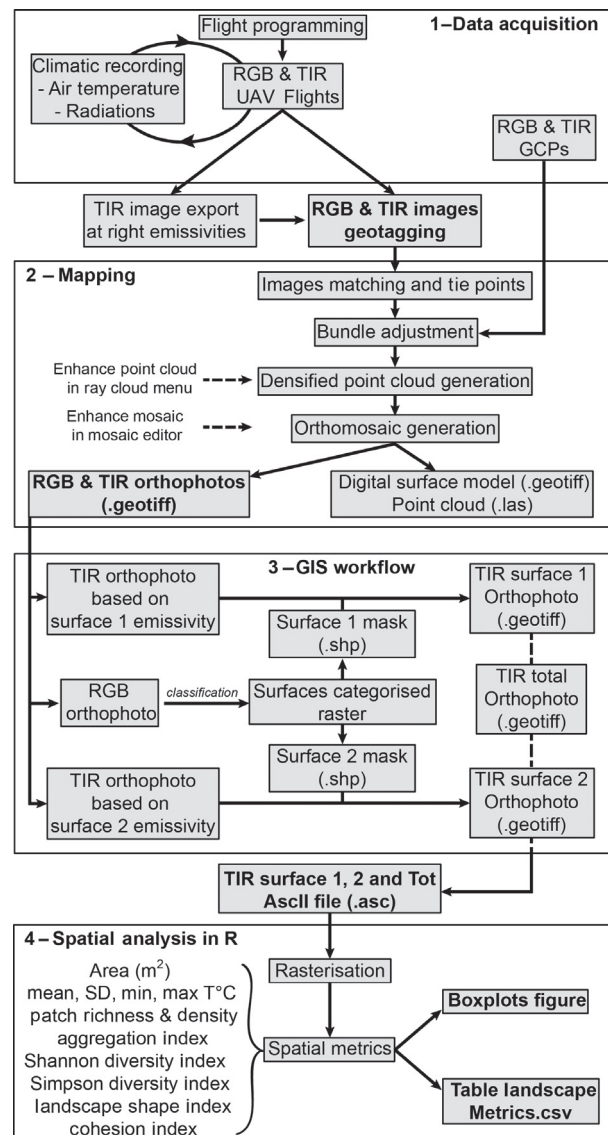


Fig. 1. Schematic workflow of the entire methodological process to analyse thermal landscapes. Each step is fully detailed in the Methods.

during programmed flight following a flight plan created with a ground station (DJI PC; DJI Inc., Shenzhen, China). Images were acquired in the visual (red, green and blue bands, RGB) and thermal infrared (TIR) spectral ranges using RGB and TIR cameras mounted simultaneously on-board. The RGB camera was a Sony Nex-7 that had a 24-megapixel sensor (Sony Corporation, New York, NY, USA) with a lens fixed to a focal length of 18 mm and operated in autofocus mode. The RGB camera was set to shutter priority with a fast shutter speed of 1/1500 to reduce motion blurs and ISO was set to 200 to limit noise in the images. The aperture adjusted automatically to achieve the desired shutter speed. The RGB camera was triggered by an infrared LED intervalometer (Pclix XT; Visual Effects Inc., Toronto, Canada). The TIR camera (HR research 680; InfaTec, Dresden, Germany) had a 640 × 480-pixel uncooled microbolometer sensor recording the long-wave infrared radiation emitted by objects in the spectral range from 7.5 to 14 μm and was equipped with a 30-mm lens. The thermal sensitivity of the TIR camera was better than 0.03 K at 30 °C, and the measurement accuracy was ±1.5 K. The TIR camera was switched

on at least ten minutes before take-off to allow sensor stabilization. The emissivity was fixed to 1 for TIR image capturing and thereafter adapted to the studied surfaces when processing the images (see step 1-TIR surface emissivity).

Ground control points

Before flying, we recorded the UTM-WGS84 geographic coordinates of at least three evenly distributed ground control points (GCPs) with a GPS (Garmin Oregon 550; Garmin, Olathe, KS, USA). GCPs allowed improving the scale, the orientation and position of the orthomosaics generated in the next step of the procedure. However, they do not enhance the spatial resolution of the orthomosaics; therefore, a basic GPS is enough for recording GCPs. Because GCPs need to be recognizable in the RGB and TIR spectral ranges, we placed black canvas sheets tenfold larger than the TIR image resolution to ensure their visibility in the infrared spectrum with recognizable forms (square, circle, triangle, cross and star) on each of the GCPs (Appendix S1).

Meteorological conditions during flights

It is crucial to record meteorological conditions while flying in order to measure potential bias on thermal images (Jones 1992; Scherrer & Koerner 2010; Cilulko et al. 2013; for discussion). We recorded global solar radiation (in W/m^2) using a datalogger equipped with a pyranometer sensor facing the sky vault (LI-1400, LI-COR, Lincoln, NE, USA) and air temperature using one temperature logger (Hobo U23-001-Pro-V2 internal temperature loggers; Onset Computer Corporation, Bourne, MA, USA). Both loggers were located <50 m from the studied area. As a standard practice in meteorological measurements, the temperature logger was fixed at 15 m high and sheltered by a 20 cm^2 white plastic roof to minimize solar radiation heating. The sampling rate for temperature and solar radiation was one and ten seconds, respectively. These measurements were performed during each flight to ensure stable meteorological conditions while obtaining TIR images. If not (i.e. standard deviation >10%), flight had to be conducted again (Fig. 1 – Data acquisition).

Flight description

Flight planning is a trade-off between the desired final resolution of the images, the site area aimed to cover, the flight time capacity of the UAV and the characteristics (e.g. weight, focal) of the on-board cameras (Ballesteros et al. 2014). From this, trade-off can be defined cruise speed, flight elevation and camera trigger frequency. These parameters will then define the frontal and side overlapping of the images. As the aim here was to maximize the image resolution, we fixed the flight parameters according to the size of the studied area and to the smallest sensor we had on-board: the TIR camera. Therefore, we flew at 60 m above-ground level at a speed of 2 m s^{-1} with a trigger of 1 s for each camera which delivered a frontal and side overlapping of more than 80 and 70%, respectively, for the TIR images and more than 95 and 90%, respectively, for the RGB images. Moreover, flying at 60 m a.g.l. guaranteed yielding relatively stable and accurate TIR information applied to during-flight height variations (Fig. 2).

TIR surface emissivity

Emissivity, the ability of an object's surface to emit thermal radiation affects temperature readings made by any TIR camera (Rubio, Caselles & Badenas 1997). Therefore, depending on how many surfaces with different emissivity value the study focuses on, one should consider the emissivity of each surface in the analysis. We exemplify this process using two surfaces that have two different values of emissivity (surface_1 and surface_2), but the same methodology can be applied for surfaces. To produce images with the appropriate emissivity for each surface, all TIR images of the original set were replicated into two image sets: one was set to the emissivity of the surface_1 and the other one to the emissivity of the surface_2. We therefore obtained two TIR image data sets corresponding to the emissivity of the two surfaces studied: the surface_1-emissivity-based TIR images and the surface_2-emissivity-based TIR images. Later on, we extracted each surface area on the RGB orthoimage and assigned the appropriate emissivity TIR values (step 3). Emissivity adjustments were performed using the IRBIS software (InfraTec, Dresden, Germany).

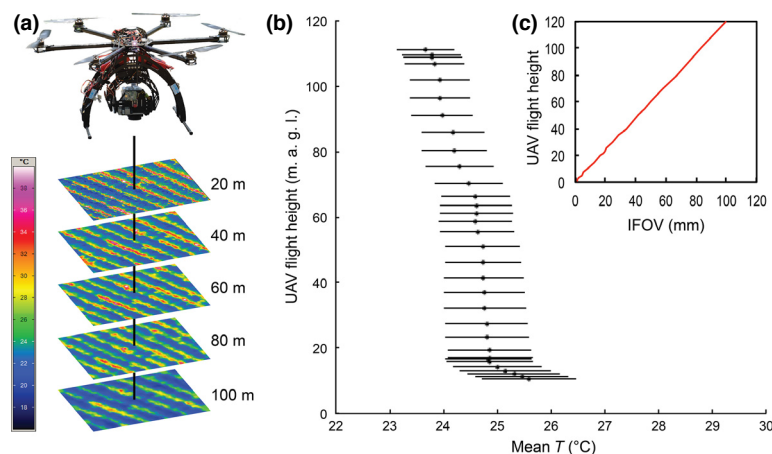


Fig. 2. Unmanned aerial vehicle (UAV)-based TIR information versus flying height. One TIR vertical flight was performed under clear sky conditions from 10 m to 110 m a.g.l. The UAV carried the same TIR camera used in this study, triggered every second with a focus fixed at infinity (i.e. 5 m). The UAV was flying in GPS mode to hover a fixed point with a manual control of the upward speed. (a) The hexacopter used in this study with some sample pictures of surface temperatures (note changes in colour with flight height). Mean surface temperatures at different UAV heights were measured for a same area (10 \times 6 m). (b) Mean and standard deviation of TIR surface temperatures plotted vs. the UAV flight height. (c) TIR camera instantaneous field of view (i.e. projected pixel size) in mm versus the UAV flight height in m.

STEP 2: MAPPING

Image geotagging

After a visual pre-selection (deleting blurred images, i.e. <5% of the total images in our case), coordinates were assigned to the UAV-acquired and emissivity-corrected TIR and RGB images (i.e. geotagging). The UAV flight path (GPS points registered on-board the UAV at logging rate of 1 Hz) was linked to the images taken on-board using the time settings of the cameras, which were synchronized with GPS time of the UAV before flight. We used the GeoSetter software (www.geosetter.de/en/) to write the UAV GPS coordinates into the corresponding RGB and TIR image EXIF headers.

RGB/TIR orthophotographs generation

We used a mapping software (Pix4Dmapper 1.3; Pix4D SA, Lausanne, Switzerland) for generating RGB and TIR orthophotographs from the geotagged UAV-acquired RGB and TIR images (Fig. 1 – Mapping, and Appendix S2 for details). The mapping process detected and bundled the characteristic image objects (i.e. tie points) between overlapping images to create a densified point cloud. The georeferencing of the densified point cloud (i.e. the orientation, scale and direction) is enhanced by the use of geotagged images and

ground control points. Blending the images based on the point cloud, the software can export an orthophotograph (i.e. a georeferenced aerial image geometrically corrected) and/or a digital surface model (Appendix S2). In our case, we generated one RGB orthophotograph and two TIR orthophotographs (one for each studied surface emissivity) with high resolution (1 and 5 centimetres/pixel, respectively).

STEP 3: GIS WORKFLOW (FIG. 1 – GIS WORKFLOW AND FIG. 3)

We then imported the RGB and TIR orthophotographs into ArcGIS 10.1 (ESRI, Redlands, CA, USA). To determine independent surface area (including the two defined studied surfaces) in the TIR orthophotograph, we classified the high-resolution RGB orthophotograph using the Image Classification tool included in the ArcGIS Spatial Analyst extension. We performed an Interactive Supervised Classification based on five training sample polygons for each studied surface within the RGB orthophotographs (i.e. five polygons of surface_1 and five polygons of surface_2; see Appendix S3 for parameters of the RGB classification). The result was a categorized raster with identified pixels belonging to the respective studied surfaces (areas not assigned to the studied surfaces were left aside). From this raster, we created a shapefile mask of the surface_1 area and another for surface_2 area (using the Raster to polygon tool in the Conversion tools menu). We then used

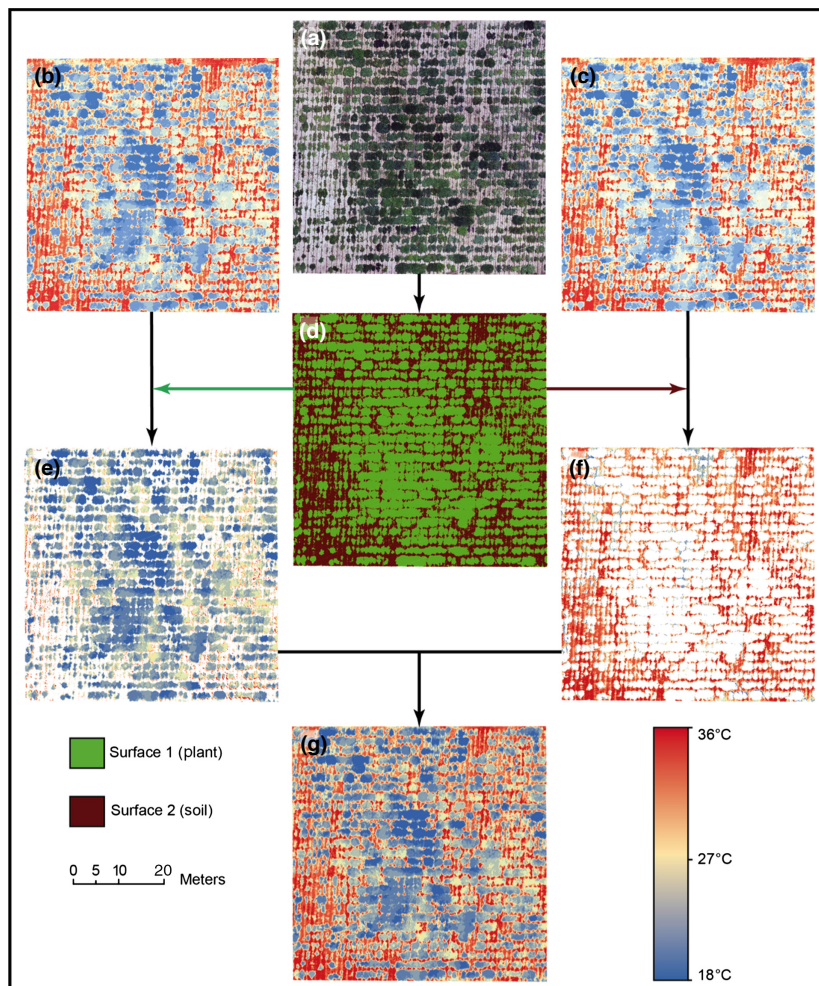


Fig. 3. GIS workflow of the visual (red-green-blue, RGB) and Thermal InfraRed (TIR) orthophotographs for a studied field. (a) RGB high-resolution orthophotograph of the field; (b and c) emissivity-based TIR orthophotograph of surface_1 (plant surface) and surface_2 (soil surface); (d) classified raster from the RGB orthophotograph including the two surfaces – the green part (surface_1/plant) and the brown part (surface_2/soil) serve to create masks to extract pixels of pure surface_1 and 2 in their respective TIR orthophotographs. (e and f) TIR orthophotographs of surface_1 and 2 at their appropriate emissivity. (g) merged TIR orthophotograph of the entire studied field with the appropriate surface emissivity and therefore the correct surface temperatures.

these masks to extract pure surface₁ pixels and pure surface₂ pixels in the corresponding emissivity-based TIR orthophotographs (with the Extract by mask tool in the Spatial Analyst extension). This allowed us to obtain two TIR orthophotographs: one representing only surface₁ surfaces and the other one, only surface₂ surfaces (each with their appropriate emissivity; Fig. 3). Finally, we merged the surface emissivity-based TIR orthophotographs to obtain a complete TIR orthophotograph with the appropriate emissivity for each surface. We assumed therefore that those TIR orthophotographs displayed the correct surface temperatures for surface₁ and surface₂ surfaces (Fig. 3g). Finally, we exported these three TIR orthophotographs into ASCII files (using the Raster to ASCII Conversion tool in ArcGIS, which permits to export raster without formatting options) for further spatial analyses.

STEP 4: SPATIAL ANALYSES IN R (Fig. 1 – Spatial Analysis in R)

Spatial analyses of the thermal orthophotographs were performed using the R software version 3.1.2 (R Development Core Team 2014; see Appendix S4 for the R script used in this study). Our script imports the ASCII files of the TIR orthophotographs and converts them into raster files using the R packages RASTER (Hijmans 2014) and MAPTOOLS (Bivand & Lewin-Koh 2014). Adapted from the class metrics calculated by Fragstats (Mc Garigal & Marks 1994), we used the CLASSSTAT function of the SDM TOOLS package (VanDerWal et al. 2014) to quantify the spatial configuration and composition at the landscape level of the thermal raster images (each index was computed as the sum of the index at the class level, weighted by its proportional area in the total landscape, Appendix S4 for details). We propose seven complementary metrics to fully describe the characteristics of the raster thermal landscapes: (i) thermal patch richness (number of patch types, i.e. temperature classes, present in the landscape), (ii) thermal patch density (number of patches per unit area), (iii) thermal aggregation index (quantifies to what extent temperature pixels of a same value are spatially aggregated), (iv) Simpson's thermal diversity index (probability that two pixels selected at random would be different temperature classes), (v) Shannon's thermal diversity index (which quantifies the uncertainty in predicting the temperature of one pixel that is taken at random in the thermal landscape), (vi) thermal landscape shape index (standardized measure of the total edge of a given thermal patch) and (vii) the thermal cohesion index (physical connectedness among patches of the same temperature). As a final output, for each of the TIR orthophotographs processed, thermal landscape metrics are automatically concatenated into a single table together with a boxplot display. Additional basic thermal statistics (e.g. mean, standard deviation, maximum, minimum temperature and area) are also provided in the table.

Study case

This toolbox might be applied to various ecologically relevant study cases such as presented in Fig. 4: quantifying the spatiotemporal heterogeneity in thermal environment for dragonflies in ponds, studying the relationship between surface temperature and the spatial structure of invasive plant in natural meadows or identifying thermal refuges in palm groves in the semi-arid desert. Here, we applied our toolbox to the study of the spatial heterogeneity in surface

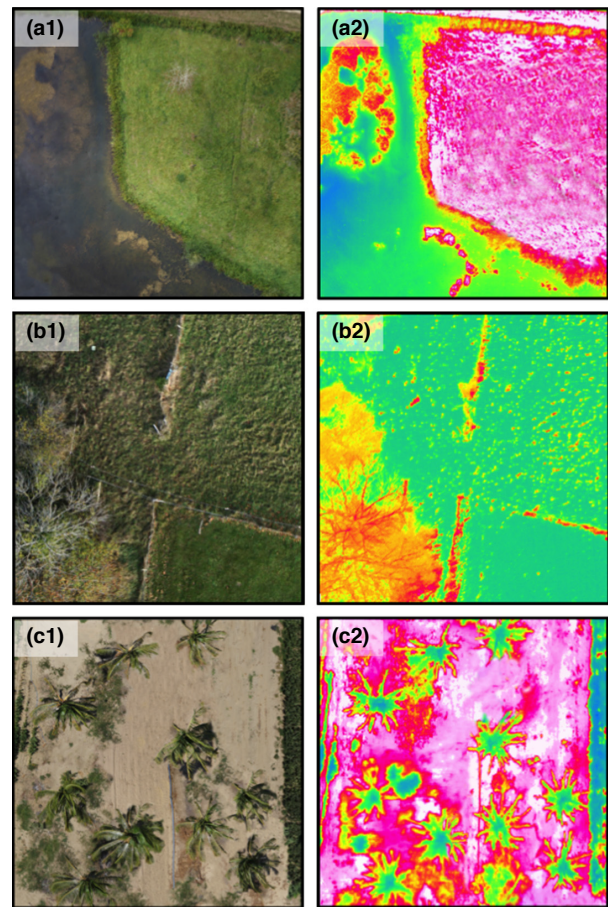


Fig. 4. Visual and thermal orthophotographs (column 1 and 2, respectively) of various natural landscapes. (a) Riverbank of a natural pond in Loire, France. (b) Natural pastures for livestock grazing, Auvergne, France. (c) Palm grove in the semi-arid desert of Piura, North Peru.

temperatures in agricultural landscapes (Faye et al. 2014), with the view to assessing how microscale thermal features of crop fields change across plant phenology. Our study was conducted in an Andean agricultural landscape located in the Cotopaxi province of Ecuador. We selected 12 potato fields (*Solanum tuberosum* L.) so that they could be evenly distributed into three phenological stages (leaf development, inflorescence and mature stages, Table 1 and Appendix S5). For each field at a specific phenological stage, we measured the leaf area index (Wilhelm, Ruwe & Schlemmer 2000) by estimating the ratio of leaf area within a 1 m² quadrant subdivided into 0.1 m² cells delimited by strings. In February 2014, we performed one RGB and TIR flight per field following the method described above between 11:00 AM and 15:00 PM under clear sky conditions (Table 1). This time window generally showed stable meteorological conditions and allowed reducing the shadow effects on images due to the zenithal position of the sun. The number of CGPs depended on the field size (Table 1) and meteorological data were recorded during flights to ensure comparisons among TIR images (see the low standard deviation of mean air temperature and mean solar radiations in Table 1). As

Table 1. Description of the studied fields and abiotic parameters recorded during unmanned aerial vehicle flights.

Field	Coordinates (DD ^a)	Elevation (m.a.s.l. ^b)	Field area (m ²)	Phenology	LAI ^c (%)	Time (h:min)	Flight duration (min:sec)	Mean air temperature (°C)	Mean solar radiations (watt/m ²)	Mean flight altitude (m.a.g.l. ^d)	GCPs ^e
F1	−1.044475° −78.570443°	2718	926	P1	25	11:47	5:24	26.4 (±1.2)	1020 (±24.3)	58.90 (±2.69)	3
F2	−1.026193° −78.566117°	2693	1047	P1	34	13:05	6:55	25.2 (±0.4)	894 (±19.6)	61.32 (±2.42)	5
F3	−1.026285° −78.566620°	2697	871	P1	30	14:11	5:38	24.8 (±1.8)	827 (±57.3)	60.62 (±1.32)	4
F4	−1.026322° −78.565606°	2695	964	P1	35	14:52	6:55	22.7 (±0.7)	732 (±27.5)	58.92 (±2.20)	5
F5	−1.044334° −78.570457°	2720	929	P2	65	11:23	6:10	26.7 (±0.9)	936 (±39.1)	59.90 (±2.69)	3
F6	−1.054945° −78.567388°	2747	985	P2	67	12:48	7:33	29.3 (±0.3)	1014 (±8.2)	58.64 (±3.11)	4
F7	−1.012548° −78.531975°	3166	1224	P2	51	14:30	8:28	27.4 (±1.1)	1091 (±77.7)	59.58 (±1.46)	5
F8	−1.052141° −78.570058°	2733	1053	P2	60	13:56	7:17	26.2 (±1.4)	847 (±61)	62.31 (±2.81)	4
F9	−1.019801° −78.556391°	2742	851	P3	100	11:08	6:43	24.9 (±0.3)	763 (±20.6)	60.58 (±2.37)	3
F10	−1.020283° −78.556352°	2742	1176	P3	94	11:44	7:13	25 (±0.3)	904 (±31.8)	60.79 (±1.63)	5
F11	−1.019543° −78.555662°	2751	1096	P3	88	14:42	7:37	28.7 (±0.2)	1023 (±2.8)	57.87 (±3.81)	4
F12	−1.020596° −78.555491°	2750	1084	P3	92	12:32	5:57	25.7 (±0.5)	962 (±15.3)	61.75 (±1.28)	4

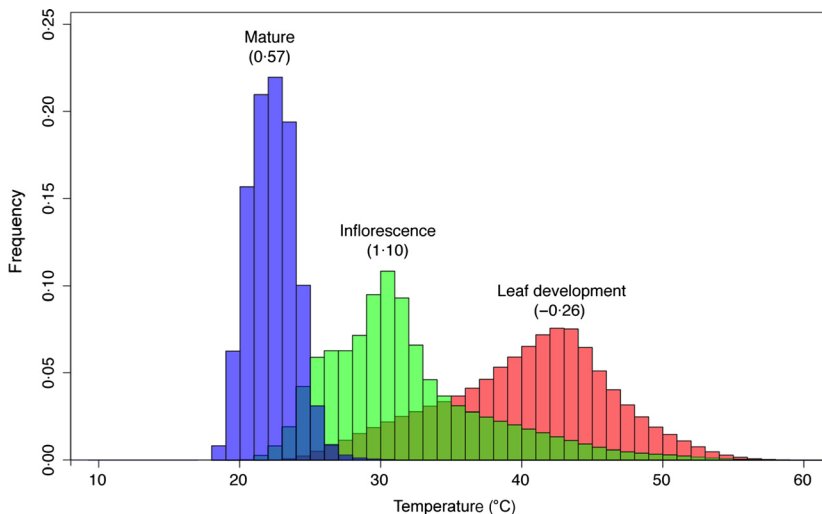
^aDecimal degree (Latitude; Longitude).^bMetres above sea level.^cLeaf area index.^dMetres above-ground level.^eGround control points.

Fig. 5. Frequency histograms of TIR surface temperatures for all the studied fields at the three phenological stages: leaf development (red bars), inflorescence (green bars) and mature (blue bars). The skewness of each distribution is given between brackets.

we were interested in the thermal metrics of two surfaces that had different emissivities (soil and plant), we produced two sets of TIR images with the appropriate emissivities (Rubio, Caselles & Badenas 1997) for each surface: the emissivity of plant canopy (0.98) and that of dry bare soil (0.94). Therefore, for each of the twelve fields flown over, we obtained two TIR data sets corresponding to the two

emissivity of the surface studied in this study case: the plant emissivity-based TIR images and the soil-emissivity-based TIR images. Once processed in the mapping software we obtained RGB and TIR orthophotographs with resolution of 1.3 and 5 cm per pixel, respectively. After following the GIS workflow as described above, we run spatial analyses of configuration and composition for each phenology on

the twelve surface TIR orthophotographs (Appendix S6). We then plotted frequency histograms of surface temperatures for all fields belonging to the same phenology and for one individual field for each phenological stage. Finally, we plotted across plant phenology four thermal metrics of particular interest for our study (mean temperature, thermal patch richness, thermal aggregation and thermal cohesion index), for soil, plant and entire field surfaces.

Results

Crop phenology was a strong modifier of fine-scale surface temperatures in potato fields as the mean temperature of the whole surfaces (entire fields) decreased as plant growth increased: from $40.3 \pm 6.0^\circ\text{C}$ for the 'leaf development stage' fields to $31.8 \pm 5.7^\circ\text{C}$ for the 'inflorescence stage' fields, to $22.33 \pm 1.66^\circ\text{C}$ for the 'mature stage' fields (Fig. 5). Interestingly, standard deviation of surface temperature strongly decreased with phenology as well. The skewness of the histograms of the frequency classes shifted from left skewed to right skewed distributions according to the phenological stage of the fields (from 0.57 for leaf development stage field to -0.26 for mature stage fields; see Fig. 5).

By decomposing temperature frequency distribution between the studied surfaces, we found that the frequency distributions of surface temperatures were bimodal with mean soil temperatures always exceeding mean plant temperatures by $13\text{--}22^\circ\text{C}$ (Fig. 6). As expected, the proportion of each surface area changed over crop phenology: during the 'leaf development' stages, soil temperatures covered a larger area than plant temperatures (Fig. 6a) and vice versa at the mature stage (Fig. 6c). Interestingly, plant and soil mean temperatures decreased by 10°C and 12°C , respectively, as crop phenology increased: at the 'leaf development' stages large surfaces of soil warmed small surfaces of plant while at 'mature stages', small surfaces of soil were cooled by large surface of plants.

Thermal patch richness of plant and soil surfaces displayed a bell-shaped trend across phenology with a low number of patches at both ends of crop development (Fig. 7-c2). A combined reading of mean temperature and patch richness highlights the fact that the relatively high temperatures of soil surfaces for the mature stage phenology (Fig. 7-c1) did not affect much the mean temperature of the entire surface (Fig. 7-a1, due to its low patch richness index (Fig. 7-c2). Thermal aggregation index rose gradually for the plant surfaces, while it rose steeply at the mature phenology for the combined surfaces (Fig. 7-a3 and b3). This index decreased gradually with increasing phenology for the soil surfaces (Fig. 7-c3). Cohesion index for combined surfaces tended to increase with phenology, as well as for plant surfaces (Fig. 7-a4 and b4). Conversely, the cohesion index in soil surfaces decreased with growth plant phenology (Fig. 7-c4).

Discussion

The proposed toolbox provides a user-friendly, repeatable method for studying ecologically relevant fine-scale thermal

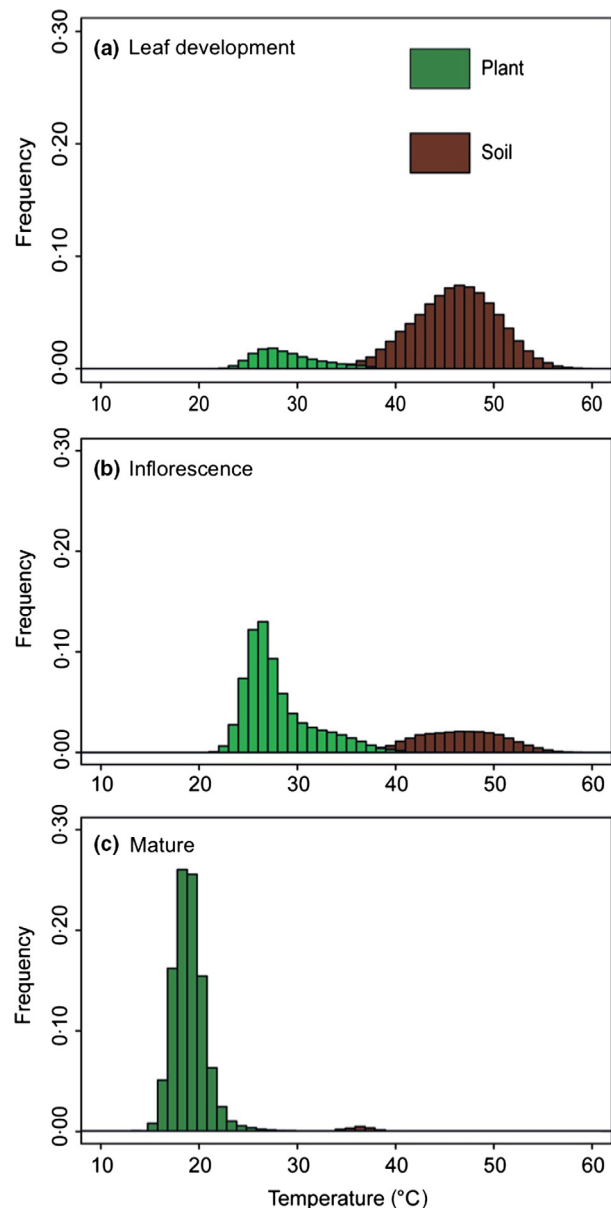


Fig. 6. Plant (green) and soil (brown) temperature frequency histograms from the TIR orthophotograph of a single potato field at each of the three studied phenology stages: leaf development (a), inflorescence (b) and mature (c).

patterns in a landscape. We discuss below the several advances and limits of this method in the field of thermal ecology.

Various studies have attempted to reconcile the spatial resolutions of thermal data with the species ecology using mechanistic modelling of microclimates at coarse spatial scale (Hijmans et al. 2005; Kearney, Isaac & Porter 2014), downscaling of climatic models (Fridley 2009; Palmer 2014) or spatial distribution inferences of microclimates based on structural landscape characteristics (Bennie et al. 2008; Dobrowski 2011; Sears, Raskin & Angilletta 2011). However, the obtained spatiotemporal resolution is still far from the body size of the studied organisms (Potter, Woods & Pincebourde 2013). Moreover, the optimal spatial resolution of cli-

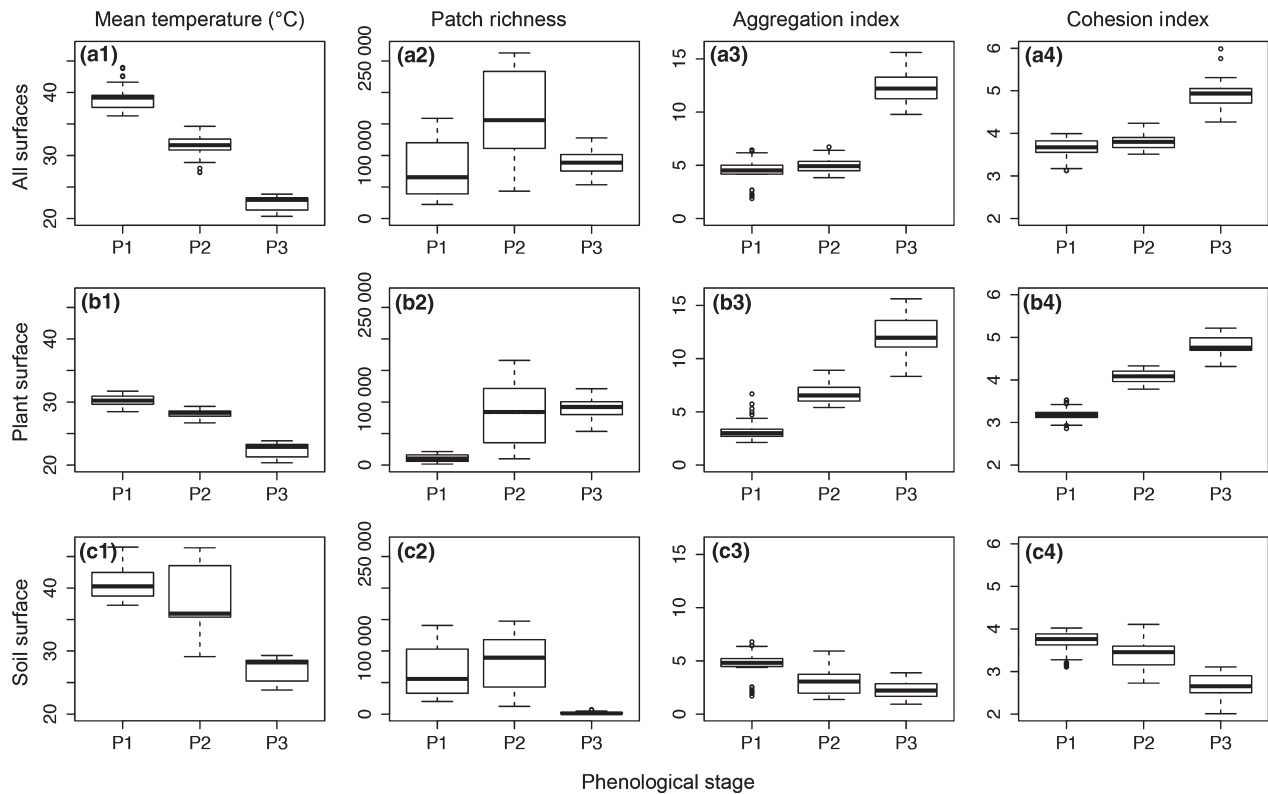


Fig. 7. Boxplots of selected thermal landscape metrics from the TIR orthophotographs for entire surface (a), plant surface (b) and soil surface (c) for the mean temperature (1), patch richness (2), aggregation index (3) and cohesion index (4). Data from the 12 studied potato fields are pooled. Phenological stages are given in abscise where P1 = leaf development stage, P2 = inflorescence stage and P3 = mature stage.

matic data to be used depends on the body size and the ability to move of the study organism: 1-m resolution might be plenty enough for trees and mobile animals, but is too coarse for tiny insects or small reptiles (Hannah et al. 2014; Sears & Angilletta 2015). Technical solutions, such as spacecraft or aircraft remote-sensing TIR imagery, are nowadays expensive and limited to the medium resolution of microbolometer sensor, which commonly offers c.a. 100 m resolution thermal images (ASTER and Landsat images, Kuenzer & Dech 2013; but see Lee et al. 2015) and c.a. 1 m resolution for aircraft TIR imagery. Our method surpassed this technical limitation by delivering maps of surface temperatures with centimetre resolution, allowing the study of the heterogeneity of thermal natural landscapes at spatial resolution relevant for the studied organism (Anderson & Gaston 2013; Potter, Woods & Pincebourde 2013).

As a topical technological breakthrough, our toolbox used image classification techniques to identify a large number of study surfaces in the visual landscape, based on their spectral components (e.g. different types of vegetation, soil, rock, water). In case of difficulties for separating different surfaces in the RGB orthophotographs because of their similar spectral properties (e.g. different plant species), one could increase the number of training sample polygons for each surface. If still insufficient, the toolbox could be completed with a multispectral sensor recording new spectral bands allowing a finer delimitation of surfaces (Liebisch et al. 2015). Then, the thermal

metrics associated to these surfaces can then be analysed separately or as an entity of the entire thermal landscape. Furthermore, our method resolves the current and difficult problem of emissivity associated with object surfaces in thermal images (Rubio, Caselles & Badenas 1997; Cilulko et al. 2013): by selecting surfaces with different emissivity values and creating as many sets of thermal orthophotographs as surfaces selected, our toolbox easily produces thermal orthophotographs with the appropriate emissivity for each considered surface. Consequently, surface temperatures obtained with our toolbox display the correct surface temperatures. Interestingly, our toolbox therefore highlights a poorly used outcome of UAV imagery in thermal ecology: the cross-analysis between RGB and TIR orthophotographs (Bulanon, Burks & Alchanatis 2009). For example, it would be possible to select thermal niches on the thermal orthophotograph suited for a given species (e.g. butterflies in mountainous landscapes, Ashton, Gutierrez & Wilson 2009) and identify the elements that create these refuges in the corresponding visual images, and vice versa. In this context, the metrics developed in our toolbox would allow revisiting some basic landscape ecology issues (e.g. influence of habitat shape index, edge effect, patch distribution and connectivity) from a thermal point of view, opening new opportunities towards thermal landscape ecology. Still, UAV-TIR measurements provide no information on temperatures of beneath-surface layers (i.e. under canopy, under rock or soil temperatures), which are important for ecological

studies. Combining precise climatic time series of these beneath-surface layers (Faye et al. 2014) to UAV-TIR imagery could therefore be a promising route to better understand the landscape scale thermal ecology processes that affect living organism. Our toolbox can also be used for assessing the temporal evolution of the thermal heterogeneity of natural landscape by repeating the data acquisition's step. Indeed, because UAV flights are GPS based and follow a same flight plan, they can be repeated over day and night at short time steps (e.g. each hour) to yield a complete picture of the thermal landscape experienced by organisms during 24 h or more.

The spatial extent at which microclimates can be explored with this methodology is determined by the flight time capacity of the UAV (Watts, Ambrosia & Hinkley 2012; Anderson & Gaston 2013; Ballesteros et al. 2014), that is at least tens of hectares at once (depending on the resolution needed), or larger if thermal orthophotographs are merged. Consequently, our toolbox would be most useful to ecologist interested in exploring the thermal ecology of a vast number of study models such as: the microdistribution of alpine plants (Scherrer & Koerner 2010), the microclimate at the leaf surface in tree canopies (Pincebourde et al. 2007), the spatial segregation of terrestrial insects along thermal gradients (Dangles et al. 2008; Wittman et al. 2010), thermally complex urban ecosystems (Meineke et al. 2013) or the distribution of desert lizards' thermal refuges (Sears & Angilletta 2015). Moreover, our methodological framework would facilitate the monitoring of microclimates in out-of-reach areas such as top forest canopies or extensive intertidal zones (Helmuth & Hofmann 2001), with appropriate thermal resolution for the study of flora and fauna that live in these remote environments.

The framework proposed here provides a way to link the various mechanisms operating at different spatial scales. On one hand, sophisticated toolboxes are available to compute the body temperatures (e.g. Gates 1980), or the plant surface temperatures (e.g. Jones 1992), from bioclimatological data. These models operate at the scale of the organism or the plant organ, and they integrate eco-physiological knowledge (e.g. transpiration rate of plants) with physical laws of heat transfers. On the other hand, remote sensing of surface temperatures taken by satellites (e.g. MODIS, Kuenzer & Dech 2013) operates at very large scale. These data are widely used in macroecological studies, including ecosystem functioning, carbon cycles. Linking fine-scale mechanisms to large-scale processes requires specific tools to describe how the thermal variations at fine-scale translate into detectable surface temperature shifts at coarse scale. Complex biophysical models exist to describe the spatial thermal heterogeneity at regional extent, but these models demand huge effort to be parameterized (Bennie et al. 2008; Dobrowski 2011; Kearney, Isaac & Porter 2014). Our toolbox establishes empirically this link between fine-scale eco-physiological mechanisms and large-scale processes in a straightforward fashion, with interest ultimately for global change biology and ecosystem services studies.

Finally, two constraints might hamper the adoption of this toolbox: first, UAV and TIR systems are cheap but not inex-

pensive (e.g. 30 000\$ for the all system used in this study) and 6 months of practise will be necessary to gain UAV and mapping proficiency. Secondly, the administrative restrictions such as the governmental approval for flying (Watts, Ambrosia & Hinkley 2012; Allan et al. 2015; Vincent, Werden & Dittmer 2015), mainly in the United States and Europe for now, are the most time consuming and difficult step to achieve for using UAVs in scientific research.

Acknowledgements

This work was part of the project 'Adaptive management in insect pest control in thermally heterogeneous agricultural landscapes' (MAN-PEST) funded by the Agence Nationale pour la Recherche (ANR-12-JSV7-0013-01) and an 'Action Incitative' funded from the Research Institute for Development (IRD). We warmly thank Carlos Carpio, Mario Herrera for their help at various stages of the study. Additionally, we are grateful to the Pix4Dmapper team, Bettina Heider and Dr. Sylvain Pincebourde for insightful comments and advice on earlier drafts of this work. The authors thank H. Arthur Woods and one anonymous reviewer for their valuable comments and constructive suggestions on the manuscript.

Data accessibility

R script: uploaded as online supporting information (Appendix S4).

References

- Allan, B.M., Ierodiaconou, D., Nimmo, D.G., Herbert, M. & Ritchie, E.G. (2015) Free as a drone: ecologists can add UAVs to their toolbox. *Frontiers in Ecology and the Environment* 13, 354–355.
- Anderson, K. & Gaston, K.J. (2013) Lightweight unmanned aerial vehicles will revolutionize spatial ecology. *Frontiers in Ecology and the Environment* 11, 138–146.
- Ashton, S., Gutierrez, D. & Wilson, R.J. (2009) Effects of temperature and elevation on habitat use by a rare mountain butterfly: implications for species responses to climate change. *Ecological Entomology*, 34, 437–446.
- Ballesteros, R., Ortega, J.F., Hernández, D. & Moreno, M.A. (2014) Applications of georeferenced high-resolution images obtained with unmanned aerial vehicles. Part I: description of image acquisition and processing. *Precision Agriculture*, 15, 579–592.
- Bennie, J., Huntley, B., Wiltshire, A., Hill, M.O. & Baxter, R. (2008) Slope, aspect and climate: spatially explicit and implicit models of topographic microclimate in chalk grassland. *Ecological Modelling*, 216, 47–59.
- Berni, J.A.J., Zarco-Tejada, P.J., Sepulcre-Cantó, G., Fereres, E. & Villalobos, F.J. (2009) Mapping canopy conductance and CWSI in olive orchards using high resolution thermal remote sensing imagery. *Remote Sensing of Environment* 113, 2380–2388.
- Bivand, R. & Lewin-Koh, N. (2014) Maptools: Tools for reading and handling spatial objects. R package version 0.8-30.
- Bulanon, D.M., Burks, T.F. & Alchanatis, V. (2009) Image fusion of visible and thermal images for fruit detection. *Biosystems Engineering* 103, 12–22.
- Ciulko, J., Janiszewski, P., Bogdaszewski, M. & Szczygalska, E. (2013) Infrared thermal imaging in studies of wild animals. *European Journal of Wildlife Research*, 59, 17–23.
- Dangles, O., Carpio, C., Barragan, A.R., Zeddarn, J.L. & Silvain, J.F. (2008) Temperature as a key driver of ecological sorting among invasive pest species in the tropical Andes. *Ecological Applications*, 18, 1795–1809.
- Dobrowski, S.Z. (2011) A climatic basis for microrefugia: the influence of terrain on climate. *Global Change Biology*, 17, 1022–1035.
- Dugdale, S.J., Bergeron, N.E. & St-Hilaire, A. (2015) Spatial distribution of thermal refuges analysed in relation to riverscape hydromorphology using airborne thermal infrared imagery. *Remote Sensing of Environment* 160, 43–55.
- Faye, E., Herrera, M., Bellomo, L., Silvain, J.F. & Dangles, O. (2014) Strong discrepancies between local temperature mapping and interpolated climatic grids in tropical mountainous agricultural landscapes. *PLoS ONE* 9, e105541.
- Floreano, D. & Wood, R.J. (2015) Science, technology and the future of small autonomous drones. *Nature*, 521, 460–466.
- Fridley, J.D. (2009) Downscaling climate over complex terrain: high finescale (<1000 m) spatial variation of near-ground temperatures in a montane

- forested landscape (Great Smoky Mountains). *Journal of Applied Meteorology and Climatology*, 48, 1033–1049.
- Gates, D.M. (1980) *Biophysical ecology*. Dover Publications, New York, USA.
- Gillingham, P.K., Huntley, B., Kunin, W.E. & Thomas, C.D. (2012) The effect of spatial resolution on projected responses to climate warming. *Diversity and Distributions*, 18, 990–1000.
- Hannah, L., Flint, L., Syphard, A.D., Moritz, M.A., Buckley, L.B. & McCullough, I.M. (2014) Fine-grain modeling of species' response to climate change: holdouts, stepping-stones, and microrefugia. *Trends in Ecology & Evolution*, 29, 390–397.
- Haselwimmer, C., Prakash, A. & Holdmann, G. (2013) Quantifying the heat flux and outflow rate of hot springs using airborne thermal imagery: case study from Pilgrim Hot Springs, Alaska. *Remote Sensing of Environment* 136, 37–46.
- Helmut, B.S. & Hofmann, G.E. (2001) Microhabitats, thermal heterogeneity, and patterns of physiological stress in the rocky intertidal zone. *The Biological Bulletin*, 201, 374–384.
- Hijmans, R.J. (2014) Raster: raster: Geographic data analysis and modelling. R package version 2.3-0.
- Hijmans, R.J., Cameron, S.E., Parra, J.L., Jones, P.G. & Jarvis, A. (2005) Very high resolution interpolated climate surfaces for global land areas. *International Journal of Climatology*, 25, 1965–1978.
- Jones, H.G. (1992) *Plants and microclimate: a quantitative approach to environmental plant physiology*. Cambridge University Press, Cambridge.
- Kearney, M.R., Isaac, A.P. & Porter, W.P. (2014) Microclim: global estimates of hourly microclimate based on long-term monthly climate averages. *Scientific Data*, 1, 1–9.
- Kuenzer, C. & Dech, S. (2013) *Thermal Infrared Remote Sensing*. Springer, London, UK.
- Lee, C.M., Cable, M.L., Hook, S.J., Green, R.O., Ustin, S.L., Mandl, D.J. & Middleton, E.M. (2015) An introduction to the NASA Hyperspectral Infra-Red Imager (HyspIRI) mission and preparatory activities. *Remote Sensing of Environment*, 167, 6–19.
- Liebig, F., Kirchgeßner, N., Schneider, D., Walter, A. & Hund, A. (2015) Remote, aerial phenotyping of maize traits with a mobile multi-sensor approach. *Plant Methods*, 11, 9.
- Marris, E. (2013) Fly, and bring me data. *Nature*, 498, 156–158.
- McGarigal, K. & Marks, B.J. (1994) *Fragstats: Spatial Pattern Analysis Program for Quantifying Landscape Structure*. Oregon State University, Forest Science Department, Corvallis.
- Meineke, E.K., Dunn, R.R., Sexton, J.O. & Frank, S.D. (2013) Urban warming drives insect pest abundance on street trees. *PLoS ONE*, 8, e59687.
- Palmer, T. (2014) Climate forecasting: build high-resolution global climate models. *Nature*, 515, 338–339.
- Pincebourde, S. & Casas, J. (2015) Warming tolerance across insect ontogeny: influence of joint shifts in microclimates and thermal limits. *Ecology*, 96, 986–997.
- Pincebourde, S., Sinoquet, H., Combes, D. & Casas, J. (2007) Regional climate modulates the canopy mosaic offavourable and risky microclimates for insects. *Journal of Animal Ecology*, 76, 424–438.
- Potter, K.A., Woods, H.A. & Pincebourde, S. (2013) Microclimatic challenges in global change biology. *Global Change Biology*, 19, 2932–2939.
- Rubio, E., Caselles, V. & Badenas, C. (1997) Emissivity measurements of several soils and vegetation types in the 8–14 mm wave band: analysis of two field methods. *Remote Sensing of Environment* 59, 490–521.
- Scheffers, B.R., Edwards, D.P., Diesmos, A., Williams, S.E. & Evans, T.A. (2014a) Microhabitats reduce animal's exposure to climate extremes. *Global Change Biology*, 20, 495–503.
- Scheffers, B.R., Evans, T.A., Williams, S.E. & Edwards, D.P. (2014b) Microhabitats in the tropics buffer temperature in a globally coherent manner. *Biology Letters*, 10, 20140819.
- Scherrer, D. & Koerner, C. (2010) Infra-red thermometry of alpine landscapes challenges climatic warming projections. *Global Change Biology*, 16, 2602–2613.
- Sears, M.W. & Angilletta, M.J. (2015) Costs and benefits of thermoregulation revisited: both the heterogeneity and spatial structure of temperature drive energetic costs. *The American Naturalist*, 185, E94–E102.
- Sears, M.W., Raskin, E. & Angilletta, M.J. (2011) The world is not flat: defining relevant thermal landscapes in the context of climate change. *Integrative and Comparative Biology*, 51, 666–675.
- Storlie, C., Merino-Viteri, A., Phillips, B., VanDerWal, J., Welbergen, J. & Williams, S. (2014) Stepping inside the niche: microclimate data are critical for accurate assessment of species' vulnerability to climate change. *Biology Letters*, 10, 20140576.
- Tonolla, D., Wolter, C., Ruhtz, T. & Tockner, K. (2012) Linking fish assemblages and spatiotemporal thermal heterogeneity in a river-floodplain landscape using high-resolution airborne thermal infrared remote sensing and in-situ measurements. *Remote Sensing of Environment* 125, 134–146.
- VanDerWal, J., Falconi, L., Januchowski, S., Shoo, L. & Storlie, C. (2014) *SDMTools: Species Distribution Modelling Tools: Tools for processing data associated with species distribution modelling exercises*. R package version 1.1-221.
- Vincent, J.B., Werden, L.K. & Dittmer, M.A. (2015) Barriers to adding UAVs to the ecologist's toolbox: peer-reviewed letter. *Frontiers in Ecology and the Environment* 13, 74–75.
- Watts, A.C., Ambrosia, V.G. & Hinkley, E.A. (2012) Unmanned aircraft systems in remote sensing and scientific research: classification and considerations of use. *Remote Sensing* 4, 1671–1692.
- Wilhelm, W.W., Ruwe, K. & Schlemmer, M.R. (2000) Comparisons of three-leaf area index meters in a corn canopy. *Crop Science*, 40, 1179–1183.
- Wittman, S.E., Sanders, N.J., Ellison, A.M., Jules, E.S., Ratchford, J.S. & Gotelli, N.J. (2010) Species interactions and thermal constraints on ant community structure. *Oikos*, 119, 551–559.
- Woods, H.A., Dillon, M.E. & Pincebourde, S. (2014) The roles of microclimatic diversity and of behavior in mediating the responses of ectotherms to climate change. *Journal of Thermal Biology*, in press. doi:10.1016/j.jtherbio.2014.10.002.

Received 8 June 2015; accepted 23 September 2015

Handling Editor: Andrew Tatem

Supporting Information

Additional Supporting Information may be found in the online version of this article.

Appendix S1. Ground control point for RGB and TIR orthophoto.

Appendix S2. Generation of RGB and TIR orthophotos.

Appendix S3. RGB orthophoto classification.

Appendix S4. R script for spatial analysis of thermal raster images.

Appendix S5. Phenological stages of potato crop.

Appendix S6. Boxplots of the spatial metrics.

Supporting Information of “Faye, E., Rebaudo, F., Yáñez, D., Cauvy-Fraunié, S. & Dangles O. (2015). A toolbox for studying thermal heterogeneity across spatial scales: from unmanned aerial vehicle imagery to landscape metrics. *Methods in Ecology and Evolution*. Doi: 10.1111/2041-210X.12488

Appendix S1: Ground control point for RGB and TIR orthophoto

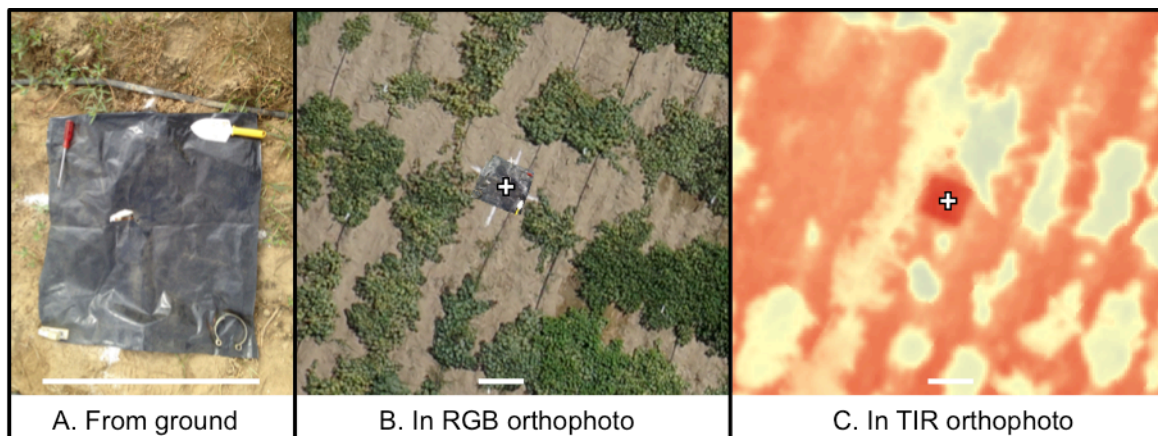
Appendix S2: Generation of RGB and TIR orthophotos

Appendix S3: RGB orthophoto classification

Appendix S4: R script for spatial analysis of thermal raster images

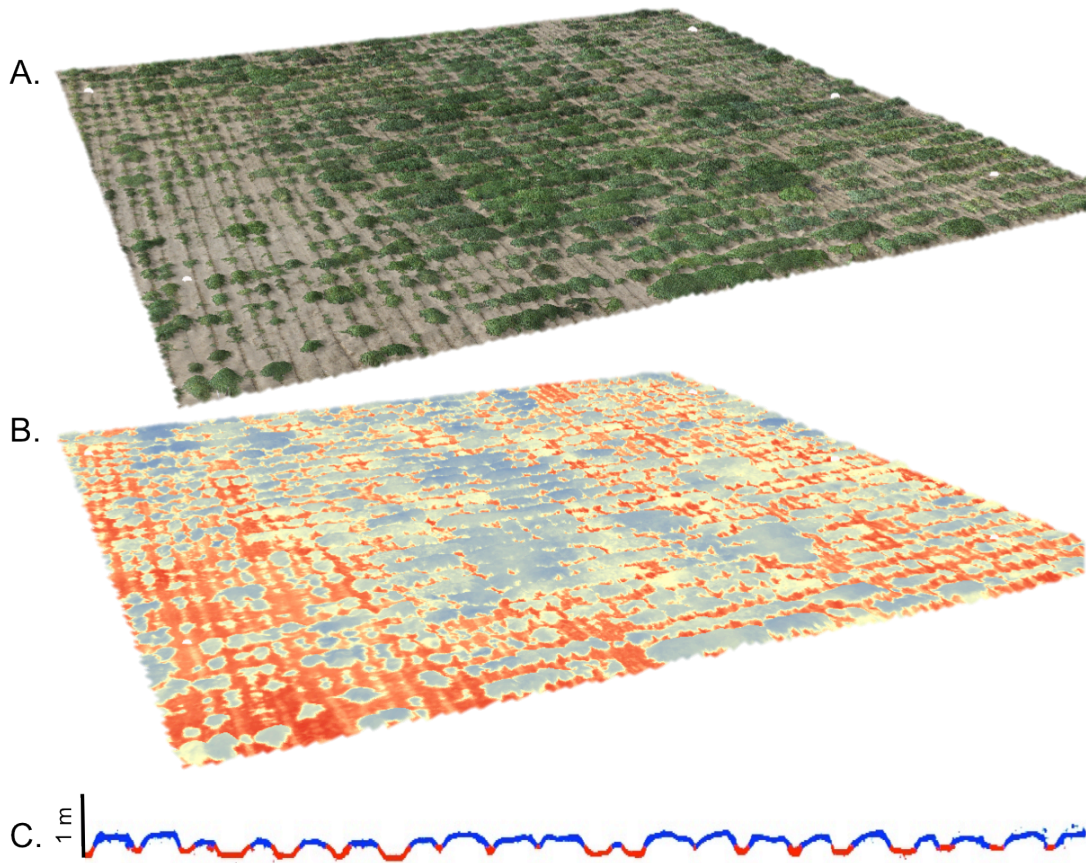
Appendix S5: Phenological stages of potato crop

Appendix S6: Boxplots of the spatial metrics



Appendix S1: Example of a ground control point (GCP) for RGB and TIR orthophoto. A. Photograph of the 1m² black square canvas sheet placed on the CGP location. B. The GCP identified in the RGB orthophoto. C. The GCP identified in the TIR orthophoto. The white crosses show the GPS position of the GCP measured on field before flying. The white bars are scale bars of 80 cm.

Appendix S2: RGB and TIR orthophotos aligned with the digital surface model exported from the mapping software for one of the studied field. A. The 3D RGB orthophoto. B. The 3D TIR orthophoto. C. Simple 2D TIR cross-section of the length of the studied field. Red and blue colours show temperature gradient.



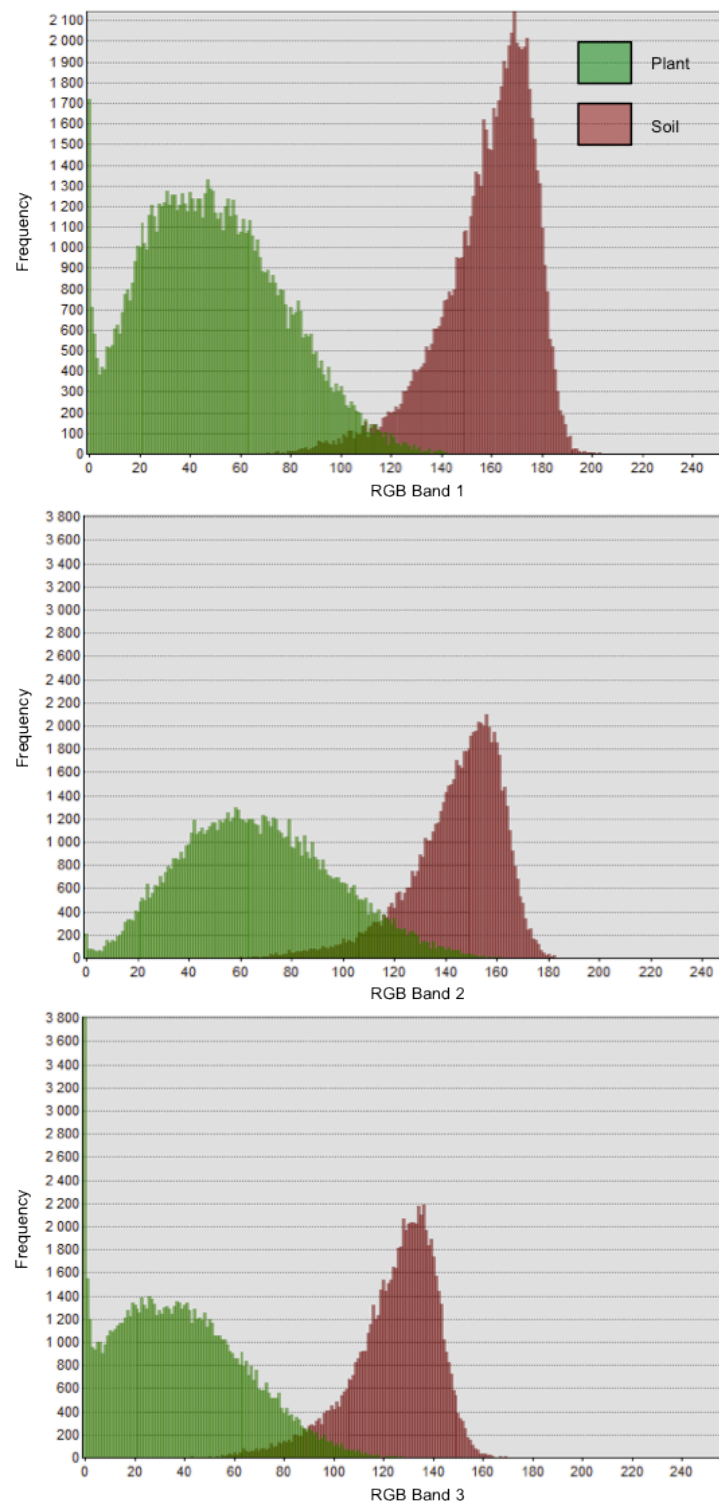
Generally, the mapping process starts with the selection of the photographs with sufficient overlap from multiple positions. Next, an image feature recognition algorithm (similar to the one described by [Lowe 2004](#)) is used to automatically detect and match the tie points between overlapping images, i.e. characteristic image objects. After a bundle adjustment on the matched features ([Triggs *et al.* 2000](#)), using the image position, orientation and the camera parameters, the software creates a densified point cloud based on multi-view stereo algorithms ([Furukawa & Ponce 2009](#)). The georeferencing of the densified point cloud (i.e. the orientation, scale and direction) in the coordinate system defined by the user is enhanced by the use of geotagged images and ground control points. Then based on this densified point cloud, the aerial images are gridded into a digital surface model, which is used to orthorectify

the images (geometrical correction for standardizing the scales and directions). The orthomosaic of all acquired images is adjusted (brightness, contrast, mesh configuration, etc.) using the Mosaic editor menu.

References appendix S2:

- Furukawa, Y., & Ponce, J. (2009). Accurate & camera calibration from multi-view stereo and bundle adjustment. *International Journal of Computer Vision*, 84(3), 257-268.
- Lowe, D. G. (2004). Distinctive image features from scale-invariant keypoints. *Journal of International Computer Vision*, 60, 91–110.
- Triggs, B., McLauchlan, P., Hartley, R., & Fitzgibbon, A. (2000). Bundle adjustment - a modern synthesis. *Lecture Notes in Computer Science*, 1883, 298–372.

Appendix S3: RGB orthophoto classification. Histograms showing the spectral signature of the ten training polygons - sample areas in the RGB image that represent different surfaces in the interactive supervised classification, i.e. 5 for plant and 5 for soil surfaces-, for each band of the RGB orthophoto. These polygons were used to check the separability (low overlapping) and distribution of the training samples to classify the rest of the pixels of the orthophoto using the classification tool in ArcGIS.



Appendix S4: R script for spatial analysis of thermal raster images

```
#!/usr/bin/env RScript
#####
### Supplementary Information
### A toolbox for studying fine-scale spatial thermal heterogeneity: from unmanned
### aerial vehicle imagery to landscape metrics
### E. Faye, F. Rebaudo, D. Yanez, S. Cauvy-Fraunié, O. Dangles
#####

### This script describes how to use thermal information contained in text files
### exported from a GIS software. The first part specifies the required packages in R.
### The second part specifies how to convert text files into ascii files, then the third
### part how to compute metrics. Please do not hesitate to contact us for any question:
### E. Faye: <ehfaye@gmail.com> ; F. Rebaudo: <francois.rebaudo@ird.fr> ;
### O. Dangles: <olivier.dangles@ird.fr>

#####
### environmental variables
#####
wd<-getwd() # working directory (change getwd() for something like "/home/mynome/Documents/")
myFilesPattern<-"(.txt)$" # text files selection using a regular expression (?regex() for help)
NAvalues<-TRUE # TRUE if NA values, FALSE otherwise
locNAvalue<-c(1,1) # location of a pixel known to have a NA value (if NAvalues<-TRUE)
trans<-1000 # if values need to be transformed: x = x / trans (set to 1 if no transformation)
nbDigitsSign<-0 # number of digits for the temperature
pxsize<-0.0025 # pixel size in m2
### The following script will create a CSV file tableLandMetrics.csv which can be read in R
### using read.table("tableLandMetrics.csv",header=TRUE,sep=",")
#####

### [1] install and load packages
### [2] select text files from working directory and transform to ascii
### [2.1] set working directory
### [2.2] select files
### [2.3] transform to ascii files
### [3] perform metrics on the files imported and return results within a data.frame
### [4] graphics

### [1] install and load packages
pkgCheck <- function(x){ # check for a package, install and load
  if (!require(x,character.only = TRUE)){
    install.packages(x,dependencies=TRUE)
    if(!require(x,character.only = TRUE)) {
      stop()
    }
  }
}
pkgCheck("SDMTTools")
pkgCheck("raster")
pkgCheck("sp")
pkgCheck("maptools")

### [2] select Text files from working directory and transform to ascii
# [2.1] set working directory
setwd(wd)
# [2.2] select files
myTextFiles<-list.files(pattern=myFilesPattern)
print(myTextFiles)

# [2.3] transform to ascii files
lapply(myTextFiles,function(x){
  rasterFile<-raster(x)
  ascFile<-asc.from.raster(rasterFile)
  if (NAvalues==TRUE){ascFile[ascFile==ascFile[locNAvalue[1],locNAvalue[2]]]<-NA}
  ascFile<-round(ascFile/trans,digits=nbDigitsSign)
  write.asc(ascFile,file=strsplit(x,"\\.")[[1]][1])
  return(paste("File: ",x," -> ",strsplit(x,"\\.")[[1]][1],".asc [ok]",sep=""))
})

### [3] perform metrics on the area of interest and return results within a data.frame
myAsciiFiles<-list.files(pattern=".asc$")
myAsciiContent<-lapply(myAsciiFiles,function(x){read.asc(x)})
metrics<-sapply(seq(length(myAsciiContent)),function(myAsc){
  Px_TIR<- length (myAsciiContent[[myAsc]][!is.na(myAsciiContent[[myAsc]])]) # Number of
pixels

```

```

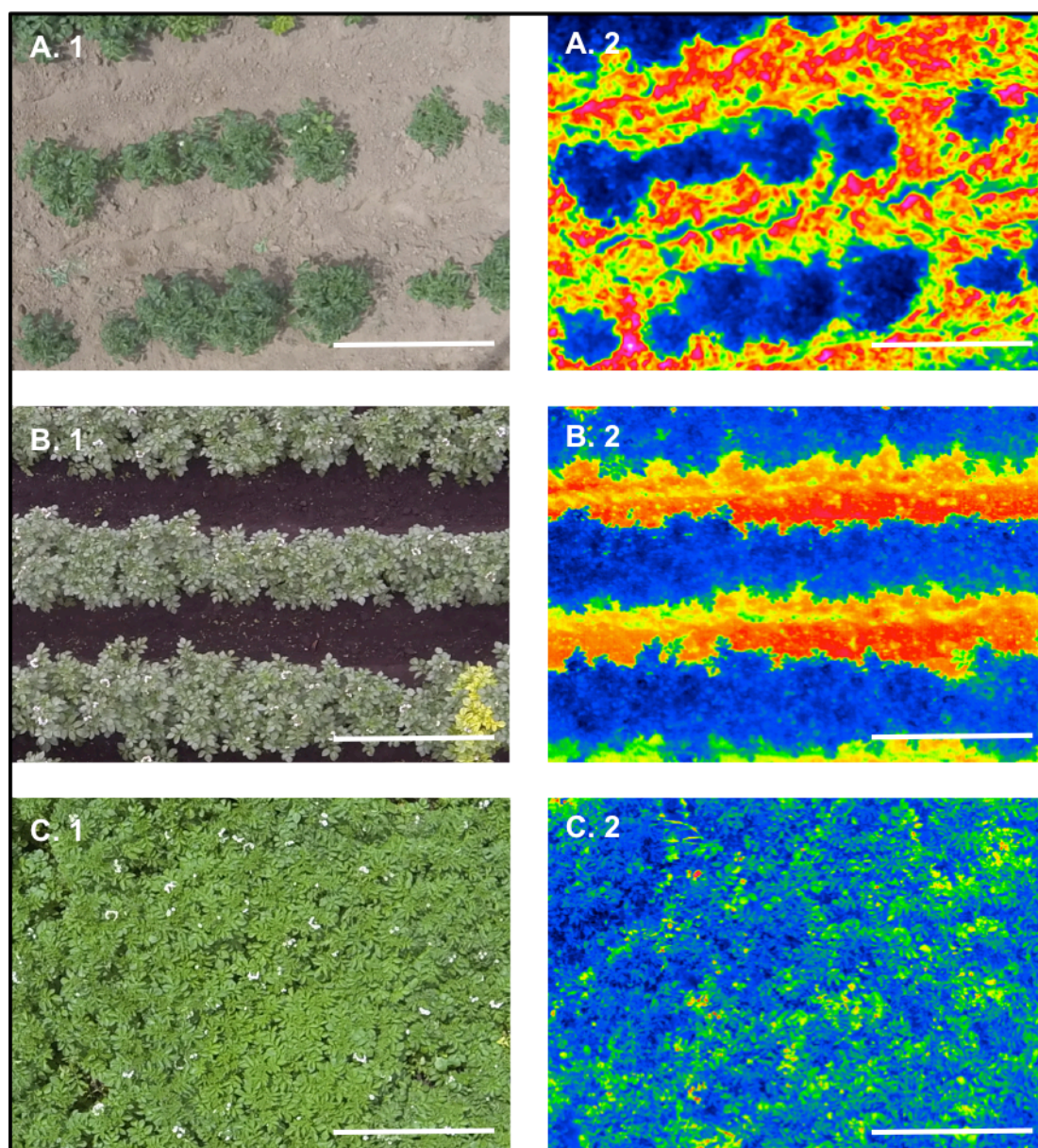
Area_TIR<-Px_TIR*pxsize # Area (m2)
cclmyAsc<- ConnCompLabel(myAsciiContent[[myAsc]]) # Define a simple binary matrix of the
same size and extent
stats_TIR<-unlist(ZonalStat(myAsciiContent[[myAsc]], cclmyAsc, FUN =
c("mean", "sd", "min", "max"))) # Descriptive statistics at the landscape level
land_metrics_TIR<-ClassStat(myAsciiContent[[myAsc]], cellsize = pxsize, latlon =
FALSE) # landscape metrics
PR_TIR<- sum (land_metrics_TIR [,2]) # Patch Richness
AI_TIR<- sum(land_metrics_TIR [,34]*land_metrics_TIR [,4]) # Aggregation Index at
Landscape level
SHDI_TIR<- -sum(land_metrics_TIR [,4]*log(land_metrics_TIR [,4])) # Shanon Diversity
Index
PD_TIR<- PR_TIR/Px_TIR # Patch density
SIDI_TIR<- 1 - sum (land_metrics_TIR [,4]*land_metrics_TIR [,4]) # Simpon's Diversity
Index
LSI_TIR <- sum (land_metrics_TIR [,8]*land_metrics_TIR [,4]) # Landscape shape index
CI_TIR <- sum((replace(land_metrics_TIR [,38], is.na(land_metrics_TIR
[,38]), 0))*land_metrics_TIR [,4]) # Landscape cohesion index
return(matrix(c(Px_TIR, Area_TIR, stats_TIR[2], stats_TIR[3], stats_TIR[4], stats_TIR[5], PR_
TIR, AI_TIR, SHDI_TIR, PD_TIR, SIDI_TIR, LSI_TIR, CI_TIR), dimnames=list(c("Px_TIR", "Area_TIR", "stats_
TIR_mean", "stats_TIR_sd", "stats_TIR_min", "stats_TIR_max", "PR_TIR", "AI_TIR", "SHDI_TIR", "PD_TIR
", "SIDI_TIR", "LSI_TIR", "CI_TIR"), c(myAsciiFiles[myAsc]))))
})

metrics<-
matrix(metrics, ncol=length(myAsciiContent), dimnames=list(c("Px_TIR", "Area_TIR", "stats_TIR_mean
", "stats_TIR_sd", "stats_TIR_min", "stats_TIR_max", "PR_TIR", "AI_TIR", "SHDI_TIR", "PD_TIR", "SIDI_T
IR", "LSI_TIR", "CI_TIR"), c(myAsciiFiles)))
tableLandMetrics<-t(data.frame(metrics, row.names=rownames(metrics))) # convert matrix to table
print(tableLandMetrics)
write.csv(tableLandMetrics, "tableLandMetrics.csv", quote = FALSE) # save data into a csv file

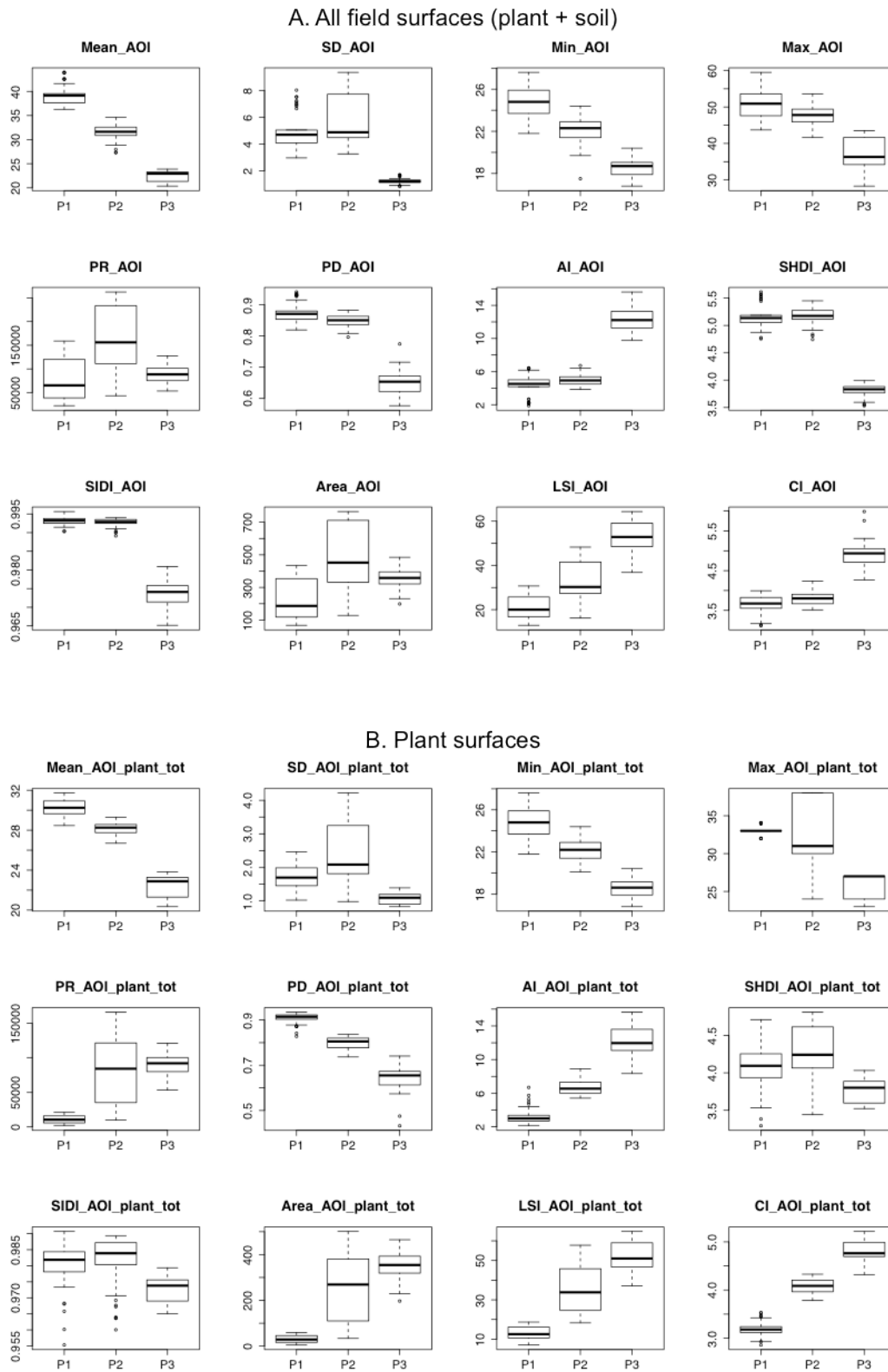
### [4] graphics
pdf(file="BOXPLOT_tableLandMetrics.pdf")
par(mfrow=c(4,4), mar=c(4,4,1,1))
sapply(1:length(tableLandMetrics[1,]),
function(x){boxplot(tableLandMetrics[,x], xlab=colnames(tableLandMetrics)[x], main="" )})
dev.off()
pdf(file="HIST_tableLandMetrics.pdf")
par(mfrow=c(4,4), mar=c(4,4,1,1))
sapply(1:length(tableLandMetrics[1,]),
function(x){hist(tableLandMetrics[,x], xlab=colnames(tableLandMetrics)[x], main="" )})
dev.off()

```

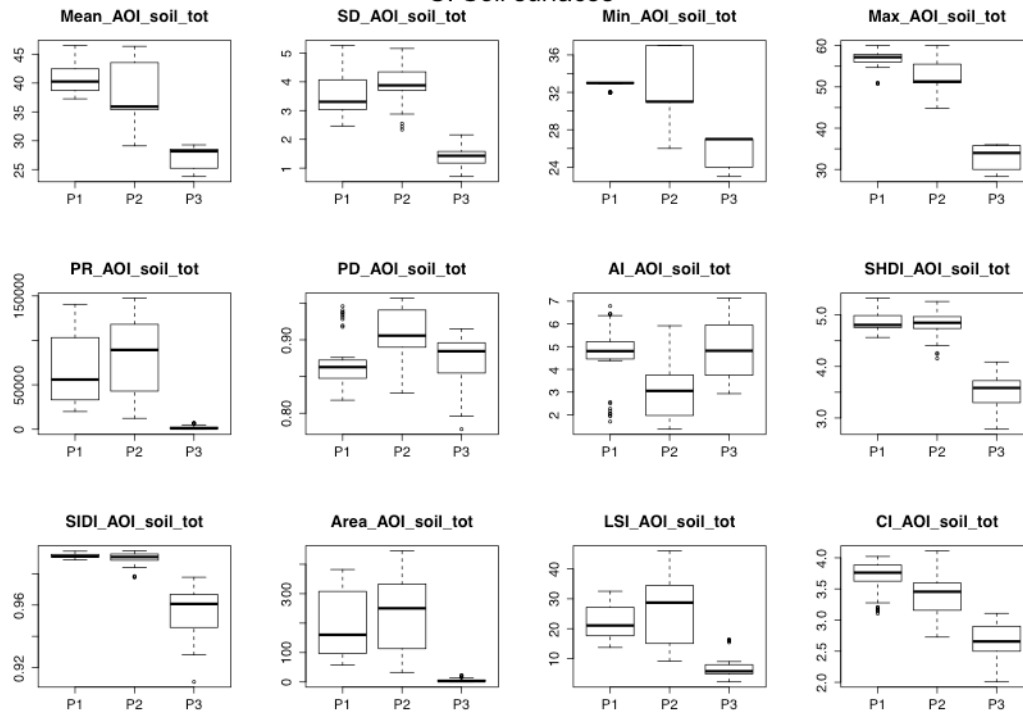
Appendix S5: Potato crop phenological stages' used in the main document. The figure shows images of potato crop fields in the visual (column #1) and thermal infrared (column #2) spectral range at the A. Leaf development, B. Inflorescence, and C. Mature growth stage. The white scale bars represent 1-meter length.



Appendix S6: Boxplots of the spatial metrics performed on TIR orthophotos across plant phenology for all the studied fields for A. all surfaces, B. Plant surfaces and C. Soil surfaces. Phenological stages are given in abscise where P1 = leaf development stage, P2 = inflorescence stage and P3 = mature stage. The acronym AOI refers to area of interest.



C. Soil surfaces



CHAPTER III

Microclimates and pests *in situ*

The last Chapter of this thesis is the application *in situ* of the methods developed in Chapter II in view to understand the relationship between crop microclimates and pest occurrences in potato fields. For this, we assessed the thermal heterogeneity of surface temperatures at the field scale with aerial infrared thermography done at fine spatial resolution. In the same time, a sampling of four major potato pests in the study region was performed in the studied fields. We then evaluated the fine-scale thermal heterogeneity of crop canopy implications for pest performance and mobility regarding their thermal tolerance for development. Finally, we compared a variety of spatial metrics of the surface microclimates in crops with the pest abundance and richness measured in fields. This work took place on 38 potato fields of the central Ecuadorian Andes and revealed that few centimetres matter when considering optimal thermal environments for pest performances.

This work was performed in collaboration with the ‘Instituto Nacional de Investigaciones Agropecuarias’ (INIAP) and the ‘Escuela Superior Politécnica de Chimborazo’, Ecuador. This last Chapter is a manuscript to submit to *Journal of Applied Ecology*:

- **Faye, E.**, Rebaudo, F., Carpio, C., Herrera, M., & Dangles, O. Does heterogeneity in crop canopy microclimate matter for pests? Evidence from aerial high-resolution thermography. To submit in *Journal of Applied Ecology*.

Title: Does heterogeneity in crop canopy microclimate matter for pests? Evidence from aerial high-resolution thermography

Running title: Crop canopy microclimates and pests

Authors: E. FAYE^{1,2,3}, F. REBAUDO¹, C. CARPIO⁴, M. HERRERA⁵, O. DANGLES^{1,3}

Affiliations:

¹ Institut de Recherche pour le Développement, UMR EGCE, IRD-247 CNRS-UP Sud-9191, 91198 Gif-sur-Yvette cedex, France.

² Sorbonne Universités, UPMC Univ Paris 06, IFD, 4 Place Jussieu, 75252 Paris cedex 05, France.

³ Pontifica Universidad Católica del Ecuador, Facultad de Ciencias Exactas y Naturales, Quito, Ecuador.

⁴ Facultad de Recursos Naturales, Escuela Superior Politécnica de Chimborazo.

⁵ Instituto Nacional de Investigaciones Agropecuarias (INIAP) - Dirección de Investigaciones, Quito-Ecuador.

Corresponding authors: Emile Faye - ehfaye@gmail.com; Olivier Dangles - olivier.dangles@ird.fr

Paper type: Standard paper

Word count (between Title to Supporting information): 6942

Keywords: high-resolution thermal imagery, microclimate heterogeneity, spatial metrics, potato pests, surface temperature.

Abstract

- 1- A vast majority of agricultural pests and diseases are strongly influenced by microclimatic conditions that affect their performance and distribution. Thermal heterogeneity experienced by crop pests at fine spatial scales is potentially key to understand pest dynamics, yet its study over entire fields has never been performed.
- 2- We used aerial infrared thermography to yield fine-resolution measurements (5 millimetres pixel side) of crop canopy temperatures in 38 potato fields in the Ecuadorian Andes. In each field, we characterized the spatiotemporal thermal heterogeneity of crop canopy and sampled populations of four common potato pests (trips, aphids, dipterans, and fungi) in 30 different plots (total of 1140 thermal images). We then evaluated the fine-scale thermal heterogeneity implications for pest performance and compared a variety of thermal metrics with pest abundance and richness measured in field.
- 3- We found that the range of temperatures available for pests in crop canopies was mostly independent on scale: pests can access in their close vicinity (1.2 m) most of the thermal microenvironments recorded at the field level. Also, the availability of thermal microenvironments was strongly dependent on solar radiations: with increasing radiation levels, pests have to travel less distance to reach a variety of temperatures.
- 4- At the plot level, we found no relationship between pest abundance and thermal metrics: the four studied pests were not clumped in their supposedly preferred thermal conditions but distributed rather evenly. However, pest richness was significantly correlated to both thermal aggregation and diversity index: more diverse and distinctly distributed thermal environments presented higher diversity of pest. Finally crop pests always have a wide range of possibilities to regulate the temperature of their

environment within very short distances.

- 5- By measuring crop microclimates at fine spatial resolution over entire fields, our study revealed that a few centimetres suffice for providing enough optimal thermal environments for crop pests to enhance their performances.

Introduction

Microclimate effects on ectotherm populations have long been studied from an ecological perspective ([Cloudsley-Thompson 1962](#), [Ferro *et al.* 1979](#), [Willmer 1982](#), [Frazier *et al.* 2006](#), [Scheffers *et al.* 2014](#), [Storlie *et al.* 2014](#), [Rojas *et al.* 2014](#)). The spatiotemporal heterogeneity of microclimates ([Woods *et al.* 2014](#), [Sears & Angilletta 2015](#)) and the biophysics connecting their properties to those of local macroclimates ([Holmes & Dingle 1965](#), [Bakken 1992](#), [Gates 1980](#), [Kearney *et al.* 2014](#)) are widely recognized for shaping ectotherms distribution and metabolism ([Porter *et al.* 2002](#), [Storlie *et al.* 2014](#), [Raghu *et al.* 2014](#)). Body temperature is strongly altered by changes in the organism's physical environment, inducing a direct relationship between environmental parameters and the metabolism of the organism ([Sears & Angilletta 2015](#)). The relatively small size of most ectotherms (e.g., insects) allows them to exploit a great diversity of small-scale variations in microclimate that are not available to larger animals ([Ashton 2009](#)). Consequently, it is well acknowledged that quantifying the spatiotemporal heterogeneity of the thermal environment as perceived by small organisms (i.e., at the proper scale) is of prime importance for understanding their distribution and biological responses in their microhabitats ([Potter *et al.* 2013](#), [Storlie *et al.* 2014](#)).

Although the spatiotemporal structure of microclimates has been shown to affect insect populations ([Cloudsley-Thompson 1962](#), [Willmer 1982](#), [Porter *et al.* 2002](#), [Raghu *et al.* 2004](#), [Scheffers *et al.* 2014](#), [Storlie *et al.* 2014](#), [Woods *et al.* 2014](#)), implications in the context

of agricultural pests have been poorly explored. Being ectotherms, agricultural pests respond to the rules of thermal dependency for achieving their optimal performances (Davis *et al.* 2006, Angilletta 2009). That is why precise information on pests' thermal responses is crucial for understanding their occurrence and dynamics (Travis *et al.* 2011). However, very few studies have focused on the potential effects of microclimates on pest distribution at the field scale (Ferro 1979, Juroszek & Von Tiedemann 2013, Sutherst 2014). Tompkins *et al.* (1993) and Suh *et al.* (2002) showed how agronomic practices and canopy closure influenced the infestation of crop diseases and pests by modifying the components of the inside field microclimates (*Septoria sp* in wheat field and *Trichogramma exiguum* in cotton field, respectively). Also, Willmer *et al.* (2008) reported how intra-field microclimates constrained the distribution patterns of raspberry beetle (*Byturus tomentosus*). But these studies concentrated on punctual measurements of microclimatic parameters rather than a continuous assessment of the spatial heterogeneity of microclimates at fine spatial scale in the field.

Technical limitations in microclimate measurements have long impeded the exploring to what extent the spatiotemporal heterogeneity in microclimatic conditions can potentially influence crop pest distribution and their damages at the field level. However, recent developments in thermal infrared camera resolution and mobility (e.g., using unmanned-aerial vehicles – UAV) now allow characterizing microclimates experienced by tiny insect pests over large field surfaces (Faye *et al.* 2015). Here, we used aerial thermal infrared (TIR) cameras (both fixed on UAV and long perches) to yield accurate estimate of the spatiotemporal heterogeneity of surface temperature at the field scale and relate this information with the occurrence of four major potato pests. We sampled 38 potato fields (*Solanum tuberosum* L.) with aerial thermal infrared and visual imagery (5 mm resolution and 3.2 x 2.4 m extent for the perches based thermal images) to obtain, after a GIS processing, the surface temperatures of crop canopies only. With this methodology we reached an average

TIR coverage of 21.41% ($\pm 7.91\%$) of the 38 potato fields. The main objectives of this study were 1) to characterize the intra-field spatiotemporal heterogeneity in surface temperature at a scale relevant for pests (both insects and fungi) living at the leaf surface, and 2) to assess whether such thermal heterogeneity can be related to pest performance and occurrence in various parts of the field. We hypothesized that 1) the range of temperatures available for pests in crop canopies within the field was mostly independent upon the spatial scale considered, 2) daily variations in radiations influence microclimate habitats available for pests, 3) pest performance is affected by thermal heterogeneity in space and time, 4) pests would be found at higher densities in thermal microclimates optimal for them, and 5) higher diversity of microclimates would allow a co-occurrence of higher richness of pest species.

Materials and methods

Data acquisition in the field

Study area. Measurements were carried out during the last two weeks of January 2014 in 38 potato fields located 115 km south from the equatorial line ($01^{\circ}01'36''\text{S}$, $78^{\circ}32'16''\text{W}$) at 2850 \pm 135 m.a.s.l. in the Cotopaxi province of Ecuador. The low seasonality occurring in this region (less than 1°K average mean monthly temperature variations) allows potato crops to be planted and harvested all year round, making convenient the study of crops at different growth stages at the same time (Faye *et al.* 2014). Therefore, the 38 fields provided a variety of potato phenology from leaf development to mature stage (Appendix 1). The studied fields were planted with 1-m spaced rows (± 0.16) and with 0.5-m spaced plants (± 0.06) within a row. Fields were not irrigated since at least 3 days before sampling. The field areas were relatively small, ranging from 630 to 3072 m^2 (average of 1265 m^2). Additional characteristics of studied fields and the dates of measurements are given in Appendix 1.

Solar radiation recordings. During the period of data acquisition, we recorded in each studied field global solar radiation (in watt/m^2) using a pyranometer sensor facing the sky vault (LI-1400, LI-COR, Lincoln, USA). The global solar radiation logger was located nearby the studied field and recorded the global solar radiation for each TIR image taken.

Acquisition of aerial TIR and visible images. Thermal infrared (TIR) images were acquired using a TIR camera (HR research 680, InfaTec, Dresden, Germany) equipped with a 640×480 -pixel uncooled micro-bolometer sensor and a 30 mm lens. The TIR camera recorded the long-wave infrared radiation emitted by objects in the spectral range from 7.5 to 14 μm . The thermal sensitivity of the TIR camera was $< 0.03\text{K}$ at 30°C , and the measurement accuracy was $\pm 1.5\text{K}$. The TIR camera was switched on at least ten minutes before measurements to allow sensor stabilization. The emissivity was fixed to 0.98, the emissivity of potato plant surface ([Rubio et al. 1997](#)). Digital RGB images were acquired with a GoPro (GoPro 3+ black edition, GoPro Inc., USA) that was attached to the thermal camera with both lenses pointing the same direction (Fig. 1). The GoPro camera had a 12-megapixel sensor and was settled in photo mode with a narrow field of view to avoid image distortions.

Both types of images were acquired using either an unmanned aerial vehicle (UAV) or a gutter pipe. We first carried on UAV flights over twelve potato fields to assess the scale-dependence of thermal heterogeneity (hypothesis 1), by following the method described in [Faye et al. \(2015\)](#). Briefly, we flew a hexacopter UAV 60 m a.g.l. over 12 fields to yield one TIR and one RGB orthophoto with a resolution of 5 cm^2 and 1.2 cm^2 , respectively. For technical reasons we were not able to fly over all the 38 potato fields using the UAV so we developed an alternative method in which the cameras were mounted on a 6-m long gutter pipe with a $+20^\circ$ angle to the pipe axis. Then, the pipe was tilted by $+70^\circ$ to the ground to obtain perfectly perpendicular TIR and RGB images, as it is the case with UAV acquisition

(Fig. 1). At this distance from the ground, the field of view of the TIR camera was 3.2 x 2.4 m with a pixel side of 5 millimetres. Within each field, we evenly selected 10 study points at which microclimatic conditions were recorded following [Faye *et al.* \(2014\)](#) (see Appendix 5 for details). At each of the ten study points within a field, we simultaneously triggered the TIR and RGB camera at 3 locations around the point: on the front side, at 90° rotation on the left side and at 90° rotation on the right side of the point (corresponding to a total of 1140 TIR and 1140 RGB images acquired, i.e., 10 study points x 3 image locations x 38 fields). The pipe method allowed us an average TIR coverage of 21.41% ($\pm 7.91\%$) in the 38 potato fields (Appendix 1). The thermal heterogeneity recorded by pipe was comparable to that recorded by the UAV (see Fig. 2)

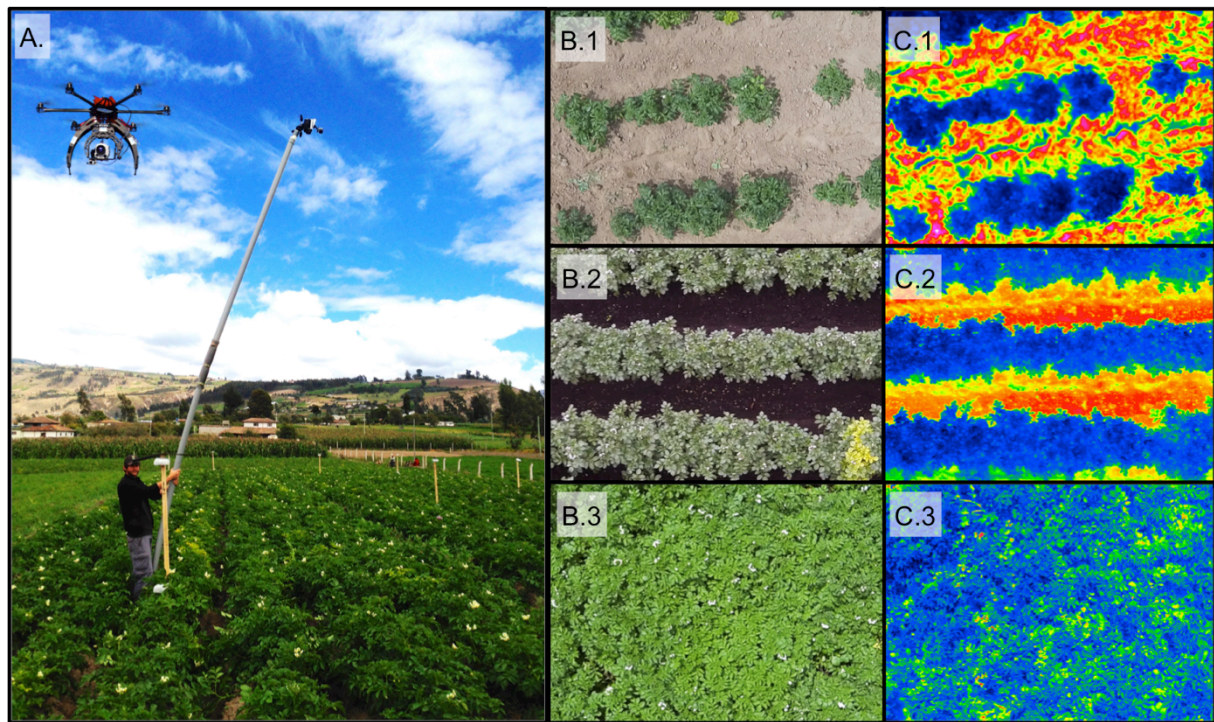


Figure 1: Aerial thermal infrared methodologies used for the experiments. A. Photograph of the UAV and the 6 m high gutter pipe equipped with the TIR and RGB cameras. B. RGB images for three potato fields at different phenologies: B.1. leaf development, B.2. inflorescence, and B.3. mature stages. C. TIR images of the same 3 fields. Dimension of TIR and RGB images: 3.2 x 2.4 m.

Pest assessment. Simultaneously to the microclimate data acquisition, we assessed, in each of the 30 image extents per fields (see above), population levels of most common potato pests and diseases. Pest assessments were made by the same persons (CC and MH), both experts in potato pest identification. They enumerated the following pests: *Frankliniella tuberosi* (Moulton), *Liriomyza huidobrensis* (Blanchard), *Myzus persicae* (Sulzer) and *Phytophthora infestans* (Mont.). The sampling of adults thrips (*F. tuberosi*), aphids (*M. persicae*) and diptera leafminers (*L. huidobrensis*) was made by plant beating on a white plastic tray (35 cm length \times 30 cm width \times 5 cm of depth) repeated twice and a direct counting of the remaining insects on the lower leaf surfaces (Weisz *et al.* 1996). Because *P. infestans* is an oomycete responsible for the potato late blight, its infestation has been measured as the rate of the total plant surfaces affected by the disease. These four pests are among the most damaging pests of potato worldwide and represent alone 70% of the potato pest occurrence in the study area (Pumisacho & Sherwood 2002).

Image treatment and data sets

Image processing. TIR and RGB images were processed following Faye *et al.* 2015. Briefly, images were paired using the camera's clock and then aligned and geometrically-matched using ArcGIS 10.2 (ESRI, Redlands, USA). Afterward, images were processed in ArcGIS for extracting in the TIR images the surfaces belonging to the plant canopy only. This procedure used RGB image classification (between soil and plant surfaces) to provide a shapefile mask of the plant surface that was used for extracting the plant surfaces in the TIR image. As we were interested in relating microclimatic conditions to pest population levels, and assuming that mobile pests can move independently in all directions from their initial location, we selected the largest circle (1.2 m-radius) that could be drawn within the 3.2 x 2.4 m extent of the TIR images. These circles avoided potential bias in quantifying thermal heterogeneity

available for pests as they ‘provided’ a pest moving further away from its initial location with the same number of pixels in all directions.

Pests’ optimal temperatures data. Among all studied pest, four have been intensely studied for their agronomical and economical interests. Consequently, we searched in the literature information on the thermal biology of the adult stages of these four pests. In particular, we gathered minimum and maximum critical temperatures (CT_{min} and CT_{max}) to identify growth performance ranges (or thermal tolerance ranges, Huey & Stevenson 1979). The optimal temperature ($Topt$) at which the growth rate is maximal was either extracted directly from the literature or estimated as the last quartile of the growth performance range. Indeed, thermal performance curves of growth rate for insect are known to display a marked negative skewness and a rapid drop after the $Topt$, making the $Topt$ likely to be situated within the last quartile of the growth performance range (Huey & Stevenson 1979, Frazier *et al.* 2006). These thermal parameters for each pest growth performance and their related references are given in Table 1.

Pest	$Topt$	$T_{min} - T_{max}$	Last quartile	References
<i>Frankliniella tuberosi</i>	28	15 – 30	26.25 – 30	Chaisuekul & Riley 2005
<i>Liriomyza huidobrensis</i>	24	20 – 25	23.75 – 25	Lanzoni <i>et al.</i> 2002
<i>Myzus persicae</i>	34	6.5 – 37.3	29.60 – 37.3	Davis <i>et al.</i> 2006
<i>Phytophthora infestans</i>	21	13 – 22	19.75 – 22	Sparks <i>et al.</i> 2014

Table 1: Thermal parameters of the growth performances for the four studied potato pests as identified in the literature. $Topt$, T_{min} - T_{max} and Last quartile are expressed in °C.

Data analyses

To assess the effect of the spatial scale on thermal heterogeneity (*hypothesis 1*), we computed the distance and the difference in surface temperatures between all the pixels of the TIR images and two specifically chosen pixels P1 and P2. These two pixels, different for each image, were chosen to be both the nearest from the central pixel of the image and the closest possible to the mean temperature value of the image. P1 and P2 were selected with various thresholds to ensure the accuracy of their location on the images and the proximity to the selected temperature value (see R script provided in Appendix 2 for details). The temperature value of P1 and P2 was compared to the temperature value of all the pixels of the TIR circle ($P1 - P_i$). Additionally, the distance separating P1 (and P2) with all of the others pixels of the TIR circle (P_i) was calculated using the Pythagorean theorem and expressed in metre (Appendix 2 for details). Consequently, we obtained the distance (in m) and the Δ temperature (in Kelvin) between each pixel of the image and P1 (and P2). We then computed a bivariate binning of the calculated distance and Δ temperature and plotted it in a hexagonal binning plot. In these plots, hexagonal cells with count > 0 are plotted using a colour ramp in proportion to the counts (i.e., the number of pixels of the image that fall within this cell). Using this procedure, and following the concepts proposed by [Jackson & Fahrig \(2015\)](#), we assessed how spatial scale affected the thermal heterogeneity of potato crop canopies by selecting five circles of different radius (1.2 m, 6 m, 12 m, 18 m, and 24 m) on the twelve UAV orthophotos (Fig. 2 present this analysis for one of them). All circles were centred onto the middle point of the entire field. All analyses were coded in R (R Core Team, 2014) using various packages (Hexbin, Mass, SP, and Raster; see Appendix 2 for the full code and details).

To assess the effect of radiations on thermal heterogeneity (*hypothesis 2*), we plotted the relationship between the minimums, maximums, means and standard deviations of the

plant surface temperatures versus the global solar radiation for the 1140 TIR images (Fig. 3). Fit significance was assessed using a Spearman-rank test using Table Curve 5.01 software (Systat Software, Chicago, Illinois).

To explore how thermal spatiotemporal heterogeneity would affect pest performance (*hypotheses 3-5*), we first plotted the bivariate binning of distance and Δ temperatures and all other pixels included in the last quartile of the thermal tolerance range for pest development depending on radiations classes (Fig. 5). P1 and P2 were chosen to be the closest to the T_{opt} of each pest. We then related pest abundance (i.e., the number of individuals on a given potato plant) with the mean surface temperatures (Fig. 6) and plotted two spatial metrics of thermal landscapes configuration (i.e., Aggregation index and the Shannon's diversity index, see [Faye et al. 2015](#) versus pest richness (Fig. 7, Appendix 3).

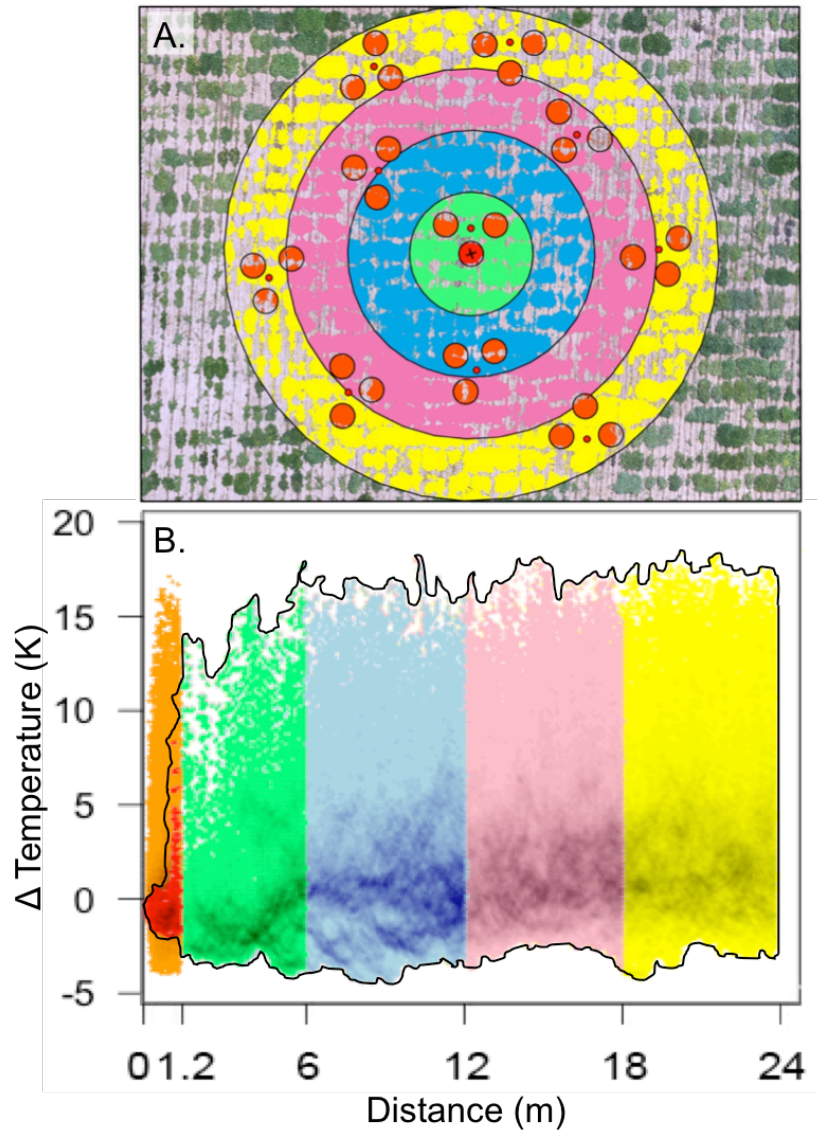


Figure 2: Effect of spatial scale on surface temperature heterogeneity in potato fields. A. RGB orthophoto acquired from an unmanned aerial vehicle. Red dots represent the ten study points evenly distributed in the field (yellow circle). Coloured surfaces show the TIR pixels of the plant canopy extracted from the TIR orthophoto: orange for the thirty 1.2 m-radius circles, and red, green, blue, pink and yellow for 1.2, 6, 12, 18 and 24 m-radius circles, respectively, all centred on the same central point of the field (black cross). B. Hexagonal binning plot of the Δ distance (in m) and Δ temperature (in K) for the different TIR circles with corresponding colours. The black line displayed the contour of the hexagonal binning plot of the largest circle.

Results

Spatiotemporal heterogeneity in crop surface temperatures

Micro-environmental temperatures of potato crop canopies were highly heterogeneous at the field level, in a range comprised between +15°C and -5°C when compared to the mean field temperature (Fig. 2). This heterogeneity was poorly affected by the scale considered as the temperature deviation that occurred within 30 repeated 1.2 m TIR circles (total area of 45 m²) ranged from -4.47 to +17.33 K around the mean temperature of the larger TIR circle (in yellow) while the thermal heterogeneity of larger circles (i.e., green circle of 113 m², blue circle of 452 m², pink circle of 1017 m² and yellow circle of 1808 m²) spanned between -4.69 to + 17.69 K (Fig. 2 B.). However, a single 1.2-m TIR circle of 4.53 m² encompassed a smaller range of temperatures (-2.25 to +8.97 K, red TIR circle in Fig. 2 A.) suggesting that temperature heterogeneity may be affected at very small scales. Thermal spatial metrics (i.e., Patch density, Aggregation index, Shannon's diversity index and Patch connectivity index) were also globally consistent across spatial scales (Table 2).

Name	Area (m ²)	Mean (°C)	PD	AI	SHDI	PCI
Orange	1808	22.38	0.14	65.30	2.64	9.20
Red	4.53	19.54	0.09	73.10	1.63	8.69
Green	113	20.88	0.10	69.73	2.46	9.21
Blue	452	21.69	0.11	67.31	2.52	9.27
Pink	1017	22.44	0.12	64.52	2.57	9.20
Yellow	1808	22.80	0.14	62.45	2.65	9.10

Table 2: Spatial metrics of the 5 TIR circles and 30 repeated 1.2m TIR circles. Orange are the 30 repeated 1.2m TIR circles, red, green, blue, pink and yellow the TIR circles of 1.2, 6, 12, 18, 24 m radius, respectively. Metrics presented in this table are commonly used metrics for featuring the spatial composition and configuration of landscape, here applied to thermal surface crop canopies (see [Faye et al. 2015](#) for details). PD is Patch density, AI, SHDI and PCI are Aggregation index, Shannon's diversity index and Patch connectivity index, respectively.

Temporal changes in solar radiations strongly affected thermal patterns in potato field canopies (Fig. 3). Minimum, maximum and mean temperatures all increased at higher radiations (from 10.37, 10.53, 10.60°C at 120 watt/m² to 36.60, 26.37, 23.48°C at 1500 watt/m², respectively). Interestingly, thermal heterogeneity also varied by 400% between both extreme radiation levels, with highest radiation levels showing highest thermal heterogeneity.

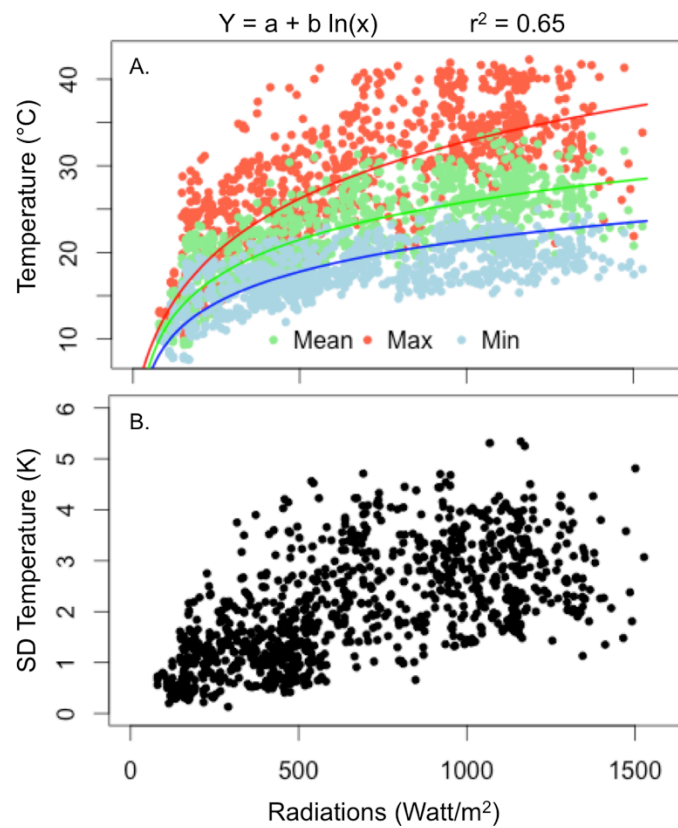


Figure 3: Scatter plots of the 1140 TIR image temperatures (SD) temperatures versus solar radiations. A. mean (green dots), minimum (blue dots) and maximum (red dots) temperatures versus radiations fitted to a log-model ($R^2 = 0.65$ for the three fits). B. Standard deviation of the 1140 TIR image temperatures versus the solar radiations.

Thermal microenvironments and crop pests

We found that the range of surface temperatures that a pest can access in crop canopies increased with the distance it travelled from its initial position (Fig. 4). While a pest can always find a wide range of temperature at short distance, these microenvironments are very rare (light grey in Fig. 4). Interestingly, the probability for a pest to find wide range of temperatures not only increases with distance but also with solar radiations. When travelling 0.2 m from its starting point, a pest disposed of a span of high frequency cells of ± 1.29 K at the 0-400 watt/m² levels while it reached a span of ± 3.24 K at 1201-1600 watt/m². When crossing the maximum distance considered (1.2 m from the initial pixel) this temperature range increases from ± 2.68 K (0-400 watt/m²) to ± 6.93 K (1201-1600 watt/m²). In other words, to access a range of temperatures of ± 2.68 K, a pest would have to travel 1.2 m under low radiation conditions, but only 0.11 m under high radiation conditions.

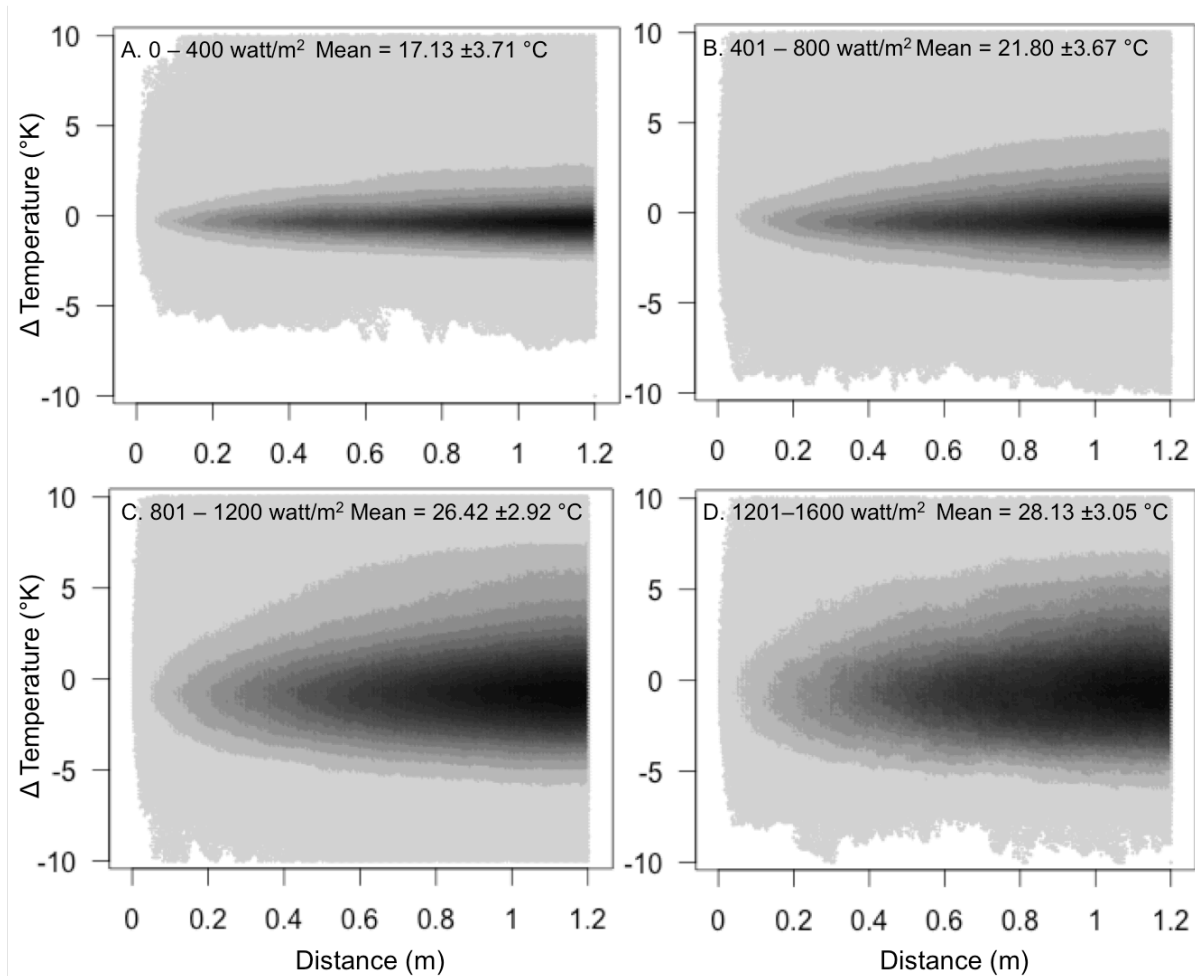


Figure 4: Hexagonal binning plot of the distance (in m) and Δ temperature (in K) for the 1140 TIR images as a function of solar radiation classes (A. R1= 0-400, B. R2= 401-800, C. R3=801-1200 and D. R4=1201-1600 watt/m²). The colour scale shows the occurrence of the TIR pixels that falls into the hexagonal cell. Light grey cells show an occurrence of 1 (the lowest).

When exploring how thermal heterogeneity in potato field surface temperature may potentially affect pest development (here the last quartile of the thermal tolerance range for each pest), we found that the four studied pest had many possibility to stay within their thermal tolerance range by travelling relatively short distances at the surface of crop potato canopy (Fig. 5). As a general pattern, pests under low radiation conditions have more opportunities to find cooler than warmer microenvironments at all distances, but still keep many available pixels to increase their environmental temperature. Only species as *M.*

persicae, with a high optimal temperature for growth performance (34°C), would experience thermal constraints under such conditions (Fig. 5 third row, first column). At high radiation levels, pests with high optimal temperatures (*F. tuberosi* and *M. persicae*) would need to travel larger distances to increase their chance of finding warmer microenvironments than cooler ones. The opposite pattern is found for species with low optimal temperature (e.g., *L. huidobrensis*).

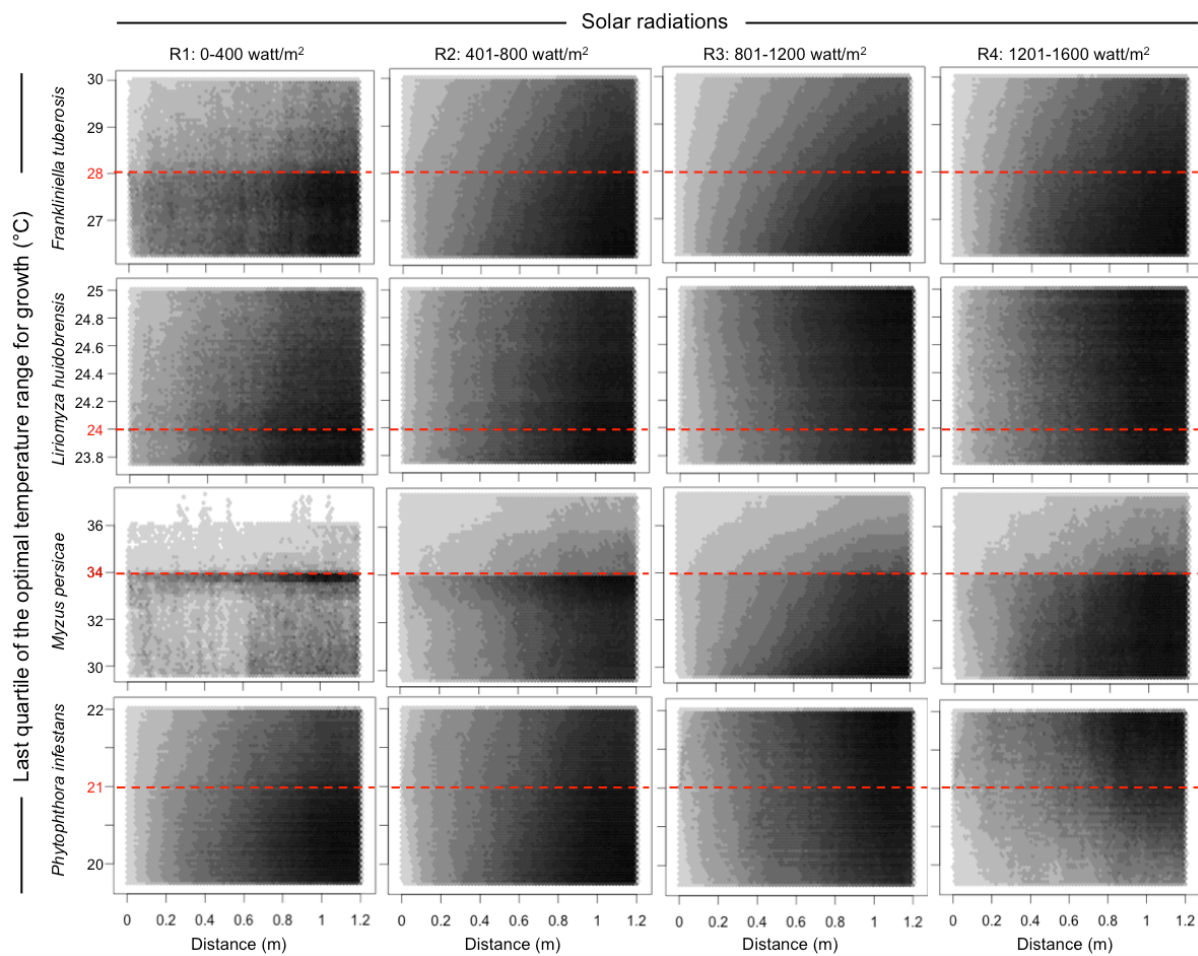


Figure 5: Hexagonal binning plot of the distance (in m) temperatures included in the last quartile of the thermal tolerance range for each pest species, as a function of solar radiation classes. Optimal temperature for the growth performance for each pest in given in red. The colour scale shows the occurrence of the TIR pixels that falls into the hexagonal cell. Light grey cells show a occurrence of 1 (the lowest).

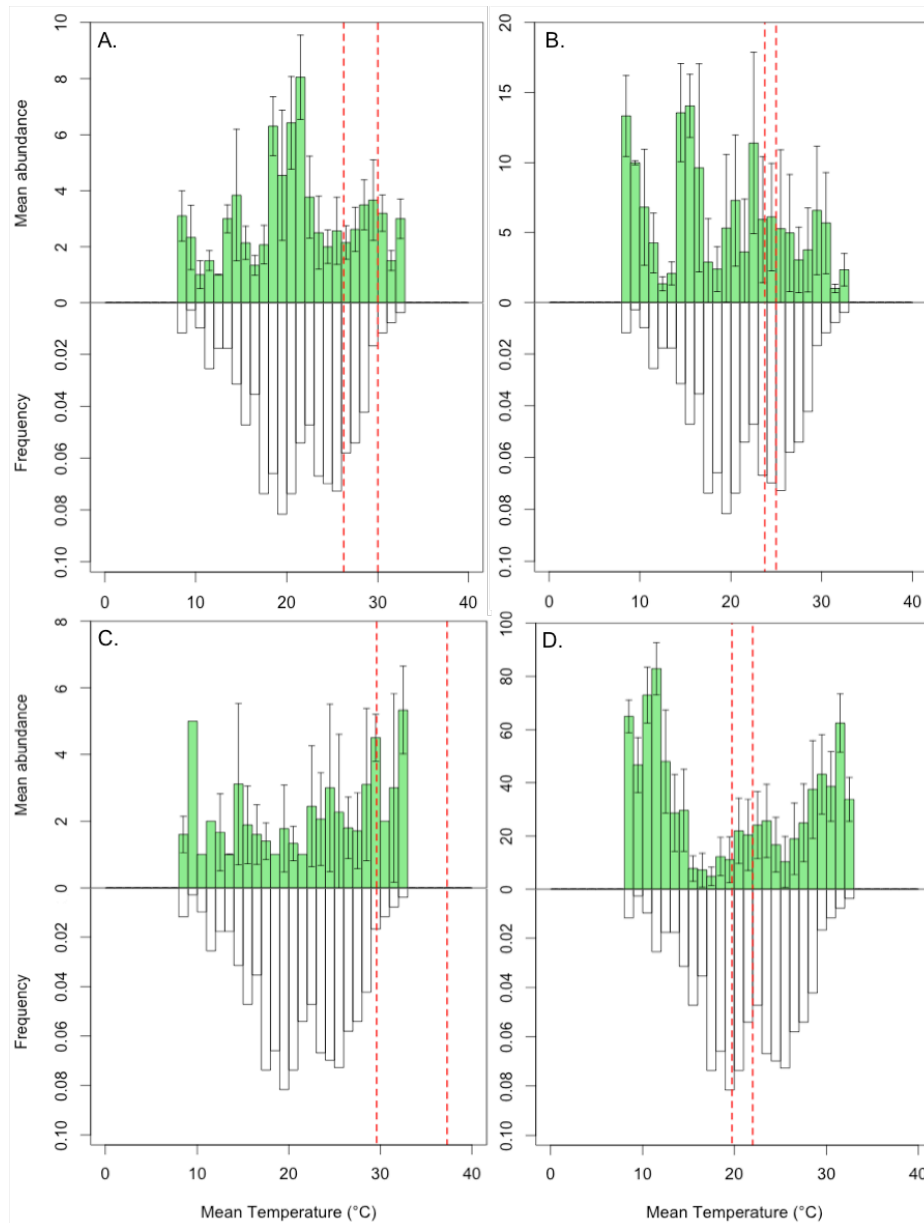


Figure 6: Distributions of mean (\pm SD) pest abundances (green) and frequency of image pixels (white), as a function of surface mean temperatures in the 1140 TIR images A. *Frankliniella tuberosi*, B. *Liriomyza huidobrensis*, C. for *Myzus persicae*; D. *Phytophthora infestans*. The red dotted line indicates the last quartile of the thermal tolerance range for growth rate for the respective pests.

We found no association between mean pest abundance and the mean temperature measured in the TIR images (Fig. 6). The four studied pests were not clumped in their supposedly preferred thermal conditions but distributed rather evenly and found in the whole

range of mean thermal conditions. However, our study revealed that pest richness significantly increased as thermal aggregation index decreased and thermal Shannon's diversity index increased (Fig. 7). Crop canopies with high thermal aggregation (86%) and low Shannon's diversity (1.42) had poorly diverse species while those with low aggregation (57%) and high Shannon's diversity index (2.48), were those infested by the highest diversity of species.

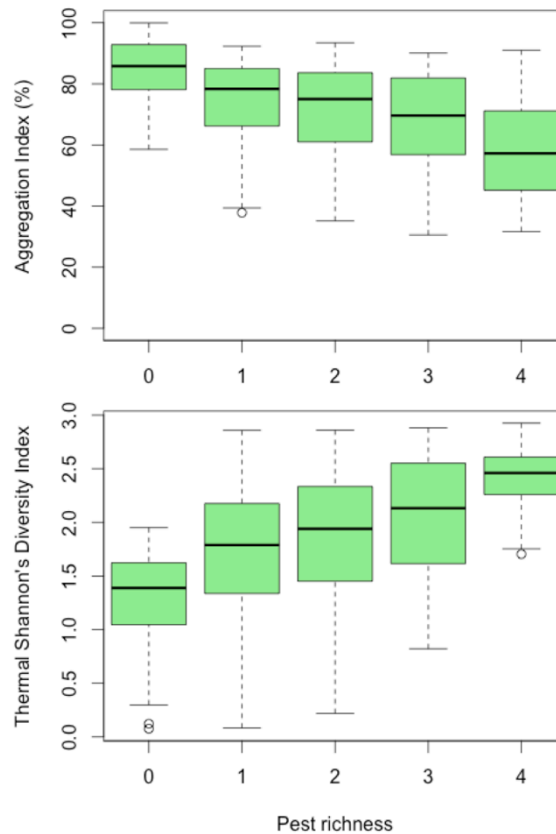


Figure 7: Boxplots of the pest richness (number of pest species in the plot) vs. the Aggregation Index (AI) and the Shannon's Diversity Index (SHDI) of the thermal patches of the 1140 TIR circles. AI = 100% when the TIR circle consists in a single patch. SHDI = 0 when the TIR circle contains only 1 thermal patch (i.e., no diversity).

Discussion

Thermal heterogeneity at relevant spatial scale for pests

Current species distribution models, based on the concept of ecological niche, integrate principles of biophysical, population and spatial ecology (Kearney & Porter 2009, Buckley *et al.* 2013) to forecast the response of ectotherms to their changing environments. However, despite their sophistication (Kearney *et al.* 2014), these models fail to take into account the thermal heterogeneity at the scale of the studied organism (Sears *et al.* 2011, Potter *et al.* 2013, Scheffers *et al.* 2014), which fundamentally biases their predictions. Typically, climatic features are considered constant over areas as large as 1 km² (Potter *et al.* 2013) while drivers of microclimates such as micro-topography (Sears *et al.* 2011) or plant structures (Faye *et al.* 2014) are known to take place at finer scales. Consequently, a general mismatch between the resolutions of climatic data and organism's processes introduces great uncertainty about the predictions of species performance and occurrences (Potter *et al.* 2013). The same mismatch occurs for pest in agricultural landscapes (Juroszek & Von Tiedemann 2013, Sutherst 2014) and many studies forecast pest distribution based on macroclimates only (e.g., Bebbier *et al.* 2014, Sparks *et al.* 2014, Crespo-Perez *et al.* 2015). Moreover, it also exists a gap in the spatial scale at which studies focusing on pest distribution are conducted (Juroszek & Von Tiedemann 2013, Sutherst 2014). On one hand, many studies focused on pest distribution at a regional or global scale due to the availability of the data needed to run the models: climatic data such as the WorldClim, land use database such as the one of the Landcover Institute (e.g., Kroschel *et al.* 2013, Sparks *et al.* 2014). On the other hand, mechanistic models relying on biophysical processes of pest individual and microclimates (Garcia *et al.* 2014, and heat balance or thermal budget, Gates 1980) or empirical experiments under controlled conditions (Pincebourde & Casas 2006) are often used to understand pest infestation at the plant scale (Ferro *et al.* 1979, Willmer 1992, Chaisuekul & Riley 2005). Between these two scales very

few studies tried to focus on the plant-pest interactions in relation with the microclimates at the field scale. Notwithstanding, it is at this local scale that the foremost spatiotemporal heterogeneity of microclimatic conditions experienced by pests occurs, and it is at this local scale also that farmers manage their pests (Christensen *et al.* 1996, Flint & Van den Bosch 2012). Considering this scale gap in the pest-based studies, one might conclude that quantifying thermal heterogeneity at relevant scale for pest organism (i.e., at the local scale) constitutes a major challenge for researchers interested in pest distribution. Our study demonstrated that methodologies exist for characterizing the intra-field spatiotemporal heterogeneity in surface temperature at a scale and resolution relevant for crop pests. Indeed, we showed that integrating 22% of the field area in TIR analysis was enough for accurately estimate the entire field composition and configuration in microclimates (Fig. 2). Therefore, we pinpointed that the thermal heterogeneity available for pests within the field was mostly independent on the spatial scale considered.

Spatiotemporal heterogeneity of microclimates

In crop habitats, thermal heterogeneity is produced spatially through vegetation structure (phenological stages, Faye *et al.* 2014) and dynamically through differential heating of surfaces as the sun moves across the sky (Wang & Dillon 2014). These patterns of surface temperatures related to solar radiation highlighted the temporal variability of the thermal heterogeneity available for pests in their environment (Fig. 3). Moreover, using high spatial resolution of climatic data in crop fields allowed us to reveal the robust relationship between the spatiotemporal heterogeneity of microclimates available for pests and solar radiation levels. Indeed, it is well known that solar radiation represents an important heat source, and numerous insect species develop thermoregulatory strategies in order to maximise or minimise the amount of radiative heat absorbed according to their thermal needs (Gates 1980,

[Kingsolver 1985](#), [Rojas *et al.* 2014](#), [Sears & Angilletta 2015](#)). Therefore, when studying surface temperature, one should take into account the temporal variability of solar radiations to yield a complete panel of the thermal possibilities that are available for crop pests.

Furthermore, the spatial heterogeneity of microclimates in vegetation landscape such as crops is also driven by the 3D structure of the plants. Indeed, the canopy structure of plant determines directly the light interception by leaves and under surfaces elements (soils, shadowed leaves, stems...), which provide insect pests with additional dimensions of microclimates variability to improve their performances or buffer lethal events ([Saudreau *et al.* 2013](#)). By recordings the temperature within the air, air inside canopies and ground layers simultaneously with the 1140 TIR images, we revealed that the 3D structure of potato crops offered others thermal opportunities for pests (Appendix 5).

Linking microclimates to pest distribution

Assessing the relationship between plant microclimates and pest occurrences and distribution in crop fields is not straightforward due to the fine spatiotemporal scales of microclimate variability and the relative mobility of pests measured in the field. Our study revealed that crop pests have the possibility to regulate the temperature of their environment in a range of various degrees Celsius within very low distances (few centimetres to 1.2 metre) and that this distance depended on radiations levels (i.e., shortened with increasing radiations; Fig. 4 and 5). Similarly, [Otero *et al.* 2015](#) showed that “A few meters matter” for the performances of tropical lizards in open and forest landscapes of Puerto Rico regarding their thermal habitats. [Sears & Angilletta 2015](#) also demonstrated that the fine-scale spatial heterogeneities of climatic conditions experienced by *Sceloporus* lizards drove their energetic costs of thermoregulation. Likewise, our study revealed that a few centimetres matter in crop microclimates for providing enough optimal thermal environments for pests to use for

enhancing their performances. However, pest occurrence is not only the result of the microclimatic conditions but rather the consequence of the integration of various factors: nutrition, reproduction, species interactions (natural enemies, competitiveness) and the conditions of the biotic and abiotic environments ([Andrewartha & Birch 1960](#), [Juroszek & Von Tiedemann 2013](#), [Sutherst 2014](#)). Among these parameters, farmer practices should be addressed as they can significantly modify pest occurrences in their fields (e.g., uses of chemical insecticides, [Flint & Van den Bosch 2012](#)).

An efficient way for studying the plant microclimate – pest interactions is spatially explicit and mechanistic modelling based on relevant biological processes and that include spatiotemporal heterogeneity of microclimates observed in the crop fields or mechanistically estimated ([Sutherst 2014](#)). Individual based model of pest traits and movements combined with spatially structured models such as cellular automata representing the spatiotemporal heterogeneity of microclimates would permits to precisely study the effect of crop microclimate aside onto pest distribution ([Garcia *et al.* 2014](#)). This theoretical approach could be a way for studying whether the pests modify their microclimate heterogeneity through mechanical alterations of the plants or whether the microclimate features attract the pests by providing favourable thermal niches.

Acknowledgements

This work was part of the project “Adaptive management in insect pest control in thermally heterogeneous agricultural landscapes” (MAN-PEST) funded by the Agence Nationale pour la Recherche (ANR-12-JSV7-0013-01). We are grateful to all farmers who collaborated with us during fieldwork. We thank Sylvain Pincebourde for lending us the pyranometer. We thank the *Instituto Ecutoriano Especial* (IEE), and particularly Danilo Yanez and Patricio Salazar

Benavides, for their collaboration in obtaining permits for UAV studies. We thank Sophie Cauvy-Fraunié for her help in UAV piloting.

References

- Andrewartha, H. G., & Birch, L. C. (1960). Some recent contributions to the study of the distribution and abundance of insects. *Annual Review of Entomology*, **5**, 219-242.
- Angilletta, M. J. (2009). *Thermal adaptation: a theoretical and empirical synthesis*. Oxford University Press.
- Ashton, S., Gutierrez, D., & Wilson, R. J. (2009). Effects of temperature and elevation on habitat use by a rare mountain butterfly: implications for species responses to climate change. *Ecological Entomology*, **34**(4), 437-446.
- Bakken, G. S. (1992). Measurement and application of operative and standard operative temperatures in ecology. *American Zoologist*, **32**(2), 194-216.
- Bebber, D. P., Holmes, T., & Gurr, S. J. (2014). The global spread of crop pests and pathogens. *Global Ecology and Biogeography*, **23**(12), 1398-1407.
- Chaisuekul, C., & Riley, D. G. (2005). Host plant, temperature, and photoperiod effects on ovipositional preference of *Frankliniella occidentalis* and *Frankliniella fusca* (Thysanoptera: Thripidae). *Journal of Economic Entomology*, **98** (6), 2107-2113.
- Christensen, N. L., Bartuska, A. M., Brown, J. H., Carpenter, S., D'Antonio, C., Francis, R., ... & Woodmansee, R. G. (1996). The report of the Ecological Society of America committee on the scientific basis for ecosystem management. *Ecological applications*, **6** (3), 665-691.
- Cloudsley-Thompson, J. L. (1962). Microclimates and the distribution of terrestrial arthropods. *Annual Review of Entomology*, **7** (1), 199-222.

- Crespo-Pérez, V., Régnière, J., Chuine, I., Rebaudo, F., & Dangles, O. (2015). Changes in the distribution of multispecies pest assemblages affect levels of crop damage in warming tropical Andes. *Global Change Biology*, **21** (1), 82-96.
- Davis, J. A., Radcliffe, E. B., & Ragsdale, D. W. (2006). Effects of high and fluctuating temperatures on *Myzus persicae* (Hemiptera: Aphididae). *Environmental Entomology*, **35**(6), 1461-1468.
- Faye, E, Herrera, M, Bellomo, L, Silvain, J-F, Dangles, O. (2014). Strong discrepancies between local temperature mapping and interpolated climatic grids in tropical mountainous agricultural landscapes. *PLoS ONE*, **9**(8), e105541. doi:10.1371/journal.pone.0105541
- Faye, E., Rebaudo, F., Yáñez, D., Cauvy-Fraunié, S. & Dangles O. (2015). A toolbox for studying thermal heterogeneity across spatial scales: from unmanned aerial vehicle imagery to landscape metrics. *Methods in Ecology and Evolution*, In press.
- Ferro, D. N., Chapman, R. B., & Penman, D. R. (1979). Observations on insect microclimate and insect pest management. *Environmental Entomology*, **8** (6), 1000-1003.
- Flint, M. L., & Van den Bosch, R. (2012). *Introduction to integrated pest management*. Springer Science & Business Media.
- Frazier MR, Huey RB, & Berrigan D. (2006). Thermodynamics constrains the evolution of insect population growth rates: “Warmer is better.” *The American Naturalist*, **168**, 512–520.
- Garcia, A., Cônsoli, F. L., Godoy, W. A. C., & Ferreira, C. P. (2014). A mathematical approach to simulate spatio-temporal patterns of an insect-pest, the corn rootworm *Diabrotica speciosa* (Coleoptera: Chrysomelidae) in intercropping systems. *Landscape Ecology*, **29** (9), 1531-1540.
- Gates, D. M. (1980). *Biophysical ecology*. Springer-Verlag.

- Holmes, R. M., & Dingle, A. N. (1965). The relationship between the macro-and microclimate. *Agricultural Meteorology*, **2** (2), 127-133.
- Huey, R. B., & Stevenson, R. D. (1979). Integrating thermal physiology and ecology of ectotherms: A discussion of approaches. *American Zoologist*, **19**, 357-366.
- Jackson, H. B., & Fahrig, L. (2015). Are ecologists conducting research at the optimal scale?. *Global Ecology and Biogeography*, **24**(1), 52-63.
- Juroszek P, & Von Tiedemann, A. (2013). Plant pathogens, insect pests and weeds in a changing global climate: a review of approaches, challenges, research gaps, key studies and concepts. *Journal of Agricultural Science*, **151**, 163–188.
- Kearney, M. R., Shamakhy, A., Tingley, R., Karoly, D. J., Hoffmann, A. A., Briggs, P. R., & Porter, W. P. (2014). Microclimate modelling at macro scales: a test of a general microclimate model integrated with gridded continental-scale soil and weather data. *Methods in Ecology and Evolution*, **5** (3), 273-286.
- Kingsolver, J. G. (1985). Thermal ecology of *Pieris* butterflies (Lepidoptera: Pieridae): a new mechanism of behavioral thermoregulation. *Oecologia*, **66** (4), 540-545.
- Kroschel, J., Sporleder, M., Tonnang, H. E. Z., Juarez, H., Carhuapoma, P., Gonzales, J. C., & Simon, R. (2013). Predicting climate-change-caused changes in global temperature on potato tuber moth *Phthorimaea operculella* (Zeller) distribution and abundance using phenology modeling and GIS mapping. *Agricultural and Forest Meteorology*, **170**, 228-241.
- Lanzoni, A., Bazzocchi, G. G., Burgio, G., & Fiacconi, M. R. (2002). Comparative life history of *Liriomyza trifolii* and *Liriomyza huidobrensis* (Diptera: Agromyzidae) on beans: effect of temperature on development. *Environmental Entomology*, **31** (5), 797-803.
- McGarigal, K. & Marks, B.J. (1994) Fragstats: Spatial Pattern Analysis Program for

- Quantifying Landscape Structure. Oregon state university, Forest science department, Corvallis.
- Otero, L. M., Huey, R. B., & Gorman, G. C. (2015). A Few Meters Matter: Local Habitats Drive Reproductive Cycles in a Tropical Lizard. *The American Naturalist*, **186**(3), E72-E80.
- Pincebourde, S., & Casas, J. (2006). Leaf miner-induced changes in leaf transmittance cause variations in insect respiration rates. *Journal of Insect Physiology*, **52** (2), 194-201.
- Porter, W.P., Sabo, J.L., Tracy, C.R., Reichman, O.J. & Ramankutty, N. (2002). Physiology on a landscape scale: plant-animal interactions. *Integrative and Comparative Biology*, **42**, 431–453.
- Potter, K. A., Arthur Woods, H., & Pincebourde, S. (2013). Microclimatic challenges in global change biology. *Global Change Biology*, **19** (10), 2932-2939.
- Pumisacho, M., & Sherwood, S. (2002). *El cultivo de la papa en Ecuador*. INIAP and CIP, Quito, Ecuador.
- Raghu, S., Drew, R. A., & Clarke, A. R. (2004). Influence of host plant structure and microclimate on the abundance and behavior of a tephritid fly. *Journal of Insect Behavior*, **17** (2), 179-190.
- Rojas, J. M., Castillo, S. B., Folguera, G., Abades, S., & Bozinovic, F. (2014). Coping with daily thermal variability: behavioural performance of an ectotherm model in a warming world. *Plos One*, DOI: 10.1371/journal.pone.0106897
- Rubio E., Caselles V., Badenas C. (1997). Emissivity measurements of several soils and vegetation types in the 8–14 mm wave band: analysis of two field methods. *Remote Sensing of Environment*, **59** (3), 490–521.
- Saudreau, M., Pincebourde, S., Dassot, M., Adam, B., Loxdale, H. D., & Biron, D. G. (2013). On the canopy structure manipulation to buffer climate change effects on insect

- herbivore development. *Trees*, **27** (1), 239-248.
- Scheffers, B. R., Edwards, D. P., Diesmos, A., Williams, S. E., & Evans, T. A. (2014). Microhabitats reduce animal's exposure to climate extremes. *Global Change Biology*, **20** (2), 495-503.
- Sears, M. W., & Angilletta Jr, M. J. (2015). Costs and benefits of thermoregulation revisited: both the heterogeneity and spatial structure of temperature drive energetic costs. *The American Naturalist*, **185**(4), E94-E102.
- Sears, M. W., E. Raskin, & M. J. Angilletta (2011). The world is not flat: defining relevant thermal landscapes in the context of climate change. *Integrative and Comparative Biology*, **51**, 666–675.
- Sparks, A. H., Forbes, G. A., Hijmans, R. J., & Garrett, K. A. (2014). Climate change may have limited effect on global risk of potato late blight. *Global Change Biology*, **20** (12), 3621-3631.
- Storlie, C., Merino-Viteri, A., Phillips, B., VanDerWal, J., Welbergen, J., & Williams, S. (2014). Stepping inside the niche: microclimate data are critical for accurate assessment of species' vulnerability to climate change. *Biology Letters*, **10** (9), 20140576.
- Suh, C. P. C., Orr, D. B., Van Duyn, J. W., & Borchert, D. M. (2002). Influence of cotton microhabitat on temperature and survival of *Trichogramma* (Hymenoptera: Trichogrammatidae) within cardboard capsules. *Environmental Entomology*, **31** (2), 361-366.
- Sutherst, R. W. (2014). Pest species distribution modelling: origins and lessons from history. *Biological Invasions*, **16** (2), 239-256.
- Tompkins, D. K., Fowler, D. B., & Wright, A. T. (1993). Influence of agronomic practices on canopy microclimate and *Septoria* development in no-till winter wheat produced in the

- Parkland region of Saskatchewan. *Canadian Journal of Plant Science*, **73**(1), 331-344.
- Wang, G., & Dillon, M. E. (2014). Recent geographic convergence in diurnal and annual temperature cycling flattens global thermal profiles. *Nature Climate Change*, **4**, 988-992.
- Weisz, R., Fleischer, S., & Smilowitz, Z. (1996). Site-specific integrated pest management for high-value crops: impact on potato pest management. *Journal of Economic Entomology*, **89** (2), 501-509.
- Willmer, P. G. (1982). Microclimate and the environmental physiology of insects. *Advances in Insect Physiology*, **16**, 1-57.
- Willmer, P. G., Hughes, J. P., Woodford, J. A. T., & Gordon, S. C. (2008). The effects of crop microclimate and associated physiological constraints on the seasonal and diurnal distribution patterns of raspberry beetle (*Byturus tomentosus*) on the host plant *Rubus idaeus*. *Ecological Entomology*, **21**(1), 87-97.
- Woods, H. A., Dillon, M. E., & Pincebourde, S. (2014). The roles of microclimatic diversity and of behavior in mediating the responses of ectotherms to climate change. *Journal of Thermal Biology*. doi:10.1016/j.jtherbio.2014.10.002

Supporting Information of “Faye, E., Herrera, M. A., Carpio, C., Rebaudo, F., & Dangles, O. Does heterogeneity in crop canopy microclimate matter for pests? Evidence from aerial high-resolution thermography. To submit in *Journal of Applied Ecology*”.

Appendix 1: Table of the studied field descriptions

Appendix 2: R script used in this study

Appendix 3: Boxplots of the spatial metrics versus pest richness on the 1140 TIR circles

Appendix 4: Schematic interpretation of the Aggregation Index and the Shannon’s Diversity Index

Appendix 5: Spatial heterogeneity of crop microclimates in three-dimensional layers

Appendix 1: Table of the studied field descriptions. Field area is expressed in squared meters, Phenology and Damage were estimated for the entire field and Cov is the TIR coverage of the field in percentage of the field area.

Name	Date	Area	Phenol	Dam	Cov	Name	Date	Area	Phenol	Dam	Cov
1	14/01/14	726	C	3	31.7	20	24/01/14	1010	2	2	22.8
2	15/01/14	1147	C	3	20.1	21	24/01/14	1604	3	2	14.4
3	15/01/14	1292	B	2	17.8	22	24/01/14	958	1	1	24.1
4	15/01/14	1454	B	1	15.8	23	24/01/14	1118	3	2	20.6
5	16/01/14	2217	A	1	10.4	24	27/01/14	1136	2	1	20.3
6	16/01/14	1192	B	3	19.3	25	27/01/14	831	2	1	27.7
7	16/01/14	1188	A	1	19.4	26	28/01/14	725	3	2	31.8
8	16/01/14	2277	C	3	10.1	27	28/01/14	982	1	3	23.5
9	21/01/14	705	C	3	32.7	28	28/01/14	759	1	1	30.4
10	21/01/14	1914	A	1	12.0	29	28/01/14	818	3	1	28.2
11	21/01/14	850	C	2	27.1	30	29/01/14	1456	3	3	15.8
12	22/01/14	861	C	3	26.8	31	29/01/14	1200	2	2	19.2
13	22/01/14	924	C	2	24.9	32	29/01/14	1597	2	1	14.4
14	22/01/14	1293	B	3	17.8	33	29/01/14	2016	2	2	11.4
15	22/01/14	1970	C	3	11.7	34	31/01/14	630	3	2	36.6
16	23/01/14	631	C	2	36.5	35	31/01/14	2328	2	2	9.9
17	23/01/14	814	B	2	28.3	36	31/01/14	1778	2	2	13.0
18	23/01/14	881	C	3	26.2	37	31/01/14	3072	1	1	7.5
19	23/01/14	816	B	3	28.2	38	31/01/14	921	1	2	25.0

Phenology A = Leaf development, B = Inflorescence and C = Mature stage

Appendix 2: R script used in this study

```
#!/usr/bin/env RScript
#####
###
### Script to compute the difference between points in terms of temperature and distance.
###
### This script is part of the publication Does heterogeneity in crop canopy microclimate
### matter for pests?
### Evidence from aerial high-resolution thermography. Faye, E., Herrera, M. A., Carpio, C.,
### Rebaudo, F., & Dangles, O.
### Contacts : E. Faye: <ehfaye@gmail.com>; F. Rebaudo: <francois.rebaudo@ird.fr>;
### O. Dangles: <olivier.dangles@ird.fr>
### September 2015
###
#####

### working directory
mywd<-"/home/my/working/directory/"
# mywd<-"D:/SYNC_UMSA/_PAPIERS_/EF_FR_OD_Tube/"
setwd(mywd)
### packages
pkgCheck <- function(x){ # check for a package, install and load
  if (!require(x,character.only = TRUE)){
    install.packages(x,dependencies=TRUE)
    if(!require(x,character.only = TRUE)) {
      stop()
    }
  }
}
pkgCheck("MASS")
pkgCheck("sp")
pkgCheck("raster")
pkgCheck("hexbin")

### load raster files and compute distances and dif in temperature
getDist<-
function(numPoints=2,temp="insect",tempOptInsect=23,tempMinInsect=22.5,tempMaxInsect=25,myFile
s=list.files(pattern="rda"),type="",rangeMinMax=0.1,useOnlyTmean=FALSE){
  xxx<-NULL
  yyy<-NULL
  for (i in myFiles){
    if(type=="rda"){
      load(i) # load raster file
      matRaster<-as.matrix(Plant_rast) # convert to matrix
    }else{
      matRaster<-as.matrix(read.table(i,skip=6,na.strings = -9999)/1000)
      if(temp=="mean"){
        tempOptInsect<-mean(matRaster,na.rm=TRUE)
        tempMinInsect<-tempOptInsect-rangeMinMax*tempOptInsect
        tempMaxInsect<-tempOptInsect+rangeMinMax*tempOptInsect
      }
    }
    meanRast<-mean(matRaster,na.rm=TRUE) # get mean temperature
    sdRast<-sd(matRaster,na.rm=TRUE) # get sd temperature

    if(useOnlyTmean==TRUE){
      tempOptInsect<-meanRast
      print(paste0("Tmean: ",meanRast))
    }
    # [1] matPointsMean = coordinates of all points with temperature between
tempMinInsect and tempMaxInsect
    matPointsMean<-which(matRaster<=tempMaxInsect & matRaster>=tempMinInsect,
arr.ind=TRUE)
    pointsIntoRange<-matPointsMean
    origin<-length(matPointsMean[,1])
    if(length(matPointsMean[,1])>1000*numPoints){#
      for(z in seq(from=0.01,to=0.9,by=0.005)){
        getMax<-tempMaxInsect-tempMaxInsect*z
        getMin<-tempMinInsect+tempMinInsect*z
        if(getMax<tempOptInsect+0.05){getMax<-tempOptInsect+0.05}
        if(getMin>tempOptInsect-0.05){getMin<-tempOptInsect-0.05}

        matPointsMeanAltMAX<-which(matRaster<=getMax &
matRaster>=getMin, arr.ind=TRUE)
        if(length(matPointsMeanAltMAX[,1])>1000*numPoints){
```

```

                                matPointsMean<-matPointsMeanAltMAX
                                }
                                }
                                }
numPointsGood<-length(matPointsMean[,1])
print(paste0(i,": ",numPointsGood, " / ", origin))
if(length(matPointsMean[,1])>10000*numPoints){
  for(z in seq(from=0,to=100,by=0.05)){
    getMax<-tempMaxInsect-z
    getMin<-tempMinInsect+z
    if(getMax<tempOptInsect+0.05 & getMin>tempOptInsect-0.05){break}
    if(getMax<tempOptInsect+0.05){getMax<-tempOptInsect+0.05}
    if(getMin>tempOptInsect-0.05){getMin<-tempOptInsect-0.05}

    matPointsMeanAltMAX<-which(matRaster<=getMax &
matRaster>=getMin, arr.ind=TRUE)
    if(length(matPointsMeanAltMAX[,1])>1000*numPoints){
      matPointsMean<-matPointsMeanAltMAX
    }
  }
}
numPointsGood<-length(matPointsMean[,1])
print(paste0(i,": ",numPointsGood, " / ", origin))
xx<-NULL
yy<-NULL
myX<-1:length(matRaster[,1])
myY<-1:length(matRaster[,1])
centralPoint<-c(length(myX)/2,length(myY)/2)
distToCentralPoint<-sqrt((centralPoint[1]-
matPointsMean[,1])^2+(centralPoint[2]-matPointsMean[,2])^2)

if (numPointsGood>=numPoints){
  # [2] matPointsMean = coordinates of (100 * numPoints) points close to
the center of the matrix
  while (nrow(matPointsMean) > (100*numPoints)) { # limit matPointsMean to
numPoints*100

    cdists <- distToCentralPoint
    closest <- which(cdists == max(cdists))[1]
    matPointsMean <- matPointsMean[-closest,]
    distToCentralPoint <- distToCentralPoint[-closest]
  }
  # [3] matPointsMean = coordinates of (5 * numPoints) points close to the
center of the matrix and closest to tempOptInsect
  selectedTemp<-matPointsMean
  myTemp<-NULL
  difTemp<-NULL
  for(k in 1:length(selectedTemp[,1])){
    difTemp<-
c(difTemp,abs(matRaster[matPointsMean[k,1],matPointsMean[k,2]]-tempOptInsect))
    myTemp<-
c(myTemp,matRaster[matPointsMean[k,1],matPointsMean[k,2]])
  }
  selectedTemp<-cbind(selectedTemp,difTemp)
  selectedTemp<-cbind(selectedTemp,myTemp)
  while (nrow(matPointsMean) > numPoints) { # limit matPointsMean to
5*numPoints

    cdists <- selectedTemp[,3]
    closest <- which(cdists == max(cdists))[1]
    matPointsMean <- matPointsMean[-closest,]
    selectedTemp <- selectedTemp[-closest,]
  }
  for(j in 1:numPoints){
    randomPointCoo<-matPointsMean[j,]
    print(paste0("XY: ",matPointsMean[j,]))
    allMyDist<-
sapply(1:length(pointsIntoRange[,1]),function(ii){myDist<-
as.vector(sqrt(((pointsIntoRange[ii,1]-randomPointCoo[1]))^2+((pointsIntoRange[ii,2]-
randomPointCoo[2]))^2))) # get distances from the random point in PIXELS
    allMyTempDif<-
sapply(1:length(pointsIntoRange[,1]),function(ii){myTempDif<-
matRaster[pointsIntoRange[ii,1],pointsIntoRange[ii,2]]-
matRaster[randomPointCoo[1],randomPointCoo[2]]}) # get dif in temperature from the random
point
    xx<-c(xx,allMyTempDif[!is.na(allMyTempDif)]) # vector of dif in
temperature for all random points numPoints
    yy<-c(yy,allMyDist[!is.na(allMyTempDif)]) # vector of distances
for all random points numPoints

```

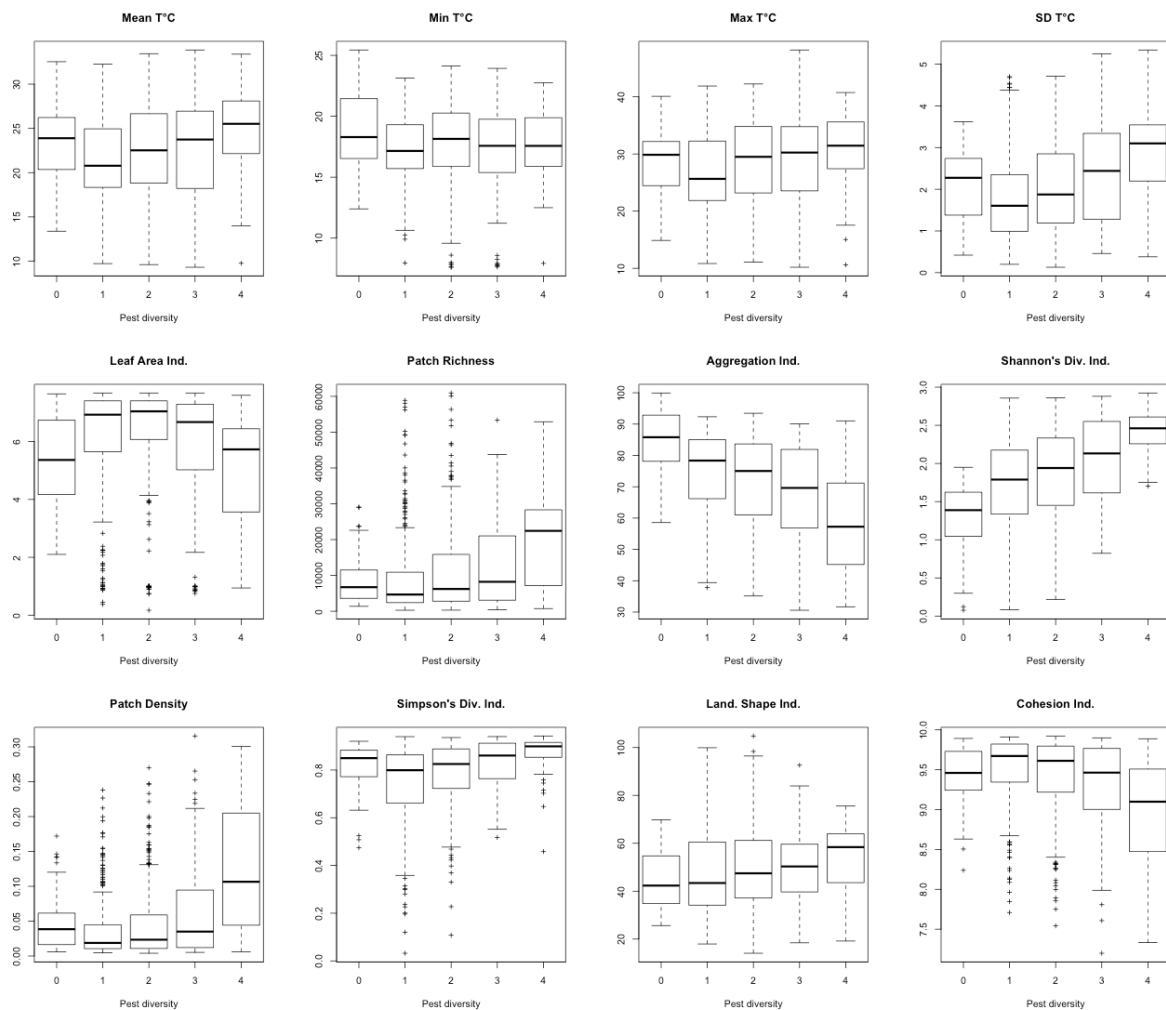
```

    }
    print(paste0(i, ": OK, ", numPoints, " selected from ", origin))
  } else{
    print(paste0(i, ": no ", numPoints, " points between ", tempMinInsect, " and
", tempMaxInsect, " degrees"))
  }
  xxx<-c(xxx,xx)
  yyy<-c(yyy,yy)
}
return(data.frame(deltaTemp=xxx,deltaCoo=yyy))
}
mywdFiles<-
getDist(numPoints=2,tempOptInsect=22.5,tempMinInsect=15,tempMaxInsect=30,type="rda");
save(mywdFiles,file="MywdFiles_R1_Fra.rda"); rm(mywdFiles);

hist((mywdFiles$deltaCoo)*0.005)
bin<-hexbin (mywdFiles$deltaCoo,mywdFiles$deltaTemp, xbnbs =
c(min(mywdFiles$deltaCoo),max(mywdFiles$deltaCoo)), ybnbs
=c(min(mywdFiles$deltaTemp),max(mywdFiles$deltaTemp)))
plot(bin)

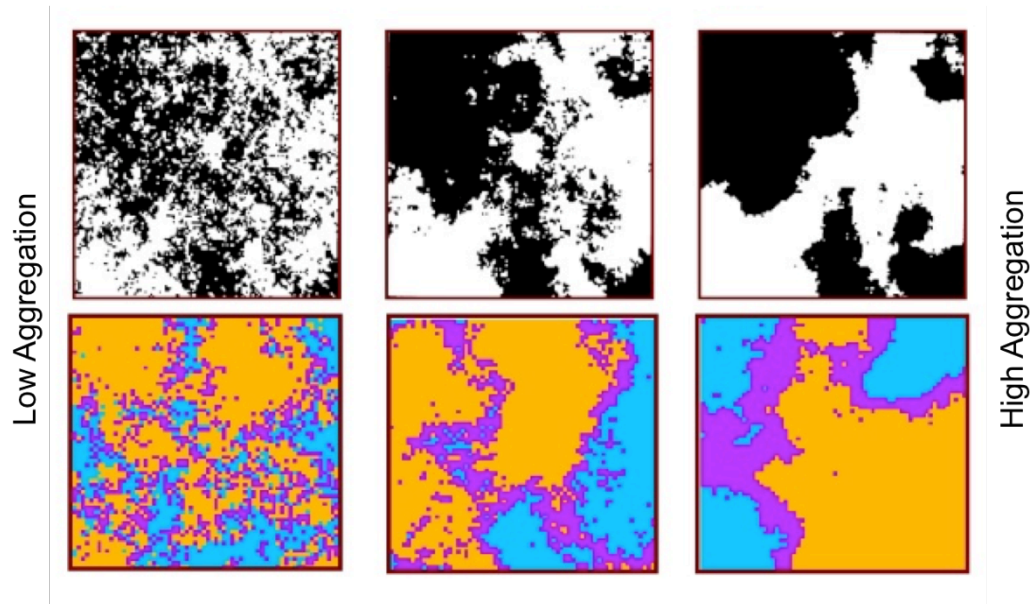
```

Appendix 3: Boxplots of the spatial metrics versus pest richness on the 1140 TIR circles

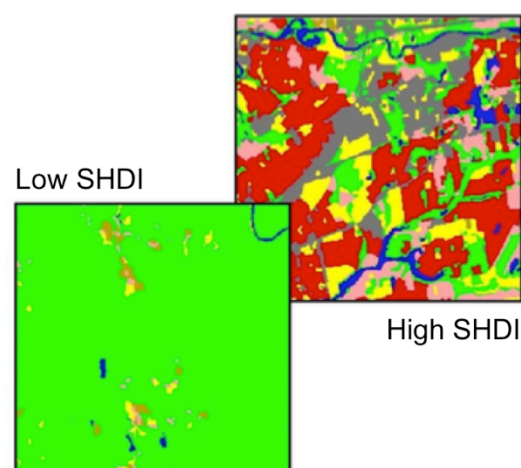


Appendix 4: Schematic interpretation of the Aggregation Index and the Shannon's Diversity Index (SHDI)

Aggregation Index – Metric of landscape configuration

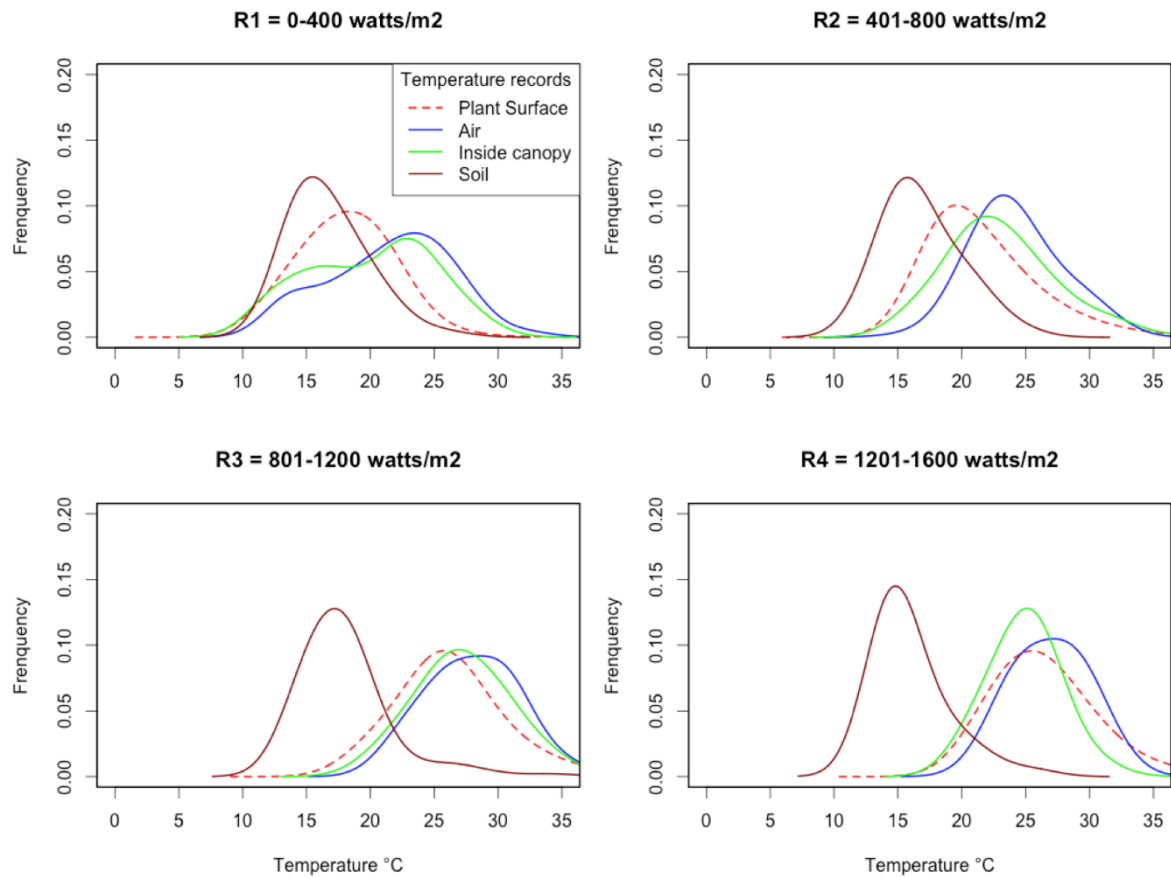


Shannon's Diversity Index – Metric of landscape composition



Adapted from McGarigal & Marks (1994)

Appendix 5: Spatial heterogeneity of crop microclimates in three-dimensional layers (Air, Surface, Air inside canopy and ground).



Within each of the ten study points per fields, we recorded microclimatic temperatures in the layers potentially experienced by crop pests along their life cycle: temperature in the air above canopy, air inside canopy and soil (see [Faye et al. 2014](#) for details). Within each field, we recorded microclimatic temperatures using three temperature loggers (Hobo U23-001-Pro-V2 internal temperature loggers, Onset Computer Corporation, Bourne, USA) fixed on wooden sticks in the three layers following the method described in [Faye et al. \(2014\)](#). The time-step recording was 10 seconds for the 30 temperature loggers located in each field. In the figure S5 above, plant surface temperatures were obtained from the 1140 TIR circles and the Air, Air inside canopy and ground layer temperatures have been recorded at the same time of the TIR image shots with temperature loggers.

DISCUSSION

In this thesis, we investigated the effects of microclimates on pest occurrence and distribution, and highlighted the scale gap that currently exists in the spatial resolution between the studied insects and the climatic data used in agro-ecosystems. We also developed innovative methodologies to yield and analyse thermal data and their spatiotemporal dynamics at the appropriated scale and resolution for studying tiny crop pests and diseases. Finally, we integrated all this information for relating the microclimatic landscapes with the occurrence and distribution of pests observed in crop fields. In particular, we showed the importance of microclimates in providing short distance thermal niches that crop pests can take advantage of. In the following, we choose to discuss these main results by following a leaning from 1) theoretical issues, 2) relevance of thermal ecology for agronomical applications and 3) to challenges to put microclimate research into practice in developing countries. This plan adheres to the design of the entire thesis in which we firstly presented the microclimates *In silico*, methodologies to deal with thermal heterogeneity at fine spatiotemporal scales in agro-ecological disciplines and the applications of theses methods *in situ*. Moreover, we present in the discussion additional studies that have been performed during this thesis but that are still under process and analyses. They will be used to illustrate some specific issues.

I. Microclimates: Is exactness in the details?

1. Scale effects in microclimates

The “scale effect” issue has a long history in ecology ([Wiens 1989](#), [Levin1992](#), [Willis & Whittaker 2002](#), [Storch et al. 2007](#), [McGill 2010](#), [Gillingham et al. 2012](#), [Jackson & Fahrig 2015](#)). In its influential paper ‘On the problem of pattern and scale in ecology’, [Levin’s \(1992\)](#) demonstrated that ecological processes act at a variety of spatial and temporal scales. Later [McGill \(2010\)](#) pointed out the scale dependency of ecological patterns. For instance, in a study relating the percentage forest cover to the abundance of 12 wood beetle species,

Holland *et al.* (2004) found that, depending on the scale at which forest cover was measured (from 20 to 2000 m radius), the correlation between forest cover and beetle abundance ranged from strongly positive to negligible. Therefore, the scale at which landscape attributes are measured has a strong impact on inferred species–landscape relationships (Jackson & Fahrig 2015). Scales are defined by their resolution and extent (Elith & Leathwick 2009). The extent usually reflects the purpose of the analysis: global change studies tend to be continental to global in scope (e.g., Deutsch *et al.* 2008), whereas studies targeting detailed ecological patterns tend toward local to regional extents (e.g., Sears & Angilletta 2015). The resolution usually belongs to the data used: i.e., the grid cell size of abiotic variables but also the spatial accuracy of the species records (Willis & Whittaker 2002, Gillingham *et al.* 2012). Conceptually, there is no single natural scale at which ecological patterns should be studied (Levin 1992). Rather, the appropriate scale is dictated by the study objectives, the study system, and available data (Kearney & Porter 2009).

In terms of climatic data, the effect of the chosen scale might have important consequences on the study issues, such as modifying the estimates of species declines and extinction (Gillingham *et al.* 2012, Logan *et al.* 2013). Indeed, global predictions use ambient temperature data gathered from weather stations, but the temperature experienced by ectotherms results from a complex interplay among many biophysical parameters (including convection, conduction, and radiation, see Introduction) and thus consistently deviate from ambient conditions (Bakken, 1992). Our work showed that this might be a key issue in agricultural and mountainous landscapes, where coarse-resolution grid cells (e.g., the WorldClim) may contain a wide variability of thermal environments driven by microtopography (Sears *et al.* 2011) and plant structure (Faye *et al.* 2014). Within such a grid square, there is likely a wide range of microclimatic conditions resulting in the presence of locally-suitable conditions for ectotherms (e.g., crop pests but also natural enemies, Bianchi *et*

al. 2006, *Fahrig et al.* 2011, *Veres et al.* 2013) at their thermal margins, the existence of which might not be apparent at a coarser resolution (*Storlie et al.* 2014). Consequently, it is intuitive that scales in climatic data will influence the results of the study. *Gillingham et al.* (2012) downscaled spatial climates at four spatial resolutions to explain the abundance of sampled ground beetles over their study area (Fig. 1). In their analysis, different resolutions resulted in different predictions about the abundance of the populations: higher resolution analyses provided more accurate estimates of observed patterns, but also highlighted potential microclimatic refugia for the conservation of species that otherwise might appear to be threatened with regional or global extinction under climate change.

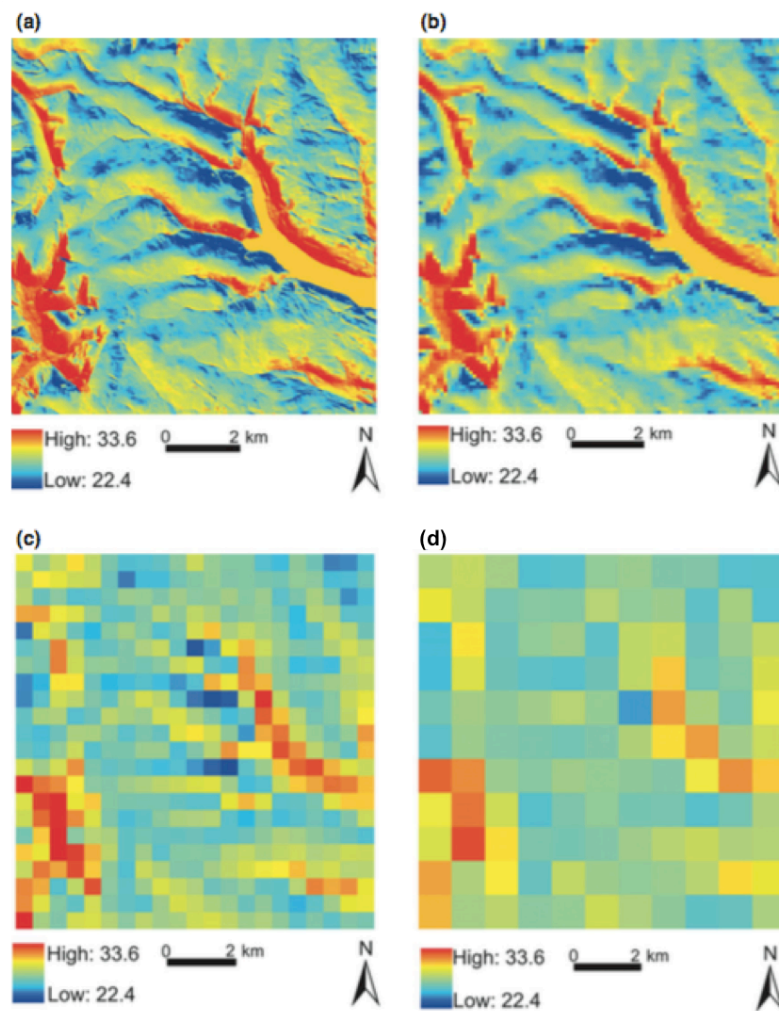


Figure 1: Mean temperature modelled at different spatial scales: a) 5x5, b) 100x100, c) 500x500 and d) 1000x1000 m. This climatic data were used for predicting the species abundance of ground beetles. Adapted from *Gillingham et al.* (2012).

Similarly to [Gillingham *et al.* \(2012\)](#), we predicted potato pest abundance with thermal performance models using different spatiotemporal resolutions of climatic data and compared the results of the models with observed data measured in the field (see paragraph II.3. of this discussion). Generally, our study revealed that microclimatic data (measured at the field scale) were more relevant for predicting crop pest performances and abundance than the coarser scales (Fig. 7 below). Our results highlight the need for incorporating fine-scale climate data for studying ecological patterns that occur at fine spatial scale: e.g., incorporation into pest' performance analyses ([Faye *et al.* 2014](#)). Therefore, a clear understanding of ectotherms occurrence and distribution at the local and regional scale will depend critically on the fine spatial and temporal structure of their thermal environments. In other words, accurate ectotherm forecasts will require biologically relevant measures of thermal heterogeneity.

However, studies with more generalist scopes, such as biogeographic distribution of organisms, range shifts, population dynamics, and extinctions at global scales may not always need such fine-scale resolutions for their climatic data used in models. For instance, [Deutsch *et al.* \(2008\)](#), estimate the general impact of climate change on insect thermal tolerances across latitude using coarse-scale climatic data. As a general pattern, they concluded (as in [Janzen 1967](#)) that because tropical species generally have narrow tolerance ranges and acclimation capacities compared to temperate species, the greatest extinction risks from global warming may occurs in the tropics. Moreover, some authors defended that the apparent mismatch between the scale of climate data and the size of organisms is implicitly bridged in most species distribution models (SDMs) with the “mean field approximation” ([Bennie *et al.* 2014](#)). They assumed that the grid-cell average climatic variables are statistically meaningful predictors of the probability of species persistence. The mean field approach simply states that macroclimate is a good predictor of the aggregated population-level effect of many individual responses to the spatial and temporal variations in microclimate that influence individual

performances (Bennie *et al.* 2014). Therefore, climatic data at coarse resolution and large extent may also be sufficient to assess main changes in distribution.

So, what is the appropriate scale for climate data?

Predicting how organisms will respond to their environment will require reducing the mismatch between the spatial scales of climatic data used versus organisms (Austin & Van Niel 2011, Potter *et al.* 2013). But how fine is fine enough? The question of optimal spatial resolution has been debated since the birth of SDMs (Guisan & Thuiller 2005), with some authors suggesting that finer-scaled SDMs provide better predictions (Elith & Leathwick 2009, Hannah *et al.* 2014, Storlie *et al.* 2014) and others that do not (Guisan *et al.* 2007, Bennie *et al.* 2014). Focal organisms and their habitat requirements are a starting point for informing the choice of appropriate scales for climatic data and others type of data (Hannah *et al.* 2014). Fine-resolution spatial data may be less important for organisms in spatially homogeneous environments or for wide-ranging studies that focus on a general purpose and trends. Also, high temporal resolution data may be less important in environments where diurnal or seasonal variability is limited, at least relative to the environmental tolerances of organisms (Potter *et al.* 2013). The biological question of the study also influences the choice of climate data: temporal resolution may be more crucial for studies of survival and reproduction and spatial resolution for studies of distribution (Buckley *et al.* 2010).

For biologists, the greatest challenge resides nowadays in the availability of high-resolution climate data, because constructing these surfaces requires new physical modelling skills (Kearney *et al.* 2014) both with the development of new thermal recording technics (Faye *et al.* 2015). Lee *et al.* (2015) presented the new HypsIRI satellite sensor (Hyperspectral InfraRed Imager) that will soon start recording thermal infrared orthoimages within the 4-13 μm range with 60 m spatial resolution and a revisit time of 5 days. For finer

spatiotemporal resolution in temperatures, the toolbox presented in this work, [Faye et al. \(2015\)](#), provides an innovative methodological framework to better assess the thermal heterogeneity of natural landscapes at fine spatiotemporal scales. In particular, this toolbox would be of topical interest for ecologists trying to bridge the gap between the resolution of their climatic data and the body size of their study organisms.

2. Is microclimate enough?

Not only temperatures – While it becomes increasingly admitted that microclimatic conditions, especially temperatures, are critical for the assessment of species' responses to their environments (changing or not), insights on others factors that composed microclimates would be of topical interest too. Indeed, solar radiations, relative humidity, soil moisture, microtopography, wind speed and direction are parameters that shape the microclimatic environment experienced by organisms ([Geiger 1965](#), [Gates 1980](#), [Jones 1992](#)). These additional parameters were faintly studied in this thesis as temperatures had been identified as the main factor influencing potato pest dynamics in the tropical Andes ([Dangles et al. 2008](#)). Notwithstanding, as for temperature, these abiotic variables are also highly heterogeneous in space and in time at very small spatiotemporal scales ([Gates 1980](#), [Bakken 1992](#)). Thus, a complete assessment of microclimates in the environment inhabited by species should include a measure of these parameters. However, these additional parameters remain poorly studied and methodologies for measuring them produce a high degree of uncertainty ([Unwin 1980](#), [Porter et al. 2002](#)). To address this issue, recent advances in mechanistic models use complex energy balance equations which incorporate spatially mapped variables such as surface albedo, relative humidity, incoming solar radiation and wind speed to generate estimates of microclimate at relatively fine scales ([Kearney et al. 2014](#)). This arrangement of highly heterogeneous variables composing the microclimate makes even more complex our

understanding of the relationship between organisms and their environments. In other words, species with specific thermal tolerances may exhibit habitat associations for thermal reasons, as well as because of others specific abiotic constraints.

Not only microclimates – Many others environmental variables (not only climatic) may influence species' occurrence and distribution at fine spatiotemporal scales. Certainly, many organisms can disperse through environments that are thermally unsuitable to achieve others essentials requirements ([Buckley et al. 2010](#)). Needs in nutrition, reproduction, or species interactions (prey/target, competitiveness, positive interactions) can significantly influence species distribution ([Cloudsley-Thompson 1962](#), [Porter et al. 2002](#)). For example, many plants may be limited by patterns of water availability or soil nutrients, rather than temperature ([Jones 1992](#)); thus even if insects that rely on these plants are limited by temperature (i.e., because they are ectotherms), they are further constrained by the nutrition requirements of their hosts ([Huey, 1978](#)). Similarly, pests in agricultural landscapes may be constrained by their microclimatic thermal environment and their relative thermal tolerances, but their distribution will also be driven by other parameters such as plant host quality, natural enemies' occurrences, and chemical insecticide spraying. Consequently, even with all the scientific and technological breakthroughs that appeared over the years, the identification, understanding and integration of the complete array of processes that drive organisms in their microhabitat is still likely to be a challenging endeavour.

3. Does microclimate reduce tropical mountain passes?

The work presented in this thesis may have broader implications for the study of tropical ectotherms' ecology, as it would allow revisiting some influential concepts on the physiological thermal tolerances of tropical- versus temperate-zone organisms. In 1967, Daniel Janzen published an influential paper entitled "Why mountain passes are higher in the tropics?" Janzen derived a simple climatic-physiological model predicting that tropical mountain passes would be more effective barriers to ectotherms dispersal than would be temperate-zone passes of equivalent elevation ([Janzen 1967](#)). This prediction resulted from the recognition that the annual variation in ambient temperature at any site is relatively low in the tropics compare to the temperate-zones. Consequently, altitudinally separated sites in the tropics will have little overlap in their thermal regimes at any given time or even over the course of a full year. Temperate-zones show a strikingly different pattern because both low- and high-altitude sites experience marked seasonal variations in temperature (Fig. 2). As a result, low- and high-altitude sites in the temperate-zones have considerable overlap in thermal regimes, at least computed over a full year. In the tropics, the low variation within sites reduces or even prevents the overlap in thermal regimes between low- and high-altitude sites.

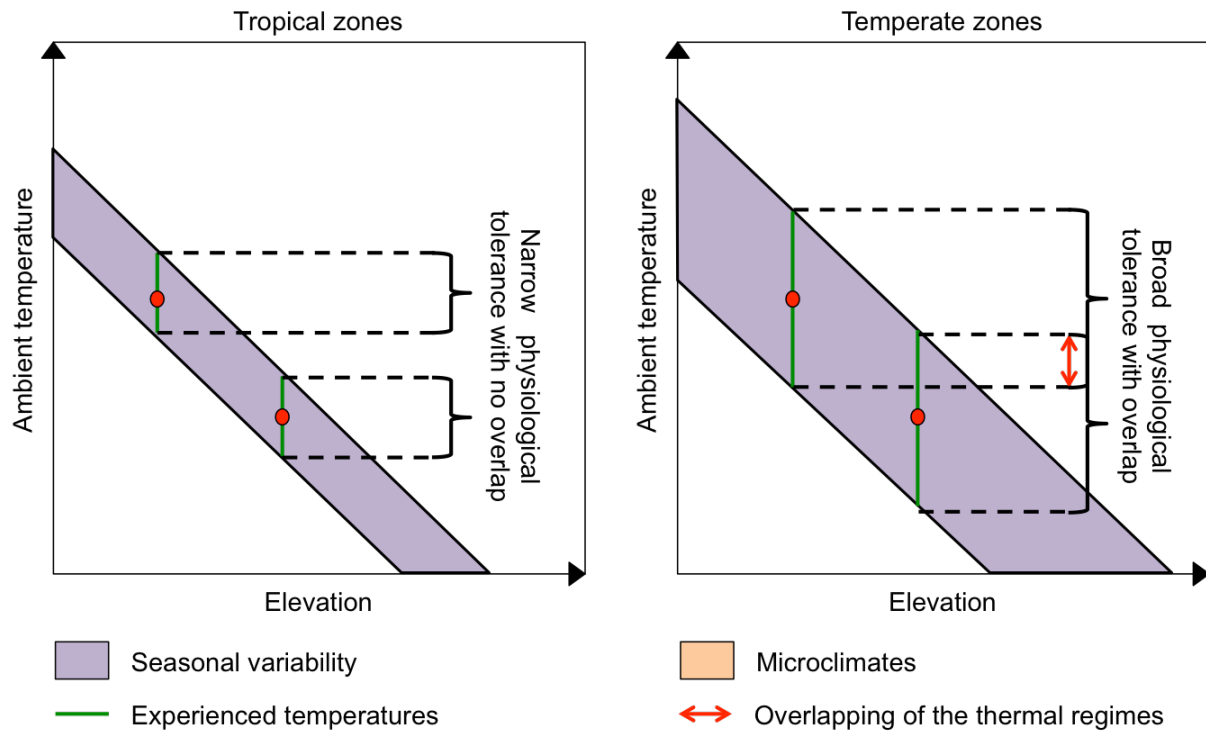


Figure 2: Graphical illustration of Janzen's hypothesis: low seasonal variations of temperature at tropical localities necessarily result in low overlapping in climate between valleys and mountain passes and therefore select for organisms that had narrow tolerances to temperature. On the contrary temperate-zones, marked by strong seasonal variations in temperature, lead to considerable overlaps in thermal regimes between valleys and mountain passes. Consequently, tropical mountain passes are stronger physiological barriers to dispersal than those in temperate-zones.

Organisms develop physiological adaptations and acclimation capacities that reflect the range of climatic variation typically encountered ([Angilletta 2009](#), [Sunday *et al.* 2011](#), [Sheldon & Tewksbury 2014](#)). Thus, temperate-zone organisms possess broad thermal tolerances as well as marked acclimation capacities to cope with the large seasonal changes in climate ([Bonebrake & Deutsch 2012](#)). In contrast, tropical organisms evolve narrow thermal tolerance and reduced acclimation responses, appropriate to the less variable climate of the tropics ([Deutsch *et al.* 2008](#), [Sunday *et al.* 2011](#)). As a result, Janzen predicted that tropical lowland organisms have narrow tolerances to temperature and were more likely to encounter a mountain pass as a physiological barrier to dispersal ([Janzen 1967](#), [Ghalambor *et al.* 2006](#)).

Thus mountain passes are physiological, not topographic, barriers to dispersal: a mountain pass will be a greater physiological barrier if there is relatively little overlap in climate between a low-altitude valley and an adjacent high-altitude pass (Fig. 2). He finally linked these assumptions and predicted that tropical organisms would have greater difficulty in crossing mountain passes (than would temperate-zone organisms) because they would be more likely to encounter a climate to which they were not adapted.

When taking into account the microclimates experienced by organisms as presented in this thesis, two new questions may appear with respect to this hypothesis: 1) do microclimates physically provide organisms with favourable temperatures to “cross” the mountain passes of the tropics? thereby reducing tropical mountain passes, and 2) are the thermal tolerances of an organism influenced by the microclimates it experiences? In both cases, recomputing the Janzen’s hypothesis using microclimates (e.g., using operative environmental temperatures rather than ambient temperature, [Bakken 1992](#), [Kearney *et al.* 2014](#)) at a global scale and allowing for the expression of behavioural and other adaptations that buffer variation in ambient temperatures (see Introduction) would permit to detail how much microclimatic patterns influence the evolution of the physiological capacities of organisms ([Huey 1991](#), [Logan *et al.* 2013](#)). Moreover this will be a great opportunity to test the effect of latitude and elevations on the microclimatic patterns (i.e., seasonal variability of microclimates, [Scheffers *et al.* 2014b](#)).

Using the same graphical illustration of the Janzen’s hypothesis, we displayed the potential effect of microclimate temperatures in modifying the thermal regimes and leading to a thermal overlapping between valleys and mountain passes in the tropics (Fig. 3). Thus, tropical organisms would have physical possibilities to cross mountain passes when taking into account microclimates, because they would be more likely to encounter favourable

thermal niches. Similarly, in the temperate-zones the overlapping of the thermal regimes will increase if the microclimatic patterns remain constants across latitudes. Actually, high-altitude tropical sites can experience great daily fluctuations in temperature compared to similar altitudes in temperate locations ([Dangles *et al.* 2008](#)). Our work showed that these temperature variations increased by various degree when taking into account the microclimates experienced by organisms ([Faye *et al.* 2014](#)).

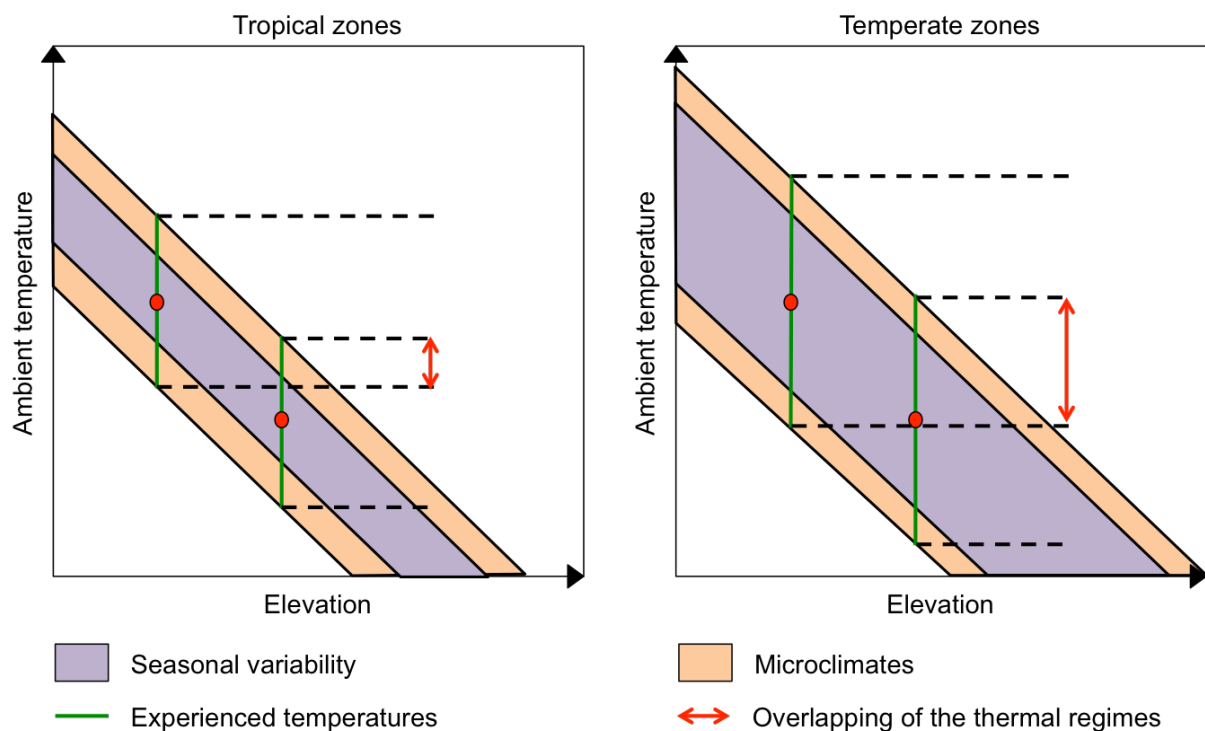


Figure 3: Graphical illustration of Janzen's hypothesis considering the microclimatic patterns.

In the context of climate change, Janzen's hypothesis is relevant as it corresponds to change in ambient temperatures. [Scherrer & Koerner \(2011\)](#) exemplify how a shift in 2 K warmer of the surface temperature distribution will result in the loss of less than 3% of the microclimates observed within one kilometre-squared area [see Fig. 6 of their paper]. Only the species confined to the coldest microclimates will have to move to higher elevations, but the majority of the species will find suitable thermal habitats (as rated by their current thermal

tolerance) in a distance of just a few centimetres or metres. In the Chapter III of our work, we found a similar pattern in crop fields in which pests have to move few centimetres only to modulate their thermal environment and find thermal niches that foster their performances. The large variation of microclimatic conditions in landscapes may buffer the impacts of climate change on biodiversity by offering stepping stones and refugia (Hannah *et al.* 2014, Scheffers *et al.* 2014a), rather than forcing all species upslope in order to track climatic warming. In conclusion (and opening for future research), microclimates might both reduce tropical mountain passes and reduce species' vulnerability to climate change.

II. Thermal ecology for agronomists

1. Pest control based on thermal ecology?

Currently, there is a relatively small but growing community of researchers working on thermal ecology. Some of them were gathered at the HeteroClim workshop '*The response of organisms to climate change in heterogeneous environments*' that took place in July 2014 in Loches, France (see Appendix S2 for the poster I presented there). This workshop faced the challenges of bringing together scientists from various key disciplines (climate, genetics, physiology, ecology, agronomy, statistics) to promote the interconnections between their different expertise and skills. One of the major outputs of this conference was that interdisciplinary blends would bring innovative solutions to topical issues related to thermal ecology.

Similarly, interdisciplinary studies linking ecological, agronomical and social issues are essentials to build a complete understanding of agrosystems. Indeed, further investigations should focused on the interconnections that occur between farmers, pests and their abiotic environments (Fig. 4). Our team already focused on the Pest – Farmer interactions (Fig. 4.1) and revealed the importance of collaborative actions among farmers for more efficient pest

management (Rebaudo & Dangles 2011, Rebaudo *et al.* 2011, Rebaudo & Dangles 2015). This thesis opens a new pathway towards thermal agroecology based both on agronomical and thermal ecology processes: indeed, we showed how crop microclimates influenced pest occurrences and how pests modify their environments leading to new microclimatic conditions (Fig. 4.1). Indeed, when pests damage their host plant, they are often modifying the structure and/or composition of the plant (e.g., colour of the leaves, water content of the plants, senescence, leaf area index...). These modifications lead in turn to a modification of the microclimates experienced by the pests (e.g., diminution of shadow, increased emission of thermal radiations). The next step for the development of innovative pest control strategies will be to study how farmer practices can shape the thermal environment of crop pests, which will subsequently hampers crop infestation by pest. Certainly, agricultural practices such as row- or plant-spacing, intercropping, adapted plant prune may turn the microclimates experienced by pest unfavourable regarding their thermal tolerance, thereby limiting their infestation (Fig. 4.3).

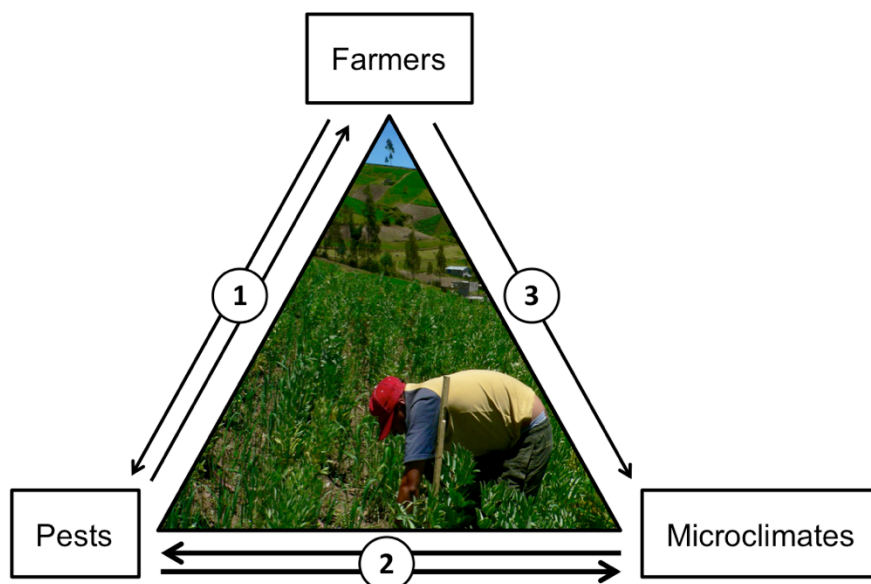


Figure 4: Schematic representation of the interconnections that occurs in agrosystems between farmers, pests, microclimates. The #2 arrows pointed out the integration of this thesis in this triptych.

Based on the outputs shown in this thesis, strategies aiming at enhancing a thermal-based pest control should be explored by setting up spatially explicit models (e.g., cellular automata combined with agent based simulations). These simulations implemented at the field or agricultural landscape scales should test the efficiency of specific farmer practices and collaborations for improving pest control. For instance, different kinds of field management (field clustering, heterogeneity in sowing dates, row spacing, intercropping...) should be explored for their impact on microclimate patterns and subsequent effect on pest levels. We could identify specific crop (e.g., corn) that act as a physical obstacle to cross due to its thermal properties (i.e., a thermal barrier) for potato pests. We could also test the efficiency of appropriate landscape manipulations by farmers for hampering infestation by pests (different levels of composition and configuration in space and in time of crops, [Veres *et al.* 2013](#), [Schneider *et al.* 2015](#)) based on the thermal properties of the agricultural landscape ([Parsa *et al.* 2011](#)). The results of these modelling explorations would provide a range of theoretical pest control strategies to be tested under real conditions. Consequently, the next step will be to test these new assumptions under experimental setting or real-world situations.

2. Moving to experimental approaches

Experimental field manipulation has proven to be an efficient way to test the response of crops to specific treatments or perturbations ([Mead *et al.* 2002](#)). It allows randomizing sampling units into treatment and control groups to statistically examine the outcomes between these groups. Contrary to laboratory experiments, hypotheses can be tested “in the real world” with natural settings rather than in a constrained laboratory environment. This kind of experiment might provide great insights for understanding the effects of microclimates on pest distribution. Indeed, experimental field permits to get rid off part of the variability that may influence pests in crop fields: for instance farmers practices can be

homogenized (application of chemical insecticides) or modified to test a hypothesis (row spacing, prune, ... and see above). In this context, a collaboration with the International Potato Centre (CIP - www.cipotato.org) during my thesis gave me some insights about how to move to more experimental approaches.

Based in Lima, Peru, the CIP is a CGIAR research centre (Consultative Group for International Agricultural Research) that seeks to achieve food security for people in the developing world by improving root and tuber farming and food systems. One of their fields of investigation is to study sweet potato to improve plant tolerance to heat as it could both improve crop productivity and facilitate the use of more marginal heat prone production areas (e.g., in sub-sahelian countries in Africa). To achieve this purpose, the team of *Bettina Heider* (researcher at the Global Genetic Resources department) implemented a massive field screening of 1973 sweet potato accessions from the CIP Genebank in the semiarid region of Piura, in northern Peru. This area displays a dry and hot climate with an annual mean temperature of 24.4°C and an annual mean precipitation of only 72 mm ([Rollenbeck et al. 2015](#)). During summer 2014, the CIP team sowed a total of 2039 accessions of sweet potato (including 1973 sweat potato accessions and 66 additional test clones) within plots of 3.3 m² (Fig. 5). This experimental field was replicated in a field aside from the first one, amounting to a total number of 4078 plots spreading over 3 ha.

We collaborated with Bettina's team in this project by flying an UAV equipped with visual and thermal sensors to yield high-resolution visual and infrared orthophotos (Fig. 5, [Faye et al. 2015](#)) at two decisive stages of the physiological crop developpement: the root initiation (60 d.a.p. days after planting), the maximum root bulking (90 d.a.p.). The aim of this collaboration was to rapidly conduct a thermal selection of sweet potato plants in experimental fields using remote sensing. Indeed, thermal evaluation of all the repetition units

using a thermal infrared ground-based methodology took more than four weeks with four people employed full-time, but only a few hours with the UAV.

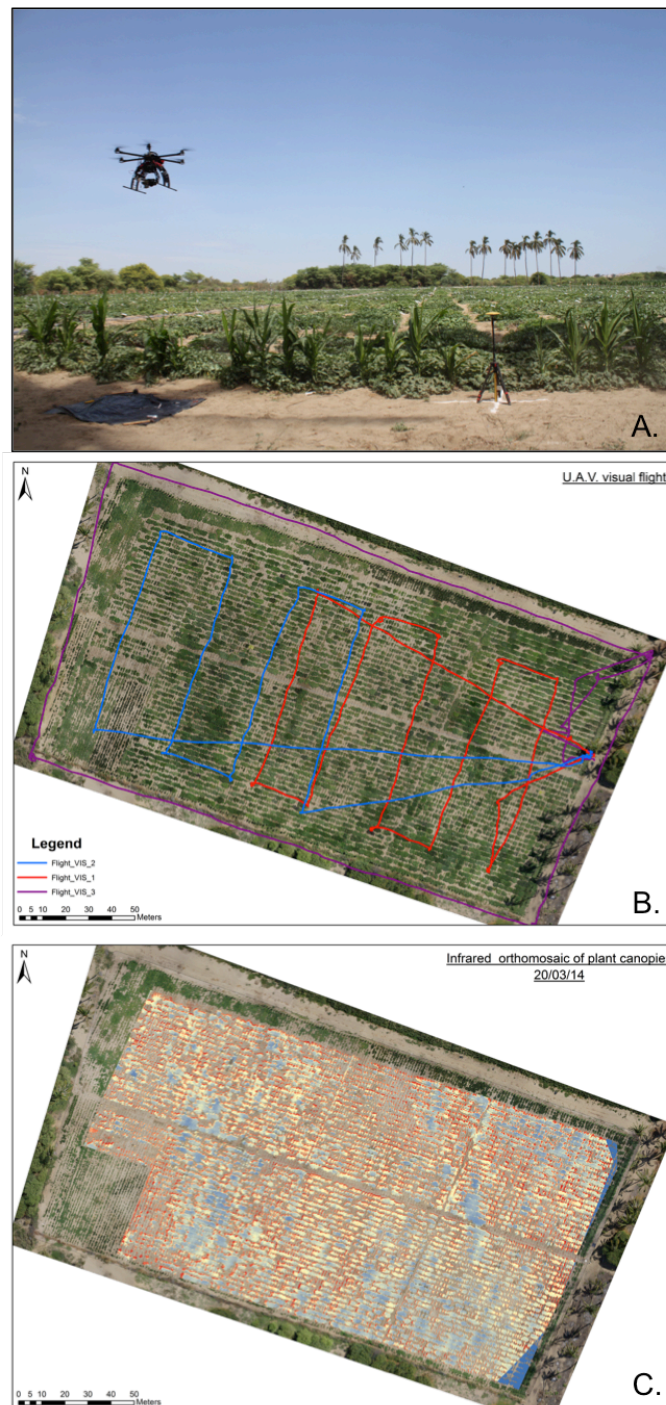


Figure 5: UAV thermal and visual orthophotos of a 3 ha experimental field of sweet potato screening for heat tolerance. A. The UAV taking off with visual and infrared thermal camera on-board. B. The visual orthophoto (1.2 cm^2 resolution) yielded from the UAV with the onboard GPS recording flight tracks. C. The infrared orthophoto of the plant canopy only (5 cm^2 resolution) produced with the UAV images.

Additionally, the use of UAV-based assessment greatly increased the accuracy of the thermal and visual measurements. By recording the entire fields in ten minutes compared, the UAV-based methodology significantly reduced the variability of the thermal measurements that is due to solar radiation and weather changes. This experiment allowed us to relate the thermal signature of the plant canopy surface and the vegetation index recorded by the UAV methodology to the effective yield of each plot empirically measured in the field. We also related the worldwide geographical origins of the sweet potato accessions with the thermal responses of plant canopies during extremes heat events.

3. Pest modelling for agro-ecological purposes

In agronomy, a great variety of temperature-based models (e.g., cohort-based models [Logan 1988](#), individual-based models [Guichard *et al.* 2012](#), cellular automata [Rebaudo *et al.* 2011](#)) have been developed to assess pest occurrences across agricultural landscapes. Such models are becoming a key component of pest-risk assessments both under current and predicted climatic conditions ([Venette *et al.* 2010](#), [Garcia *et al.* 2014](#), and [Sutherst *et al.* 2014](#) for a review). In view to improve the accuracy of the predictions of these models for farming applications, our group conducted a study on the effect of climate dataset resolution on pest performance models. Our objective was to assess whether microclimate data were more relevant than less accurate climate data in predicting crop pest performances. We therefore compared simulated pest performance of three potato tuber moths (see Fig. 26 and paragraph III.3.b. of the Introduction) using three temperature data set obtained at three different spatial resolutions: i) at the regional scale (mean air temperature data from WorldClim - resolution near 1km²), ii) at the landscape scale (air temperature from weather stations), and iii) at the field scale (microclimate in crops). We then compared these simulations with field data of pest abundance. Interestingly, we found that microclimate datasets were best disposed to predict pest abundances at the local scale and at a fine resolution. Indeed, the microclimate

based model was more efficient in predicting pest abundance than the coarser-resolution-based models (Fig. 6). Consequently, this study quantitatively highlights the importance of considering microclimates at fine spatial scales when predicting pest performances.

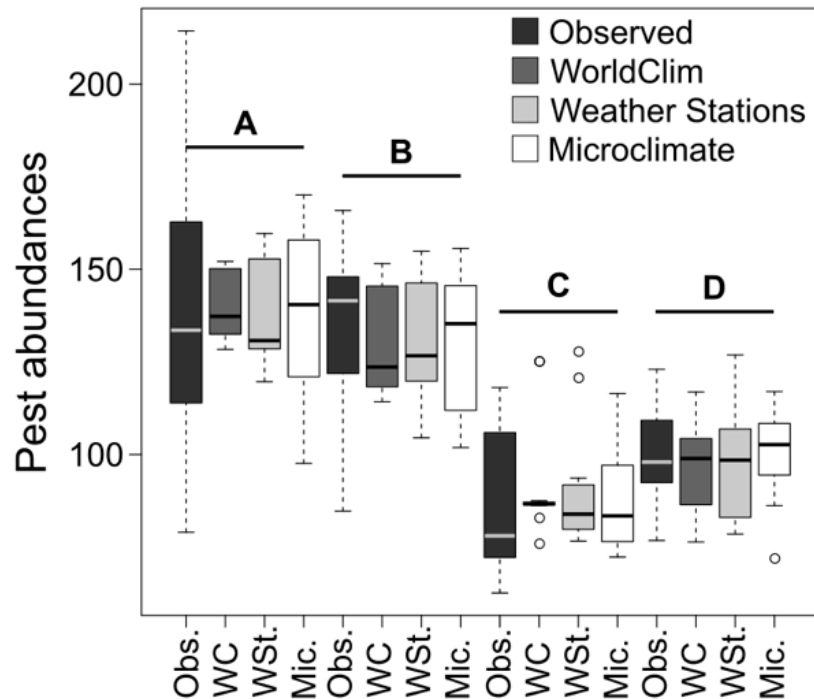


Figure 6: Comparison of observed and predicted abundances for the four studied sites. Pest abundances are represented by boxplots that correspond to mean pest abundances per month. Letters are for the various study sites.

III. Putting thermal ecology into practices in developing countries

1. The importance of data in the tropics

Working with scarce data – Data from ecological monitoring, including pest distribution and climate, are scarce in many developing countries located in the tropical region. This shortage of data hinders the development of pest distribution understandings in these regions. Due to less developed scientific research information concerning insects' responses to their environment, data is often scarce and many times incomplete. Moreover, much of the existing information has not been published and has remained as “grey” literature, hardly available for researchers. For our concerns, the low number of weather stations in tropical regions causes climatic data to be even scarcer (Hijmans *et al.* 2005). This lack of weather data also increases the already high uncertainty of climate change predictions (Buytaert *et al.* 2010). Additionally, information regarding land-use and agronomy is usually out-dated and existing maps have a very coarse spatiotemporal resolution (Ministerio de Agricultura Ganaderia Acuacultura y Pesca del Ecuador, www.agricultura.gob.ec). Finally, monitoring data on pests is usually completely lacking. Therefore, this shortage of data demands great efforts for researchers either to find existing information or to develop and record it themselves in order to achieve adequate analysis regarding their scientific interests. Below we propose two ways to deal with this shortage of data.

“Big data” insights into pest distribution – The need for a coordinated monitoring system, complemented by robust diagnostic networks and widely accessible information systems on pest and plant diseases, has never been greater (Chakraborty & Newton 2011). Pest problems are likely to increase in the future (Oerke 2006, Garrett 2013), so we need to move from a pest specific, short-term and demand-driven approach to the establishment of a general framework of understanding and managing insect pests. But the cost of effective

surveillance can be high for many developing countries. In this context, the *Centre for Agricultural Bioscience International* (CABI) has been developing a Global Plant Clinic network where ‘plant doctors’ provide quality-controlled data for a community surveillance system, leading to early detection of new pests and diseases (<http://www.cabi.org>). It is nowadays the largest global pest distributions repository available: the CABI features an extensive global coverage of more than 20 000 pests, diseases, weeds and their natural enemies, the crops that are their hosts, and the countries in which they occur. Moreover, the CABI provides up-to-date information on the latest literature on the spread, detection and control of pests and diseases worldwide.

Another example of large scale pest monitoring is the *INNOMIP* project (INNOvative approaches to Manage Insect Pest risks in changing Andes), led by the French Institute for Research and Development (IRD) in collaboration with the Entomology Laboratory of the Pontifical Catholic University of Ecuador (PUCE). This program was developed to improve the capacity of North Andean farmers to fight agricultural pests. This participative monitoring was made of 51 study points spread over Ecuador, Peru and Bolivia (Fig. 7). At each point from 2006 to 2012, climatic data were recorded at a 1-minute time-step using an air temperature and relative humidity logger placed at 1.5 m high. The INNOMIP project also established a participative monitoring of potato tuber moth infestation with pheromone traps, revised by either technicians or farmers every three weeks. Data recorded by this project were available through a web-base interface. This thesis has benefited from such a project mainly through the availability of data on pests and climate monitoring at a regional scale. For instance, long term temperature monitoring in the field with data-loggers in the study site of this thesis were used as a reference for assessing the actual seasonality in the study sites (see Appendices S4 and S6 of Chapter I). Also, pest data issued from this monitoring were used as observed data for validating our modelling outcomes in the work presented in paragraph II.3.

of this discussion (see above). Approaches such as this one to manage and make accessible data constitute important advances towards improving both knowledge about these pests' and the capacity to understand their dynamics in the North Andean Region.

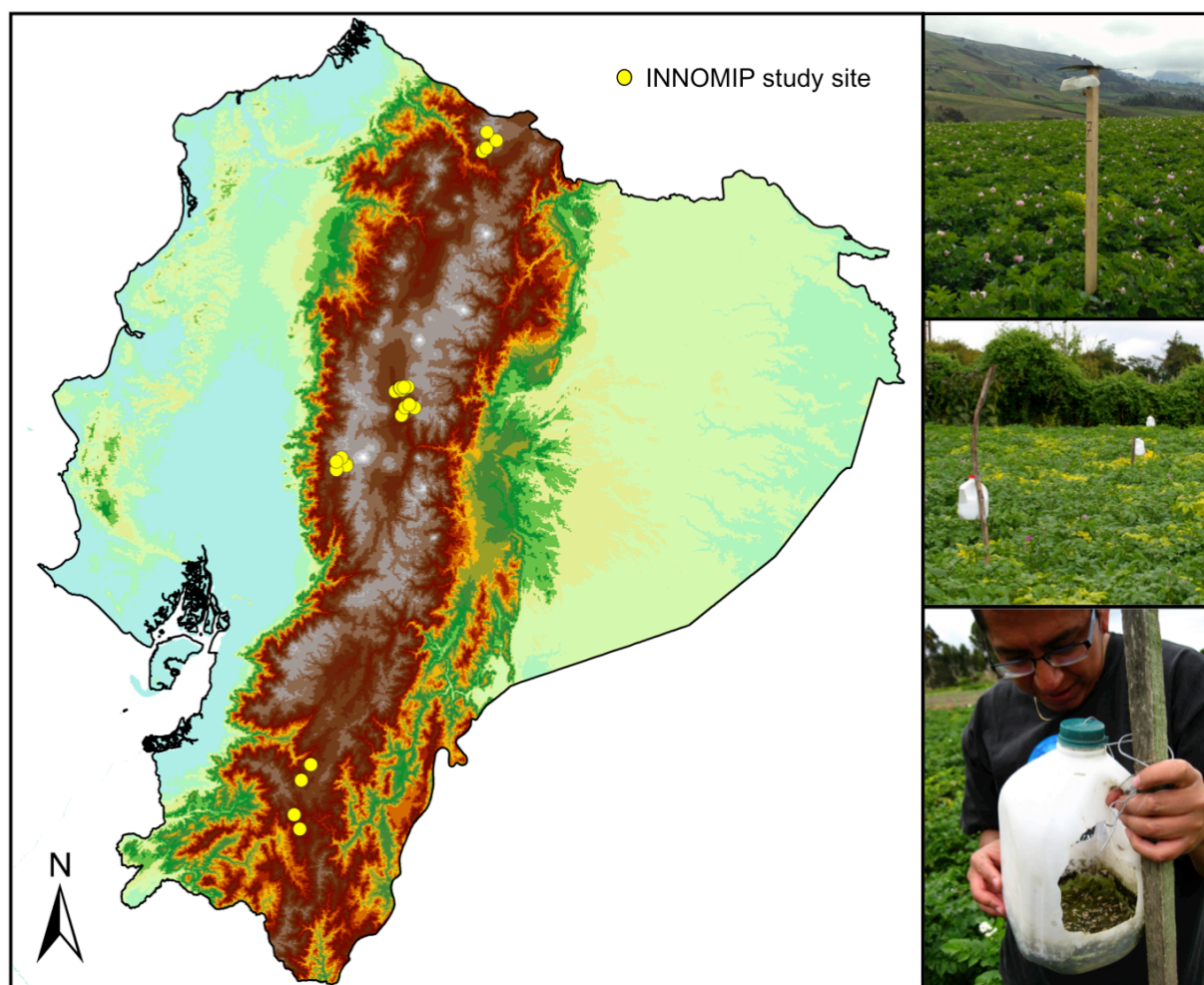


Figure 7: Map of the 27 study sites of the *INNOMIP* pest and climate monitoring over the Ecuadorian Andes. Photographs from top to bottom illustrate the temperature logger, pheromone traps of the three studied pests, and pest enumerating. Photo credits: IRD – Emile Faye and Olivier Dangles.

2. UAV: Limits and promises for developing countries

Limits of the technology – As claimed by [Anderson & Gaston \(2013\)](#), “drones are on their way to revolutionize spatial ecology” and to become an indispensable device for ecologists ([Grémillet et al. 2012](#)). But applying such technologies for research, in particular in developing countries, faces different obstacles that have to be overcome. The price of technologies such as thermal cameras and UAVs, even if constantly decreasing, is still expensive. A complete UAV system (including the drone, the ground control station, the remote control, the data link, etc...) combined with on-board visual and infrared cameras will cost between 10.000 and 50.000 US dollars. After what, the learning of piloting, flight programming, UAV maintenance, thermal and visual image processing, mapping software will last in average for 1 year of practice. Weather conditions are also restricting UAV flights: wind, rain and thunderstorms are the main factors that can constrain UAV flight and they have to be appreciated by the pilot himself. Generally, wind speeds above 30 km/h will keep the UAV on the ground or force the pilot to return to land. Rain is no flight conditions because it may interfere with the on-board electronic components and also affect data values of the images due to high water content in the light path ([Jones & Vaughan 2010](#)). Ground elevation a.s.l. also hampers the uses of UAVs for research, in particular those of hexacopters (compared to wing shape UAVs which possess more lifting power): indeed, for the purpose of another study interested in glacier melt effects of plant biodiversity, we tried to fly over a glacier snout with a light UAV (<1 kg) and due to the low air density at that altitude, we were not able to hover (Fig. 8). Based on flights performed at various elevations in the tropical Andes, we estimated that the elevation limits for flying with ready-to-fly commercial drones was 3500 m high. Of course, the flying aptitude of the UAV can be adjusted by decreasing the total flying weight, and by increasing the power of the motors and the capacity of the batteries. Additionally, care should be taken when conducting UAV experiments on wild

animals because if practised without caution UAV flights can disrupt animals' behaviour (Ditmer *et al.* 2015, Vas *et al.* 2015). Last but not least, despite a strong interest and enthusiasm from the scientific community for such a promising tool, one critical constraint that still hampers the adoption of UAVs by the scientific community concerns administrative restrictions such as the governmental approval for flying (Allan *et al.* 2015). For instance, the use of UAV system in this thesis was achieved thanks to the support of the official authorities of Ecuador (IEE – [Instituto Espacial Ecuatoriano](#)). As declared by Vincent *et al.* (2015), “UAV technology will revolutionize ecology, but only if it can be widely and easily implemented”.



Figure 8: Photographs of a light commercial UAV flying over the glacier snout of the Carihuairazo mountain at 4850 m.a.s.l. (Ecuador). Photo credit: S. Cauvy-Fraunié.

Transferring UAV knowledge and methodology – Knowledge diffusion is one of the most important challenges for global development (Hoekman *et al.* 2005). The transfer of skills, knowledge, technologies and methods among scientists worldwide is a key step for making it accessible to a wide range of stakeholders who can further develop and exploit this knowledge. A trustful collaboration with southern partners is decisive for addressing the international development issues; and researchers from developed countries should not

monopolize new technologies such as UAVs and thermal cameras. That is why during this thesis, we collaborated with scientific partners of Ecuador, Peru and Bolivia and tried to transfer UAV knowledge and technology through various talks, workshops and training in universities as well as scientific vulgarisation in schools (Fig. 9).



Figure 9: Supports and vulgarisation of Sciences and technologies in Ecuador. First row: field training on the uses of different sensors for Thermal ecology with students (June 2015), UAV fieldwork with our Ecuadorian partners (January 2014). Second row: vulgarisation of our researches for the 2015 ‘*Fête de la Sciences*’ for the school pupils (April 2015). Third row: UAV piloting course at the ‘*Escuela Politecnica Nacional*’ in Ecuador (December 2013).

3. The broader picture: facing obstacles to IPM

This thesis revealed that thermal ecology might bring relevant insights into our knowledge of agricultural landscape and pest dynamics. We think that the recognition of the effect of landscape microclimatic heterogeneity on pest distribution may afford a valuable contribution to the theory and practice of integrated pest management (IPM). IPM involves the coordinated integration of multiple complementary methods to suppress pests in a safe, cost-effective, and environmentally friendly manner (Ehler 2006, Morse 2009). In this context, both methodological and conceptual issues proposed in this thesis may be added to the IPM toolbox, a viewpoint supported by a recent study performed by our group on IPM obstacles worldwide (Parsa *et al.* 2014 in Appendix S3). Indeed, an important result of this survey (that involved 96 countries) was that developing-country respondents rated “IPM requires collective action within a farming community” as their top obstacle to IPM adoption. Such recognition of the need of managing pest at the landscape level (and not by individual farms) is totally in phase with the conclusions of our thesis that thermal landscapes heterogeneity may have a key effect on pest dynamics. Moreover, the Parsa *et al.*’s (2014) survey showed that respondents from developing and developed countries rated the obstacles differently. This difference in perception between actors highlighted for the first time the need to improve the participation of all stakeholders of the developing countries in the debate on adoption of the IPM worldwide. In this context, research on thermal ecology applied to agronomy, to date developed mainly in developed countries, should also involved developing country stakeholders and academics so that the regional and local specificities of tropical agroscares may be taken into account. From theory to practices, training a new generation of agro-ecologists with the most recent knowledge and methodologies available for the survey of pest dynamics should be one of the best bet to address food security problems in a context of climate change and variability.

REFERENCES

REFERENCES

- Agam, N., Segal, E., Peeters, A., Levi, A., Dag, A., Yermiyahu, U., & Ben-Gal, A. (2014). Spatial distribution of water status in irrigated olive orchards by thermal imaging. *Precision agriculture*, **15**(3), 346-359.
- Alcázar, J., & Cisneros, F. (1997). Taxonomy and bionomics of the Andean potato weevil complex: *Premnotrypes* spp. and related genera. *Impact on a changing world: Program report*, **98**, 141-151.
- Allan, B. M., Ierodiaconou, D., Nimmo, D. G., Herbert, M., & Ritchie, E. G. (2015). Free as a drone: ecologists can add UAVs to their toolbox. *Frontiers in Ecology and the Environment*, **13**(7), 354-355.
- Alyokhin, A., Baker, M., Mota-Sanchez, D., Dively, G., & Grafius, E. (2008). Colorado potato beetle resistance to insecticides. *American Journal of Potato Research*, **85**(6), 395-413.
- Anderson, K., & Gaston, K. J. (2013). Lightweight unmanned aerial vehicles will revolutionize spatial ecology. *Frontiers in Ecology and the Environment*, **11**(3), 138-146.
- Anderson, M. C., Kustas, W. P., & Norman, J. M. (2007). Upscaling flux observations from local to continental scales using thermal remote sensing. *Agronomy Journal*, **99**(1), 240-254.
- Andrewartha, H. G., & Birch, L. C. (1960). Some Recent Contributions to the Study of the Distribution and Abundance of Insects. *Annual Review of Entomology*, **5**, 219-242.
- Angilletta, M. J. (2006). Estimating and comparing thermal performance curves. *Journal of Thermal Biology*, **31**, 541-545.
- Angilletta, M. J. (2009). *Thermal adaptation: a theoretical and empirical synthesis*. Oxford University Press.
- Angilletta, M. J., Niewiarowski, P. H., & Navas, C. A. (2002). The evolution of thermal physiology in ectotherms. *Journal of Thermal Biology*, **27**, 249-268.
- Ashcroft, M. B., Gollan, J. R., Warton, D. I., & Ramp, D. (2012). A novel approach to quantify and locate potential microrefugia using topoclimate, climate stability, and isolation from the matrix. *Global Change Biology*, **18**(6), 1866-1879.
- Austin, M. P., & Van Niel, K. P. (2011). Improving species distribution models for climate change studies: variable selection and scale. *Journal of Biogeography*, **38**(1), 1-8.
- Ayers, D.Y. & Shine, R., (1997). Thermal influences on foraging ability: body size, posture and cooling rate of an ambush predator, the python *Morelia spilota*. *Functional Ecology*, **11**, 342-347.
- Bakken, G. S. (1992). Measurement and application of operative and standard operative temperatures in ecology. *American Zoologist*, **32**(2), 194-216.
- Baldocchi, D. D., Verma, S. B., & Rosenberg, N. J. (1983). Microclimate in the soybean canopy. *Agricultural Meteorology*, **28**(4), 321-337.
- Bale, J.S., Masters, G.J., Hodkinson, I.D., Awmak, C., Bezemer, T.M., Brown, V., Butterfield, J., Buse, A., Coulson, J.C., Farrar, J., Good, J.E.G., Hartley, R., Jones, T.H., Lindroth, R.L., Press, M.C., Symrnioudis, I., Watt, A., Whittaker, J.B., 2002. Herbivory in global climate change research: direct effects of rising temperature on insect herbivores. *Global Change Biology*, **8**, 1-16.
- Barbour, M. G., & Racine, C. H. (1967). Construction and performance of a temperature-gradient bar and chamber. *Ecology*, 861-863.
- Bartholomew, G. A. (1966). Interaction of physiology and behavior under natural conditions in the Galápagos. *Proceedings of the Symposia of the Galápagos International Scientific Project* (No. 13, p. 39). Univ of California Press.

- Batugal, P. A., de la Cruz, A., Libunao, W. H., & Khwaja, A. M. (1990). Intercropping potato with maize in lowland Philippines. *Field Crops Research*, **25**(1), 83-97.
- Bebber, D. P., Holmes, T., & Gurr, S. J. (2014). The global spread of crop pests and pathogens. *Global Ecology and Biogeography*, **23**(12), 1398-1407.
- Becker, A., Körner, C., Brun, J. J., Guisan, A., & Tappeiner, U. (2007). Ecological and land use studies along elevational gradients. *Mountain Research and Development*, **27**(1), 58-65.
- Bellvert, J., Zarco-Tejada, P. J., Girona, J., & Fereres, E. (2014). Mapping crop water stress index in a 'Pinot-noir' vineyard: comparing ground measurements with thermal remote sensing imagery from an unmanned aerial vehicle. *Precision agriculture*, **15**(4), 361-376.
- Bennie J, Wilson, R.J., Maclean, I.M.D., & Suggitt, A.J. (2014). Seeing the woods for the trees – when is microclimate important in species distribution models? *Global Change Biology*. doi: 10.1111/gcb.12525.
- Bennie, J., Huntley, B., Wiltshire, A., Hill, M. O., & Baxter, R. (2008). Slope, aspect and climate: spatially explicit and implicit models of topographic microclimate in chalk grassland. *Ecological Modelling*, **216**(1), 47-59.
- Benton, T. G., Vickery, J. A., & Wilson, J. D. (2003). Farmland biodiversity: is habitat heterogeneity the key? *Trends in Ecology & Evolution*, **18**(4), 182-188.
- Benzinger, T. H., Pratt, A. W., & Kitzinger, C. (1961). The thermostatic control of human metabolic heat production. *Proceedings of the National Academy of Sciences of the United States of America*, **47**(5), 730.
- Berni, J. A. J., Zarco-Tejada, P. J., Sepulcre-Cantó, G., Fereres, E., & Villalobos, F. J. (2009). Mapping canopy conductance and CWSI in olive orchards using high resolution thermal remote sensing imagery. *Remote Sensing of Environment*, **113**, 2380–2388.
- Bianchi, F. J. J. A., Booij, C. J. H., & Tscharrntke, T. (2006). Sustainable pest regulation in agricultural landscapes: a review on landscape composition, biodiversity and natural pest control. *Proceedings of the Royal Society of London B: Biological Sciences*, **273**(1595), 1715-1727.
- Birch, A.N.E., Begg, G.S., & Squire, G.R. (2011). How agro-ecological research helps to address food security issues under new IPM and pesticide reduction policies for global crop production systems. *Journal of Experimental Botany*, **62**, 3251–3261.
- Bonebrake, T. C., & Deutsch, C. A. (2012). Climate heterogeneity modulates impact of warming on tropical insects. *Ecology*, **93**(3), 449-455.
- Bozinovic, F., Bastias, D. A., Boher, F., Clavijo-Baquet, S., Estay, S. A., & Angilletta, M. J. (2011). The mean and variance of environmental temperature interact to determine physiological tolerance and fitness. *Physiological and Biochemical Zoology*, **84**(6), 543-552.
- Brader, L. (1982). Recent trends of insect control in the tropics. *Entomologia Experimentalis et Applicata*, **31**, 111–20.
- Briscoe, N. J., Handasyde, K. A., Griffiths, S. R., Porter, W. P., Krockenberger, A., & Kearney, M. R. (2014). Tree-hugging koalas demonstrate a novel thermoregulatory mechanism for arboreal mammals. *Biology Letters*, **10**(6), 20140235.
- Broadbent, L. (1950). The microclimate of the potato crop. *Quarterly Journal of the Royal Meteorological Society*, **76**(330), 439-454.
- Brown, J. H., Gillooly, J. F., Allen, A. P., Savage, V. M., & West, G. B. (2004). Toward a metabolic theory of ecology. *Ecology*, **85**(7), 1771-1789.
- Buckley, L. B., Ehrenberger, J. C., & Angilletta, M. J. (2015). Thermoregulatory behaviour limits local adaptation of thermal niches and confers sensitivity to climate change. *Functional Ecology*.

- Buckley, L. B., Tewksbury, J. J., & Deutsch, C. A. (2013). Can terrestrial ectotherms escape the heat of climate change by moving? *Proceedings of the Royal Society of London B: Biological Sciences*, **280**(1765), 20131149.
- Buckley, L. B., Urban, M. C., Angilletta, M. J., Crozier, L. G., Rissler, L. J., & Sears, M. W. (2010). Can mechanism inform species' distribution models? *Ecology Letters*, **13**(8), 1041-1054.
- Buytaert, W. B. W., Vuille, M., Dewulf, A., Urrutia, R., Karmalkar, A., & Celleri, R. (2010). Uncertainties in climate change projections and regional downscaling in the tropical Andes: implications for water resources management. *Hydrology and Earth System Sciences*, **14**, 1247-1258.
- Calderón, R., Montes-Borrego, M., Landa, B. B., Navas-Cortés, J. A., & Zarco-Tejada, P. J. (2014). Detection of downy mildew of opium poppy using high-resolution multi-spectral and thermal imagery acquired with an unmanned aerial vehicle. *Precision Agriculture*, **15**(6), 639-661.
- Camacho, A., Rodrigues, M. T., & Navas, C. (2015). Extreme operative temperatures are better descriptors of the thermal environment than mean temperatures. *Journal of Thermal Biology*, **49**, 106-111.
- Campbell, A., Frazer, B. D., Gilbert, N. G. A. P., Gutierrez, A. P., & Mackauer, M. (1974). Temperature requirements of some aphids and their parasites. *Journal of Applied Ecology*, 431-438.
- Capitanio, F., Faccenna, C., Zlotnik, S., & Stegman, D. (2011). Subduction dynamics and the origin of Andean orogeny and the Bolivian orocline. *Nature*, **480**, 83-86.
- Cauvy-Fraunié, S. (2014). Hydroecology of invertebrate communities in equatorial glacier-fed streams. Life Sciences. Universités Pierre et Marie Curie – Paris VI.
- Chaisuekul, C., & Riley, D. G. (2005). Host plant, temperature, and photoperiod effects on ovipositional preference of *Frankliniella occidentalis* and *Frankliniella fusca* (Thysanoptera: Thripidae). *Journal of Economic Entomology*, **98**(6), 2107-2113.
- Chakraborty S. & Newton A. C. (2011). Climate change, plant diseases and food security: an overview. *Plant Pathology*, **60**(1), 2-14.
- Chang, J. H. (1974). *Climate and agriculture: an ecological survey*. Transaction Publishers.
- Christensen, N. L., Bartuska, A. M., Brown, J. H., Carpenter, S., D'Antonio, C., Francis, R., ... & Woodmansee, R. G. (1996). The report of the Ecological Society of America committee on the scientific basis for ecosystem management. *Ecological applications*, **6**(3), 665-691.
- Chuanyan, Z., Zhongren, N., & Guodong, C. (2005). Methods for modelling of temporal and spatial distribution of air temperature at landscape scale in the southern Qilian mountains, China. *Ecological Modelling*, **189**(1), 209-220.
- Church, N. S. (1960). Heat loss and the body temperatures of flying insects II. Heat conduction within the body and its loss by radiation and convection. *Journal of Experimental Biology*, **37**(1), 186-212.
- Cloudsley-Thompson, J. L. (1962). Microclimates and the distribution of terrestrial arthropods. *Annual Review of Entomology*, **7**(1), 199-222.
- Coll, C., Caselles, V., Galve, J. M., Valor, E., Niclos, R., Sánchez, J. M., & Rivas, R. (2005). Ground measurements for the validation of land surface temperatures derived from AATSR and MODIS data. *Remote Sensing of Environment*, **97**(3), 288-300.
- Colville, W. L. (1968). Influence of plant spacing and population on aspects of the microclimate within corn ecosystems. *Agronomy Journal*, **60**(1), 65-67.
- Cooper, J. P. (1964). Climatic variation in forage grasses. I. Leaf development in climatic races of *Lolium* and *Dactylis*. *Journal of Applied Ecology*, 45-61.

- Cossins, A. R., & Bowler, K. (1987). *Temperature Biology of Animals*. Springer Science & Business Media.
- Crespo-Perez V., Rebaudo, F., Silvain, J.F., & Dangles, O. (2011) Modeling invasive species spread in complex landscapes: the case of potato moth in Ecuador. *Landscape Ecology*, **26**, 1447–1461.
- Crespo-Pérez V., Régnière J., Chuine I, Rebaudo F., & Dangles O. (2014). Changes in the distribution of multispecies pest assemblages affect levels of crop damage in warming tropical Andes. *Global Change Biology*, **21**(1), 82-96.
- Crespo-Pérez, V., Dangles, O., Régnière, J., & Chuine, I. (2013). Modeling temperature-dependent survival with small datasets: insights from tropical mountain agricultural pests. *Bulletin of Entomological Research*, **103**(03), 336-343.
- Dangles, O., Carpio, C., Barragan, A. R., Zeddarn, J. L., & Silvain, J. F. (2008). Temperature as a key driver of ecological sorting among invasive pest species in the tropical Andes. *Ecological Applications*, **18**(7), 1795-1809.
- Dangles, O., Carpio, F.C., Villares, M., Yumisaca, F., Liger, B., Rebaudo, F., & Silvain, J.F. (2010). Community-based research helps farmers and scientists to manage invasive pests in the Ecuadorian Andes. *Ambio*, **39**, 325-335.
- Dangles, O., Herrera, M., Mazoyer, C., & Silvain, J.F. (2013). Temperature-dependent shift in herbivore performance and interactions drive non-linear changes in crop damages. *Global Change Biology*, **19**, 1056-1063.
- Dangles, O., Mesías, V., Crespo-Perez, V., & Silvain, J.F. (2009). Crop damage increases with pest species diversity: evidence from potato tuber moths in the tropical Andes. *Journal of Applied Ecology*, **46**, 1115-1121.
- Danks, H. V. (2004). Seasonal adaptations in arctic insects. *Integrative and Comparative Biology*, **44**(2), 85-94.
- Davis, J. A., Radcliffe, E. B., & Ragsdale, D. W. (2006). Effects of high and fluctuating temperatures on *Myzus persicae* (Hemiptera: Aphididae). *Environmental Entomology*, **35**(6), 1461-1468.
- Dawson, W.R. (1975). On the physiological significance of the preferred body temperatures of reptiles. In: Gates, D.M., Schmerl, R.B. (Eds.), *Perspectives in Biophysical Ecology*. Springer, Berlin, pp. 443–473.
- De Frenne, P., Rodríguez-Sánchez, F., Coomes, D. A., Baeten, L., Verstraeten, G., Vellend, M., ... & Verheyen, K. (2013). Microclimate moderates plant responses to macroclimate warming. *Proceedings of the National Academy of Sciences*, **110**(46), 18561-18565.
- Deutsch, C. A., Tewksbury, J. J., Huey, R. B., Sheldon, K. S., Ghalambor, C. K., Haak, D. C., & Martin, P. R. (2008). Impacts of climate warming on terrestrial ectotherms across latitude. *Proceedings of the National Academy of Sciences*, **105**(18), 6668-6672.
- Devaux, A., Ordinola, M., Hibon, A., & Flores, R. (2010). *El sector papa en la región andina: Diagnóstico y elementos para una visión estratégica* (Bolivia, Ecuador y Perú). Centro Internacional de la Papa.
- Dillon, M. E., Liu, R., Wang, G., & Huey, R. B. (2012). Disentangling thermal preference and the thermal dependence of movement in ectotherms. *Journal of Thermal Biology*, **37**(8), 631-639.
- Dillon, M. E., Wang, G., Garrity, P. A., & Huey, R. B. (2009). Thermal preference in *Drosophila*. *Journal of Thermal Biology*, **34**(3), 109-119.
- Ditmer, M. A., Vincent, J. B., Werden, L. K., Tanner, J. C., Laske, T. G., Iaizzo, P. A., ... & Fieberg, J. R. (2015). Bears Show a Physiological but Limited Behavioral Response to Unmanned Aerial Vehicles. *Current Biology*, **25**(17), 2278-2283.

- Dobrowski, S. Z. (2011). A climatic basis for microrefugia: the influence of terrain on climate. *Global Change Biology*, **17**(2), 1022-1035.
- Dormann, C.F., Schymanski, S.J., Cabral, J., Chuine, I., Graham, C., Hartig, F. et al. (2012). Correlation and process in species distribution models: bridging a dichotomy. *Journal of Biogeography*, **39**, 2119–2131.
- Easterling, D. R., Meehl, G. A., Parmesan, C., Changnon, S. A., Karl, T. R., & Mearns, L. O. (2000). Climate extremes: observations, modelling, and impacts. *Science*, **289**(5487), 2068-2074.
- Ehler, L. E. (2006). Integrated pest management (IPM): definition, historical development and implementation, and the other IPM. *Pest Management Science*, **62**(9), 787-789.
- Elith, J., & Leathwick, J. R. (2009). Species distribution models: ecological explanation and prediction across space and time. *Annual Review of Ecology, Evolution, and Systematics*, **40**(1), 677.
- Estay, S. A., Lima, M., & Bozinovic, F. (2014). The role of temperature variability on insect performance and population dynamics in a warming world. *Oikos*, **123**(2), 131-140.
- Fahrig, L., Baudry, J., Brotons, L., Burel, F. G., Crist, T. O., Fuller, R. J., ... & Martin, J. L. (2011). Functional landscape heterogeneity and animal biodiversity in agricultural landscapes. *Ecology letters*, **14**(2), 101-112.
- Faye, E, Herrera, M, Bellomo, L, Silvain, J-F, Dangles, O. (2014). Strong discrepancies between local temperature mapping and interpolated climatic grids in tropical mountainous agricultural landscapes. *PLoS ONE*, **9**(8), e105541. doi:10.1371/journal.pone.0105541
- Faye, E., Rebaudo, F., Yáñez, D., Cauvy-Fraunié, S. & Dangles O. (2015). A toolbox for studying thermal heterogeneity across spatial scales: from unmanned aerial vehicle imagery to landscape metrics. *Methods in Ecology and Evolution*, In press.
- Fleisher, L. A., Frank, S. M., Sessler, D. I., Cheng, C., Matsukawa, T., & Vannier, C. A. (1996). Thermoregulation and heart rate variability. *Clinical Science*, **90**(2), 97-104.
- Frazier MR, Huey RB, & Berrigan D. (2006). Thermodynamics constrains the evolution of insect population growth rates: “Warmer is better.” *The American Naturalist*, **168**, 512–520.
- Furrer, E. M., & Katz, R. W. (2007). Generalized linear modeling approach to stochastic weather generators. *Climate Research*, **34**(2), 129.
- Garrett, K. A. (2013). Agricultural impacts: Big data insights into pest spread. *Nature Climate Change*, **3**(11), 955-957.
- Gates, D. M. (1980). *Biophysical ecology*. Springer-Verlag.
- Gaum, W. G., Giliomee, J. H., & Pringle, K. L. (1994). Life history and life tables of western flower thrips, *Frankliniella occidentalis* (Thysanoptera: Thripidae). *Bulletin of Entomological Research*, **84**(02), 219-224.
- Geiger, R. (1965). *The Climate near the Ground*. Cambridge Mass.
- Ghalambor, C. K., Huey, R. B., Martin, P. R., Tewksbury, J. J., & Wang, G. (2006). Are mountain passes higher in the tropics? Janzen's hypothesis revisited. *Integrative and Comparative Biology*, **46**(1), 5-17.
- Gilbert, C., Robertson, G., Le Maho, Y., & Ancel, A. (2008). How do weather conditions affect the huddling behaviour of emperor penguins? *Polar Biology*, **31**(2), 163-169.
- Gilbert, E., Powell, J. A., Logan, J. A., & Bentz, B. J. (2004). Comparison of three models predicting developmental milestones given environmental and individual variation. *Bulletin of Mathematical Biology*, **66**, 1821-1850.
- Gilchrist, G. W. (1995). Specialists and generalists in changing environments .1. Fitness Landscapes of Thermal Sensitivity. *The American Naturalist*, **146**, 252-270.

- Gillingham, P. K., Huntley, B., Kunin, W. E., & Thomas, C. D. (2012). The effect of spatial resolution on projected responses to climate warming. *Diversity and Distributions*, **18**(10), 990-1000.
- Gillooly, J. F., Brown, J. H., West, G. B., Savage, V. M., & Charnov, E. L. (2001). Effects of size and temperature on metabolic rate. *Science*, **293**(5538), 2248-2251.
- Glenn, E. P., Huete, A. R., Nagler, P. L., Hirschboeck, K. K., & Brown, P. (2007). Integrating remote sensing and ground methods to estimate evapotranspiration. *Critical Reviews in Plant Sciences*, **26**(3), 139-168.
- Gonzalez-Dugo, V., Zarco-Tejada, P., Nicolás, E., Nortes, P. A., Alarcón, J. J., Intrigliolo, D. S., & Fereres, E. (2013). Using high resolution UAV thermal imagery to assess the variability in the water status of five fruit tree species within a commercial orchard. *Precision Agriculture*, **14**(6), 660-678.
- Graae, B. J., De Frenne, P., Kolb, A., Brunet, J., Chabrierie, O., Verheyen, K., ... & Milbau, A. (2012). On the use of weather data in ecological studies along altitudinal and latitudinal gradients. *Oikos*, **121**(1), 3-19.
- Grémillet, D., Puech, W., Garcon, V., Boulinier, T. & Le Maho, Y. (2012). Robots in ecology: welcome to the machine. *Open journal of ecology*, **2**(2).
- Guichard, S., Kriticos, D. J., Leriche, A., Kean, J. M., & Worner, S. P. (2012). Individual-based modelling of moth dispersal to improve biosecurity incursion response. *Journal of Applied Ecology*, **49**(1), 287-296.
- Guisan, A., & Thuiller, W. (2005). Predicting species distribution: offering more than simple habitat models. *Ecology Letters*, **8**(9), 993-1009.
- Guisan, A., Graham, C. H., Elith, J., & Huettmann, F. (2007). Sensitivity of predictive species distribution models to change in grain size. *Diversity and Distributions*, **13**(3), 332-340.
- Hanafi, A. (1999). Integrated pest management of potato tuber moth in field and storage. *Potato Research*, **42**, 373-380.
- Hannah, L., Flint, L., Syphard, A. D., Moritz, M. A., Buckley, L. B., & McCullough, I. M. (2014). Fine-grain modeling of species' response to climate change: holdouts, stepping-stones, and microrefugia. *Trends in Ecology & Evolution*, **29**(7), 390-397.
- Hardwick, S. R., Toumi, R., Pfeifer, M., Turner, E. C., Nilus, R., & Ewers, R. M. (2014). The relationship between leaf area index and microclimate in tropical forest and oil palm plantation: forest disturbance drives changes in microclimate. *Agricultural and Forest Meteorology*, **201**, 187-195.
- Hare, J. D. (1990). Ecology and management of the Colorado potato beetle. *Annual Review of Entomology*, **35**(1), 81-100.
- Harris, P. M. (2012). *The potato crop: the scientific basis for improvement*. Springer Science & Business Media.
- Harrison, J. F., Fewell, J. H., Roberts, S. P., & Hall, H. G. (1996). Achievement of thermal stability by varying metabolic heat production in flying honeybees. *Science*, **274**(5284), 88-90.
- Heath, J. E., & Adams, P. A. (1967). Regulation of heat production by large moths. *Journal of Experimental Biology*, **47**(1), 21-33.
- Heinrich, B. (1990). Is 'Reflectance' Basking Real? *The Journal of Experimental Biology*, **154**(1), 31-43.
- Heinrich, B. (1993). *The hot-blooded insects: strategies and mechanisms of thermoregulation*. Harvard University Press.
- Helmuth, B. S., & Hofmann, G. E. (2001). Microhabitats, thermal heterogeneity, and patterns of physiological stress in the rocky intertidal zone. *The Biological Bulletin*, **201**(3), 374-384.

- Herrera, M.A., & Dangles, O. (2012). Preferencia de oviposición en tres especies de polillas de la papa (Lepidoptera: Gelechiidae). *Revista Ecuatoriana de Medicina y Ciencias Biológicas*, **33**, 82-87.
- Hijmans, R. J., Cameron, S. E., Parra, J. L., Jones, P. G., & Jarvis, A. (2005). Very high resolution interpolated climate surfaces for global land areas. *International Journal of Climatology*, **25**(15), 1965-1978.
- Hijmans, R.J. (2001). Global distribution of the potato crop. *American Journal of Potato Research*, **78**, 403-412.
- Hirano, M., & Rome, L.C. (1984). Jumping performance of frogs (*Rana pipiens*) as a function of temperature. *Journal of Experimental Biology*, **108**, 429-439.
- Hoekman, B. M., Maskus, K. E., & Saggi, K. (2005). Transfer of technology to developing countries: Unilateral and multilateral policy options. *World Development*, **33**(10), 1587-1602.
- Holland, J.D., Bert, D.G. & Fahrig, L. (2004). Determining the spatial scale of species' response to habitat. *Bioscience*, **54**, 227-233.
- Holmes, R. M., & Dingle, A. N. (1965). The relationship between the macro-and microclimate. *Agricultural Meteorology*, **2**(2), 127-133.
- Hook, S., & Prata, A. J. (2001). Land surface temperature measured by ASTER First results. In *Geophysical research abstracts*, 26th general assembly (Vol. 3, p. 71).
- Huang, L. H., Chen, B., & Kang, L. (2007). Impact of mild temperature hardening on thermotolerance, fecundity, and Hsp gene expression in *Liriomyza huidobrensis*. *Journal of Insect Physiology*, **53**(12), 1199-1205.
- Huey, R. B. (1974). Behavioral thermoregulation in lizards: importance of associated costs. *Science*, **184**(4140), 1001-1003.
- Huey, R. B. (1978). Latitudinal pattern of between-altitude faunal similarity: mountains might be "higher" in the tropics. *The American Naturalist*, 225-229.
- Huey, R.B. (1991). Physiological consequences of habitat selection. *The American Naturalist*, **137**, S91-S115.
- Huey, R.B., & Stevenson, R. D. (1979). Integrating thermal physiology and ecology of ectotherms: A discussion of approaches. *American Zoologist*, **19**, 357-366.
- Huey, R.B., Kearney, M.R., Krockenberger, A., Holtum, J.A.M., Jess, M. & Williams, S.E. (2012). Predicting organismal vulnerability to climate warming: roles of behaviour, physiology and adaptation. *Philosophical Transactions of the Royal Society B - Biological Sciences*, **367**, 1665-1679.
- Inagaki, M. N., & Nachit, M. M. (2008). Visual monitoring of water deficit stress using infrared thermography in wheat. In *The 11th International Wheat Genetics Symposium proceedings* edited by Rudi Appels Russell Eastwood Evans Lagudah.
- IPCC (2014). *Climate Change 2014: Impacts, Adaptation, and Vulnerability*. Cambridge University Press, Cambridge.
- Jackson, H. B., & Fahrig, L. (2015). Are ecologists conducting research at the optimal scale?. *Global Ecology and Biogeography*, **24**(1), 52-63.
- Jacob, F., Petitcolin, F., Schmugge, T., Vermote, E., French, A., & Ogawa, K. (2004). Comparison of land surface emissivity and radiometric temperature derived from MODIS and ASTER sensors. *Remote Sensing of Environment*, **90**(2), 137-152.
- Janzen, D. H. (1967). Why mountain passes are higher in the tropics. *The American Naturalist*, **11**, 233-249.
- Jones, H. G. (1992). *Plants and microclimate: a quantitative approach to environmental plant physiology*. Cambridge university press.
- Jones, H. G., & Vaughan, R. A. (2010). *Remote sensing of vegetation: principles, techniques, and applications*. Oxford university press.

- Josse, C., Cuesta, F., Navarro, G., Barrena, V., Becerra, M. T., Cabrera, E., ... & Naranjo, L. G. (2011). Physical geography and ecosystems in the tropical Andes. *Climate change and biodiversity in the tropical Andes, Inter-American Institute for Global Change Research (IAI) and Scientific Committee on Problems of the Environment (SCOPE)*, 152-169.
- Kadochová, S., & Frouz, J. (2013). Thermoregulation strategies in ants in comparison to other social insects, with a focus on red wood ants (*Formica rufa* group). *F1000Research*, 2.
- Kalma, J. D., McVicar, T. R., & McCabe, M. F. (2008). Estimating land surface evaporation: A review of methods using remotely sensed surface temperature data. *Surveys in Geophysics*, **29**(4-5), 421-469.
- Karl, T. R., Knight, R. W., & Plummer, N. (1995). *Trends in high-frequency climate variability in the twentieth century*.
- Kearney, M. R., Isaac, A. P., & Porter, W. P. (2014). microclim: Global estimates of hourly microclimate based on long-term monthly climate averages. *Scientific data*, **1**.
- Kearney, M., & Porter, W.P. (2009). Mechanistic niche modelling: combining physiological and spatial data to predict species' ranges. *Ecology letters*, **12**(4), 334-350.
- Kearney, M., Shine, R., & Porter, W.P. (2009). The potential for behavioral thermoregulation to buffer cold-blooded animals against climate warming. *Proceedings of the National Academy of Sciences*, **106**, 3835-3840.
- Keasar, T., Kalish, A., Becher, O., & Steinberg, S. (2005). Spatial and temporal dynamics of potato tuberworm (Lepidoptera: Gelechiidae) infestation in field-stored potatoes. *Journal of Economic Entomology*, **98**, 222-228.
- Keller, S. (2003). *Integrated Pest Management of the Potato Tuber Moth in Cropping Systems of Different Agroecological Zones*. Margraf Publishers, Germany.
- Kemp, D. J., & Krockenberger, A. K. (2002). A novel method of behavioural thermoregulation in butterflies. *Journal of Evolutionary Biology*, **15**(6), 922-929.
- Kinahan, A.A., Pimm, S.L., & van Aarde, R.J. (2007). Ambient temperature as a determinant of landscape use in the savanna elephant, *Loxodonta africana*. *Journal of Thermal Biology*, **32**: 47-58.
- Kingsolver, J. G. (1985). Thermal ecology of *Pieris* butterflies (Lepidoptera: Pieridae): a new mechanism of behavioral thermoregulation. *Oecologia*, **66**(4), 540-545.
- Kingsolver, J. G., & Buckley, L. B. (2015). Climate variability slows evolutionary responses of *Colias* butterflies to recent climate change. *Proceedings of the Royal Society of London B: Biological Sciences*, **282**(1802), 24-70.
- Kingsolver, J.G., (2009). The well-temperated biologist. *The American Naturalist*, **174**, 755-768.
- Kingsolver, J.G., & Woods, H.A., (1997). Thermal sensitivity of growth and feeding in *Manduca sexta* caterpillars. *Physiological and Biochemical Zoology*, **70**, 631-638.
- Knapp, G. (1991). *Andean ecology: adaptive dynamics in Ecuador*. Westview Press.
- Korb, J. (2003). Thermoregulation and ventilation of termite mounds. *Naturwissenschaften*, **90**, 212-219.
- Körner, C. (2013). Mountain ecosystems in a changing environment. 5th Symposium for research in protected areas Mittersill (NP Hohe Tauern, Austria) 10 -12 June 2013. Conference Volume, pp 409-412
- Kuenzer, C., & Dech, S. (2013). *Thermal Infrared Remote Sensing*. Springer.
- Kühne, M. (2007). *The Andean potato weevil *Premnotrypes suturicallus**.
- Langer, F., & Fietz, J. (2014). Ways to measure body temperature in the field. *Journal of Thermal Biology*, **42**, 46-51.
- Langridge, J., & McWilliam, J. R. (1967). *Heat responses of higher plants. Thermobiology*. Academic Press, New York, 231-292.

- Lee, C. M., Cable, M. L., Hook, S. J., Green, R. O., Ustin, S. L., Mandl, D. J., & Middleton, E. M. (2015). An introduction to the NASA Hyperspectral InfraRed Imager (HyspIRI) mission and preparatory activities. *Remote Sensing of Environment*, **167**, 6-19.
- Legates, D. R., & Willmott, C. J. (1990). Mean seasonal and spatial variability in gauge-corrected, global precipitation. *International Journal of Climatology*, **10**, 111-127.
- Lenoir, J., Graae, B. J., Aarrestad, P. A., Alsos, I. G., Armbruster, W. S., Austrheim, G., ... & Svenning, J. C. (2013). Local temperatures inferred from plant communities suggest strong spatial buffering of climate warming across Northern Europe. *Global Change Biology*, **19**(5), 1470-1481.
- Leopold, A. C. (1964). *Plant growth and development*. New York, USA. McGraw-Hill eds.
- Levin, S.A. (1992). The problem of pattern and scale in ecology. *Ecology*, **73**, 1943–1967.
- Logan, J. A. (1988). Toward an expert system for development of pest simulation models. *Environmental Entomology*, **17**(2), 359-376.
- Logan, M. L., Cox, R. M., & Calsbeek, R. (2014). Natural selection on thermal performance in a novel thermal environment. *Proceedings of the National Academy of Sciences*, **111**(39), 14165-14169.
- Logan, M. L., Huynh, R. K., Precious, R. A., & Calsbeek, R. G. (2013). The impact of climate change measured at relevant spatial scales: new hope for tropical lizards. *Global Change Biology*, **19**(10), 3093-3102.
- Lookingbill, T. R., & Urban, D. L. (2003). Spatial estimation of air temperature differences for landscape-scale studies in montane environments. *Agricultural and Forest Meteorology*, **114**(3), 141-151.
- Luck, J., Spackman, M., Freeman, A., Griffiths, W., Finlay, K., & Chakraborty, S. (2011). Climate change and diseases of food crops. *Plant Pathology*, **60**(1), 113-121.
- Lutterschmidt, W. I., & Hutchison, V. H. (1997). The critical thermal maximum: history and critique. *Canadian Journal of Zoology*, **75**(10), 1561-1574.
- Maclean, I. M. D., Hopkins, J. J., Bennie, J., Lawson, C. R., & Wilson, R. J. (2015). Microclimates buffer plant community responses to climate change. *Global Ecology and Biogeography*, **24**(11), 1340-1350.
- May, R. M. (1988). How many species are there on earth? *Science*, **241**(4872), 1441-1449.
- Mc Garigal, K. & Marks, B.J. (1994). *Fragstats: Spatial Pattern Analysis Program for Quantifying Landscape Structure*. Oregon state university, Forest science department, Corvallis. *US Department of Agriculture, Forest Service, Pacific Northwest Research Station*.
- McCain, C. (2007). Could temperature and water availability drive elevational species richness patterns? A global case study for bats. *Global Ecology and Biogeography*, **16**(1), 1-13.
- McCain, C. (2009). Vertebrate range sizes indicate that mountains may be “higher” in the tropics. *Ecology Letters*, **12**, 550-560.
- McConnell, E., & Richards, A.G. (1955). How fast can a cockroach run? *Bulletin of Brooklyn Entomological Society*, **50**, 36–43.
- McGill, B. J. (2010). Matters of scale. *Science*, **328**(5978), 575-576.
- Mead, R., Curnow, R. N., & Hasted, A. M. (2002). *Statistical methods in agriculture and experimental biology* (Vol. 55). CRC Press.
- Meron, M., Tsipris, J., Orlov, V., Alchanatis, V., & Cohen, Y. (2010). Crop water stress mapping for site-specific irrigation by thermal imagery and artificial reference surfaces. *Precision Agriculture*, **11**(2), 148-162.
- Millones, J. (1982). Patterns of land use and associated environmental problems of the Central Andes: an integrated summary. *Mountain Research and Development*, 49-61.

- Mondal, S., & Rai, U. (2001). In vitro effect of temperature on phagocytic and cytotoxic activities of splenic phagocytes of the wall lizard, *Hemidactylus flaviviridis*. *Comparative Biochemistry and Physiology Part A: Molecular & Integrative Physiology*, **129**, 391-398.
- Monteith, J. L., & Elston, J. F. (1971). *Microclimatology and crop production*. Potential crop production.
- Morales, F. J., Lastra, R., De Uzcátegui, R. C., & Calvert, L. (2001). Potato yellow mosaic virus: a synonym of Tomato yellow mosaic virus. *Archives of virology*, **146**(11), 2249-2253.
- Moran, M. S., Clarke, T. R., Inoue, Y., & Vidal, A. (1994). Estimating crop water deficit using the relation between surface-air temperature and spectral vegetation index. *Remote sensing of environment*, **49**(3), 246-263.
- Moran, M. S., Inoue, Y., & Barnes, E. M. (1997). Opportunities and limitations for image-based remote sensing in precision crop management. *Remote Sensing of Environment*, **61**(3), 319-346.
- Morse, S. (2009). IPM, Ideals and realities in developing countries. *Radcliffe EB, Hutchison WD and*.
- Navas, C.A. & Bevier, C. (2001). Thermal dependency of calling performance in the eurythermic frog *Colostethus subpunctatus*. *Herpetologica*, **57**, 384-395.
- New, M., Lister, D., Hulme, M., & Makin, I. (2002). A high-resolution data set of surface climate over global land areas. *Climate Research*, **21**(1), 1-25.
- Nowicki, M., Foolad, M. R., Nowakowska, M., & Kozik, E. U. (2012). Potato and tomato late blight caused by *Phytophthora infestans*: an overview of pathology and resistance breeding. *Plant Disease*, **96**(1), 4-17.
- Nwilene, F. E., Nwanze, K. F., & Youdeowei, A. (2008). Impact of integrated pest management on food and horticultural crops in Africa. *Entomologia experimentalis et Applicata*, **128**(3), 355-363.
- Oerke E. C. (2006). Crop losses to pests. *The Journal of Agricultural Science*, **144**(01), 31-43.
- Otero, J., & Onaindia, M. (2008). Landscape structure and live fences in Andes Colombian agrosystems: upper basin of the Cane-Iguaque River. *International Journal of Tropical Biology and Conservation*, **57**(4).
- Paaijmans, K. P., Heinig, R. L., Seliga, R. A., Blanford, J. I., Blanford, S., Murdock, C. C., & Thomas, M. B. (2013). Temperature variation makes ectotherms more sensitive to climate change. *Global Change Biology*, **19**(8), 2373-2380.
- Parmesan, C. (2006). Ecological and evolutionary responses to recent climate change. *Annual Review of Ecology, Evolution, and Systematics*, 637-669.
- Parrella, M. P. (1987). Biology of *Liriomyza*. *Annual Review of Entomology*, **32**(1), 201-224.
- Parsa, S., Ccanto, R., & Rosenheim, J. A. (2011). Resource concentration dilutes a key pest in indigenous potato agriculture. *Ecological Applications*, **21**(2), 539-546.
- Parsa, S., Morse, S., Bonifacio, A., Chancellor, T. C., Condori, B., Crespo-Pérez, V., ... & Dangles, O. (2014). Obstacles to integrated pest management adoption in developing countries. *Proceedings of the National Academy of Sciences*, **111**(10), 3889-3894.
- Peacock, J. M. (1975). Temperature and leaf growth in *Lolium perenne*. II. The site of temperature perception. *Journal of Applied Ecology*, 115-123.
- Penning de Vries, F. W. T., & Laar, H. V. (1982). *Simulation of plant growth and crop production*. Simulation of plant growth and crop production.
- Perez, C., Nicklin, C., Dangles, O., Vanek, S., Sherwood, S., Halloy, S., Martinez, R., Garret, K., & Forbes, G. (2010). Climate change in the high Andes: Implications and adaptation strategies for small scale farmers. *International Journal of Environmental, Cultural, Economic and Social Sustainability*, **6**, 78-88.

- Petach, A. R., Toomey, M., Aubrecht, D. M., & Richardson, A. D. (2014). Monitoring vegetation phenology using an infrared-enabled security camera. *Agricultural and Forest Meteorology*, **195**, 143-151.
- Pielke, R. A., Avissar, R., Raupach, M., Dolman, A. J., Zeng, X., & Denning, A. S. (1998). Interactions between the atmosphere and terrestrial ecosystems: influence on weather and climate. *Global Change Biology*, **4**(5), 461-475.
- Pincebourde, S., & Casas, J. (2006a). Multitrophic biophysical budgets: thermal ecology of an intimate herbivore insect-plant interaction. *Ecological Monographs*, **76**(2), 175-194.
- Pincebourde, S., & Casas, J. (2006b). Leaf miner-induced changes in leaf transmittance cause variations in insect respiration rates. *Journal of Insect Physiology*, **52**(2), 194-201.
- Pincebourde, S., Sanford, E., & Helmuth, B. (2013). Survival and arm abscission are linked to regional heterothermy in an intertidal sea star. *The Journal of Experimental Biology*, **216**(12), 2183-2191.
- Pollet, A., Onore, G., Chamorro, F., & Barragan A. (2004). *Avances en investigacion y manejo integrado de la polilla guatemalteca de la papa, Tecia solanivora*. Pontificia universidad catolica del Ecuador.
- Porter, W. P., & Gates, D. M. (1969). Thermodynamic equilibria of animals with environment. *Ecological Monographs*, 227-244.
- Porter, W. P., Sabo, J. L., Tracy, C. R., Reichman, O. J., & Ramankutty, N. (2002). Physiology on a landscape scale: plant-animal interactions. *Integrative and Comparative Biology*, **42**(3), 431-453.
- Pörtner, H. O. (2002). Climate variations and the physiological basis of temperature dependent biogeography: systemic to molecular hierarchy of thermal tolerance in animals. *Comparative Biochemistry and Physiology - Part A: Molecular & Integrative Physiology*, **132**, 739-761.
- Potter, K. A., Arthur Woods, H., & Pincebourde, S. (2013). Microclimatic challenges in global change biology. *Global Change Biology*, **19**(10), 2932-2939.
- Poveda, G., Alvarez, D. M., & Rueda, O. A. (2011). Hydro-climatic variability over the Andes of Colombia associated with ENSO: a review of climatic processes and their impact on one of the Earth's most important biodiversity hotspots. *Climate Dynamics*, **36**, 2233-2249.
- Prange, H. D. (1996). Evaporative cooling in insects. *Journal of Insect Physiology*, **42**(5), 493-499.
- Prinzinger, R., Pressmar, A., & Schleucher, E. (1991). Body temperature in birds. *Comparative Biochemistry and Physiology Part A: Physiology*, **99**(4), 499-506.
- Puillandre, N., Dupas, D., Dangles, O., Zeddani, J.L., Barbin, K. & Silvain, J.F. (2008). Genetic bottleneck in invasive species: the potato tuber moth adds to the list. *Biological Invasions*, **10**: 319-333.
- Pumisacho, M., & Sherwood, S. (2002). *El cultivo de la papa en Ecuador*. INIAP and CIP, Quito, Ecuador.
- Quattrochi, D. A., & Luvall, J. C. (1999). Thermal infrared remote sensing for analysis of landscape ecological processes: methods and applications. *Landscape Ecology*, **14**(6), 577-598.
- Raymundo, R., Asseng, S., Cammarano, D., & Quiroz, R. (2014). Potato, sweet potato, and yam models for climate change: A review. *Field Crops Research*, **166**, 173-185.
- Rebaudo F. & Dangles, O. (2013). An agent-based modeling framework for integrated pest management dissemination programs. *Environmental Modelling and Software*, **45**, 141-149.

- Rebaudo, F., & Dangles, O. (2011). Coupled information diffusion - pest dynamics models predict delayed benefits of farmer cooperation. *PLoS Computational Biology*, **7**(10), e1002222.
- Rebaudo, F., & Dangles, O. (2015). Adaptive management in crop pest control in the face of climate variability: an agent-based modeling approach. *Ecology and Society*, **20**(2), 18.
- Rebaudo, F., Crespo-Perez, V., Silvain, J.F., & Dangles, O. (2011). Agent-based modeling of human-induced spread of invasive species in agricultural landscapes: insights from the potato moth in Ecuador. *Journal of Artificial Societies and Social sciences*, **14** (3), 7.
- Rhines, A., & Huybers, P. (2013). Frequent summer temperature extremes reflect changes in the mean, not the variance. *Proceedings of the National Academy of Sciences*, **110**(7), E546-E546.
- Robert, E. J. F., Buck, K. W., & Coutts, R. H. A. (1986). A new geminivirus infecting potatoes in Venezuela. *Plant Disease*, **70**(6), 592-603.
- Rojas J. M., Simon, B., Guillermo Folguera, C, Abades, S., & Bozinovic, F. (2014). Coping with daily thermal variability: behavioural performance of an ectotherm model in a warming world. *Plos One*, e106897.
- Rollenbeck, R., Bayer, F., Münchow, J., Richter, M., Rodriguez, R., & Atarama, N. (2015). Climatic cycles and gradients of the El Niño core region in North Peru. *Advances in Meteorology*, 2015.
- Rondon, S. I. (2010). The potato tuberworm: a literature review of its biology, ecology, and control. *American Journal of Potato Research*, **87**,149-16.
- Rosenberg, N. J. (1966). Influence of snow fence and corn windbreaks on microclimate and growth of irrigated sugar beets. *Agronomy Journal*, **58**(5), 469-475.
- Rubio, E., Caselles, V., & Badenas, C. (1997). Emissivity measurements of several soils and vegetation types in the 8–14 mm wave band: analysis of two field methods. *Remote Sensing of Environment*, **59**(3), 490–521.
- Sakschewski, B., von Bloh, W., Huber, V., Müller, C., & Bondeau, A. (2014). Feeding 10 billion people under climate change: How large is the production gap of current agricultural systems? *Ecological Modelling*, **288**, 103-111.
- Saudreau, M., Marquier, A., Adam, B., Monney, P., & Sinoquet, H. (2009). Experimental study of fruit temperature dynamics within apple tree crowns. *Agricultural and Forest Meteorology*, **149**(2), 362-372.
- Savage, V. M., Gillooly, J. F., Brown, J. H., West, G. B., & Charnov, E. L. (2004). Effects of body size and temperature on population growth. *The American Naturalist*, **163**(3), 429-441.
- Scheffers, B. R., Edwards, D. P., Diesmos, A., Williams, S. E., & Evans, T. A. (2014a). Microhabitats reduce animal's exposure to climate extremes. *Global Change Biology*, **20**(2), 495-503.
- Scheffers, B. R., Evans, T. A., Williams, S. E., & Edwards, D. P. (2014b). Microhabitats in the tropics buffer temperature in a globally coherent manner. *Biology Letters*, **10**(12), 20140819.
- Scherrer, D., & Koerner, C. (2010). Infra-red thermometry of alpine landscapes challenges climatic warming projections. *Global Change Biology*, **16**(9), 2602-2613.
- Scherrer, D., & Körner, C. (2011). Topographically controlled thermal-habitat differentiation buffers alpine plant diversity against climate warming. *Journal of Biogeography*, **38**(2), 406-416.
- Schoolfield, R. M., Sharpe, P. J. H., & Magnuson, C. E. (1981). Non-linear regression of biological temperature-dependent rate models based on absolute reaction-rate theory. *Journal of Theoretical Biology*, **88**(4), 719-731.

- Schneider, G., Krauss, J., Riedinger, V., Holzschuh, A., & Steffan-Dewenter, I. (2015). Biological pest control and yields depend on spatial and temporal crop cover dynamics. *Journal of Applied Ecology*. DOI: 10.1111/1365-2664.12471.
- Sears, M. W., & Angilletta Jr, M. J. (2015). Costs and benefits of thermoregulation revisited: both the heterogeneity and spatial structure of temperature drive energetic costs. *The American Naturalist*, **185**(4), E94-E102.
- Sears, M. W., Raskin, E., & Angilletta, M. J. (2011). The world is not flat: defining relevant thermal landscapes in the context of climate change. *Integrative and Comparative Biology*, **51**(5), 666-675.
- Seebacher, F., & Shine, R. (2004). Evaluating thermoregulation in reptiles: the fallacy of the inappropriately applied method. *Physiological and Biochemical Zoology*, **77**, 688-695.
- Sharaiha, R. K., & Battikhi, A. (2002). A study on potato/corn intercropping - microclimate modification and yield advantages. *Agricultural Sciences*, **29**(2).
- Sharaiha, R., & Kluson, R. (1994). Dinitrogen fixation of faba bean as affected by intercropped systems with Pea and Lettuce, **21**, 243-266.
- Sharpe, P. J., & DeMichele, D. W. (1977). Reaction kinetics of poikilotherm development. *Journal of Theoretical Biology*, **64**(4), 649-670.
- Sheldon, K. S., & Tewksbury, J. J. (2014). The impact of seasonality in temperature on thermal tolerance and elevational range size. *Ecology*, **95**(8), 2134-2143.
- Smart, R. E. (1985). Principles of grapevine canopy microclimate manipulation with implications for yield and quality. A review. *American Journal of Enology and Viticulture*, **36**(3), 230-239.
- Smith, E. N. (1979). Behavioral and physiological thermoregulation of crocodilians. *American Zoologist*, **19**(1), 239-247.
- Sobolev, S. V. & Babeyko, A. Y. (2005). What drives orogeny in the Andes? *Geology*, **33**, 617-620.
- Soer, G. J. R. (1980). Estimation of regional evapotranspiration and soil moisture conditions using remotely sensed crop surface temperatures. *Remote Sensing of Environment*, **9**(1), 27-45.
- Sparks, A. H., Forbes, G. A., Hijmans, R. J., & Garrett, K. A. (2014). Climate change may have limited effect on global risk of potato late blight. *Global Change Biology*, **20**(12), 3621-3631.
- Sporleder, M., Kroschel, J., Quispe, M. R. G., & Lagnaoui, A. (2004). A temperature-based simulation model for the potato tuberworm, *Phthorimaea operculella* Zeller (Lepidoptera; gelechiidae). *Environmental Entomology*, **33**, 477-486.
- Steen, I., & Steen, J. B. (1965). Thermoregulatory importance of the beaver's tail. *Comparative Biochemistry and Physiology*, **15**(2), 267-270.
- Stern, C. R. (2004). Active Andean volcanism: its geologic and tectonic setting. *Revista*
- Stevenson, R.D., Peterson, C.R., & Tsuji, J.S. (1985). The thermal dependence of locomotion, tongue flicking, digestion, and oxygen consumption in the wandering garter snake. *Physiological Zoology*, **58**, 46-57.
- Stigter, C. J., & Baldy, C. M. (1995). Manipulation of the microclimate by intercropping: making the best of services rendered. In: *Ecophysiology of tropical intercropping*, H. Sinoquet, P. Cruz (eds.). INRA, Paris (1995) 29-44.
- Storch, D., Marquet, P. A., & Brown, J. H. (Eds.). (2007). *Scaling biodiversity*. Cambridge: Cambridge University Press.
- Storlie, C., Merino-Viteri, A., Phillips, B., VanDerWal, J., Welbergen, J., & Williams, S. (2014). Stepping inside the niche: microclimate data are critical for accurate assessment of species' vulnerability to climate change. *Biology Letters*, **10**(9), 20140576.

- Stoskopf, N. C., & Klinck, H. R. (1966). Temperature variations in the microclimate of oats. *Canadian Journal of Plant Science*, **46**(2), 155-162.
- Suggitt, A. J., Gillingham, P. K., Hill, J. K., Huntley, B., Kunin, W. E., Roy, D. B., & Thomas, C. D. (2011). Habitat microclimates drive fine-scale variation in extreme temperatures. *Oikos*, **120**(1), 1-8.
- Suh, C. P. C., Orr, D. B., Van Duyn, J. W., & Borchert, D. M. (2002). Influence of cotton microhabitat on temperature and survival of *Trichogramma* (Hymenoptera: Trichogrammatidae) within cardboard capsules. *Environmental entomology*, **31**(2), 361-366.
- Sunday, J. M., Bates, A. E., & Dulvy, N. K. (2011). Global analysis of thermal tolerance and latitude in ectotherms. *Proceedings of the Royal Society of London B: Biological Sciences*, **278**(1713), 1823-1830.
- Sutherst, R. W. (2014). Pest species distribution modelling: origins and lessons from history. *Biological Invasions*, **16** (2), 239-256.
- Thomas, M. B. (1999). Ecological approaches and the development of “truly integrated” pest management. *Proceedings of the National Academy of Sciences*, **96**(11), 5944-5951.
- Thornton, P. K., Ericksen, P. J., Herrero, M., & Challinor, A. J. (2014). Climate variability and vulnerability to climate change: a review. *Global change biology*, **20**(11), 3313-3328.
- Tilman D., Balzer C., Hill J., & Befort, B. L. (2011). Global food demand and the sustainable intensification of agriculture. *Proceedings of the National Academy of Sciences*, **108**(50), 20260-20264.
- Tompkins, D. K., Fowler, D. B., & Wright, A. T. (1993). Influence of agronomic practices on canopy microclimate and *Septoria* development in no-till winter wheat produced in the Parkland region of Saskatchewan. *Canadian Journal of Plant Science*, **73**(1), 331-344.
- Tovar, C., Arnillas, C. A., Cuesta, F., & Buytaert, W. (2013). Diverging responses of tropical Andean biomes under future climate conditions. *PloS one*, **8**, e63634.
- Travis, J. M., Harris, C. M., Park, K. J., & Bullock, J. M. (2011). Improving prediction and management of range expansions by combining analytical and individual-based modelling approaches. *Methods in Ecology and Evolution*, **2**(5), 477-488.
- Unwin, D. M. (1980). *Microclimate measurement for ecologists*. Academic Press Inc.
- Van Noorden, R. (2014). Global scientific output doubles every nine years. *Nature*.
- Vas, E., Lescroël, A., Duriez, O., Boguszewski, G., & Grémillet, D. (2015). Approaching birds with drones: first experiments and ethical guidelines. *Biology Letters*, **11**(2), 20140754.
- Vasseur, C., Joannon, A., Aviron, S., Burel, F., Meynard, J. M., & Baudry, J. (2013). The cropping systems mosaic: How does the hidden heterogeneity of agricultural landscapes drive arthropod populations? *Agriculture, ecosystems & environment*, **166**, 3-14.
- Vasseur, D. A., DeLong, J. P., Gilbert, B., Greig, H. S., Harley, C. D., McCann, K. S., ... & O'Connor, M. I. (2014). Increased temperature variation poses a greater risk to species than climate warming. *Proceedings of the Royal Society of London B: Biological Sciences*, **281**(1779), e20132612.
- Vázquez, D. P., Gianoli, E., Morris, W. F., & Bozinovic, F. (2015). Ecological and evolutionary impacts of changing climatic variability. *Biological Reviews*. doi: 10.1111/brv.12216.
- Venette, R.C., Kriticos, D.J., Magarey, R.D., Koch, F.H., Baker, R.H., Worner, S.P., Raboteaux, N.N.G., McKenney, D.W., Dobesberger, E.J., & Yemshanov, D., (2010). Pest risk maps for invasive alien species: a roadmap for improvement. *BioScience*, **60**, 349–362.

- Veres, A., Petit, S., Conord, C., & Lavigne, C. (2013). Does landscape composition affect pest abundance and their control by natural enemies? A review. *Agriculture, Ecosystems & Environment*, **166**, 110-117.
- Vernon, R. S., & Thomson, D. (1993). Effects of soil type and moisture on emergence of tuber flea beetles, *Epitrix tuberis* (Coleoptera: Chrysomelidae) from potato fields. *Journal of the Entomological Society of British Columbia*, **90**, 3-10.
- Vincent, J. B., Werden, L. K., & Ditmer, M. A. (2015). Barriers to adding UAVs to the ecologist's toolbox: Peer-reviewed letter. *Frontiers in Ecology and the Environment*, **13**(2), 74-75.
- Vizy, E. K., & Cook, K. H. (2007). Relationship between Amazon and high Andes rainfall. *Journal of Geophysical Research: Atmospheres*, **112**, 1984-2012.
- Vogel, S. (1970). Convective cooling at low airspeeds and the shapes of broad leaves. *Journal of Experimental Botany*, **21**(1), 91-101.
- Wang, G., & Dillon, M. E. (2014). Recent geographic convergence in diurnal and annual temperature cycling flattens global thermal profiles. *Nature Climate Change*.
- Waterhouse, F. L. (1955). Microclimatological profiles in grass cover in relation to biological problems. *Quarterly Journal of the Royal Meteorological Society*, **81**(347), 63-71.
- Watson, D. J., & Baptiste, E. C. D. (1938). A comparative physiological study of sugar-beet and mangold with respect to growth and sugar accumulation: I. growth analysis of the crop in the field. *Annals of Botany*, 437-480.
- Weinstein, R.B., 1998. Effects of temperature and water loss on terrestrial locomotor performance in land crabs: integrating laboratory and field studies. *American Zoology*, **38**, 518-527.
- Weiss, S. B., Murphy, D. D., & White, R. R. (1988). Sun, slope, and butterflies: topographic determinants of habitat quality for *Euphydryas editha*. *Ecology*, **69**(5), 1486-1496.
- Wiens, J. A. (1989). Spatial scaling in ecology. *Functional ecology*, 385-397.
- Willis, K. J., & Whittaker, R. J. (2002). Species diversity: scale matters. *Science*, **295**(5558), 1245-1248.
- Willmer, P. G., Hughes, J. P., Woodford, J. A. T., & Gordon, S. C. (2008). The effects of crop microclimate and associated physiological constraints on the seasonal and diurnal distribution patterns of raspberry beetle (*Byturus tomentosus*) on the host plant *Rubus idaeus*. *Ecological Entomology*, **21**(1), 87-97.
- Wilson, E.O. (1992). *The diversity of life*. Harvard University Press, Cambridge, MA).
- Woods, H. A., Dillon, M. E., & Pincebourde, S. (2014). The roles of microclimatic diversity and of behavior in mediating the responses of ectotherms to climate change. *Journal of Thermal Biology*.
- Woodward, F. I. (1987). *Climate and Plant Distribution*. Cambridge University Press.
- Wu, T. H., Shiao, S. F., & Okuyama, T. (2014). Development of insects under fluctuating temperature: a review and case study. *Journal of Applied Entomology*, **139**, 592-599.
- Young, K. R. 2009. Andean land use and biodiversity: Humanized landscapes in a time of change. *Annals of the Missouri Botanical Garden*, **96**, 492-507.
- Zarco-Tejada, P. J., González-Dugo, V., & Berni, J. A. (2012). Fluorescence, temperature and narrow-band indices acquired from a UAV platform for water stress detection using a micro-hyperspectral imager and a thermal camera. *Remote Sensing of Environment*, **117**, 322-337.

GENERAL APPENDICES

Appendix S1: Press communications – *Sciences au sud* – November 2013

sciences au sud

n° 72 - novembre-décembre 2013
bimestriel

Le journal de l'IRD

© IRD / S. Cauby



Drone avec caméra thermique embarquée.

Les drones au secours de la science

De moins en moins coûteux et plus souples d'utilisation, les drones sont fréquemment utilisés par les scientifiques pour l'écologie, l'agronomie et l'étude du climat.

Après les militaires, les policiers et les pompiers, les drones séduisent désormais de nouveaux adeptes : les scientifiques. Capables d'embarquer de multiples capteurs, les aéronefs sans pilote deviennent de précieux alliés pour l'acquisition de données à vocation scientifique. En particulier dans les domaines où la mesure *in situ* peut s'avérer complexe voire impossible avec des moyens traditionnels. Depuis quelques années, des drones ont ainsi déjà été assignés à des missions aussi variées que l'étude de l'atmosphère à proximité de cyclones, le prélèvement d'échantillons de gaz toxiques dans des fumerolles volcaniques ou l'étude de la qualité de la glace en Antarctique, par -40 °C. « Ils sont en passe de devenir une technologie indispensable et révolutionnaire », résumait Adam Watts, chercheur en écologie à l'Université de Floride, dans un article publié cet été dans le magazine *Nature* sur l'essor des drones dans la science.

Ils peuvent aussi s'avérer efficaces pour des missions dans des disciplines telles que la biologie ou l'écologie, pour lesquelles les satellites et les avions classiques n'offrent pas une résolution spatiale suffisante (un mètre au mieux), ni la même souplesse d'utilisation. C'est ce qui a poussé les laboratoires Biodiversité et évolution des complexes plantes-insectes ravageurs-antagonistes et Botanique et bioinformatique de l'architecture des plantes de l'IRD à faire l'acquisition commune, l'été dernier, d'un de ces appareils. Il vient de rejoindre Quito, en Équateur, où il renforcera le programme BIO-ICE dédié à l'étude de la dynamique de la biodiversité (à la fois des insectes et des plantes) dans les hautes Andes tropicales. Les premiers essais au champ seront réalisés en collaboration avec l'Institut Spatial Équatorien, très intéressé par cette nouvelle technologie. Ce drone multirotor à 6 hélices d'une valeur de 12 000 euros, équipé d'une caméra thermique (20 000 euros) permettra de mesurer précisément l'évolution

et la distribution de la température du sol et des plantes des zones survolées, jusqu'à la limite des glaciers, à 5 000 m d'altitude. Le tout avec une précision de quelques centimètres, contre au

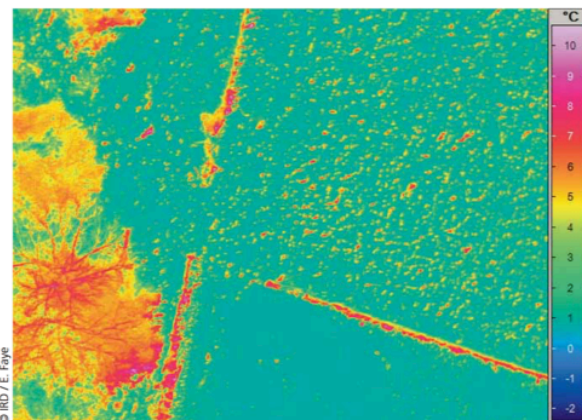
mieux un mètre pour les images satellites. Ces données permettront de mieux comprendre la dynamique des insectes et des plantes dont les distributions sont actuellement rapidement déplacées en amont en raison du réchauffement climatique. « Les images prises par ce drone, qui volera jusqu'à 80 mètres de hauteur, nous permettront de reconstituer le relief en 3D et d'y superposer un paysage thermique, explique Olivier Dangles, chercheur à l'IRD ».

Cerise sur le gâteau, la prise en main de ces robots volants est à la portée de tous. « C'est vraiment surprenant de facilité. Pourtant, je n'avais jamais piloté ce genre d'appareil auparavant », témoigne Émile Faye, thésard au BEI chargé des vols d'essais. L'appareil peut, selon les missions, être télépiloté manuellement ou préprogrammé pour suivre de façon autonome un parcours grâce à un guidage GPS. Ceci à toute heure de la journée ou de la nuit, tout en étant capable de maintenir sa position par grand vent (40 km/h). Seul handicap : un rayon d'action de 1 km et une autonomie des batteries limitée à une dizaine de minutes pour ce modèle. Mais en cas de panne, tout est prévu : un parachute de secours pourra ramener l'engin, sa caméra et ses précieuses données en toute sécurité sur le plancher... des lamas.

Contacts

olivier.dangles@ird.fr
UR BEI
fabien.anthelme@ird.fr
UMR AMAP (IRD / Cirad / CNRS / Inra / Université Montpellier 2)

Image infrarouge aérienne d'une surface agricole.





24/25 JAN 14

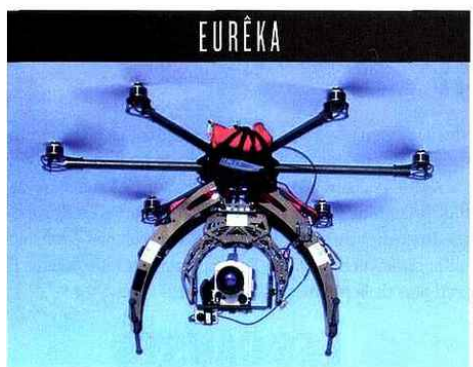
Hebdomadaire

OJD : 431865

Surface approx. (cm²) : 184

N° de page : 25

Page 1/1



Les drones au service de la science

Si, aujourd'hui, les drones ont une vocation militaire affirmée, ils ne sont cependant pas réservés aux forces armées. Ces aéronefs sans pilote, commandés à distance et dotés de toutes sortes de capteurs (caméras visibles ou à infrarouge, radars, détecteurs de pollution ou de radiation...) sont en voie de conquérir le monde civil, mais également le milieu scientifique. Simples d'emploi et accessibles financièrement, ils sont utilisés dans de nombreuses disciplines. Le plus souvent, il s'agit de drones dits tactiques ou de minidrones (moins de 25 kilos), voire de microdrones (moins de 2 kilos), qui transmettent des informations en temps réel, exploitables rapidement. Ainsi, le Centre national d'études spatiales (Cnes) expérimente, sur le site de Cessales, en Haute-Garonne, un microdrone de surveillance dont les photos et les vidéos sont diffusées en direct, par satellite, partout dans le monde. L'objectif visé est de prévenir incendies et inondations. De son côté, l'Institut de recherche pour le développement (IRD) a acquis un drone multiréacteur dédié à l'étude de la dynamique de la biodiversité. Il permettra de mesurer précisément l'évolution de la température du sol et des plantes dans les Andes tropicales, en Equateur.

Plus faciles à déployer qu'un satellite et volant à basse altitude, les drones offrent une définition d'image inégalée. Et leur champ d'action semble illimité. Au Danemark, des chercheurs de l'université de Copenhague testent l'utilisation des drones pour repérer les mauvaises herbes envahissant les terres agricoles. Les données sont envoyées à des robots déployés au sol qui se déplacent et traitent la zone affectée avec, pour résultat, une consommation de pesticides réduite de moitié. Les archéologues ont aussi recours à l'outil. Un drone quadricoptère a permis de découvrir des constructions mayas, au Mexique. D'autres ont pour fonction d'étudier l'atmosphère à proximité des cyclones, la qualité de la glace en Antarctique ou de prélever des échantillons de gaz toxiques dans des fumerolles volcaniques... D'ores et déjà, des scientifiques lui prédisent un rôle majeur.

PAR MARTINE BETTI-CUSSO

Sciences au sud – September 2014

sciences au sud

n° 76 - septembre-octobre 2014
bimestriel

Le journal de l'IRD

A chacun son climat !

L'étude de la grande variété de climat à l'échelle des petits organismes, discutée lors du colloque Heteroclim, est essentielle pour prédire leur réponse face au changement climatique.

Des insectes sous les tropiques aux plantes alpines, le comportement et la survie des organismes vivants dépendent des conditions environnementales perçues à leur échelle. « Dans les agrosystèmes d'Équateur par exemple, la différence de variétés et de stades de croissance des cultures génère une grande quantité de microclimats sur quelques mètres, raconte le chercheur Olivier Dangles. Ceux-ci influencent le développement des insectes ravageurs ! » De fait, considérer les conditions écologiques à l'échelle locale apparaît essentiel, notamment pour étudier la réponse des petites espèces au changement climatique. Une notion nouvelle, placée au cœur des discussions du colloque international Heteroclim, organisé récemment à Loches, sous l'égide du CNRS, de l'IRD et de l'université de Tours. « Il rassemble plus de 50 chercheurs de disciplines différentes », souligne-t-il. Climatologues, statisticiens, écologues, physiologistes ou encore généticiens ont répondu présent. « Tous s'accordent sur l'importance de renforcer leurs collaborations scientifiques pour mettre en commun leurs savoir-faire et bases de données », relève le chercheur. Une première étape pour répondre aux priorités de recherche définies lors de la rencontre. Celles-ci s'articulent autour du besoin d'améliorer les modèles de distribution des espèces sur différentes échelles spatio-temporelles. Pour ce faire, les chercheurs devront d'une part coupler les approches de caractérisation des climats globaux et locaux. « Les modèles ont besoin d'être affinés avec les données de petite échelle (température, humidité...) car elles sont différentes de celles mesurées au niveau



© naturexpose.com / O.Dangles et F.Nowicki.

Scarabée doré (*Euchroma gigantea*) ravageur des palmiers.

des stations météorologiques. ». D'autre part, étudier la capacité des insectes à réguler leur température dans des conditions aussi fluctuantes devient une piste de recherche importante. « La machine enzymatique qui contrôle le développement des petites espèces est étroitement liée à la température, précise-t-il. Même de faibles variations ont d'importantes conséquences que les modèles ne transcrivent pas. » In fine, les résultats de simulation permettront

aux gestionnaires d'établir des stratégies de conservation des espèces avec une meilleure considération de l'hétérogénéité des microclimats. ●

Contacts

olivier.dangles@ird.fr
IRD Equateur
Sylvain.pincebourde@univ-tours.fr
IRBI (Université de Tours, CNRS)

Roots, Tubers and Bananas Annual Report of the CGIAR – December 2014

and habitat destruction abounds, it is essential that in-situ reserves are established. In-situ conservation is complementary to genebanks and can support ongoing evolution and adaptive shifts in population genetics."

Scientists from CIP and CIAT led genebank gap analyses with partners around the world to identify gaps in potato and sweetpotato collections and geographic areas where further collecting is needed. A total of 32 species of potato wild relatives (43.8% of those studied) were assigned high priority status due to significant gaps in genebank collections. In the Andean highlands specifically – potato's center of origin – potato crop wild relatives are threatened as their habitats are impacted by climate change, land use intensification and the construction of roads and villages. The researchers recommended immediate action on both ex situ and in situ conservation.

The gap analysis for crop wild relatives of sweetpotato yielded even more dramatic results: a total of 78.6% of the species considered in the study were assessed as high priority for further collecting and conservation in ex situ collections. The research findings, published in the journal *Frontiers in Plant Science*, also indicate that diversity gaps in ex situ collections largely align with the geographic distribution of species richness of sweetpotato CWR, such as "hotspots" in central Mexico and Central America, and in the extreme southeastern USA. Further collecting of CWR germplasm should consequently be focused on these regions.

"Not only do we need more germplasm collecting activities," said Bettina Heider, a genetic resources specialist at CIP and co-lead author of the scientific paper, "we also need more research on sweetpotato overall, including its wild relatives, to better

understand the genetic diversity of the crop and tap its potential for food security."

For Rick Miller, professor of biological sciences at Southern Louisiana University, field trials can be combined with genetic approaches to identify characteristics like drought resistance in populations of the Batatas complex from around the world to be used for sweetpotato breeding. "This may sound like an ambitious goal, but for many crop species, like tomato, corn and rice, it is a reality," he said.

Both studies were undertaken as part of the project on "Adapting agriculture to climate change: collecting, protecting and preparing crop wild relatives," managed by the Global Crop Diversity Trust, Germany and the Millennium Seed Bank of the Royal Botanic Gardens at Kew in the UK.

Castañeda-Alvarez NP, de Haan S, Juárez H, Khoury CK, Achicanoy HA, Sosa CC, Bernau V, Salas A, Heider B, Simon R, Maxted N, Spooner DM (2015). Ex situ conservation priorities for the wild relatives of potato (*Solanum L.* section *Petota*). *PLOS ONE*

Khoury CK, Heider B, Castañeda-Alvarez NP, Achicanoy HA, Sosa CC, Miller RE, Scotland RW, Wood JR, Rossel G, Eserman LA, Jarret RL, Yencho G, Bernau V, Juárez H, Sotelo S, de Haan S and Struik PC (2015). Distributions, ex situ conservation priorities, and genetic resource potential of crop wild relatives of sweetpotato [*Ipomoea batatas* (L.) Lam., I. series *Batatas*]. *Front. Plant Sci.* 6:251. doi: 10.3389/fpls.2015.00251

Mass Field Screening of Sweetpotato Germplasm Reveals that CIP Genebank Holds Many Heat-Tolerant Clones

Scientists in CIP's Global Program for Genetic Resources undertook a mass field screening of 1,973 sweetpotato accessions from the CIP Genebank in the lowlands of northern Peru that resulted in the identification of 146 accessions that



Sweetpotato germplasm preserved in CIP's genebank

performed well under heat-stress conditions. The results show that CIP has ample genetic material for breeding improved sweetpotato varieties for marginal regions or the extreme conditions predicted under climate change.

"We knew that sweetpotato was a robust crop, but the results of this study show that it is very heat tolerant," said researcher Bettina Heider, who led the field screening.

She explained that the accessions were planted in Peru's northern desert, near the city of Piura, for two cropping cycles: the southern winter of 2013 and summer of 2014. Summer temperatures near Piura can reach highs of 40 °C during the day and between 20 °C and 30 °C at night. Warm soil at night typically causes sweetpotato to produce "pencil roots" with little or no value. At the end of each cycle, the researchers recorded details for each accession such as total yield, root conditions, leaf and vine biomass and any pest problems detected.

At least 21 of the accessions showed high yields and early bulking under heat-stress conditions, which makes them good candidates for further selection and breeding efforts. Heider noted that the test site has poor, sandy soil and some

plants suffered drought stress, which means the accessions that performed well have real potential for relieving hunger and malnutrition on marginal lands.

"This is really promising because we now know that we have germplasm that we can send to areas that suffer heat and related stress. In many areas of Africa and Asia, all the good farmland is already dedicated to other crops, and as the population grows, farmers are moving into marginal areas," Heider said.

She explained that her team separated accessions according to know traits such as roots with high beta-carotene, or that are sweet or not sweet, which scientists in different countries are already breeding for. She added that the accessions in the CIP genebank are from all over the world, and some of the ones that performed best under heat stress are from Asia.

"The idea is that this information strengthens the breeding program," she said. "The next step is to send the accessions that performed well for multiple testing in other regions."

In addition to producing useful information for CIP's genebank and sweetpotato breeding program, the field study was innovative in its use of remote sensing data, thanks to a collaboration with the IRD office in Ecuador, a member of RTB's global partnership with French organizations. Information from remote sensing has not only enhanced the sweetpotato mass screening, it will strengthen the future use of this type of data for evaluation of sweetpotato in the field.

"The good news is that enough of the clones performed well that we have a lot of germplasm that could be used in marginal areas or under climate change conditions. If you look at the clones that performed well under both the heat-stress and winter scenarios,

they could be well adapted to the kind of weather extremes that climate change models predict," Heider said.

Drone Technology Brings Remote Sensing to a New Level

Emile Faye, a PhD student at the Sorbonne University who is working at IRD's Ecuador office, travelled to northern Peru to collect remote sensing data for the sweetpotato heat-stress screening. Faye used a drone mounted with visual and thermal cameras to record leaf temperature and canopy cover in the sweetpotato plots at 60 days and 90 days from planting. By correlating that data with the survival rate, root weight and other information recorded during the screening harvest, Heider and Faye hope to establish thermal and visual indicators that can help scientists to evaluate the development of sweetpotato and other crops using remote sensing data.

"We hope that we can use this technology for future evaluations and that it will make it easier to do phenotype analysis earlier in trials," said Heider, noting that it could be used for "high-throughput, early analysis of sweetpotato development."

Faye will use the data to strengthen a methodological framework that he is constructing for the use of remote sensing in landscape ecology. Working with Olivier Dangles, the head of IRD in Ecuador, Faye uses drone technology to study how microclimates affect crop pests. Most remote sensing data comes from satellites and is too low-resolution for application to microclimates. Drones permit the collection of high-resolution data for a small area, and allow scientists to bridge the gap between the climatic data used in models and the conditions on the ground experienced by the organisms they study.

Global Musa Experts Improve Banana Taxonomy

In December 2014, the Global Musa Genetic Resources Network, MusaNet, held a workshop in India to address the urgent need of Musa collection curators for an unequivocal standardized characterization of germplasm and its associated management of information. This includes ensuring the correct identification of the germplasm conserved and making the information available to all users. The workshop was held at the National Research Centre for Banana (NRCB), in Tamil Nadu, India. Participants included 22 representatives of the 13 partners of the Taxonomic Reference Collection Project (TRCP), and national and regional curators, as well as NRCB scientific staff. Sessions covered topics such as field characterization, field management, documentation and information exchange, global and regional contexts, and next steps planned by the TRCP.

Pix4D webpage – [Study case](#) – November 2014



Sweet Potato Heat Tolerance Detected by High-Resolution UAV Thermal Infrared Imagery

Can high resolution, UAV-acquired thermal infrared (TIR) images permit the detection of heat tolerant varieties of sweet potato directly in the field? Could the thermal responses of sweet potato canopies be related to the plant yield at harvest? This case study asks these questions as it monitors 2100 plots in Northern Peru.



PROJECT INFO

Institution:	French Research Institute for Development - IRD
Country:	France
Industry:	Precision Agriculture
Project date:	Ongoing from 2014
Project Manager:	Olivier Dangles, PhD – IRD
Project Partner:	Bettina Heider, PhD – CIP International Potato Center Peru
Equipment:	Hexapter with DJI Wookong M autopilot / Sony Nex-7 / Infratec HR infrared camera



Actualité scientifique IRD n°488 – November 2015

Climat : des drones au service de la biodiversité



Survol d'un champ de pommes de terre en Equateur (© IRD / E. Faye)

Pour étudier la réponse du vivant au changement climatique, il est nécessaire de considérer les conditions écologiques de vie des espèces animales et végétales. Pour la plupart de ces organismes (insectes, reptiles, plantes...), les observations doivent être conduites à des échelles de l'ordre du centimètre. Comment effectuer des mesures environnementales à de si petites échelles sur de grandes surfaces ? Des chercheurs de l'IRD et leurs partenaires équatoriens viennent de publier une méthodologie complète pour répondre à cette question. Celle-ci combine l'usage de drones, de capteurs thermiques, de logiciels de cartographie et de traitement statistique. Il s'agit d'une avancée méthodologique majeure pour améliorer les prévisions des effets du climat, notamment des variations de température, sur la biodiversité.

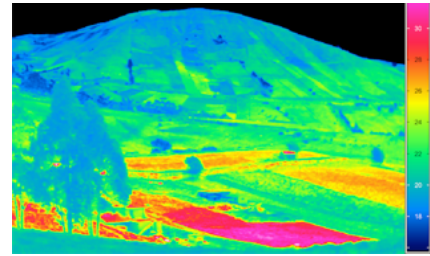
Bon à savoir

Un drone, de l'anglais « faux-bourdon », désigne un aéronef sans pilote. Depuis 10 ans, les progrès technologiques permettent une utilisation de plus en plus aisée des drones pour effectuer de nombreuses tâches de manière autonome, notamment l'acquisition d'informations sur les terres et les mers. Les limites à leur déploiement sont devenues plus réglementaires que techniques.

De plus en plus accessibles, les drones constituent une révolution technique pour l'acquisition de données scientifiques. Surtout lorsque les mesures in situ s'avèrent difficiles avec des moyens traditionnels, ou dans des domaines pour lesquels les satellites et les avions n'offrent pas la même souplesse d'utilisation ni une résolution spatiale suffisante – un mètre au mieux pour les images satellites infrarouges.

Des « paysages thermiques » en 3D

Plusieurs études récentes ont documenté les applications de ces aéronefs sans pilote, en particulier pour les recherches en écologie et en agronomie. Equipés d'une caméra thermique embarquée, ils fournissent notamment des données sur la température locale, à des échelles spatiales et temporelles adaptées. Cependant, il restait à définir un cadre méthodologique permettant d'exploiter ces données. C'est ce que viennent de proposer des chercheurs de l'IRD et leurs partenaires équatoriens dans la revue *Methods in Ecology & Evolution*. Ils y offrent une « boîte à outils » complète, permettant d'intégrer des images prises par des drones dans des logiciels de cartographie et de traitement statistique appropriés. Au final, cela permet de reconstituer en 3D le relief des zones survolées et d'y superposer un paysage thermique en haute résolution.



(© IRD)

Des essais grandeur nature

L'équipe de recherche a testé cette nouvelle méthodologie dans les paysages agricoles andins en Équateur. Dotés d'une caméra infrarouge (enregistrant les températures de surface), des drones ont passé au crible des champs de pommes de terre, qui sont communément attaqués par une grande diversité de ravageurs et maladies (chenilles, pucerons, champignons). Volant à une hauteur de 60 mètres au dessus du sol, ceux-ci ont permis de mesurer précisément sur plusieurs dizaines de mètres carrés la distribution spatiale des températures de surface, à la fois du sol et des plantes. Le tout avec une précision, respectivement pour les images visuelles et infrarouges, de 1 et 5 centimètres !

Mieux représenter les microclimats

La résolution à laquelle les données climatiques étaient collectées jusque-là ne permettait pas de rendre compte des conditions microclimatiques dans les modèles de climat globaux. Or, les microclimats modifient la réponse et la distribution des espèces locales au changement climatique. Leur mauvaise représentation dans les modèles constitue un obstacle majeur à l'étude et aux prévisions des effets climatiques, notamment sur les plantes et les animaux.

Les images collectées lors de cette étude soulignent l'urgence de quantifier, selon des échelles spatiales pertinentes, les conditions microclimatiques. Elles ont en effet révélé que le type de cultures et leur stade de croissance modifient fortement la température et les conditions écologiques dans les champs, et donc la dynamique et l'aire de répartition des populations de ravageurs de cultures, comme les teignes ou les charançons.

Partenaires

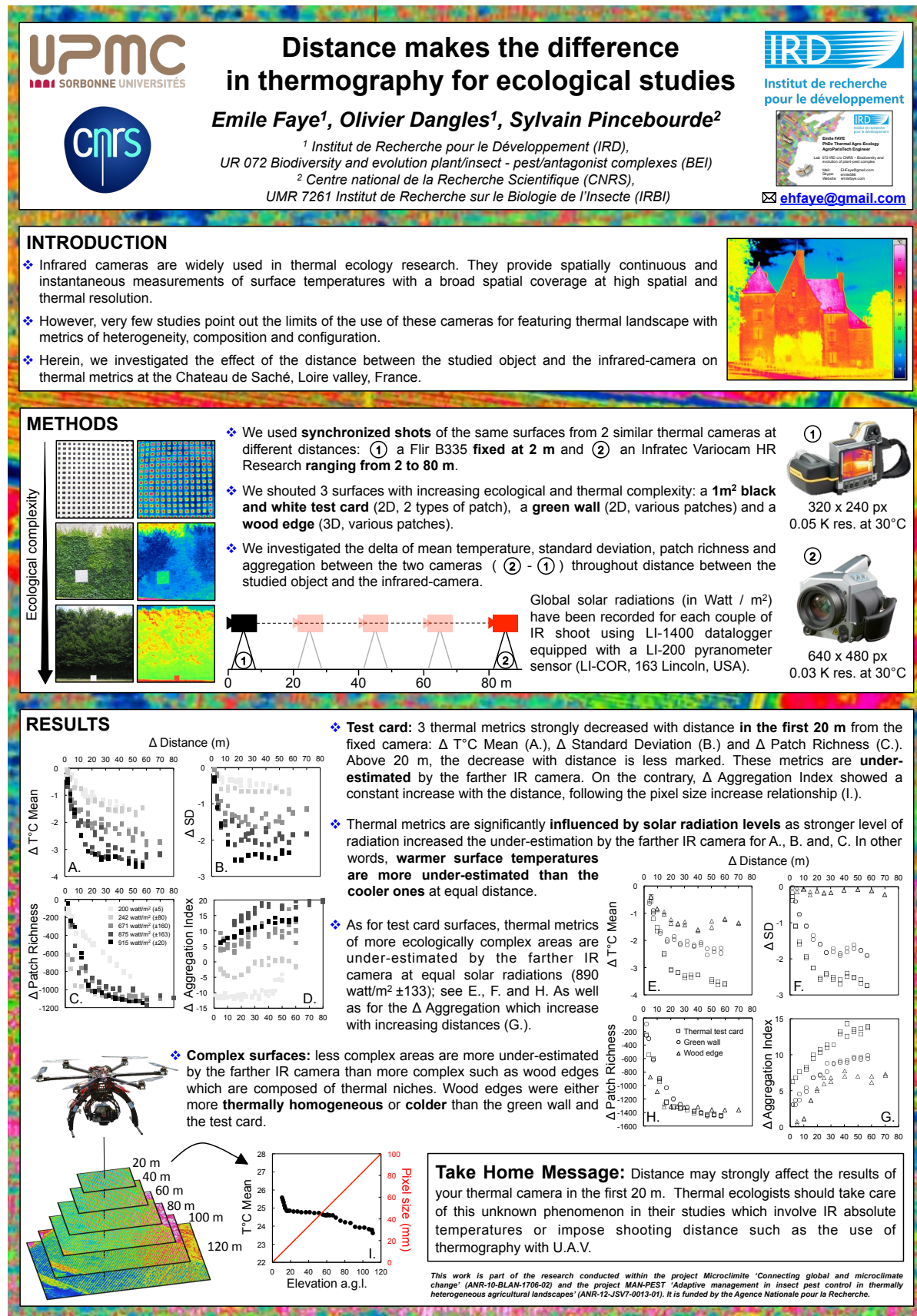
Institut spatial équatorien (IEE), Université pontificale catholique de l'Équateur (PUCE) dans le cadre du projet ANR *ManPest*.

Références

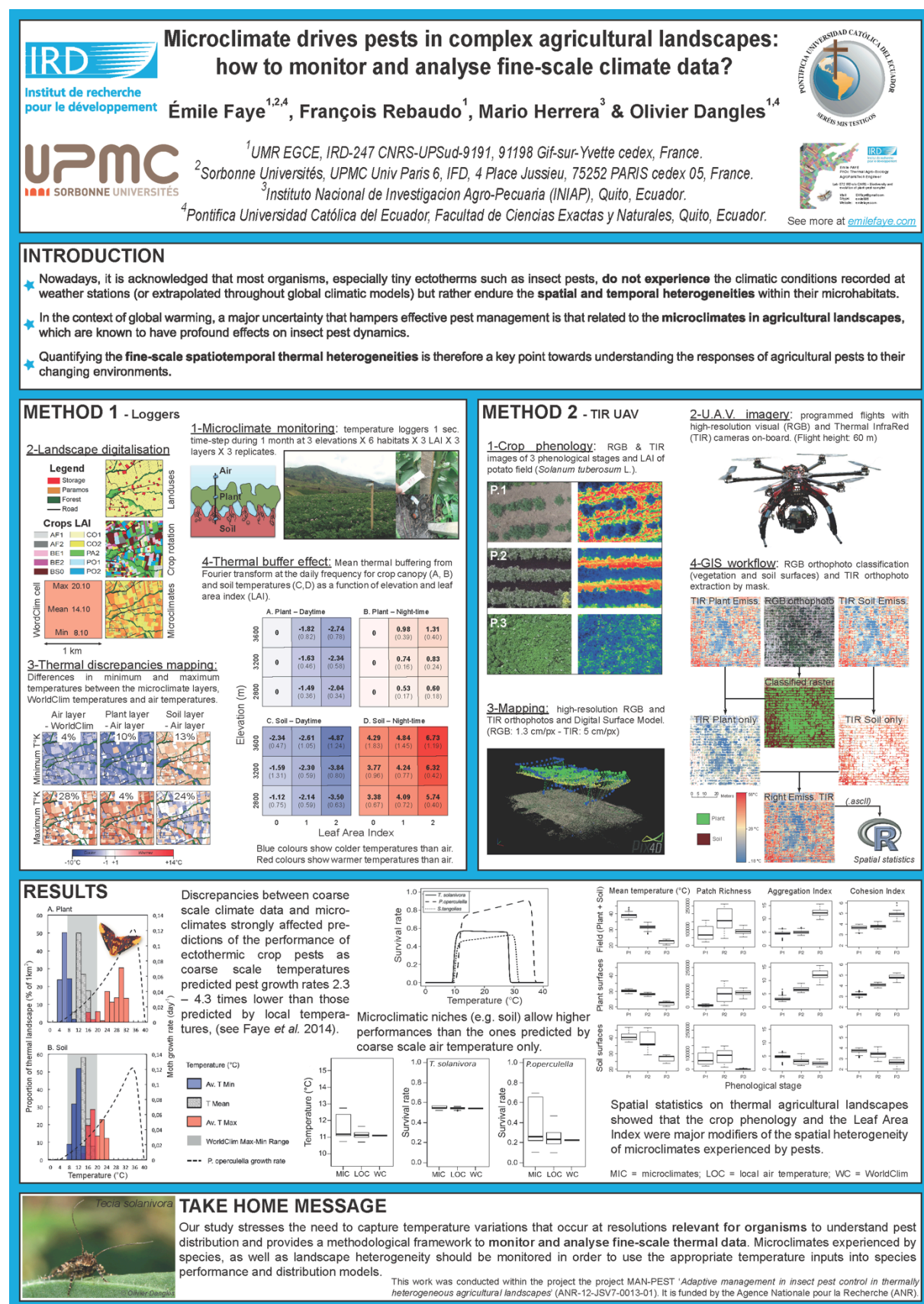
EMILE FAYE, FRANÇOIS REBAUDO, D. YANEZ-CAJO, S. CAUVY-FRAUNIE, OLIVIER DANGLES. **A toolbox for studying thermal heterogeneity across spatial scales: from unmanned aerial vehicle imagery to landscape metrics.** *Methods in Ecology & Evolution*, 2015. DOI: [10.1111/2041-210X.12488](https://doi.org/10.1111/2041-210X.12488)

Appendix S2: Posters

Poster presented at the *Heteroclim workshop* the 10-14 of June 2014. Loches, France.



Poster presented at the 3rd conference on Climate Smart Agriculture.18 of March 2015.
Montpellier, France.



Obstacles to integrated pest management adoption in developing countries

Soroush Parsa ^{a,1}, Stephen Morse ^b, Alejandro Bonifacio ^c, Timothy C. B. Chancellor ^d, Bruno Condori ^e, Verónica Crespo-Pérez ^f, Shaun L. A. Hobbs ^g, Jürgen Kroschel ^h, Malick N. Ba ⁱ, François Rebaudo ^{j,k}, Stephen G. Sherwood ^l, Steven J. Vanek ^m, Emile Faye ^j, Mario A. Herrera ^f, and Olivier Dangles ^{f,j,k,n}

^aInternational Center for Tropical Agriculture, Cali, Colombia; ^bCentre for Environmental Strategy, University of Surrey, Guildford, Surrey GU2 7XH, United Kingdom; ^cFundación para la Promoción e Investigación de Productos Andinos, Cochabamba, Bolivia; ^dNatural Resources Institute, University of Greenwich, Chatham Maritime, Kent ME4 4TB, United Kingdom; ^eLiaison Office for Bolivia, International Potato Center, La Paz, Bolivia; ^fEscuela de Ciencias Biológicas, Pontificia Universidad Católica del Ecuador, Quito, Ecuador; ^gCAB International, Wallingford, Oxon OX10 8DE, United Kingdom; ^hInternational Potato Center, Lima, Peru; ⁱInternational Crop Research Institute for the Semi-Arid Tropic, Niamey, Niger; ^jInstitut de Recherche pour le Développement (IRD), Unité Diversité, Évolution et Écologie des Insectes Tropicaux, Laboratoire Evolution, Génomes et Spéciation, 91198 Gif-sur Yvette Cedex, France; ^kUniversité Paris-Sud 11, 91405 Orsay Cedex, France; ^lKnowledge, Technology and Innovation Group, Wageningen University, Hollandseweg 1, 6706 KN, Wageningen, The Netherlands; ^mCrop and Soil Sciences, Cornell University, Ithaca, NY 14853; and ⁿInstituto de Ecología, Universidad Mayor San Andrés, La Paz, Bolivia

Edited by Hans R. Herren, Millennium Institute, Arlington, VA, and approved January 13, 2014 (received for review July 8, 2013)

Despite its theoretical prominence and sound principles, integrated pest management (IPM) continues to suffer from anemic adoption rates in developing countries. To shed light on the reasons, we surveyed the opinions of a large and diverse pool of IPM professionals and practitioners from 96 countries by using structured concept mapping. The first phase of this method elicited 413 open-ended responses on perceived obstacles to IPM. Analysis of responses revealed 51 unique statements on obstacles, the most frequent of which was “insufficient training and technical support to farmers. Cluster analyses, based on participant opinions, grouped these unique statements into six themes: research weaknesses, outreach weaknesses, IPM weaknesses, farmer weaknesses, pesticide industry interference, and weak adoption incentives. Subsequently, 163 participants rated the obstacles expressed in the 51 unique statements according to importance and remediation difficulty. Respondents from developing countries and high-income countries rated the obstacles differently. As a group, developing-country respondents rated “IPM requires collective action within a farming community as their top obstacle to IPM adoption. Respondents from high-income countries prioritized instead the “shortage of well-qualified IPM experts and extensionists. Differential prioritization was also evident among developing-country regions, and when obstacle statements were grouped into themes. Results highlighted the need to improve the participation of stakeholders from developing countries in the IPM adoption debate, and also to situate the debate within specific regional contexts.

sustainable agriculture | technology adoption | collective action dilemma

Feeding the 9,000 million people expected to inhabit Earth by 2050 will present a constant and significant challenge in terms of agricultural pest management (1–3). Despite a 15- to 20-fold increase in pesticide use since the 1960s, global crop losses to pests—arthropods, diseases, and weeds—have remained unsustainably high, even increasing in some cases (4). These losses tend to be highest in developing countries, averaging 40–50%, compared with 25–30% in high-income countries (5). Alarmingly, crop pest problems are projected to increase because of agricultural intensification (4, 6), trade globalization (7), and, potentially, climate change (8).

Since the 1960s, integrated pest management (IPM) has become the dominant crop protection paradigm, being endorsed globally by scientists, policymakers, and international development agencies (2, 9–15). The definitions of IPM are numerous, but all involve the coordinated integration of multiple complementary methods to suppress pests in a safe, cost-effective, and environmentally friendly manner (9, 11). These definitions also recognize IPM as a dynamic process in terms of design, implementation, and evaluation (11). In practice, however, there is a continuum of

interpretations of IPM (e.g., refs. 14, 16, 17), but bounded by those that emphasize pesticide management (i.e., “tactical IPM”) and those that emphasize agroecosystem management (i.e., “strategic IPM,” also known as “ecologically based pest management”) (16, 18, 19). Despite apparently solid conceptual grounding and substantial promotion by the aforementioned groups, IPM has a discouragingly poor adoption record, particularly in developing-country settings (9, 10, 15–23), raising questions over its applicability as it is presently conceived (15, 16, 22, 24).

The possible reasons behind the developing countries poor adoption of IPM have been the subject of considerable discussion since the 1980s (9, 15, 16, 22, 25–31), but this debate has been notable for the limited direct involvement from developing-country stakeholders. Most of the literature exploring poor adoption of IPM in the developing world has originated in the developed world (e.g., refs. 15, 16, 22). An international workshop, entitled “IPM in Developing Countries,” was held at the Pontificia Universidad Católica del Ecuador (PUCE) from October 31 to November 3, 2011. Poor IPM adoption spontaneously became a central discussion point, creating an opportunity to address the apparent participation bias in the IPM adoption debate.

It was therefore decided to explore the topic further by eliciting and mapping the opinions of a large and diverse pool of IPM

Significance

Integrated pest management (IPM) has been the dominant crop protection paradigm promoted globally since the 1960s. However, its adoption by developing country farmers is surprisingly low. This article reports 51 potential reasons why, identified and prioritized by hundreds of IPM professionals and practitioners around the world. Stakeholders from developing countries prioritized different adoption obstacles than those from high-income countries. Surprisingly, a few of the obstacles prioritized in developing countries appear to be overlooked by the literature. We suggest that a more vigorous analysis and discussion of the factors discouraging IPM adoption in developing countries may accelerate the progress needed to bring about its full potential.

Author contributions: S.P., A.B., T.C.B.C., B.C., V.C.-P., S.L.A.H., J.K., M.N.B., F.R., S.G.S., S.J.V., E.F., M.A.H., and O.D. designed research; S.P. and O.D. performed research; S.P. and O.D. analyzed data; and S.P. and S.M. wrote the paper.

The authors declare no conflict of interest.

This article is a PNAS Direct Submission.

Freely available online through the PNAS open access option.

¹To whom correspondence should be addressed. E-mail: s.parsa@cgiar.org.

This article contains supporting information online at www.pnas.org/lookup/suppl/doi:10.1073/pnas.1312693111/-DCSupplemental.

professionals and practitioners from around the world, including many based in developing countries. The objective was to generate and prioritize a broad list of hypotheses to explain poor IPM adoption in developing-country agriculture. We also wanted to explore differences as influenced by respondents' characteristics, particularly their region of practice. To achieve these objectives, we used structured concept mapping (32), an empirical survey method often used to quantify and give thematic structure to open-ended opinions (33).

We know of only one other similar study that characterizes obstacles to IPM. It was based on the structured responses of 153 experts, all from high-income countries (30). Our survey was designed to progress from unstructured to structured responses, and to reach a much larger and diverse pool of participants, particularly those from the "Global South." Considering that the vast majority of farmers live in developing countries (34), it would seem imperative that the voices from this region be heard.

Results

Fig. 1 provides a summary of the study's results. The study began with a brainstorming phase that used an open-ended question that asked participants to identify one obstacle to IPM adoption

in developing countries. We received 413 responses, 80% of which came from professionals and practitioners based in developing countries (Table S1). Most participants (56.4%) had more than 10 y of experience in developing-country agriculture. They were demographically diverse (Table S1), although with an important male bias (75.5%), but nevertheless reflecting the wider discipline of crop protection. After eliminating redundancies and editing for conciseness and clarity, we generated statements on 51 unique obstacles (Table 1), which were then used in subsequent steps of the concept mapping. The obstacle most frequently cited was "insufficient training and technical support to farmers" [coded as "outreach weakness" (OUT)-1; Table 1], accounting for 12.8% of total responses. This was followed by "lack of favorable government policies and support" [coded as "weak adoption incentive" (INC)-1], accounting for 9.4% of total responses. Later, 12 respondents sorted the obstacles into similar groups. Their responses were submitted to multidimensional scaling (MDS) analysis, which identified six distinct clusters (Fig. S1) that were designated as follows: FMR, for "farmer weaknesses"; INC, for "weak adoption incentives"; IPM, for "IPM weaknesses"; OUT, for "outreach weaknesses"; PST, for

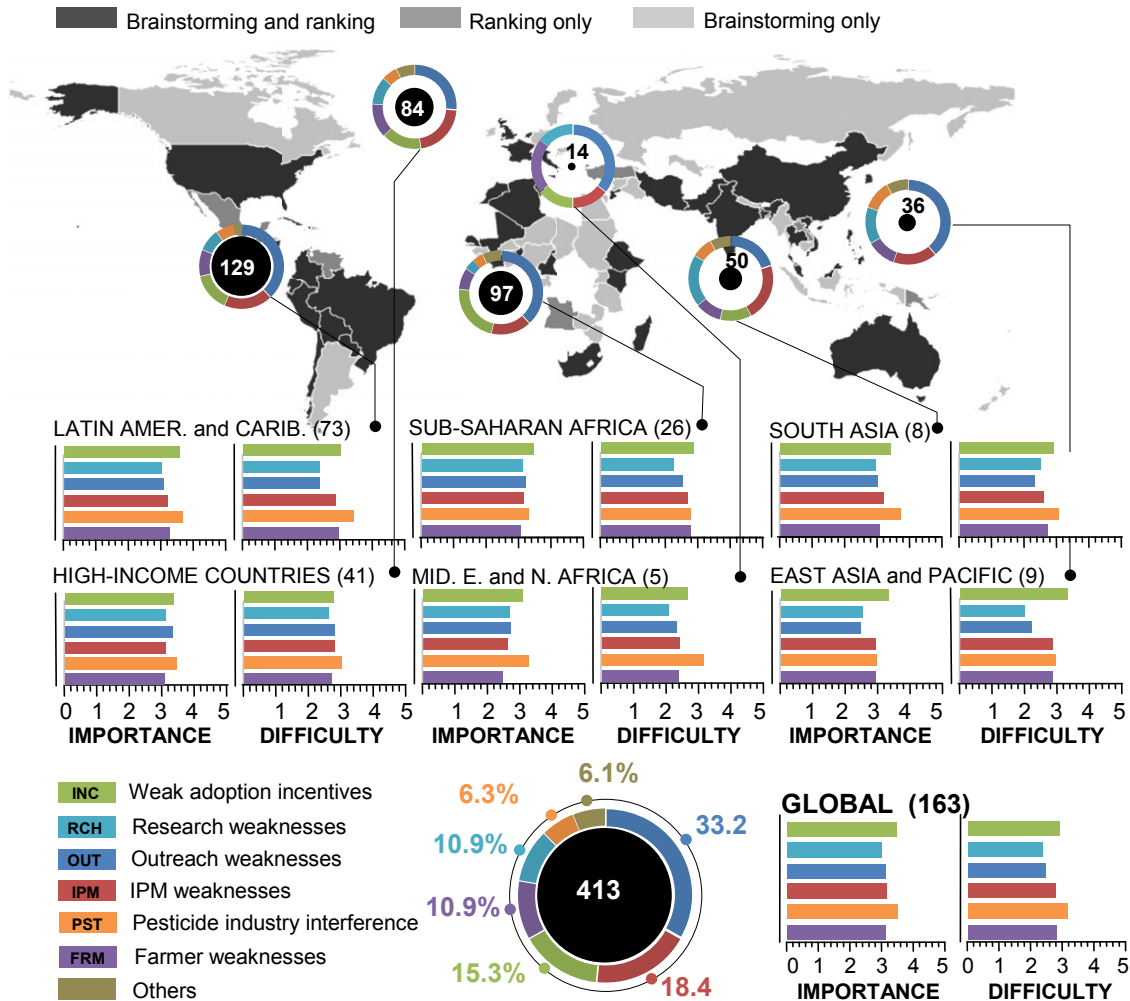


Fig. 1. Summary of a concept map identifying obstacles to IPM in developing countries. The world map captures the global participation in developing the concept map. Doughnut charts represent the proportion of open-ended responses that matched one of six obstacle themes or were otherwise assigned to the generic category "others." The size of the circle inside each doughnut is proportional to the number (labeled in or next to it) of open-ended responses. Bar charts represent ratings on a scale from 1 to 5, ranging from least to most important or difficult obstacle. The number of rating responses is presented in parentheses next to the region's name. Responses from Europe and Central Asia were omitted from the graph because of poor representation.

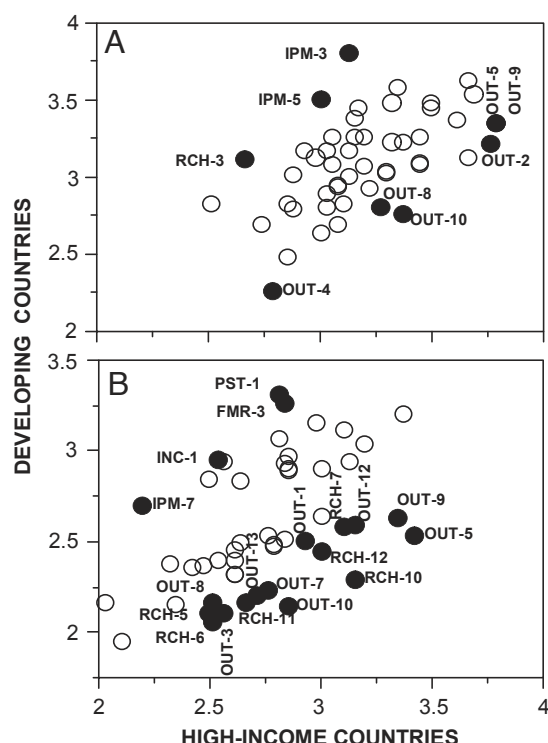


Fig. 2. Respondents from high-income and developing countries rated 51 unique obstacles in terms of their importance (A) and the difficulty (B) of solving them. Differences in ratings are based on a scale from 1 to 5, ranging from least to most important or difficult obstacle. Solid circles represent obstacles that were rated significantly differently ($df = 161$; $P \leq 0.05$). Labels represent codes for obstacle themes. FMR, farmer weaknesses; INC, weak adoption incentives; IPM, IPM weaknesses; OUT, outreach weaknesses; PST, pesticide industry interference; RCH, research weaknesses.

the statement "IPM requires collective action within a farming community" (IPM-3) as the most important obstacle. This rating differed significantly with that from high-income country participants, who rated it 28th of 51 responses for importance ($df = 161$; $F = 12.56$; $P < 0.01$; Fig. 2).

Analyses of ratings by region pointed to overall agreement on the importance and remedial difficulty for most of the 51 obstacles (Table S2). However, top-rated statements differed, often significantly (Table 2). For example, high-income countries rated the statement "shortage of well-qualified extensionists" (OUT-9) as one of the two most important obstacles to IPM in developing countries, but there was low agreement on its importance and difficulty across regions (Table 2).

Statistical analyses conducted on obstacle themes (clusters) showed less agreement by region than those conducted on the obstacles themselves (Table 3 and Table S2). Nevertheless, regions notably agreed on the importance of "weak adoption incentives," which was the top-ranked theme for Asia and sub-Saharan Africa (Table 3).

Discussion

Our objective was to elicit and prioritize a broad list of hypotheses to explain relatively low IPM adoption in developing countries. Our list of 51 obstacles to IPM adoption is reasonably comprehensive, but not necessarily exhaustive. For example, the list did not include the argument that, under conditions of low productivity that are common in developing countries, the yield saved by IPM vs. doing nothing may be too inconsequential to justify adoption (15). According to this argument, IPM is

economically justifiable only under conditions of high productivity under which the cost of investment will be covered by increased revenue (15).

A retrospective review of our open-ended responses revealed the statement "...in regions with low yields, the economic incentive for IPM is very limited," which we simplified and coded as "IPM is too expensive" (IPM-4). However, of course, much depends on pest pressure and the extent of losses incurred by farmers. Even within subsistence systems that have relatively low productivity, a high degree of pest pressure could make IPM important. Indeed farmers may be using practices that help suppress pest numbers without necessarily being aware of the effect.

Given the ambitious scope and reach of our survey, we believe these types of omissions or simplifications are unlikely to substantially influence the outcome of our study. Indeed, many of the points raised in this study have been reported before (16), and should not be surprising. The failure of extension to function as a vehicle providing technical support and training to farmers, the lack of investment in research, and the prominence of pesticide-based solutions have long been put forward as reasons for poor IPM adoption. What is interesting is that these issues have persisted as long as they have. Clearly, all the calls for action that have been expressed since the early IPM adoption studies of the 1980s (35) have gone unheard.

However, some obstacle statements in our list appeared to be new to the literature on IPM adoption. Most noteworthy was the statement "IPM requires collective action within a farming community." This was ranked by developing-country respondents as their single most important obstacle to IPM adoption (Fig. 2). The recognition that pest management is most effective when implemented collectively at the regional level precedes IPM itself, and gave rise to the development of area-wide pest management (36) and metapopulation theory (37). Indeed, some pest management decisions are subject to a collective action dilemma (38), whereby the payoffs from adopting a technology depend on whether others adopt it too (39, 40). For example, smallholder farmers in Peru are encouraged to plow their previous-season potato fields to kill overwintering weevils before they colonize newly planted fields, but this practice is ineffective if their neighbors do not also plow their fields (41).

This phenomenon may be particularly acute for preventive, as opposed to therapeutic, management tactics, which are in fact the most heavily championed by IPM (13, 23). However, collective action may be more important for IPM in developing countries because pests can more easily move between farms that are small and therefore separated by short distances. Aware of

Table 2. Ratings by region for the most important obstacles to IPM adoption in developing countries

Code*	Importance					Difficulty				
	HIC	Asia	LAC	SSA	P value [†]	HIC	Asia	LAC	SSA	P value [†]
OUT-5	3.78	3.29	3.47	3.27	0.228	3.41	2.71	2.51	2.65	0.000
OUT-9	3.78	3.24	3.22	3.73	0.064	3.34	2.53	2.51	3.12	0.001
IPM-9	3.32	3.82	3.55	3.15	0.106	3.20	3.35	3.05	2.73	0.306
INC-2	3.68	3.41	3.48	3.85	0.821	3.10	3.00	3.08	3.27	0.874
IPM-3	3.12	3.41	4.05	3.54	0.000	2.83	2.71	3.11	2.73	0.085

HIC, high-income countries; LAC, Latin America and the Caribbean; SSA, sub-Saharan Africa.

*The statistical significance of the importance and difficulty of an obstacle according to rating by region was derived through multiple regression analyses using sex, education and field of expertise as covariates. Larger P values suggest greater agreement across regions.

[†]The letter coding describes six obstacle themes: FMR, farmer weaknesses; INC, weak adoption incentives; IPM, IPM weaknesses; OUT, outreach weaknesses; PST, pesticide industry interference; RCH, research weaknesses.

close to zero indicating a good fit. The stress value of the six-cluster MDS solution was 0.196, indicating a good fit.

Cluster dissimilarity was further tested by using an analysis of similarities that generated a statistical parameter R , which indicated the degree of separation between groups (where a score of 1 indicated complete separation and a score of 0 indicated no separation). After this analysis, we examined and discussed the obstacle statements within each cluster to identify their unifying theme and propose a suitable cluster name.

To visually examine global patterns within our results, we adopted the World Bank regional classification system for developing countries (<http://data.worldbank.org/about/country-classifications/country-and-lending-groups>), and consolidated responses from high-income countries into a single group.

We applied one-way ANOVA to identify differences in perceptions between high-income countries and developing countries of the importance and difficulty of resolution for each obstacle statement. Responses from South and East Asia and the Pacific were consolidated

into a single group, and poorly represented regions were omitted. Multiple regression analyses were then applied to identify differences in ratings of statements and their cluster themes by region, using sex, education, and field of expertise as covariates. Because of an unbalanced representation, all social sciences were grouped into a single expertise category.

ACKNOWLEDGMENTS. We thank Jean Vacher, director of the French regional cooperation for Andean countries; Hugo Navarrete, dean of the Faculty of Exact and Natural Sciences at PUCE, for hosting the IPM workshop, and all the conference participants for their stimulating discussions; Neal Palmer and Claire Nicklin for helping us to edit our obstacle statements; and Carlos Pérez, Jay Rosenheim, Jerome Casas, and Les Ehler for critically reading the preliminary version of the manuscript and offering their invaluable feedback. This work was supported by the McKnight Foundation Collaborative Crop Research Program, the French regional cooperation for Andean countries, the French Institute for Research and Development, and the PUCE.

- Ash C, Jasny BR, Malakoff DA, Sugden AM (2010) Food security. Feeding the future. *Introduction*. *Science* 327(5967):797.
- Thomas MB (1999) Ecological approaches and the development of "truly integrated" pest management. *Proc Natl Acad Sci USA* 96(11):5944–5951.
- Godfray HCJ, et al. (2010) Food security: The challenge of feeding 9 billion people. *Science* 327(5967):812–818.
- Oerke EC (2006) Crop losses to pests. *J Agric Sci* 144(1):31.
- Thacker J (2002) *An Introduction to Arthropod Pest Control* (Cambridge Univ Press, Cambridge, UK).
- Wilby A, Thomas MB (2002) Natural enemy diversity and pest control: Patterns of pest emergence with agricultural intensification. *Ecol Lett* 5(3):353–360.
- Perrings C, Dehnen-Schmutz K, Touza J, Williamson M (2005) How to manage biological invasions under globalization. *Trends Ecol Evol* 20(5):212–215.
- Gregory PJ, Johnson SN, Newton AC, Ingram JSI (2009) Integrating pests and pathogens into the climate change/food security debate. *J Exp Bot* 60(10):2827–2838.
- Ehler LE (2006) Integrated pest management (IPM): Definition, historical development and implementation, and the other IPM. *Pest Manag Sci* 62(9):787–789.
- World Bank (2005) *Sustainable Pest Management: Achievements and Challenges*, Report 32 714 –GBL (World Bank, Washington, DC).
- Kogan M (1998) Integrated pest management: Historical perspectives and contemporary developments. *Annu Rev Entomol* 43(1):243–270.
- Kogan M, Croft BA, Sutherst RF (1999) Applications of ecology for integrated pest management. *Ecological Entomology*, eds Huffaker CB, Gutierrez AP (Wiley, New York), pp 681–736.
- Lewis WJ, van Lenteren JC, Phatak SC, Tumlinson JH, 3rd (1997) A total system approach to sustainable pest management. *Proc Natl Acad Sci USA* 94(23):12243–12248.
- Kogan M, Bajwa WI (1999) Integrated pest management: A global reality? *Anais Soc Entomol Brasil* 28(1):1–25.
- Orr A (2003) Integrated pest management for resource-poor African farmers: Is the emperor naked? *World Dev* 31(5):831–845.
- Morse S (2009) IPM, ideals and realities in developing countries. *Integrated Pest Management: Concepts, Tactics, Strategies and Case Studies*, eds Radcliffe EB, Hutchison WD, Cancelado RE (Cambridge Univ Press, Cambridge, UK), pp 458–470.
- Jeger M (2000) Bottlenecks in IPM. *Crop Prot* 19(8):787–792.
- Barfield CS, Swisher ME (1994) Integrated pest management: Ready for export? Historical context and internationalization of IPM. *Food Rev Int* 10:215–267.
- Royer TA, Mulder PG, Cuperus GW (1999) Renaming (redefining) integrated pest management: Fumble, pass, or play? *Am Entomol* 45:136–139.
- Zalucki MP, Adamson D, Furlong MJ (2009) The future of IPM: Whither or wither? *Aust J Entomol* 48:85–96.
- Way MJ, van Emden HF (2000) Integrated pest management in practice – pathways towards successful application. *Crop Prot* 19:81–103.
- Morse S, Buhler W (1997) IPM in developing countries: The danger of an ideal. *Integr Pest Manage Rev* 2(4):175–185.
- Pedigo LP (1995) Closing the gap between IPM theory and practice. *J Agric Entomol* 12(4):171–181.
- Van Huis A, Meerman F (1997) Can we make IPM work for resource-poor farmers in sub-Saharan Africa? *Int J Pest Manage* 43(4):313–320.
- Nowak P, Padgett S, Hoban TJ (1996) Practical considerations in assessing barriers to IPM adoption. *Proceedings of the Third National IPM Symposium: Broadening Support for 21st Century IPM*. ERS Miscellaneous Publication (Citeseer, Washington, DC), pp 93–114.
- Rajotte EG, Norton GW, Luther GC, Barrera V, Heong K (2005) IPM Transfer and Adoption. *Globalizing Integrated Pest Management: A Participatory Research Process*, eds Norton GW, Heinrichs EA, Luther GC, Irwin ME (Cambridge Univ Press, Cambridge, UK), pp 143–157.
- Goodell G (1984) Challenges to international pest management research and extension in the Third World: Do we really want IPM to work? *ESA Bull* 30(3):18–26.
- Smith EH (1983) Integrated pest management (IPM): Specific needs of developing countries. *Int J Trop Insect Sci* 4(1–2):173–177.
- Bottrell DG (1983) Social problems in pest management in the tropics. *Insect Sci Appl* 4(1):179–184.
- Wearing C (1988) Evaluating the IPM implementation process. *Annu Rev Entomology* 33(1):17–38.
- Dreves AJ (1996) Village-level integrated pest management in developing countries. *J Agric Entomol* 13(3):195–211.
- Trochim WMK (1989) An introduction to concept mapping for planning and evaluation. *Eval Program Plann* 12(1):1–16.
- Cabrera D, Mandel JT, Andras JP, Nydam ML (2008) What is the crisis? Defining and prioritizing the world's most pressing problems. *Front Ecol Environ* 6(9):469–475.
- International Fund for Agricultural Development (2010) *Rural Poverty Report 2011* (IFAD, Rome).
- Morse S, Buhler W (1997) *Integrated Pest Management: Ideals and Realities in Developing Countries* (Lynne Rienner, Boulder, CO).
- Knipling E (1960) Use of insects for their own destruction. *J Econ Entomol* 53(3):415–420.
- Levins R (1969) Some demographic and genetic consequences of environmental heterogeneity for biological control. *ESA Bull* 15(3):237–240.
- Olson M (1965) *The Logic of Collective Action: Public Goods and the Theory of Groups* (Harvard Univ Press, Cambridge, MA).
- Rebaudo F, Dangles O (2011) Coupled information diffusion –pest dynamics models predict delayed benefits of farmer cooperation in pest management programs. *PLOS Comput Biol* 7(10):e1002222.
- Lazarus WF, Dixon BL (1984) Agricultural pests as common property: Control of the corn rootworm. *Am J Agric Econ* 66(4):456–465.
- Parsa S, Canto R, Rosenheim JA (2011) Resource concentration dilutes a key pest in indigenous potato agriculture. *Ecol Appl* 21(2):539–546.
- Pretty J (2003) Social capital and the collective management of resources. *Science* 302(5652):1912–1914.
- Pretty J, Ward H (2001) Social capital and the environment. *World Dev* 29(2):209–227.
- Bottrell DG (1979) *Integrated Pest Management* (Council on Environmental Quality, Washington, DC).
- Bernard H (2006) *Research Methods in Anthropology: Qualitative and Quantitative Approaches* (Altamira, Oxford).